



ATTEMPTS ON PREPARATION OF ELASTIC ABSORBENT FROM WASTE RUBBER TYRES FOR RECOVERY OF BIOBUTANOL FROM FERMENT LIQUORS

László Kótai,^[a, b] István Somogyi,^[c] Li Zhibin,^[d] Baiquan Chen,^[d] Kalyan K. Banerji,^[e] R. P. Pawar,^[f] Rajni Kant^[g] and Tünde Kocsis^[b]

Keywords: Biobutanol, extractive fermentation, superabsorbent, solid sponge, sulphonated rubber, tyre wastes.

Attempts on the preparation of elastic sorbents from waste rubber tyres, for removal of biobutanol from ferment liquor extracts, using low-distribution apolar solvent like n-heptane have been discussed. The main factors in preparation of useful sorbents are the type of the waste tyre, the type of the sulphonating agent, and the reaction conditions. The waste tyres containing large amount of styrene proved to be useful base material for preparation of elastic sorbent with concentrated sulphuric acid as sulphonation agent. The common mixed waste tyres resulted in elastic sorbents with lower absorbing capacities. Therefore, the styrene containing ones were studied over a wide range of the sulphonation conditions.

* Corresponding Authors

E-Mail: kotai.laszlo@ttk.mta.hu

- [a] Institute of Materials and Environmental Chemistry, Research Centre for Natural Sciences, Hungarian Academy of Science, H-1117, Magyar Tudósok krt. 2., Budapest, Hungary
- [b] Deuton-X Ltd., H-2030, Selmeci út 89, Érd, Hungary.
- [c] Iontech Ltd., 8196, Árpád utca 38, Litér, Hungary
- [d] China New Energy Co., Room 210, Floor 2 Integration Service Building Guangzhou Science and Technology Innovation Base, 80 Lanyue Road, Guangzhou, China.
- [e] Faculty of Science, National Law University, Jodhpur, India
- [f] Department of Chemistry, Deogiri College, Aurangabad-431005, Maharashtra, INDIA.
- [g] X-ray Crystallography Laboratory, Post-Graduate Department of Physics & Electronics, University of Jammu, Jammu, India.

aliphatic hydrocarbon extractants used in the extractive biobutanol fermentation processes are described starting from waste rubber tyres.

Experimentals

Sulphonation of the soft waste rubber tyres

A waste soft rubber tyre granulate (sample made from a cross motor tyre cubes with putting that into liquid nitrogen and grinding the cooled inelastic form with selecting a fraction with 2.5 mm average equivalent diameter) (4.1 g) was mixed with 4 ml 1,2-dichloroethane and 50 ml of 96 % sulphuric acid at room temperature. The reaction mixture was heated until 90 °C in 2 h then kept at this temperature for 3 h, and cooled left to cool to room temperature (roughly 1.5 h). The sample was thoroughly washed with water until acid-free and the ion-exchange and salt-splitting capacities were measured with a standard method.⁶

The water content was measured with drying the samples in an oven at 105 °C. Solvent absorbing capacities were measured with gravimetrically after keeping the sample in the appropriate solvent for an hour. Both the salt-splitting and the ion-exchange capacity were found to be 0.50 mequiv mL⁻¹. The binding capacity for n-BuOH and some other solvents including water is given in Table 1.

Sulphonation of the hard waste rubber tyres at high temperature

A waste hard rubber tyre granulate (made from a hard tyre cubes with putting that into liquid nitrogen and grinding the cooled inelastic form with selecting a fraction with 2.5 mm average equivalent diameter) (4.4 g) was mixed with 1,2-dichloroethane (4 mL) and 90 g of 96 % sulphuric acid at room temperature. The reaction mixture was heated until 90 °C in 2 h then kept at this temperature for 3 h, and cooled left to cool to room temperature (roughly 1.5 h). The sample was thoroughly washed with water until acid-free. The n-butanol and water absorbing capacities were found to be 21.6 and 147.0 %, respectively. The salt-splitting capacity was found to be 0.31 mequiv mL⁻¹.

Introduction

Biobutanol, one of the most promising biofuel of the near-future, is produced in fermentative processes from agricultural products and wastes.^{1,2} In order to improve the effectiveness and decreasing the process costs, the so-called extractive fermentation processes are favoured in order to avoid the accumulation of the toxic biobutanol during the fermentation process.²⁻⁴ The most effective extractants like heptanal, however, are toxic, and the non-toxic solvents like aliphatic hydrocarbons such as n-heptane have very low distribution coefficients. Combining the extractive fermentation in the presence of aliphatic hydrocarbon extractants by removing of biobutanol from the low hydrocarbon solvent with a solid phase regenerable super absorbent before recycling that to the fermentation process, is a potential way to solve this problem.⁵

In order to regenerate of the solid sponges with heat treatment (both the absorption and regeneration processes initiate large volume changes of the absorbents due to swelling and drying) in order to prevent the cracking and mechanical destroying, the supersorbents used for recovery of butanol and similar polar solvents should be elastic.

In this communication the preliminary results on attempts on preparing a cheap, elastic and regenerable solid supersorbents for recovery of biobutanol from apolar

Sulphonation of the hard waste rubber tyres at room temperature

The common waste tyre granulate (30 g) removed from car tyres prepared in a method given previously was swelled with 20 mL of 1,2-dichloroethane for 30 min, the excess of solvent was decanted and the sulphonation was performed with 120 g of 96 % sulphuric acid at room temperature for 3 h. The same methods as previously described were used to isolate and characterize the product. The salt splitting/ion exchange capacity was found to be 0.21 mequiv. mL⁻¹.

Effect of sulphuric acid on the sulphonation of the hard waste rubber tyres at room temperature

The common waste tyre granulate (25 g) removed from waste tyres prepared in a method given previously was swelled with 47.7 mL of 1,2-dichloroethane for 30 min, the excess of solvent was decanted and the sulphonation was performed with 500 g of 96 % sulphuric acid at room temperature for 3 h. The same method was used to isolate and characterize the product as earlier. The salt splitting/ion exchange capacities were found to be the same, namely 0.09 mequiv mL⁻¹.

Attempts on sulphonation of waste hard rubber tyres with chlorosulphonic acid

Waste tyre granulates (5 g, 2.5 mm fraction) were swelled in 25 mL of 1,2-dichloroethane for 30 min, the solvent was removed by decantation, then 40 g of chlorosulphonic acid was added at room temperature with stirring. The reaction mixture was heated until 40 °C in 30 min, when a weak gas evolution was started with strong H₂S smell. The gas evolution was decreased after 1.5 h and the reaction mixture was allowed to cool for 30 min. The product was a strong tar-like substance which could not be removed and processed.

Attempt on sulphonation of waste rubber tyres with chlorosulphonic acid without outer heating

Another portion of (20 g) of waste tyre granules ($d = 2.5$ mm) was mixed with 175 g of chlorosulphonic acid, when the reaction mixture was warmed up to 35 °C. After 10 min stirring, the granulates were disintegrated into powder.

Attempt on sulphonation of waste rubber tyres with chlorosulphonic acid with ice-cooling

Five gram of waste tyre granules (2.5 mm in average equivalent diameter) were swelled for 15 min in 25 mL of 1,2-dichloroethane, the mixture was cooled to 5 °C with ice and 10 mL of chlorosulphonic acid was added dropwise in an hour. The maximal temperature was observed due to reaction heat at half of the acid adding (~14 °C). The mixture was stirred for 10 min at 5 °C, and the mixture was poured into ice cubes. No further reaction (evolution of HCl gas) was observed with the residual chlorosulphonic acid.

The solvent was removed by distillation, the residue was washed five times of 400 mL of distilled water. The product was inelastic.

Swelling experiment with α -methylstyrene

Common waste rubber tyre granulate (2.5 mm in diameter in average, 7.14 gram) was mixed with 11.95 g of α -methylstyrene as swelling and copolymerizing agent, and the mixture was polymerized with 0.5 % dibenzoyl peroxide. The polymer product was a sticky material which could not be isolated from the reactor.

Results and Discussions

Extractive fermentation with using non-toxic extractants like aliphatic hydrocarbons results only low distribution coefficients. For example, this value is 0.21, 0.056 and 0.16 for n-BuOH, ethanol and acetone (ABE fermentation products) with 0.031 water equilibrium ratio.⁷ In order to remove these solvents, especially the most toxic n-butanol, a solid absorbent is needed, which is in contact with the non-toxic extractant^{5,8} before recycling that into the extractive fermentation.

There are known some polar solid absorbents which can absorb butanol and the secondary solvents of butanol production as well,^{5,8} together with the small amount of water which exists in the n-heptane in contact with the aqueous ferment liquor. The two most promising ones among them are the sulphonated⁵ and nitrated⁸ styrene-divinylbenzene copolymers. The sulphonated styrene-divinylbenzene copolymers are commercialized as microporous sulphonated cation exchangers.⁶

The main problem is with using these polymers are, that during absorption of the n-BuOH and other solvents a strong swelling and volume increasing can be observed, and during removal of the solvents from the solid sorbents (regeneration and solvent collection with thermal treatment), a strong volume contraction takes place. Alternate volume changes during the repeated use and regeneration cause formation of cracks and mechanical powdering of the solid absorbent granules.

This is a strong disadvantage due to material loss and technological problems caused by the powder formation. Since the sulphonated polymers are more polar and bound less with aliphatic hydrocarbon solvents than the nitrated ones, our efforts were focused on preparation an elastic type sulphonated type polymer material.

From economic point of view, the best choice as elastic polymer materials for sulphonation experiments was different kinds of waste rubber tyres. Two series of waste rubber tyre materials, namely a soft rubber with high styrene content and a hard rubber (average mixture of waste car rubber tyre processing) were used.

Table 1. Solvent absorbing capacity of the raw waste tyres granulates and the sulphonated soft rubber tyres*

Solvent	Raw soft waste tyre		Dry sulphonated soft tyre		69.5 % water contg. sulphonated rubber
	Absorbed amount, g/100 g	Swelling in vol. %	Absorbed amount, g/100 g	Swelling, vol. %	Absorbed amount, g/100 g
n-Butanol	7	7	63	87	27
n-BuOH-H ₂ O=82:12, v/v	-	-	12	-	-
Ethanol	5	5	73	102	-
Ethanol:water, 1:1, v/v	-	-	37	-	-
Methanol	10	10	75	105	-
Methanol:water, 1:1 (v/v)	-	-	39	-	-
1,2-Dichloroethane	292	200	92	87	39
n-Heptane	24	28	37	60	6
Water	0	-	87	97	-

*Prepared from a soft rubber (removed from a cross-motor) tyre

Since the sulphonation of polystyrene-butadiene rubbers with chlorosulphonic acid was not thermodynamically favourable (ΔH^0 , ΔS^0 , and ΔG^0 were found to be 40.708 kJ, 64.22 J K⁻¹, and 22.916 kJ, respectively),⁹ the sulphonation of styrene-based rubbers was tested only with sulphuric acid, while the common waste tyre rubber mixtures were tested with both cc. sulphuric acid and chlorosulphonic acid.

Preparation and properties of the high-styrene content sulphonated (soft) waste tyres

Sulphonation of soft waste tyres containing high amount of styrene (2.5 mm equivalent diameter) and swelled in 1,2-dichloroethane with concentrated sulphuric acid at 90 °C led to black coloured granulates having the expected elastic properties. The prepared air-dried sample contained 69.5 % water which was transformed to dry at 105 °C in an oven. The bulk density of the water-containing and the dry samples was 1.1762 g mL⁻¹ and 0.4761 g mL⁻¹, respectively. This shows highly porous structure of the formed resins. The ion-exchange capacity is the same as the salt-splitting capacity, so the all active groups proved to be strongly acidic sulphonic groups in the resin.

The solvent absorbing capacities and the volume changes during swelling in the given solvent are presented in Table 1. The pure butanol absorbing capacity of the dry resin was found to be 63 % with 87 % of volume changes. The resin without drying can absorb 27 % butanol. Taking into consideration the water content of the wet resin, the absorbing capacity of the dry material content in the wet resin is close to the result get in case of the oven-dried sample.

Comparing the absorption of other polar solvents such as ethanol, methanol, 1,2-dichloroethane and water with the dry resin, the absorbing capacities correlate with the polarity of the solvents. The more polar solvent the more solvent can be absorbed, which unambiguously support the assumption that the active sites of sorption are located in the environment of the polar sulphonic groups. The apolar n-heptane was absorbed only in 37 % and 6 % amount in case of dry and wet resin, respectively. The swelling of dry resin was found to be 39 %. It shows that only the pores play role in absorption of heptane.

The distribution coefficient of the water between the ferment liquor and the extractant selected is a key parameter in the design of biobutanol production technology, because

the presence of water decreases the absorption of polar solvents in a large extent. The butanol absorbing capacity decreases to 12 % in the case of 88 % BuOH-12 % H₂O mixture (v/v), while in case of 1:1 (v/v) mixtures of ethanol or methanol the absorbing capacity roughly decreases to the half of their original values.

The elastic sulphonated rubbers are promising candidates for recovery of the solvent mixtures from n-heptane before recycling that in the extractive ABE (acetone-butanol-ethanol) or IBE (isopropanol-butanol-ethanol) fermentation processes due to two reasons. First, the distribution coefficient values of n-butanol and other polar solvents between n-heptane and water. Secondly, the low solubility of water in n-heptane, butanol and other polar or less polar solvent containing n-heptane mixtures at low polar solvent concentration.

Preparation and properties of the sulphonated common (hard) waste tyres

The sulphonation of a rubber mixture (2.5 mm in average diameter) prepared from common waste tyres were studied in detail both with cc. sulphuric acid and chlorosulphonic acid in a wide range of reaction conditions. In the case of chlorosulphonic acid the efforts failed, because tar-like or powdered material formed in every case, even if the reaction was proceeded with strong cooling. If the reaction proceeded with gentle heating, malodorous gas (H₂S or mercaptans) were formed which strongly suggests that the disulphide bridges decomposes under the action of chlorosulphonic acid which can explain the formation of tar-like products.

Using concentrated sulphuric acid, the ion-exchange/salt-splitting capacities are the same, but these values are lower than in case of styrene-containing soft rubbers. The more drastic conditions (excess of acid, higher temperature) were used, the less sulphonic acid groups were built into the structure, and there were no elastic products formed in any of the cases. The ion-exchange capacity values decreased from 0.31 mequiv mL⁻¹ to 0.09 mequiv. mL⁻¹, which suggest that the sulphuric acid decomposes the sites where the sulphonyl groups could be attached. Similarly, loss of the elastic properties of the starting rubbers shows that the disulphide bridges are also decomposed during the sulphonation process. Since the chemical environment of disulphide bridges in case of styrene containing starting polymer chain might be

different, the favoured reaction was the sulphonation of aromatic ring and not the decomposition of disulphide bridges in the case of soft rubber tyres.

In order to introduce aromatic ring content into the waste common rubber tyres, to mimic the styrene-based rubbers, the swelling of common rubbers was done with α -methylstyrene before sulphonation. We expected that the aromatic ring containing product will be more advantageous for preparation of products with sulphonated group, keeping the elasticity of the starting rubber. The polymerization was started with 0.5 % dibenzoyl peroxide, however, the polymers formed cannot be removed from the reactor, a tar-like sticky material was only formed, so the sulphonation tests could not be performed.

Further studies on usage of the sulphonated elastic soft-rubber tyre based resins as biobutanol supersorbents in ABE and IBE extractive fermentation in the presence of aliphatic hydrocarbons as extractants are in progress.

Conclusions

The styrene-containing waste rubber tyres are valuable raw materials to prepare sulphonated elastic superabsorbent butanol sponges. The sulphonation of rubber tyres was performed with concentrated sulphuric acid, chlorosulphonic acid led to useless tar-like products at various reaction conditions. The common waste tyres resulted products with lower biobutanol absorbing ability and non-elastic properties led to limited applicability in extractive biobutanol fermentations.

References

- ¹Liu, H., Wang, G., Zhang, Y., "The promising fuel -Biobutanol", in: *Liquid, Gaseous and solid biofuels*, Ed. Z. Fang, INTEC, **2013**, Chapter 6, p. 175-198., Rijeka, Croatia.
- ²Kótai, L., Szépvölgyi, J., Szilágyi, M., Zhibin, L., Baiquan, C., Sharma, V., Sharma, P. K., "Biobutanol from renewable agricultural and lignocellulose resources and its perspectives as alternative of liquid fuels", in: *Liquid, Gaseous and solid biofuels*, Ed. Z. Fang, INTEC, **2013**, Chapter 6, p. 199-262., Rijeka, Croatia.
- ³Kótai, L., Sharma, P. K., *Int. J. Chem. (Mumbai)*, **2012**,1(4), 480-485
- ⁴Kótai, L., Gács, I., *Eur. Chem. Bull.*, **2012**, 1, 1-3.
- ⁵Kótai, L., Szépvölgyi, J., Bozi, J., Gács, I., Bálint, Sz., Gömöry, Á., Angyal, A., Balogh, J., Li, Z., Chen, M., Wang, C., Chen, B., *An integrated waste free biomass utilization system for an increased productivity of biofuel and bioenergy*, in: *Biodiesel: Feedstock and processing technologies*, ed. Stoytcheva, M., Montero, G., INTECH, **2011**, 201-228, Rijeka, Croatia.
- ⁶Inczédy, J., *Ioncserélők és analitikai alkalmazásai*, Budapest, **1978**.
- ⁷Dadgar, A. M., Foutch, G.L., *Biotechnol. Bioeng. Symp.*, **1985**, 15, 611-620.
- ⁸Larsson, M., Mattiasson, B. *Chem. Industry (London, United Kingdom)*, **1984**(12), 428-31.
- ⁹Idibie, C. A., Abdulkareem, A. S., Pienaar, H. C. Z., Iyuke, S. E., Van Dyk, L., *J. Appl. Polym. Sci.*, **2010**, 117, 1766-1771.

Received: 13.10.2016

Accepted: 20.10.2016.



SELECTIVE SENSORS FOR POTENTIOMETRIC ASSESSMENT OF IODIDE BASED ON ANION RECOGNITION THROUGH COPPER (II) [DIPEPTIDE DERIVATIVE] COMPLEX

Ayman H. Kamel^{[a]*}, Magdi E. Khalifa^[b], S. A. Abd El-Maksoud^[c] and Fadl A. Elgendy^[c]

Keywords: iodide; copper (II) [dipeptide derivative] complex; anion recognition; PVC membrane sensors; potentiometry.

New selective sensors based on potentiometric transduction for iodide assessment are described. The sensors based on the use of a newly synthesized copper (II) [N,N-bis-(1-carboxy-2-(p-hydroxybenzyl))-2,6-di(aminocarbonyl)pyridine] complex (CuL) as neutral ionophore in plasticized poly(vinyl chloride) (PVC) membranes. The influence of lipophilic cationic and anionic additives on the response properties of the sensors was evaluated. The fabricated sensors exhibited enhanced response towards iodide ions over the concentration range 6.3×10^{-6} to 1.0×10^{-2} mol L⁻¹ with a detection limit of $0.33 \mu\text{g mL}^{-1}$ and a slope of -63.6 ± 0.2 mV per decade. These sensors showed a fast and stable response, good reproducibility, and long-term stability. The sensors showed a stable potential over a wide pH range (4.5–9) and exhibited high selectivity for I⁻ ion in the presence of many common anions. The sensors were applied for direct potentiometric measurements of iodide ions over the concentration range 0.8–1270 $\mu\text{g mL}^{-1}$ and also for the titration of some metal ions (e.g. Ag⁺, Hg²⁺) and MnO₄⁻ through sequential monitoring. The sequential binding of these ions with I⁻ ensured share stepwise titration curves with consecutive end point breaks at the equivalent points.

* Corresponding Authors

Tel.: +201000361328

E-Mail: ahkamel76@sci.asu.edu.eg

[a] Chemistry Department, Faculty of Science, Ain Shams University, Abbasia, Cairo, Egypt.

[b] Chemistry Department, Faculty of Science, Mansoura University, Mansoura, Egypt.

[c] Chemistry Department, Faculty of Science, Port Said University, Port Said, Egypt.

suffer from the need for expensive instrumentation, well controlled experimental conditions, frequent maintenance and sample pretreatment. Therefore, development of analytical techniques for iodide assessment that do not require expensive or complicated equipment has become increasingly important.

On the other hand, potentiometric sensors offer an inexpensive and convenient method for fast analysis with high sensitivity and selectivity.¹⁴⁻¹⁷ They can be considered as one of the promising tools used for direct determination of various species in the biological and industrial analysis.¹⁸⁻²²

Ion selective electrodes (ISEs) for anions, based on ion exchangers such as lipophilic quaternary ammonium or phosphonium salts, displayed classical Hofmeister selectivity behavior in which membrane selectivity is controlled by the free energy of hydration of ions involved.²³ The anti-Hofmeister anion selectivity is obtained in the case of membrane electrodes incorporated with an organometallic complex,²⁴ metalloporphyrins,²⁵ metal phthalocyanines²⁶ and Schiff base metallic complexes.²⁷ This deviation arises from the steric effects coming from the structure of the ionophore and from the binding affinity of the central atom in the ionophore with the anion. Therefore, the focus of this research is on the anion-sensitive materials with anti-Hofmeister behavior.

Several iodide sensors based on a variety of ion carriers have also been reported in the literature.²⁸⁻⁵⁰ Some of these sensors showed narrow linear range^{28,30,31,41,43,44,49,50} narrow pH range,^{31-33,36,43} high detection limit,^{31,49,50} long response time.^{28,49} Others showed a serious interference from some anions such as SCN⁻,^{30,33,34,36,41-43,46,49,50} NO₂⁻,^{39,43,48} Br⁻,^{36,49} CN⁻,^{42,46} and Sal⁻.^{29,30,49,50}

In this study, we have synthesized copper(II) [N,N-bis-(1-carboxy-2-(p-hydroxybenzyl))-2,6-di(aminocarbonyl)pyri-

Introduction

Anions play an important role in biology, medicine, and environmental chemistry, so there is a constantly increasing need for their online monitoring. Among them, iodide is of particular interest because of its presence in food, drug compounds and in drinking water. Moreover, it is often added to table salt for preventing iodine deficiency disorders.¹ It is also used as a catalyst and stabilizer in the production of polymers and as a disinfectant. Iodine is an essential micronutrient that are required for the biosynthesis of the thyroid hormones thyroxine and triiodothyronine by the thyroid gland. Iodine deficiency is widely known as a global problem because 30% of the world's population lives in an environment where the soil has low iodine content. Also, its deficiency in human causes hypothyroidism and formation of goiter in adults or cretinism in children.² An excess of iodine or iodide ingestion can produce goiter and hypothyroidism as well as hyperthyroidism.^{3,4} Therefore, determination of iodide and other iodine species is an important analytical task in a variety of fields such as food, clinical, biological and environmental samples. Numerous analytical methods have been reported in the literature for iodide determination at trace levels. These include gas chromatography (GC-MS),⁵ neutron activation analysis,⁶ polarography,⁷ spectrophotometry,⁸ chemiluminescence,⁹ pulse stripping analysis,¹⁰ inductively coupled plasma-atomic emission spectrometry¹¹ and capillary electrophoresis.^{12,13} These approaches, although sensitive,

dine] complex (CuL) as a new ionophore in the fabrication of polymeric membrane sensors for iodide ion assessment. The performance characteristics of the sensors were evaluated and satisfactorily used for accurate determination of μg quantities of iodide. Sequential monitoring of Ag^+ , Hg^{2+} , Bi^{3+} and MnO_4^- in single or binary mixtures via the titration with iodide was also performed. The sequential binding of these ions with I^- shared stepwise titration curves with consecutive breaks at the equivalent points.

Experimental

Reagents and solutions

All chemicals were of analytical-reagent grade. Twice-distilled water was used to prepare all solution and in all experiments. Dioctyl phthalate (DOP), *p*-chlorotetrakis-tetraphenyl borate (*p*CITPB) and high molecular weight polyvinylchloride (PVC) were obtained from Sigma-Aldrich (Steinheim, Germany). Tridodecylmethylammonium chloride (TDMAC) and THF were purchased from Fluka (S.A.G. Buchs, Switzerland). All anions used were in their sodium salts and purchased from Merck [Dermsdat, Germany]. The ligand [N,N-bis-(1-carboxy-2-(*p*-hydroxybenzyl))-2,6-di(aminocarbonyl)pyridine] (Figure 1) was synthesized as described before.⁵¹ Standard iodide solution, 0.1 mol L^{-1} , was prepared by dissolving accurately weighed NaI in 100 mL twice-distilled water. Iodide solutions used for the sensor characterization (1×10^{-6} – $1 \times 10^{-2} \text{ mol L}^{-1}$) were prepared daily from the stock solution. The ionic strength (IS) was adjusted to 0.01 mol L^{-1} by means of a $3.5 \times 10^{-3} \text{ mol L}^{-1} \text{ Na}_2\text{SO}_4$ solution. The pH adjustment was carried out with 0.01 mol L^{-1} phosphate buffer solutions of pH 6 in addition to 0.01 mol L^{-1} IS.

Equipment

All potentiometric measurements were made at $25 \pm 0.1 \text{ }^\circ\text{C}$ with a Cole-Parmer pH/mV meter (USA model 59003-05) and iodide-PVC membrane sensors in conjunction with a Sentek, Ag/AgCl double junction reference electrode (UK model R2/2MM) filled with $1.0 \text{ mol L}^{-1} \text{ KNO}_3$ in the outer compartment. A combination glass pH electrode (Schott blue line 25, Germany) was used for all pH measurements. The IR spectra were measured on Prestige-21 FT-IR instrument (SHIMADZU, Japan). The thermal studies were carried out using DTG 60 AH (SHIMADZU, Japan) under the following conditions: temperature ranges 25–1000 $^\circ\text{C}$, heating rate $25 \text{ }^\circ\text{C min}^{-1}$ and sample weight 6.0 mg. Elemental analyzes were carried out on Elementar Vario EL cube, Germany. Cu-content was determined by Perkin Elmer Atomic Absorption Spectrometer (Model 3100 USA). The molar conductivity of the complex was measured by using OAKTON (Model CON510 USA) conductivity meter.

Syntheses of the complexes

A 20 mL of a methanolic solution containing 2.77 g (10 mmol) of $\text{Cu}(\text{NO}_3)_2 \cdot 5\text{H}_2\text{O}$ was added to a hot 20 mL methanolic solution containing 10 mmol of the ligand. After stirring for 1 h, the formed green precipitate complex was filtered, collected and then washed for several times with

hot methanol until the filtrate became colorless. The complex was dried in a desiccator over anhydrous CaCl_2 under vacuum. The dried ligands and complex were subjected to IR, elemental and thermal gravimetric analysis. The complex is air-stable, nonhygroscopic, insoluble in H_2O , slightly soluble in ethanol. The elemental analysis of the free ligand [L] ($\text{C}_{25}\text{H}_{23}\text{N}_3\text{O}_8$) was found: C, 60.84; H, 4.69; N, 8.51. Characteristics of the complex were as follows: $[\text{CuL} \cdot \text{H}_2\text{O}]$ ($\text{C}_{25}\text{H}_{25}\text{N}_3\text{O}_9\text{Cu}$): Yield 85%. Color: green. M.P. $>300 \text{ }^\circ\text{C}$. $\Lambda_m(\Omega^{-1} \text{ cm}^{-1} \text{ mol}^{-1})$ 4.2. Elemental analysis: Found (%): C 52.358; H 4.014; N 7.3302; Cu 11.082. Calcd: C 52.21; H 4.35; N 7.31; Cu 11.05.

Sensors preparation and EMF measurement

The procedure to prepare the PVC membrane was based on mixing 190 mg of powdered PVC, 10 mg of the ionophore, 2 mg of cationic additive TMDAC and 350 mg of plasticizer DOP. The mixture was dissolved in 3 mL of dry THF. The membrane solutions were cast into conductive supports of tubular shapes and left overnight for drying. The sensors were then conditioned before use by soaking in 0.01 mol L^{-1} NaI solution (for at least 24 h) and stored in the same solution when not in use. Calibration was made by immersing the membrane sensor in conjunction with a double junction Ag/AgCl reference electrode in 25 mL beakers containing 10 mL aliquots of standard 1.0×10^{-6} – $1.0 \times 10^{-2} \text{ mol L}^{-1}$ NaI solution. The pH of the solutions was adjusted to 6 using 0.01 mol L^{-1} phosphate buffer. Potential readings were carried out for iodide until stabilization occurred. The calibration plot was constructed by plotting the measured potential as a function of the logarithm of iodide concentrations. This calibration plot was used for subsequent measurements of unknown iodide samples.

Direct potentiometric determination of iodide

Iodide / iodine in pharmaceutical samples was analyzed using $[\text{CuL} + \text{TDMAC}]$ membrane sensor. Vaginal douche and mouthwash (1–10 % w/v), collected from the local market, were diluted with de-ionized water. For total iodide + iodine measurement, the iodide sensor and a Sentek Ag/AgCl double junction reference electrode were immersed in a 25 mL beaker containing 10 mL of $1.0 \times 10^{-2} \text{ mol L}^{-1}$ phosphate buffer of pH 6 and ascorbic acid 0.1 mol L^{-1} for reduction of iodine into iodide. Aliquots (200 μL) of the diluted samples were successively added and the potential response of each sample was measured after potential stabilization. Other aliquots (200 μL) of the diluted samples were successively added to a 25 mL beaker containing 10 mL of a 0.1 mol L^{-1} resorcinol of pH 8.0. The potential response is equivalent to $\frac{1}{2} \text{ I}_2$ and I^- .

The calibration plot was constructed by plotting the potential change against the logarithm of the I^- concentration. The plot was then used for subsequent determination of unknown I^- samples.

Potentiometric titration of metal ions

A series of potentiometric precipitation titrations was performed in which the sensor was used as an indicator electrode to locate the equivalence point. Sample solutions

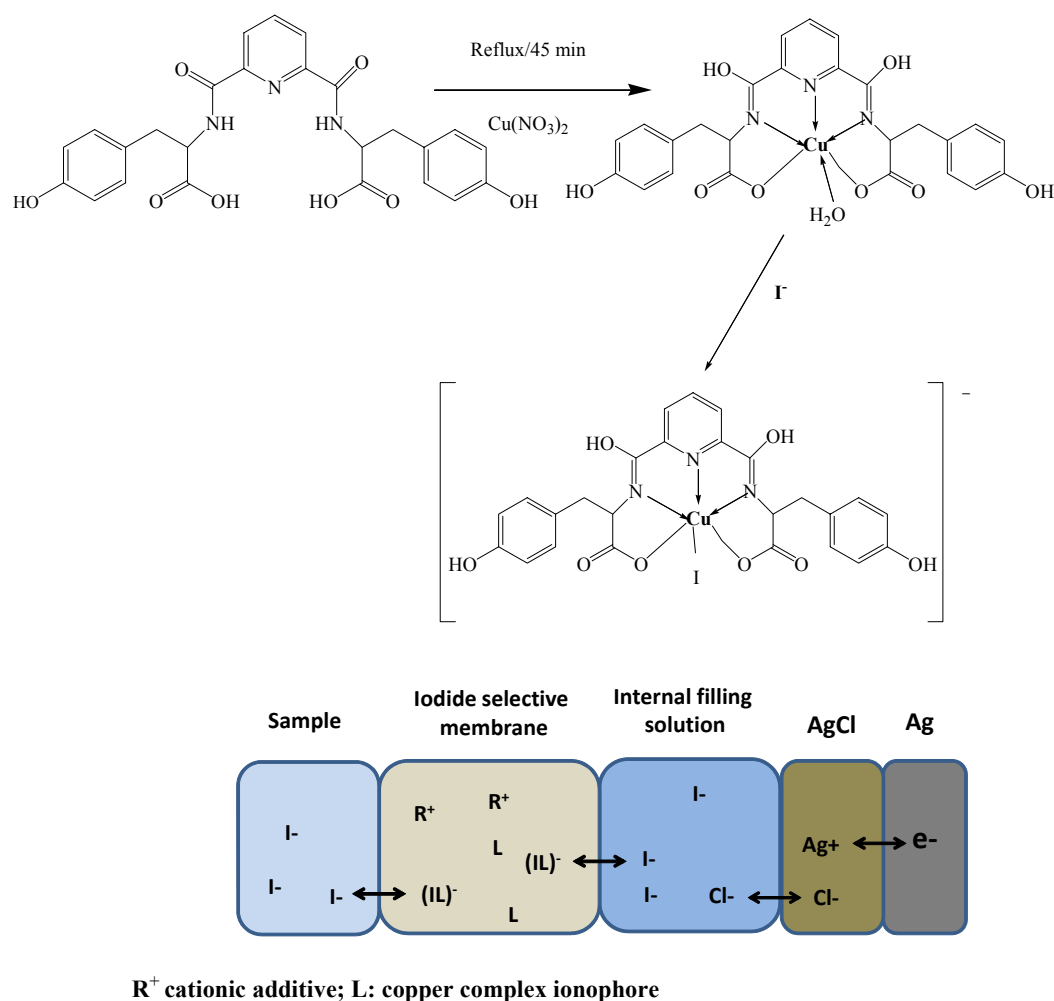


Figure 1. Chemical structure of the ionophore and an illustrative scheme describing the measuring instrument.

containing a single ion (e.g. Ag^+ , Hg^{2+} , MnO_4^-) were then titrated with $0.01 \text{ mol L}^{-1} \text{I}^-$. The equivalence points at each inflection break were determined and the concentration of each ion was assessed ($1 \text{ mol I}^- = 0.5 \text{ mol Hg}^{2+} = 1 \text{ mol Ag}^+ = 0.33 \text{ mol MnO}_4^-$).

Results and discussion

All applied ionophore in the ISE field must be able to bind the target ion via a selective (pattern) reversible reaction in order to generate a stable response in a short time.⁵² The potentiometric sensor containing the CuL ionophore significantly responded to iodide ion according to Nernstian response over other common anions. Therefore, the detailed characteristic performance of the membrane sensor based on the application of this carrier has been evaluated. In a preliminary experiment, membranes with/without the ionophore were constructed. Blank membranes showed poor selectivity toward iodide and their response was not reliable. However, the addition of the proposed ionophore to the membrane leads to the generation of a Nernstian response and remarkable response to iodide ions over several common anions. The preferential response toward iodide anion is believed to be associated with its selective coordination as a carrier to the copper center in the complex.

Structural properties

Pyridine carboxamides can be considered as a burgeoning class of multidentate ligands containing carboxamide [-CONH-] linkage. It can be prepared from condensation reactions between pyridyl-bearing amine or carboxylic acid precursors, promoted by coupling agents such as 1,1'-carbonyldiimidazole, diphenoxy phosphoryl azide or triphenyl phosphite.⁵³⁻⁵⁵ The behavior of pyridine carboxamides towards biologically relevant d-block metals has been widely investigated. These ligands support a range of coordination numbers, geometries, and nuclearities for copper (II).⁵⁶⁻⁶⁰

Elemental analysis and magnetic susceptibility data of the ligand and complex indicated the formation of 1:1 [Cu:L]. The molar conductance values of the synthesized complex determined using $1 \times 10^{-3} \text{ mol L}^{-1}$ DMF solution were in the range of $4.5\text{--}6.8 \Omega^{-1} \text{cm}^2 \text{mol}^{-1}$. These results suggested the presence of a non-electrolytic nature in the same solvent.⁶¹ These values also indicated that there were no anions in the outer coordination sphere.

The IR spectrum of the complex, in comparison with that of the free ligand, displayed significant changes that could be indicative of the type of coordination (Figure 2). The FTIR spectrum of free ligand showed characteristic bands at

3600 – 2617 (broadband, OH, and NH), 1728.2 (C=O, acid), 1662.6, 1516, 1230.5 (amide I, II and III) cm^{-1} . In the IR spectra of metal complexes, characteristic bands at 3600 – 2750 (broadband, OH phenolic, and OH iminol), 1627 (C=N, iminol), and 1384.8 (C=N, bending). The peaks at 1732, 1657, 1533 and 1225 were completely disappeared. In addition to these bands, the complex also showed weak bands at 837.1, 759.9 and 660-640 Cm^{-1} due to coordinated water. On the basis of the physical and spectral data of the free ligand and the complex discussed above, one can assume that the two imide groups coordinate to copper ion forming iminol groups in addition to (nitrogen) from pyridine and the two carboxylic groups present in the free ligand as illustrated in Figure 1.

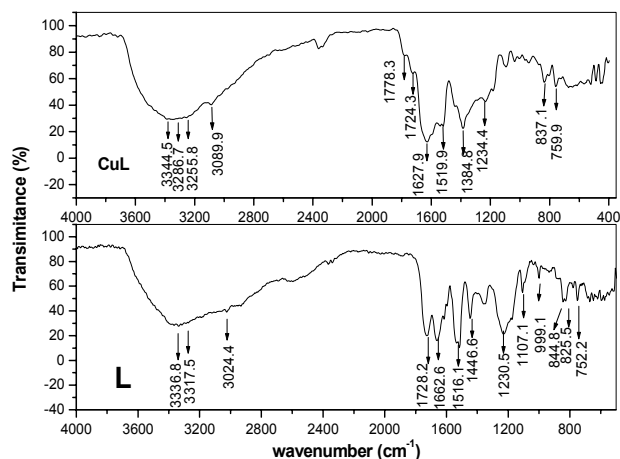


Figure 2. FTIR spectrum for the free ligand and its copper complex.

The thermal gravimetric analysis of the complex was shown in figure 3. The dehydration step in the complex occurred in the 60-120 °C range. The weight losses correspond to the loss of one water molecule and the complex decomposed in three steps via the formation of unstable intermediates. The decomposition started at 173-445 °C and ended at 450-1000 °C (oxides formation). The metal percentages of the complex were calculated from the residual metal oxide % formed in the final step and were in good agreement with data obtained by the elemental analysis. On the basis of the above observations, the following general scheme for thermal decomposition may be proposed for the metal complex.

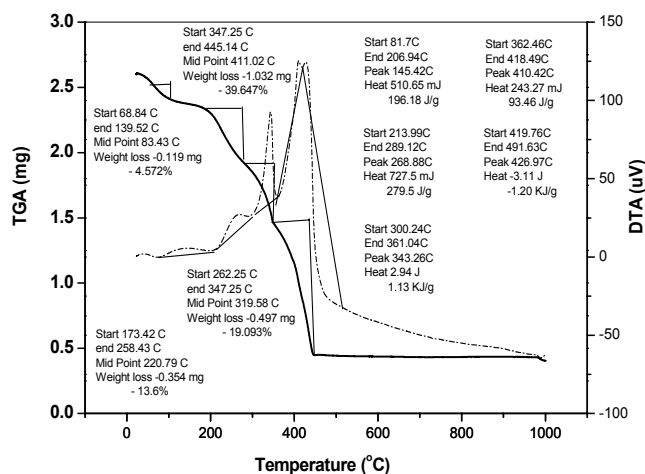


Figure 3. TG and DTG-plots of the Cu (1:1) complex.

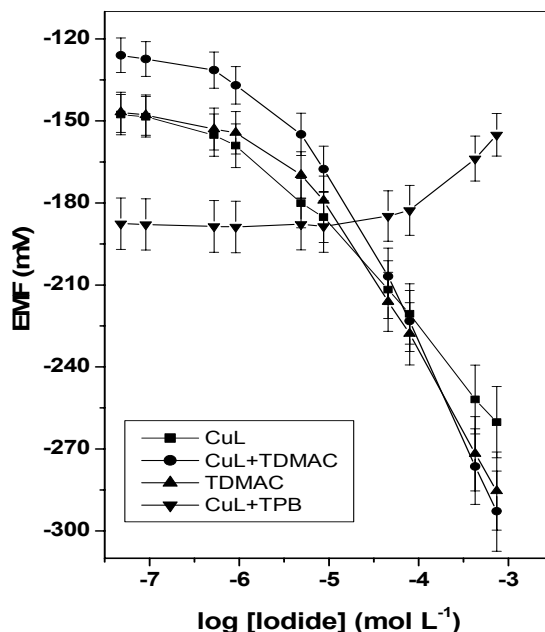
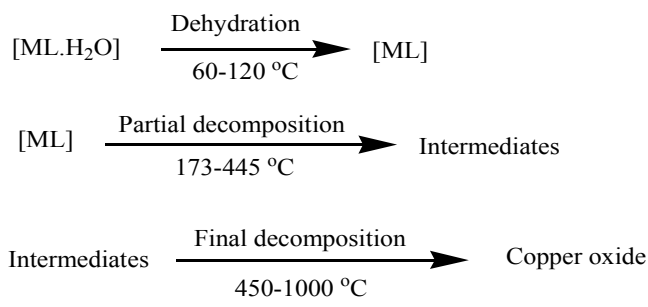


Figure 4. Potentiometric plot of iodide membrane sensors in 0.01 mol L^{-1} phosphate buffer (pH 6.0).

Response characteristics of iodide sensors

The potentiometric response characteristics of the sensors assembled with the different membranes were shown in Figure 4. The sensor based on [copper complex] showed a linear response towards iodide over the concentration range of 4.1×10^{-6} – 1.0×10^{-3} mol L^{-1} in a 0.01 mol L^{-1} phosphate buffer solution of pH 6 with a slope of -35.5 ± 2.3 mV decade^{-1} and a detection limit of $0.13 \mu\text{g mL}^{-1}$. On the other hand, the addition of 5 mg of TDMAC relative to the ionophore to the membranes showed an enhancement of the potentiometric response characteristics. These membrane electrodes exhibited a slope of -63.6 ± 0.2 mV decade^{-1} over the concentration range of 6.3×10^{-6} – 1.0×10^{-3} mol L^{-1} and detection limit of $0.32 \mu\text{g mL}^{-1}$. However, the sensor based on cationic additive alone showed a linear response towards iodide over the concentration range of 6.1×10^{-6} – 1.0×10^{-3} mol L^{-1} with a slope of -53.6 ± 0.3 mV decade^{-1} and detection limit $8.9 \mu\text{g mL}^{-1}$ (Table 1). This is in accordance with the results reported previously that the cationic sites in neutral carrier-based electrodes can stabilize the formation of the negatively charged product (iodide copper complex) in the membrane phase as well as lowering the electrical membrane resistance and improving the potentiometric response characteristics of the membrane electrodes.⁶²⁻⁶⁴

Table 1. Response characteristics of [CuL] membrane based sensors at pH 6.

Parameter	CuL	CuL+TDMAC	TDMAC
Slope, mV decade ⁻¹	-35.5±2.3	-63.6±0.2	-53.6±0.3
coefficient, r	-0.996	-0.997	0.999
Detection limit, µg mL ⁻¹	1.0 × 10 ⁻⁶	2.5 × 10 ⁻⁶	6.1 × 10 ⁻⁶
Linear range, mol L ⁻¹	4.1 × 10 ⁻⁶ - 1.0 × 10 ⁻³	6.3 × 10 ⁻⁶ - 1.0 × 10 ⁻³	7.0 × 10 ⁻⁵ - 1.0 × 10 ⁻²
Response time, s	10 - 20	10 - 20	10 - 20
Working pH range	4.5 - 9	4.5 - 9	4 - 10
SD (%)	1.3	1.5	1.5
Accuracy (%)	99.3	98.8	98.7
Precision, C _v w(%)	0.9	0.7	1.1
Between-day variability, C _v b(%)	1.1	0.9	0.9

The robustness of the method was also evaluated via testing the effect of pH and the measuring time on the potentiometric response. The influence of the pH was tested using 10⁻⁴ and 10⁻³ mol L⁻¹ iodide solutions over the pH range 2–10. Adjustment of pH values was carried out using NaOH and/or HCl. From pH-potential profiles, it was apparent that there is no change in potential response within the pH range 4.5–9 for all sensors. At high pH values (> 9), the sensor response increased, probably due to the ability of hydroxide ions to be coordinated on the axial coordination site of the central metal. At pH < 3, the response towards iodide decreased probably due to the oxidation of iodide into iodine by molecular oxygen which was stabilized in acidic medium.

The response time of the electrodes was obtained by measuring the time required to achieve a steady state potential (within ± 1mV) after successive immersion of the electrodes in a series of iodide ions solutions, each having a 10-fold increase in concentration from 1.0 × 10⁻⁶ to 1.0 × 10⁻³ mol L⁻¹. The actual potential versus time trace showed, all concentrations ranges, that the sensors reach the equilibrium response in a very short time (<10 s). These results indicate that all sensors were amenable to be used with the automated system.

Selectivity

Potentiometric selectivity coefficients ($K^{pot}_{I,B}$) were evaluated according to IUPAC guidelines using the separate solutions method^{65,66} in which the potential of a cell comprising the membrane electrode and a reference electrode is measured with two separate solutions, one containing the iodide ion *A* at the activity a_A (but no *B*), the other containing the interfering ion *B* at the same activity $a_A = a_B$ (but no *A*) and E_A and E_B are the measured values, respectively. Different interfering anions at a concentration of 1 × 10⁻³ mol L⁻¹ at pH 6 were utilized and the results were obtained using the equation:

$$\log K^{pot}_{A,B} = (E_B - E_A)/S + (1 - Z_A/Z_B) \log a_A \quad (1)$$

where

$K^{pot}_{A,B}$ is the potentiometric selectivity coefficient, *S* the slope of the calibration plot, a_A the activity of iodide and Z_A and Z_B are the charges on I⁻ and the interfering anion, respectively.

The selectivity coefficient values were shown in Table 2. The selectivity coefficients of [CuL] membrane sensor without membrane additive were in the order: I⁻ > SCN⁻ > ClO₄⁻ > IO₄⁻ > IO₃⁻ > Asco⁻ > Cl⁻ > Br⁻ > NO₂⁻ > NO₃⁻ > F⁻ > SO₄²⁻ > CH₃COO⁻ > PO₄³⁻. For [CuL] based membrane sensor doped with TDMAC as a cationic additive, the selectivity behavior of the sensor was in the order: I⁻ > ClO₄⁻ > IO₄⁻ ~ SCN⁻ > NO₃⁻ > Br⁻ > IO₃⁻ > NO₂⁻ ~ Cl⁻ > Asco⁻ > SO₄²⁻ > F⁻ > PO₄³⁻ > CH₃COO⁻ which is almost identical with the Hofmeister pattern. Membrane sensors incorporating [CuL] without additives exhibited enhanced selectivity towards iodide ions but the selectivity pattern was anti-Hofmeister. This selectivity order clarified that the response mechanism is a neutral carrier mechanism that showed a non-Hofmeister selectivity pattern. This explanation is based on the strong coordination affinity between the metal center in the ionophore and the iodide ion.

Table 2. Selectivity coefficients ($K^{pot}_{I,i}$) of iodide PVC membrane sensors.

Ion	[CuL]	[CuL]+TDMAC	TDMAC
I ⁻	0	0	0
IO ₄ ⁻	-2.60	-0.8	+1.1
IO ₃ ⁻	-3.12	-2.21	-2.85
SCN ⁻	-1.80	-0.88	+1.0
Ascorbate	-3.40	-3.27	-3.21
ClO ₄ ⁻	-2.10	-0.75	+1.7
NO ₃ ⁻	-3.81	-1.41	-1.2
NO ₂ ⁻	-3.73	-2.66	-2.3
Cl ⁻	-3.42	-2.70	-2.5
Br ⁻	-3.51	-2.06	-2.1
F ⁻	-4.22	-3.61	-3.5
SO ₄ ²⁻	-4.30	-3.42	-3.3
PO ₄ ³⁻	-4.32	-3.92	-4.1
CH ₃ COO ⁻	-4.31	-4.01	-3.9

Determination of iodide and iodine in pharmaceutical formulations

Vaginal douche and mouthwash and vaginal douche collected from local market containing iodide/iodine in pharmaceutical samples were analyzed using [CuL+TDMAC] membrane sensor. Determination of iodine in the presence of iodide ions required two potentiometric measurements. The first involved measurement of total iodine and iodide (I₂ & I⁻) after treatment with a suitable reducing agent such as 0.1 mol L⁻¹ ascorbic acid. The second measurement is done by measuring the remained iodide ions (1/2 I₂&I⁻) after reaction with resorcinol at pH 8.0 via iodination.⁶⁷ The results obtained for determining iodide and iodine in povidone iodine was in good agreement with data obtained using the titrimetric method recommended by British Pharmacopoeia⁶⁷ (Table 3).

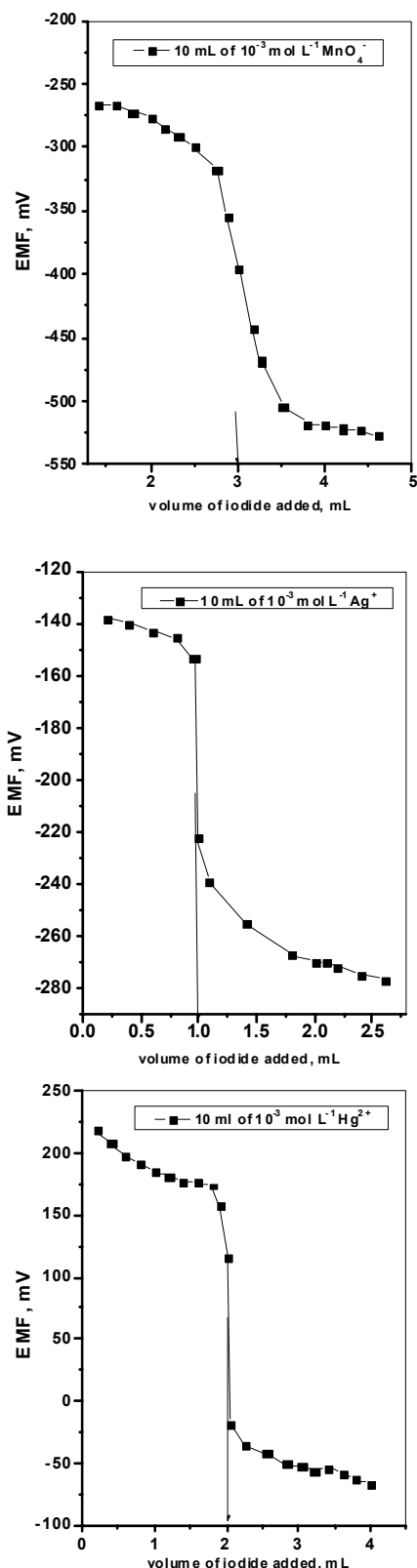


Figure 5. Potentiometric titration plot of Ag^+ , Hg^{2+} and MnO_4^- with $0.01 \text{ mol L}^{-1} \text{I}^-$ using an iodide membrane sensor.

Table 3. Potentiometric determination of povidone iodine using [CuL+TDMAC] PVC membrane based sensor.

Sample*	This work	BP ⁶⁶	Recovery, %
Betadine mouth wash	1.87 ± 0.5 $\text{mg I}_2 \text{ mL}^{-1}$	1.91 ± 0.7 $\text{mg I}_2 \text{ mL}^{-1}$	97.9
Betadine vaginal douch	10.23 ± 0.6 $\text{mg I}_2 \text{ mL}^{-1}$	10.12 ± 0.2 $\text{mg I}_2 \text{ mL}^{-1}$	101.1

*Obtained from the Nile pharm. chem., Egypt

Potentiometric titration of metal ions

The iodide membrane sensor based on ionophore (I) was also used for monitoring some ions (e.g. Ag^+ , Hg^{2+} , and MnO_4^-), single or in binary mixtures, with a standardized iodide solution. The titration curves obtained showed sharp inflection breaks ($\sim 80 \text{ mV}$) at 1:1 for I/Ag^+ and (~ 200 & 180 mV) at 1:2 and 1:3 reactions for I/Hg^{2+} and I/MnO_4^- , respectively. Typical potentiometric titration curves were shown in figure 5.

Conclusion

Novel potentiometric iodide sensors based on copper complex of [N,N- bis-(1carboxy-2-(p-hydroxy benzyl))-2,6-(diaminocarbonyl)-pyridine] were constructed and evaluated. The performance characteristics of the sensors showed stable and selective potential responses towards iodide ions over the concentration range of 6.3×10^{-6} – $1.0 \times 10^{-2} \text{ mol L}^{-1}$ with a limit of detection $2.5 \times 10^{-6} \text{ mol L}^{-1}$ and a slope of $-63.6 \pm 0.3 \text{ mV decade}^{-1}$. The addition of a cationic additive to the membranes showed a slope of $-63.6 \pm 0.2 \text{ mV decade}^{-1}$ over the concentration range of 6.3×10^{-6} – $1.0 \times 10^{-3} \text{ mol L}^{-1}$ and detection limit of 0.32 mol L^{-1} . The iodide PVC-based membrane sensor was satisfactorily used for potentiometric determination of iodide under the static mode of operation in pharmaceutical formulations. Sequential monitoring via potentiometric titration of some ions (e.g. Hg^{2+} , Ag^+ and MnO_4^-) was determined using the iodide sensor to locate the equivalent points. The sequential binding of these ions with I^- ensured share stepwise titration curves with consecutive end point breaks at their equivalent points. It is interesting to note that a comparison of the selectivity and working of the proposed iodide electrode along with those reported before clearly indicate a good enhancement in the behavior of the proposed iodide sensors.

Acknowledgments

The authors are gratefully acknowledging Dr. Abd El-Galil E. Amr (Prof. of Organic Chemistry, National Research Centre, Dokki, Cairo, Egypt) for preparing and supporting the ligand [N,N- bis-(1carboxy-2-(p-hydroxy benzyl))-2,6-(diaminocarbonyl)-pyridine] used in this work.

References

- ¹Lind, P. Kunning, G. Heinich, M. Igerc, I. Mikosch, P. Gallowitsch, H.J. Kresnik, E. Gomez, I. Unterwegen, O. Aigner, H., *Thyroid*, **2002**, *12*, 903-907.
- ²WHO, UNICEF, ICCIDD, WHO Publication, Geneva, **1994**.
- ³Azizi, F. Hedayati, M. Rahmani, M. Sheikholeslam, R. Allahverdian, S. Salarkia, N., *J. Endocrinol. Invest.*, **2005**, *28*, 23-25.
- ⁴Reid, J. R. Wheeler, S. F., *Am. Fam. Phys.*, **2005**, *72*, 623-630.
- ⁵Bichsel, Y. Von-Gunten, U., *Anal. Chem.*, **1999**, *71*, 34-38.
- ⁶Hou, X. Dahlgaard, H. Rietz, B. Jacobsen U., Nielsen, S. P. Aarkrog, A., *Anal. Chem.*, **1999**, *71*, 2745-2750.
- ⁷Turner, J. A. Abel, R. H. Osteryoung, R. A., *Anal. Chem.*, **1975**, *47*, 1343.
- ⁸Schwehr, K. A. Santschi, P. H., *Anal. Chim. Acta*, **2003**, *482*, 59-71.
- ⁹Ratanawimarnwong, N., Amornthammarong, N., Choengchan, N., Chaisuwan, P., Amatatongchai, M., Wilairat, P., McKelvie, I. D., Nacapricha, D., *Talanta*, **2005**, *65*, 756-761.
- ¹⁰Propst, R. C., *Anal. Chem.*, **1977**, *49*, 1199-1205.
- ¹¹Larsen, E. H., Ludwigsen, M. B., *J. Anal. Atom. Spectrom.*, **1997**, *72*, 435-439.
- ¹²Ito, K. Ichihara, T. Zhuo, H. Kumamoto, K. Timerbaev, A. R. Hirokawa, T., *Anal. Chim. Acta*, **2003**, *497*, 67-74.
- ¹³Yokota, K., Fukushi, K., Takeda, S., Wakida, S. I., *J. Chromatogr. A*, **2004**, *1035*, 145-150.
- ¹⁴Kamel, A. H. Soror, T. Y. Al-Romian, F. M., *Anal. Meth.*, **2012**, *4*, 3007-3012.
- ¹⁵Kamel, A. H. Al-Romian, F. M., *Int. J. Chem. Mat. Sci.*, **2013**, *1*, 1-12.
- ¹⁶Abd-Rabboh, H. S. M., Kamel, A. H., *Electroanalysis*, **2012**, *24*, 1409-1415.
- ¹⁷Gupta, V. K. Ganjali, M. R. Norouzi, P. Khani, H. Nayak, A. Agarwal, S., *Crit. Rev. Anal. Chem.*, **2011**, *41*, 282-313.
- ¹⁸Hassan, S. S. M. Badr, I. H. A. Kamel, A. H. Mohamed, M. S., *Electroanalysis*, **2013**, *25*, 1-9.
- ¹⁹Hassan, S. S. M. Kamel, A. H. Abd El-Naby, H., *Eur. Chem. Bull.*, **2013**, *2*, 232-237.
- ²⁰Kamel, A. H., Al Romian, F. M., Amr, A. E., *Eur. Chem. Bull.*, **2013**, *2*, 687-693.
- ²¹Gupta, V. K., Singh, L. P., Singh, R., Upadhyay, N., Kaur, S. P., Sethi, B., *J. Mol. Liq.*, **2012**, *174*, 11-16.
- ²²Hassan, S. S. M. Sayour, H. E. M. Kamel, A. H., *Anal. Chim. Acta*, **2009**, *640*, 75-81.
- ²³Sollner, K., Shean, G. M., *J. Am. Chem. Soc.*, **1964**, *86*, 1901-1902.
- ²⁴Zanjanchi, M. A. Arvand, M. Akbari, M., *Sens. Act. B*, **2006**, *113*, 304-309.
- ²⁵Pietrzak, M., Meyerhoff M. E., Malinowska, E., *Anal. Chim. Acta*, **2007**, *596*, 201-209.
- ²⁶Xu, W. J., Yuan, R., Chai, Y. Q., *Anal. Bioanal. Chem.*, **2008**, *392*, 297-303.
- ²⁷Xu, W. J., Zhang, Y., Chai, Y. Q., Yuan, R., *Desalination*, **2009**, *249*, 139-142.
- ²⁸Benvidi, A. Alizadeh, M. Zare, H. R. Vafazadeh, R., *J. Iran. Chem. Res.*, **2008**, *2*, 103-111.
- ²⁹Farhadi, K. Maleki, R. Yamchi, R. H., *Anal. Sci.*, **2004**, *20*, 805-809.
- ³⁰Jeong, D. C. Lee, H. K. Jeon, S., *Bull. Korean Chem. Soc.*, **2006**, *27*, 1985-1988.
- ³¹Lizondo-Sabater, J. Martynez-Manez, R. Sancenon, F., *Anal. Chim. Acta*, **2002**, *459*, 229-234.
- ³²Song, Y. Q. Yuan, R. Ying, M., *Fres. J. Anal. Chem.*, **1998**, *360*, 47-51.
- ³³Xu, W. J., Chai, Y. Q. Yuan, R., *Anal. Sci.*, **2006**, *22*, 1345-1349.
- ³⁴Pouretedal, H. R. Keshavarz, M. H., *Talanta*, **2004**, *62*, 221-225.
- ³⁵Ying, M. Yuan, R. Song, Y. Q. Li, Z. Q., *Analyst*, **1997**, *122*, 1143-1146.
- ³⁶Daunert, S., Florido, A., Bricker, J., Dunaway, W., Bachas, L. G., Valiente, M., *Electroanalysis*, **1993**, *5*, 839-843.
- ³⁷El Aamrani, F. Z., Sastre, A., Aguliar, M., Beyer, L., Florido, A., *Anal. Chim. Acta*, **1996**, *329*, 247-252.
- ³⁸Yuan, R., Chai, Y. Q., Liu, D., Gao, D., Li, J. Z., Yu, R. Q., *Anal. Chem.*, **1993**, *65*, 2572-2575.
- ³⁹Li, Z. Q., Yuan, R., Ying, M., Song, Y. Q., Shen, G. L., Yu, R. Q., *Anal. Lett.*, **1997**, *30*, 1455-1464.
- ⁴⁰Singh, A. K. Mehtab, S., *Talanta*, **2008**, *74*, 806.
- ⁴¹Shamsipur, M. Sadeghi, S. Naeimi, H. Sharghi, H., *Polish J. Chem.*, **2000**, *74*, 231-238.
- ⁴²Shamsipur, M. Soleymannpour, A. Akhond, M. Sharghi, H. Naseri, M. A., *Anal. Chim. Acta*, **2001**, *450*, 37-44.
- ⁴³Sanchez-Pedreno, C. Ortuno, J. A. Martinez, D., *Talanta*, **1998**, *47*, 305-310.
- ⁴⁴Benvidi, A. Ghanbarzadeh, M.T. Mazloum-Ardakani, M. Vafazadeh, R., *Chin. Chem. Lett.*, **2011**, *22*, 1087-1090.
- ⁴⁵Poursaberi, T. Hosseini, M. Taghizadeh, M. Pirelahi, H. Shamsipur, M., Ganjali, M. R., *Microchem. J.*, **2002**, *72*, 77.
- ⁴⁶Karimipour, G., Gharghani, S., Ahmadpour, R., *E-J. Chem.*, **2012**, *9*, 2565-2574.
- ⁴⁷Ghanei-Motlagh, M. Taher, M. A. Ahmadi, K. Sheikhshoae, I., *Mat. Sci. Eng.*, **2011**, *C31*, 1625-1631.
- ⁴⁸Ghaedi, M., Montazerzohori, M., Mousavi, A., Khodadoust, S., Mansouri, M., *Mat. Sci. Eng.*, **2012**, *C32*, 523-529.
- ⁴⁹Shvedene, N. V., Avramenko, O. A., Baulin, V. E., Tomilova, L. G., Pletnev, I. V., *Electroanalysis*, **2011**, *23*, 1067-1072.
- ⁵⁰Shvedene, N. V., Rzhevskaja, A. V., Pletnev, I. V., *Talanta*, **2012**, *102*, 123-127.
- ⁵¹Amr, A. E., Abo-Ghalia, M., Abdalah, M. M., *Z. Naturforsch.*, **2006**, *61b*, 1335-1345.
- ⁵²Bakker, E., Buhlmann, P., Pretsch, E., *Chem. Rev.*, **1997**, *97*, 3083-3132.
- ⁵³Lin, J., Zhang, J. Y., Xu, Y., Ke, X. K. and Guo, Z., *Acta Crystallogr.*, **2001**, *C57*, 192-194.
- ⁵⁴Conlon D. A. and Yasuda, N., *Adv. Synth. Catal.*, **2001**, *343*, 137-138.
- ⁵⁵Kurosaki, H., Sharma, R. K., Aoki, S., Inoue, T., Okamoto, Y., Sugiura, Y., Doi, M., Ishida, T., Otsuka M. and Goto, M., *J. Chem. Soc., Dalton Trans.*, **2001**, 441-442.
- ⁵⁶Jain, S. L., Bhattacharyya, P., Milton, H. L., Slawin, A. M. Z., Crayston, J. A., Woollins, J. D., *Dalton Trans.*, **2004**, 862-871.
- ⁵⁷Marlin, D. S. Olmstead, M. M. Mascharak, P. K., *Inorg. Chim. Acta*, **2001**, *323*, 1-4.
- ⁵⁸Rowland, J. M., Olmstead, M. M., Mascharak, P. K., *Inorg. Chem.*, **2000**, *39*, 5326-5332.
- ⁵⁹Chavez, F. A., Olmstead, M. M., Mascharak, P. K., *Inorg. Chem.*, **1996**, *35*, 1410-1412.

- ⁶⁰Rowland, J. M., Thornton, M. L., Olmstead, M. M., Mascharak, P. K., *Inorg. Chem.*, **2001**, *40*, 1069-1073.
- ⁶¹Abdel-Aziz, A. A., Kamel, A. H., *Talanta*, **2010**, *80*, 1356–1363
- ⁶²Bakker, E., Malinowska, E., Schiller, R. D., Meyerhoff, M. E., *Talanta*, **1994**, *41*, 881-890.
- ⁶³Eugster, R., Gehrig, P. M., Morf, W. E., Spichiger, U. E., Simon, W., *Anal. Chem.*, **1991**, *63*, 2285-2289.
- ⁶⁴Schaller, U., Bakker, E., Spichiger, U. E., Pretsch, E., *Anal. Chem.*, **1994**, *66*, 391-398.
- ⁶⁵Umezawa, Y., Umezawa, K. Sato, H., *Pure Appl. Chem.*, **1995**, *67*, 507-518.
- ⁶⁶Bakker, E. Pretsch, E. Buhlmann, P., *Anal. Chem.*, **2000**, *72*, 1127-1133.
- ⁶⁷British Pharmacopoeia, Her Majesty's Stationary Office, London, **2003**.

Received: 17.07.2016.

Accepted: 03.11.2016.



STUDIES ON EFFECTIVE SEGREGATION COEFFICIENTS OF IMPURITIES IN SILICON PULLED FROM MG-Si MELT

N. Kekelidze^[a], G. Tavadze^[a], E. Khutsishvili^{[a]*}, L. Gabrichidze^[a] and G. Mikaberidze^[a]

Keywords: Silicon, segregation, impurity, crystallization, purification.

Minimization of impurities content in Si, necessary for its application as semiconductor material, was performed by using directional crystallization of metallurgical grade Si (*n*-MG-Si) with 98 wt. % Si purity without intermediate stages. After pulling from melt, *n*-MG-Si goes into *p*-type Si with current carriers concentration (*p*) $\sim 10^{16} \text{ cm}^{-3}$ and Si has been purified practically from most of the impurities. The possibility of uncontrolled impurities removal from Si depends on impurities effective coefficient of segregation in Si. Therefore we have investigated the effective coefficient of segregation of unwanted impurities in Si crystals, obtained by pulling directly from MG-Si melt. In the presented article the effective segregation coefficient of major impurities in Si has been calculated and analysed in the dependence on the crystallization conditions. Effective coefficient of segregation makes possible estimate the capacity and efficiency of Si purification from impurities during crystallization from melt.

* Corresponding Author:

E-Mail: elzakhutsishvili@yahoo.com

[a] Laboratory of Semiconductor Materials Science, Ferdinand Tavadze Institute of Metallurgy and Materials Science, Tbilisi, Georgia

presented in Si. Effective coefficient of segregation makes possible estimate the capacity and efficiency of Si purification from impurities during crystallization from melt. So the objective of the presented article is the investigation of effective coefficient of segregation of unwanted impurities in Si crystals, obtained by pulling directly from metallurgical grade Si (MG-Si) melt.

Introduction

Silicon technology has had a strong influence on the world economy over the past few decades, and presently is the driving force behind the revolution in semiconductor engineering applications. Silicon has advantages over other semiconductor materials because of its abundance on the earth, meeting most required criteria and having a number of better properties.^{1, 2} It is predicted to remain the prevailing semiconductor technology for the near future. The continual reduction of the size of Si devices has led to exponential increase in their quality together with an exponential decrease in the cost per function. The size reduction of bulk crystalline Si to the nanometre dimension expands the scope of silicon application. For example, nano crystalline Si becomes light emitting. Silicon technology is gradually moving into new applications as novel silicon-base nanotechnology. However further development of Si application requires further investigations in the direction of identification of behaviour of uncontrolled impurities in Si. The main criterion of Si suitability for application in semiconductor devices is its chemical purity. Therefore the problems connected with uncontrolled impurities removal from Si are very important.

Minimization of impurity contents of Si, intended for application as semiconductor material, is achieved by using many known traditional refinement methods, among them is crystallization from the melt. As a rule, it is applied on the final stage of technological process of purification of substances. However in given work a directional crystallization is used for direct purification of metallurgical Si without any intermediate stages. The possibility of removal of unintended impurities from Si depends on effective coefficient of segregation (*k*) of impurities

Experimental

The first step product of Si obtained by restoration from quartzite with reaction to carbon is metallurgical Si. *n*-MG-Si with ~ 98 wt. % Si has been taken as initial material. Ample quantity (~ 2 wt. %) of unwanted impurities Fe, Al, P, Ca, Cu, Mg, Mn, Ni, Ti has fallen one after the other into MG-Si from quartzite and restoring materials in time of restoration process. Carbon and oxygen has been presented in MG-Si too. The known Czochralski growth method of pulling crystals has been used for obtaining Si directly from MG-Si melt. Crystals have been grown from 48 mm diameter quartz crucible. Si crystalline rods with the length of 50 mm were used as the seeds. During the process of the crystal pulling the crucible with the mother melt revolved with the rate of rotation 45 and 10 revolutions per minute in opposite directions. The optimal effect of Si purification has been achieved at $\sim 0.25 - 0.30$ mm per minute rate of crystal growth. Such conditions provide the symmetry of temperature field at the crystallization front.

First the melting camera has been pumped off up to 10^{-4} mm Hg, and then washed by flow of argon. The fusion has been carried out in the argon atmosphere at a pressure of not more than 50 kPa. *n*-type MG-Si ($n \approx 10^{18} \text{ cm}^{-3}$) have been charged into the crucible. The volatile impurities actively evaporated from the surface of MG-Si have been removed from melting camera with equipped special apparatus for gas removing (gas-extracting arrangement). An argon supply and discharge of the working chamber was regulated so, that the pressure in the chamber remained constant at the level of 50 kPa.

The content of contaminating impurities in Si before and after the directional crystallization has been defined by X-ray diffraction method, micro X-ray spectral and emissive spectral analyses. Electrical properties and microstructure analysis of Si experimental samples have been implemented too. Effective segregation coefficient of detrimental impurities in Si at the crystal pulling from MG-Si has been determined on the base of established content of unwanted impurities in Si. *n*-MG-Si after pulling goes into *p*-type Si.

Results and Discussion

Mechanisms of impurity removal

At initial step of melting at low temperatures Si has been purified from mixture of those impurities which are more volatile than basic component. The melt had sufficiently large surface. So volatile impurities actively evaporated from the surface of Si melt at low temperatures and 10^{-3} mm Hg pressure. Their content is defined by pressure and composition of atmosphere in a processing chamber. At temperatures lower than Si melting temperature (1450 °C) impurities with less fusion temperature have evaporated too. On the next step of process temperature has increased by 50–70 °C higher than 1450 °C and Si melt stayed in liquid state certain time for removal (evaporation) of uneasily meltable impurities like Fe and Ti. Under the conditions of low pressure and high temperatures those impurities, which vapor tension is higher than one of Si (P, Al, etc.), have evaporated too.

It is known,³ that quantity of impurity (*m*), which vaporizes from open unit area of the melt (reflection of molecules from crucible walls is taken into account) is defined by:

$$m = \beta P \sqrt{\frac{M}{2\pi RT}} \quad (1)$$

where

P is the equilibrium pressure of impurity steam,

M is the molecular weight of impurity,

R is the gas constant,

T is the melting temperature,

and the coefficient β can be written as

$$\beta = \frac{156.6\alpha}{1 + \alpha d l^{-1}} \quad (2)$$

where

α is the condensing coefficient,

d is the crucible diameter, and

l is the height of walls of crucible above the melt.

Purification by evaporation has been effective for those impurities, which equilibrium pressure of steam exceeds one for Si. Those impurities which equilibrium pressure of steam

is higher than for the rest of the impurities vaporized easier at the identical conditions. The ratio of equilibrium pressure of steam for impurities and Si defines the degree of their partition. It follows from expression (1) that the vaporizability or ability to be removed of easy vaporable impurities from Si melt reduces in the row of Mg > Ca > Mn > Al > Cu > Fe > Ni > Ti.

Among a great number of foreign unforeseen electrically neutral impurities carbon and oxygen in Si attract attention. They get into semiconductors because of technology equipment (quartz crucible, heated graphite). Gaseous carbon and oxygen compounds products of the reaction have been removed by gas-extracting arrangement. At the same time refractory products have precipitated at the end of crystal. IR spectroscopy measurements of carbon distribution in Si have confirmed that carbon concentration increases at the end of a crystal. It indicates the enrichment of the melt with carbon due to segregation of carbon during the growth of the crystal. This cannot be explained only by the low distribution coefficient of carbon in silicon. It is also caused by collection of carbon in the melt in the result of chemical reactions of silicon with quartz and quartz with graphite. At the melt cooling carbide compounds are in isolated state. So, it is clear, that the carbon segregation process in silicon and the enrichment of the melt with carbon depend on the time of crystal growth process. Finally carbon has been removed with cut off part of Si crystal. It is remarkable, that Fe, Ca and oxygen promote the reduction of carbon solubility in Si.

MG-Si after pulling became *p*-type with current carriers concentration $\sim 10^{16}$ cm⁻³ and has been purified practically from majority of impurities. Incidentally the impurities in MG-Si have obeyed to the procedure of purification in a variety of mechanisms because of different physical properties of impurities. During the execution of the metallurgical silicon purification process the quantity of Ca, Mn, Ni out of the whole collection of unwanted impurities has reduced so much (< 0.001 wt. %), that their concentration has been less of detection limit of applied methods of impurities determination.

The purification of silicon from Mg, Mn, Cu, Fe, Ni, Ti impurities have occurred mainly by segregation because of their small segregation coefficient in Si (10^{-4} – 10^{-6}). Equilibrium coefficients of distribution of Al and Ca impurities (k_0) in Si ($2.0 \cdot 10^{-3}$ and $8.0 \cdot 10^{-3}$ accordingly) are not sufficiently small for being removed from Si by directional crystallization. But saturation vapor pressure of Al and Ca is much more than one for Si. Thus their removal from melt surface into gaseous phase at high temperatures and afterwards by gas-extracting arrangement has been possible.

Effective coefficient of distribution of harmful impurities in Si at crystal withdrawal

It is known, that at the pulling of Si from melt impurities have redistributed between solid and liquid phases with certain ratio as mentioned above and this process is characterised by effective coefficient of segregation of impurity. *k* of impurities in Si for experimental samples has

been calculated on the base of experimentally established data of impurity composition. The dependence of k of impurities in Si on the pulling speed of crystals is shown in the Figure 1.

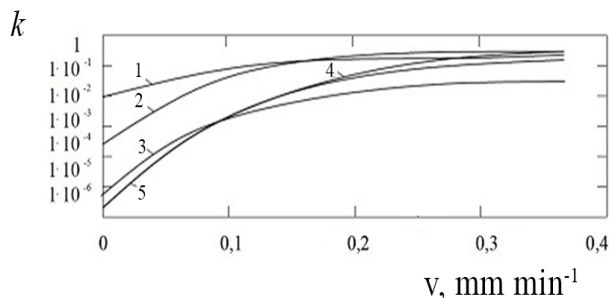


Figure 1. The dependence of effective distribution coefficients (k) of impurities in Si crystals on the pulling speed from melt. Impurities: 1 – Al; 2 – Cu; 3 – Fe; 4 – Mg; 5 – Ti.

The crystal Si pulling speed 0 mm min^{-1} belongs to the state of “equilibrium”, i.e. practically to very low pulling speed of crystal. For certain finite pulling speed magnitudes, k depends on the crystal pulling rate. It is remarkable, that equilibrium coefficient of distribution of majority of impurities in Si $k_0 < 1$. So as expected an increase in rate of crystal pulling results in k and at high pulling rates verge towards 1 (when quickly migrating separating phase is included) independently of magnitude of equilibrium coefficient of distribution of impurities k_0 .⁴ Data of effective coefficient of distribution of major impurities in Si corresponds to $k_0 \leq k \leq 1$ inequality. This result is in a good agreement with theory of Barton–Prima–Slichter.⁵ According to Barton–Prima–Slichter theory relationship between k and k_0 is defined by eqn. (3), at diffused transport of mass in δ layer (depth of melt near crystallization front-diffusion layer).

$$k = \frac{k_0}{k_0 + (1 - k_0)e^{-\Delta}} \quad (3)$$

where

$\Delta = v\delta/D$ is a dimensionless quantity, so called reduced velocity,

v is the solidification rate,

D is the diffusion coefficient of impurity

δ value depends on rate of rotation of crystal and changes in the range of $0.1\text{--}0.001 \text{ cm}$.

It can be seen from Eqn. (3), that in the first approximation k depends on the conditions of crystal growth processes i.e., solidification rate and rate of rotation of crystal (conditions of melt mixing). According to this theory when equilibrium distribution coefficient of impurities $k_0 < 1$, k increases at the growth of crystal pulling rate. While crystal is pulling from melt impurities with $k_0 < 1$ accumulate little by little in the melt because of they get into melt from crystallization front.

Accordingly impurities concentration at the surface exceeds their concentration in the melt. So $k > k_0$ and during the process of crystal growth the melt is progressively

enriched by impurities because of their bad solubility in solid phase. Therefore the end of crystal, where all residual impurities are concentrated, has always been cut off.

Impurity distribution along the ingot at crystal withdrawal

It is remarkable, that impurities are mainly concentrated at the end of Si crystal. Fig. 2 shows clearly that contaminated dark end parts of Si crystal.

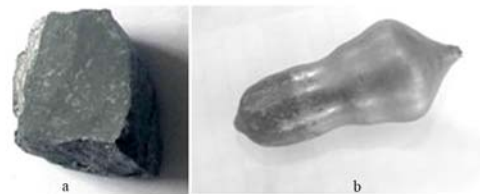


Figure 2. (a) Metallurgical Si and (b) Si crystal obtained by pulling from melt with 0.3 mm min^{-1} velocity.

The size of impure section reduces at the increase of the velocity pulling speed of crystal. It means that the effect of co-location of impurities at the end of crystal intensifies with growth of crystal pulling velocity. Impurity distribution along the crystal length during the crystal pulling from the melt is described by the following formula of Scheil.⁶

$$C = k C_0 (1 - g)^{k-1}, \quad (4)$$

where

$g = V_m/V_0$, g is the crystallized part of initial volume of melt;

V_m is the volume of crystallized phase,

V_0 is the initial volume of liquid phase,

when $g = 0$, impurity concentration in the melt C equates to its initial magnitude in the melt C_0 .

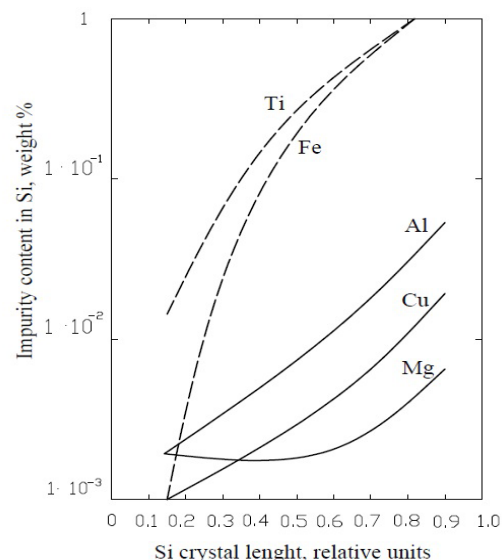


Figure 3. Dependence of impurities concentration in Si solid phase on the crystallized part of melt.

According to Eqn. (4) when $k < 1$ (at equilibrium during the process of crystal pulling, $k = \text{const}$) impurities concentration increases along the crystal length.

For majority of impurities in Si, $k \ll 1$, so Eqn. (4) can be written as Eqn. (5).

$$C \cong \frac{kC_0}{1-g} \quad (5)$$

where kC_0 is a constant. Eqn. (5) shows, that C is inversely proportional to the remaining part of melt. Dependence of impurity concentration in Si solid phase on crystallized part of melt is shown in the Figure 3.

Typical X-ray diffraction spectra have shown that obtained Si is single-phase. Consequently, there is only Si diffraction maxima on the diffractogram. Microstructure investigations has confirmed, that the tracks of different phase inclusions observed in initial microstructure of MG-Si almost disappeared after pulling Si crystal out of the melt. So crystal phase of Si is purer than liquid phase with irregular impurity distribution along length.

Conclusion

Thus Si and two or more liquid layers of slags, which differ by density, originate at Si melting and the purification of Si of impurities like Fe, Al, P, Ca, Cu, Mg, Mn, Ni, Ti take place by different mechanisms or their combination.

Concrete mechanisms processing at Si purification are defined by impurity-Si interactions and depend on impurity distribution coefficient between solid and liquid phases, degree of volatility, steam tension, melting temperature, specific weight, and other chemical properties of impurities. Because virtually all basic impurities in Si have distribution coefficient $k < 1$, their effective removal is carried out by pushing aside impurities into liquid phase.

Acknowledgement

This paper has been presented at the 4th International Conference "Nanotechnologies", October 24 – 27, 2016, Tbilisi, Georgia (Nano – 2016).

References

- ¹Green, M. A., Emery, K., Hishikawa, Y., Warta, W., Dunlop, E. D., *Progr. Photovoltaics: Res. Appl.*, **2015**, *23*, 1.
- ²Khutsishvili, E., Khutsishvili, N., Kvirkevelia, B., Kekelidze, G., Nadiradze, L., Kekelidze, N., *J. Electr. Eng.*, **2015**, *3*, 53.
- ³Sing, K. S. W., Everett, D. H. R., Haul, A. W., Moscou, I., Pierotti, R. A., Rouquerol, J., Siemieniewska, T., *Pure Appl. Chem.*, **1985**, *57*, 603
- ⁴Martorano, M. A., Neto, J. B. F., Oliveira, T. S., Tsubaki, T. O., *Mater. Sci. Eng. B*, **2011**, *76(3)*, 217.
- ⁵Burton, J. A., Prim, R. S., Slichter, W. P., *J. Chem. Phys.*, **1953**, *21*, 1987.
- ⁶Pfann, W. G., *Trans. AIME*, **1952**, *194*, 747.

Received: 30.07.2016.

Accepted: 03.11.2016.



PECULIARITIES OF “ALLOY” SCATTERING IN SEMICONDUCTORS

N. Kekelidze,^[a] E. Khutsishvili,^{[a]*} D. Kekelidze,^[a] B. Kvirkvelia,^[a] L. Nadiradze^[b] and K. Sadradze^[b]

Keywords: Semiconductor Alloys, disorders, charge carriers mobility.

The effect of nanometer size disordered regions in $\text{Si}_x\text{Ge}_{1-x}$ and $\text{InP}_x\text{As}_{1-x}$ semiconductor alloys on the mobility of charge carriers has been investigated. The investigation has shown, that the composition dependence of the mobility appears as a result of contribution of main processes of current carriers scattering on phonons, ionized impurities and “alloy” disorders in $\text{Si}_x\text{Ge}_{1-x}$ and $\text{InP}_x\text{As}_{1-x}$ alloys. We have calculated the contribution of these scattering processes towards total scattering. Share of contribution of “alloy” disorders into the total mobility is different for $\text{Si}_x\text{Ge}_{1-x}$ and $\text{InP}_x\text{As}_{1-x}$ solid solutions. Unlike $\text{Si}_x\text{Ge}_{1-x}$ alloys, the “alloy” disorders in $\text{InP}_x\text{As}_{1-x}$ practically do not disturb the crystal lattice in a tangible way at temperatures in the range of 4.2 – 300 K because of sublattices of InP and InAs retain certain individuality in $\text{InP}_x\text{As}_{1-x}$ alloys.

* Corresponding Author

E-Mail: elzakhutsishvili@yahoo.com

- [a] Laboratory of Semiconductor Materials Science, Ferdinand Tavadze Institute of Metallurgy and Materials Science, Tbilisi, 0186, Georgia
 [b] Department of Engineering Physics, Georgian Technical University, Tbilisi, 0175, Georgia

Introduction

Studies of semiconductors have shown that there might be various types of heterogeneity, which have independent scientific and practical interest in terms of materials with nanometer size disordered regions. The presence of such regions may seriously alter the transport and other properties of semiconductors. These disorders are of different origin, associated with a non-uniform distribution of impurity ions in doped and compensated semiconductors,¹ arisen at irradiation² and at the growth of crystals,³ related to the presence of crystalline boundaries in polycrystals.⁴ Independently of semiconductor crystals growth methods there always exist these or those disordered areas, which are an accompanying appearance in semiconductor technology and cannot be ignored, because may contribute to the electrical,⁵ optical⁶ properties, etc. in a greater or lesser extent. All types of the heterogeneity listed above are caused by random space distribution of impurity ions and electrons and have electrostatic nature. The main peculiarity of these kinds of heterogeneity is that they modulate the semiconductors energy bands in a way, so that the optical energy gap remains invariable.

There may be another type of heterogeneity connected with random space fluctuations of the composition⁷ so-called “alloy” disorders. This type of heterogeneity is one of the most interesting for semiconductor technology because semiconductor alloys (or so-called solid solutions) of elementary semiconductors or III–V compounds may extend the functionality and operational parameters of electronic devices based on them. Changes in the composition of these solutions allow monitoring of important physicochemical properties of the obtained materials, thereby are more widely used in modern semiconductor devices than their pure initial components. Many of semiconductor alloys devices offer higher

performance compared to silicon devices and are competitive with GaAs-based products. Presently, experimental knowledge concerning “alloy” disorders in such materials is rudimentary with a few exceptions.

This paper is devoted mainly to review the influence of “alloy disorders” on the base of electrical properties in semiconductor alloys of elementary semiconductors and III–V compounds, $\text{Si}_x\text{Ge}_{1-x}$ and $\text{InP}_x\text{As}_{1-x}$. Among the solid solutions, these systems are of great interest for engineering. In this paper, we have focused on the influence of “alloy” disorders on the mobility of charge carriers, the key parameter determining thermoelectric and microelectronic applications of semiconductors.

Experimental

The *p*-type $\text{Si}_x\text{Ge}_{1-x}$ ($0 \leq x \leq 1$) crystals were grown by the Czochralski technique. Experimental *n*-type samples of $\text{InP}_x\text{As}_{1-x}$ solid solutions were grown by the horizontal zone melting method. High degree of homogeneity of solid solutions was confirmed by several methods, among which the most important are X-ray microanalysis and application of Vegard law. Charge carriers mobility was evaluated from Hall-effect and conductivity measurements by a standard dc bridge technique. The standard deviation in the carriers' concentration was 8 – 10 % and that in the conductivity was 4 – 5%.

Results and discussion

$\text{Si}_x\text{Ge}_{1-x}$ Alloys

“Alloy” disorder scattering was observed for the first time in $\text{Si}_x\text{Ge}_{1-x}$ semiconductor alloys.⁸ Our data of current carriers mobility (μ_{exp}) for $\text{Si}_x\text{Ge}_{1-x}$ solid solutions with nearly the same carriers concentration $n \sim 10^{16}$, 10^{17} and 10^{19} cm^{-3} are presented in Figure 1. Composition dependence of the charge carriers mobility of $\text{Si}_x\text{Ge}_{1-x}$ solid solutions at 300 K with the carriers concentrations $n \sim 10^{16}$ and 10^{17} cm^{-3} (Figure 1) reveals strong minimum in the middle of solid solutions system.

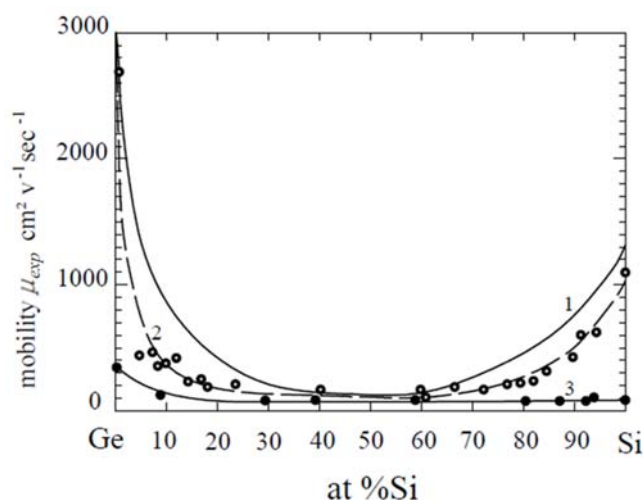


Figure 1. Composition dependence of the mobility charge carriers (μ_{exp}) at 300 K for $\text{Si}_x\text{Ge}_{1-x}$ alloys with charge concentration: 1 = $1 \times 10^{16} \text{ cm}^{-3}$, 2 = $1 \times 10^{17} \text{ cm}^{-3}$ and 3 = $2 \times 10^{19} \text{ cm}^{-3}$.

The presence of minimum in composition dependence of mobility is defined by “alloy” scattering.^{5,7} To achieve complete agreement between experimental results and the theory, it is necessary to assume the existence of an additional mechanisms of the current carriers scattering due to the disordered arrangement of solid solution atoms. Hence, we considered simultaneous action of different kinds of carriers scattering in $\text{Si}_x\text{Ge}_{1-x}$ alloys viz., the alloy disorder scattering, the scattering on acoustic lattice vibrations and the scattering on impurity ions. The individual share of contribution of these scattering mechanisms to the total varies with the compositions of $\text{Si}_x\text{Ge}_{1-x}$ solid solutions. To compare the experimental results with the theory in impurity-doped $\text{Si}_x\text{Ge}_{1-x}$ alloys, a relationship (eqn. 1), which takes into account simultaneous presence of scattering processes with different energetic dependences, was used.^{9,10} The net mobility (μ) depends on the various mobility components, associated with each scattering mechanism.

$$\frac{1}{\mu} = \frac{1}{\mu_{dis}} + \frac{1}{F} \left(\frac{1}{\mu_L} + \frac{1}{\mu_I} \right) \quad (1)$$

where,

μ_L and μ_I are the components related to the lattice vibrations and ionized impurity scattering respectively, μ_{dis} is the component related to disorder scattering and F is a correction factor, which takes into account the combined effect of different scattering processes.⁹

Comparison of experimental and theoretical mobility showed that component of mobility related to alloy disorders scattering follows the law predicted by theory^{5,7} in $\text{Si}_x\text{Ge}_{1-x}$ alloys.

Calculation of this contribution has been made by using an expression originally derived by Brooks.⁷

$$\mu_{dis} = \frac{(2\pi)^{1/2} e \hbar^4 N_0}{3(m^*)^{5/2} (kT)^{1/2} c(1-c)(E_a - E_b)^2} \quad (2)$$

where

N_0 is the number of atoms per unit volume,

c is the composition of one of the component of alloy,

E_a and E_b are energy-positions of edges of bands for two components of alloy.

According to Brooks⁷ in alloy with disorders regions the composition changes from one region to other one at the expense of statistical fluctuations. This causes energy bands deformation, peaks and dips at the edge of bands, which looks like deformation potential in theory of scattering by thermal vibration of lattice atoms. So “alloy” scattering can be considered as “frozen” scattering by thermal vibration of lattice.⁵ At low level of carriers concentration “alloy” scattering contribution to the mobility increases with increase of alloy components content. At high level of carriers concentration the mobility does not depend on alloy components content and scattering is defined by ionized impurities (Figure 1).¹⁰

The “alloy” scattering of current carriers is very important for creating of effective thermoelements on the base of $\text{Si}_x\text{Ge}_{1-x}$. The perfect combination of properties connected with “alloy” disorders and thermoelectric properties in $\text{Si}_x\text{Ge}_{1-x}$ alloys makes them high effective thermoelectric materials for use at high temperatures.¹⁰

$\text{InP}_x\text{As}_{1-x}$ alloys

Contribution of disorder scattering to the electrons mobility has been revealed also for a number of III-V compound alloys, particularly for $\text{InP}_x\text{As}_{1-x}$ solid solutions. Mobility data of current carriers for $\text{InP}_x\text{As}_{1-x}$ solid solutions with nearly the same carriers concentration $n \sim 10^{16}$ and 10^{18} cm^{-3} are presented in Figure 2.

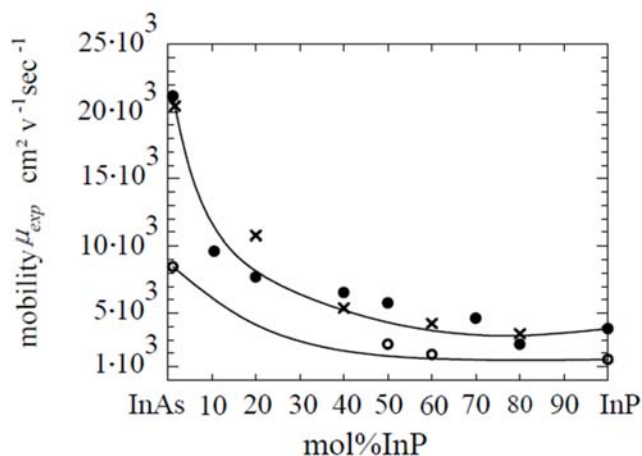


Figure 2. Composition dependence of the mobility of charge carriers (μ_{exp}) at 300 K for $\text{InP}_x\text{As}_{1-x}$ alloys with charge concentration = 10^{16} cm^{-3} (• – our data, × – data from ref. 11) and 10^{18} cm^{-3} (○ – our data).

Composition dependence of electrons mobility at 300 K for $\text{InP}_x\text{As}_{1-x}$ solid solutions with the carriers concentrations $n \sim 10^{16}$ and 10^{18} cm^{-3} (Figure 2) reveals weak minimum on the InP-rich side of solid solutions system. Such character of composition dependence of mobility is connected with the change of contribution of scattering mechanisms of separate components into the total scattering at the alteration of composition. We carried out appropriate analysis of the mobility on the basis of reasonable theories.^{7,9,12,13} Comparison with theoretical predictions in $\text{InP}_x\text{As}_{1-x}$ solid solutions with $n \sim 10^{16} \text{ cm}^{-3}$ has shown that at temperatures near 300 K the prevailing mechanism is the scattering on optical phonons.¹⁴ Contribution of the disorder scattering increases with increasing of InP composition in solid solutions system at fixed temperatures and weakens with lowering of temperature in the range of 4.2-300 K and never dominates.¹⁵ Assumption of the existence of an additional mechanism of the current carriers scattering due to the disordered arrangement of solid solution atoms allows achieving the full agreement of experimental mobility with the theory.

The composition dependence of the mobility of current carriers for $\text{InP}_x\text{As}_{1-x}$ alloys (Figure 2) differs from the similar dependence for $\text{Si}_x\text{Ge}_{1-x}$ alloys (Figure 1) with well-defined minimum in the middle of alloys system. The data for alloy scattering in $\text{InP}_x\text{As}_{1-x}$ solid solutions do not reveal such tendency.

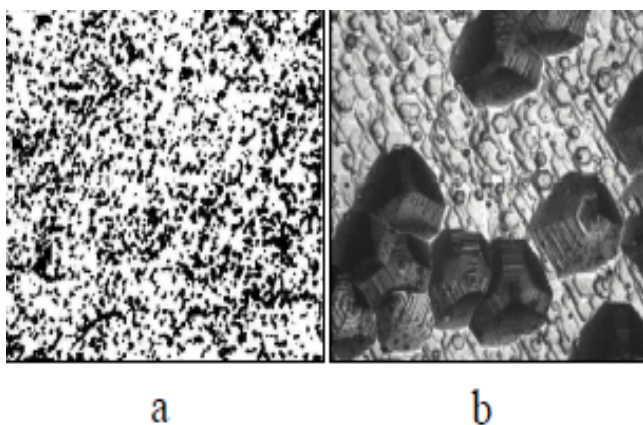


Figure 3. Dislocation structure of single crystals of semiconductor alloys on the plane (111) (a) $\text{Si}_x\text{Ge}_{1-x}$ ($\times 1000$) and (b) $\text{InP}_x\text{As}_{1-x}$ ($\times 250$).

An estimate of maximal share of disorder scattering in $\text{InP}_x\text{As}_{1-x}$ solid solutions results in the value which does not exceed $\sim 20\%$ of total magnitude of determinative scattering at 300 K and $\sim 10\%$ at lower temperatures. The reason of absence of clear minimum in the composition dependence of mobility for $\text{InP}_x\text{As}_{1-x}$ solid solutions may be apparently connected with the specific properties of $\text{InP}_x\text{As}_{1-x}$ caused by fact, that sublattices of InP and InAs retain a certain natural properties in contrast to Si and Ge in $\text{Si}_x\text{Ge}_{1-x}$ alloys. The preservation of individuality of sublattices of InP and InAs in their alloys has been previously found by us at optical properties research,¹⁴ where has been discovered two mode behavior of lattice vibrations in $\text{InP}_x\text{As}_{1-x}$ alloys.

The retention of individuality of sublattices of InP and InAs in $\text{InP}_x\text{As}_{1-x}$ alloys is confirmed by microstructural studies (see Figure 3).

This image clearly show, that InP and InAs sublattices in $\text{InP}_x\text{As}_{1-x}$ alloys retain their identity as distinct from $\text{Si}_x\text{Ge}_{1-x}$ where Si and Ge do not preserve their identity.

Conclusion

Unlike $\text{Si}_x\text{Ge}_{1-x}$, the “alloy” scattering in $\text{InP}_x\text{As}_{1-x}$ never dominates. In contrast to $\text{Si}_x\text{Ge}_{1-x}$, solid solutions InP and InAs retain a certain individuality in $\text{InP}_x\text{As}_{1-x}$ alloys. This result means, that mobility in $\text{InP}_x\text{As}_{1-x}$ solid solutions is mainly defined by the factors determining III–V compounds. A relative small contribution of disorder scattering is important for devices designed on the base of $\text{InP}_x\text{As}_{1-x}$ system.

Acknowledgement

This paper has been presented at the 4th International Conference “Nanotechnologies”, October 24 – 27, 2016, Tbilisi, Georgia (Nano – 2016).

References

- ¹Shklovski, B., Efros, A., *Electronic Properties of Doped Semiconductors*, 1984, Berlin: Springer-Verlag, 136.
- ²Gossick, B.R., *J. Appl. Phys.*, **1959**, *30*, 1214.
- ³Kekelidze, N., Kekelidze, D., Milovanova, L., Khutsishvili, E., Davitaya, Z., Kvirkvelia, B., Khomasuridze, D., *Acta Phys. Pol. A*, **2012**, *121*, 27.
- ⁴Khutsishvili, E., Kekua, M., *Phys. Stat. Sol. (a)*, **1980**, *61*, K1.
- ⁵Shik, A. Y., *Electronic Properties of Inhomogeneous Semiconductors*, Electro Component Science Monographs, Gordon & Breach Science Pub., **1995**, 153.
- ⁶Humlicek, J., Lukes, F., Schmidt, E., Kekua, M., Khutsishvili, E., *Solid State Comm.*, **1983**, *47*, 387.
- ⁷Makowski, L., Glicksman, M., *J. Phys. Chem. Solids*, **1973**, *34*, 487.
- ⁸Levitas, A., *Phys. Rev.*, **1955**, *99*, 1810.
- ⁹Mansfield, R., *Proc. Phys. Soc.*, **1956**, *B69*, 76.
- ¹⁰Kekua, M., Khutsishvili, E., *Germanium–Silicon Semiconductor Solid Solutions*, Tbilisi, Metsniereba, **1985**.
- ¹¹Weiss, H., *Zeitschrift Naturforschung Teil A*, **1956**, *11*, 430.
- ¹²Ehrenreich, H., *J. Phys. Chem. Solids*, **1959**, *12*, 1297.
- ¹³Anselm, A. I., *Introduction to the Theory of Semiconductors*, **1978**, Moscow: Nauka, 615.
- ¹⁴Kekelidze, N., Khutsishvili, E., Kvirkvelia, B., Kekelidze, G., *J. Electr. Eng.*, **2014**, *2*, 207.
- ¹⁵Kekelidze, N., Kekelidze, G., Makharadze, Z., *J. Phys. Chem. Sol.*, **1973**, *34*, 117.

Received: 09.08.2016.

Accepted: 03.11.2016.



COMPARATIVE PHYTOCHEMICAL PROFILE OF *INDONEESIELLA ECHIOIDES* (L.) NEES LEAVES

A. Elaiyaraja^{[a]*} and G. Chandramohan^[b]

Keywords: *Indoneesiella echioides* (L) Nees, phytochemical screening, separation and identification of compounds, GC-MS studies, spectral analysis.

Indoneesiella echioides (or) *Andrographis echioides* (L) Nees is an important herb widely distributed in south India. This is commonly known as False water willow. *Indoneesiella echioides* (L) Nees is used as in traditional Indian medicine. The leaf juice of this plant is used to cure fever. Different pharmacological properties of *Indoneesiella echioides* have already been reported. Thus, the present study was performed to investigate the preliminary phytochemical screening, separation, identification of compounds and compare the phytochemical composition of various fraction of *Indoneesiella echioides* using gas chromatography-mass spectrometry. The plant was extracted for various solvents in increasing order of polarity from using n-hexane, chloroform, ethyl acetate, acetone, ethanol, butanol and methanol. The result obtained after GC-MS studies were confirmed by spectral analysis.

* Corresponding Authors

Tel: +919043571103

E-Mail: raja_mscchem@rediffmail.com

[a] Department of Chemistry, A.V.V.M. Sri Pushpam College, Poondi, Thanjavur 613 503, Tamilnadu, India.

[b] Department of Chemistry, Jairams Arts and Science College, Karur-3, Tamilnadu, India.

Introduction

Indoneesiella echioides (L) Nees (Acanthaceae), also known as *Andrographis echioides* (L) Nees, is commonly known as False Water Willow and grows abundantly in south India. *Indoneesiella echioides* (L) Nees is medicinally highly important. The plants of genus *Indoneesiella* is used in goiter, liver diseases,¹ fertility problems, bacterial infection and malarial and fungal disorders.² The leaf juice of this plant is used to treating fever.³ Several *Indoneesiella* species (about 40 species) has been used in treatment of influenza, malaria, dyspepsia and respiratory diseases. The plants of *Indoneesiella* species are also used as antidote for poisonous stings of some insects.^{4,5} The leaf juice is mixed and boiled with coconut oil used to control falling and greying of hair.⁶ Phytochemistry of *Indoneesiella echioides* has been investigated and reported to contain several flavonoids^{7,8} and labdane diterpenoids.⁹⁻¹⁴

In previous literatures only flavonoids are reported as a major component in *Indoneesiella echioides* (L) Nees extracts.¹⁵⁻¹⁸ It has been reported that variety of phytoconstituents like phenols, coumarins, lignans, essential oil, monoterpenes, carotenoids, glycosides, flavonoids, organic acids, lipids, alkaloids and xanthenes are also present.¹⁹

Hence the present investigation was carried out to determine the possible phytochemical compounds of *Indoneesiella echioides* by GC-MS studies.

Experimental

Collection of plant materials

The leaves of *Indoneesiella echioides* was collected from Poondi village, Thanjavur District, Tamilnadu, India. The botanical identity (Voucher No: A.A.R 001 on 04-02-2015) of the plant was confirmed by Dr. S. John Britto, Rapinat Herbarium, St. Joseph's College, Tiruchirappalli, India.

Preparation of extracts

The fine powder (5 kg) was extracted with 95% ethanol at room temperature for ten days. The extract were filtered and concentrated under reduced pressure in a rotary evaporator and extracted with various solvents in increasing order of polarity, starting from n-hexane, chloroform, acetone, ethanol, butanol and methanol. The extract was taken in a beaker and kept in a water bath and heated at 30-40 °C till all the solvent is evaporated. The dried extracts were subjected to preliminary phytochemicals and GC-MS studies. All the extracts were tested for the presence bioactive compounds by using standard methods.

Phytochemical screening

The preliminary phytochemical analysis of *Indoneesiella echioides* (L) Nees was carried out as per standard methods (Table 1).

Identification of phytocompounds by GC-MS

GC-MS, one of the most reliable biophysical method for its specificity and repeatability, was utilized for the phytochemical profiling of *Indoneesiella echioides* (L) Nees leaves.

Table 1. Preliminary phytochemical constituents of *Indoneesiella echioides* (L) Nees leaves.

S. No.	Phytochemicals	Hexane extract	Chloroform extract	Acetone extract	Ethanol extract	Butanol extract	Methanol extract
1.	Alkaloids	-	-	Present	Present	-	-
2.	Flavonoids	-	Present	Present	Present	Present	Present
3.	Terpenes	Present	Present	-	-	-	-
4.	Triterpenoid saponins	-	Present	Present	-	-	-
5.	Saponins	-	Present	Present	Present	Present	Present
6.	Glycosides	-	-	-	-	-	-
7.	Steroids	Present	Present	Present	-	-	-
8.	Carbohydrates	-	-	-	-	-	-
9.	Phenolic compounds	Present	Present	Present	-	Present	Present
10.	Tannins	-	-	-	-	-	-
11.	Amino acids	-	-	Present	Present	-	Present

Table 2. Phytochemical components identified for n-hexane extract of *Indoneesiella echioides* (L) Nees (GC-MS study).

S.N	RT	Name of the compound	Molecular formula	Molecular weight	Peak area (%)	Compound nature	Activity
1.	12.85	Undecanoic acid, 10-methyl-, methyl ester	C ₁₃ H ₂₆ O ₂	214.3443	87	-	No activity reported.
2.	15.07	Methyl tetradecanoate	C ₁₅ H ₃₀ O ₂	242.3975	100	Myristic acid ester	Antioxidant, cancer-preventive, hypercholesterolemic, nematicide activities.
3.	15.72	Tetradecanoic acid, 12-methyl-, methyl ester	C ₁₆ H ₃₂ O ₂	256.4241	100	Fatty acid methyl ester	No activity reported.
4.	16.95	(Z)-9-Hexadecenoic acid, methyl ester,	C ₁₇ H ₃₂ O ₂	268.4348	63.9	Fatty acid methyl ester	No activity reported.
5.	17.17	Pentadecanoic acid, 14-methyl-, methyl ester	C ₁₇ H ₃₄ O ₂	270.4507	100	Palmitic acid methyl ester	Antioxidant, antifungal, antimicrobial activities.
6.	18.15	Hexadecanoic acid, 14-methyl-, methyl ester	C ₁₈ H ₃₆ O ₂	284.4772	100	-	No activity reported.
7.	18.93	10-Octadecenoic acid, methyl ester	C ₁₉ H ₃₆ O ₂	296.4879	100	Fatty acid ester	antioxidant, antimicrobial activities.
8.	19.1	Heptadecanoic acid, 16-methyl-, methyl ester	C ₁₉ H ₃₈ O ₂	298.5038	100	Stearic acid	Used against skin cancer protein.
9.	19.72	Eicosanoic acid	C ₂₀ H ₄₀ O ₂	312.5304	74.7	Fatty acid	No activity reported.
10.	20.92	Eicosanoic acid, methyl ester	C ₂₁ H ₄₂ O ₂	326.5570	100	Arachidic acid	α-Glucosidase inhibitors activity.
11.	21.18	Hexadecanoic acid, 1,1-dimethylethyl ester	C ₂₀ H ₄₀ O ₂	312.5304	54.5	-	No activity reported.
12.	22.95	Docosanoic acid, methyl ester	C ₂₃ H ₄₆ O ₂	354.6101	98.4	Fatty acid	Therapeutic, diagnostic activities.
13.	23.28	Benzoic acid, 2,4-dimethoxy-6-methyl-, (8,8-dimethoxy-2-octyl) ester	C ₂₀ H ₃₂ O ₆	368.46448	94.4	-	No activity reported.

Source: Dr. Duke's Phytochemical and Ethnobotanical Databases

Interpretation on Mass-Spectra GC-MS was conducted using the database of National Institute Standard and Technology (NIST) having more 62,000 patterns. The spectrum of the unknown components was compared with the spectrum of known components stored in the NIST library.

The name, molecular weight and structure of the components of the test materials were ascertained. In the present study many phytochemical constituents have been identified from various fractions of *Indoneesiella echioides*(L) Nees leaves by GC-MS analysis.

Analysis of n-hexane extract

Thirteen phytocomponents which appeared in the n-hexane extract of *Indoneesiella echioides* (L) Nees leaves are listed in Table 2. All these compounds were known compounds.

Analysis of chloroform extract

Nine phytocomponents were identified from the chloroform extract of *Indoneesiella echioides* (L) Nees leaves and are listed in Table 3.

Table 3. Phytochemical components identified for chloroform extract of *Indoneesiella echioides* (L) Nees (GC-MS study).

S.No.	RT	Name of the compound	Molecular formula	Molecular weight	Peak area (%)	Compound nature	Activity
1.	12.63	Phenol, 2,4-bis(1,1-dimethylethyl)-	C ₁₄ H ₂₂ O	206.3239	27	-	Antifungal, antimicrobial, antioxidant, antimalarial activities.
2.	14.52	1,4-Dicyano-2-cyclohexylbenzene	C ₁₄ H ₁₄ N ₂	210.27436	3.5	-	-
3.	15.7	Flavone	C ₁₅ H ₁₀	222.239	6.4	-	-
4.	17.15	Pentadecanoic acid, 13-methyl-, methyl ester	C ₁₇ H ₃₄ O ₂	270.4507	15.5	-	-
5.	18.03	n-Hexadecanoic acid	C ₁₆ H ₃₂ O ₂	256.4241	12.5	Fatty acid	Antioxidant, hypocholesterolemic, nematocidal, pesticide, lubricant, Antiandrogenic, flavor, hemolytic, 5- α -reductase inhibitor activities.
6.	18.83	10-Octadecenoic acid, methyl ester	C ₁₉ H ₃₆ O ₂	296.4879	13.1	Fatty acid ester	Antioxidant, antimicrobial activities.
7.	19.45	Ethyl Oleate	C ₂₀ H ₃₈ O ₂	310.52	24.9	Fatty acid ester	It is used as a vehicle for intramuscular drug delivery.
8.	21.4	3,5-Dicarbethoxy-1-methyl-1,4,5,6,7,8-hexahydropyrrolo[2,3-b]azepin-4,7-dione	-	-	7.3	Unknown compound	-
9.	23.18	Butanoic acid, 3-methyl-, hexadecyl ester.	-	-	25.8	Unknown compound	-

Source: Dr. Duke's Phytochemical and Ethnobotanical Databases

Table 4. Phytochemical components identified for acetone extract of *Indoneesiella echioides* (L) Nees (GC-MS study).

S.N o.	RT	Name of the compound	Molecular formula	Molecular weight	Peak Area (%)	Compound nature	Activity
1.	17.97	Hexadecanoic acid, ethyl ester	C ₁₈ H ₃₆ O ₂	284	100	Fatty acid	Antioxidant, Hypocholesterolemic, Nematocidal, Pesticide, Lubricant, Antiandrogenic, Flavor activities.
2.	19.57	Ethyl Oleate	C ₂₀ H ₃₈ O ₂	310.52	100	Fatty acid ethyl ester	It is used for vehicle for intramuscular drug delivery.
3.	19.8	14-Hydroxy-15-methylhexadec-15-enoic acid, ethyl ester	C ₁₉ H ₃₆ O ₃	312.48734	91.2	-	No activity reported.
4.	21.75	2a,3b,5b,6a-Tetramethoxy carbonyl-bicyclo(2,2,2)oct-7-ene	C ₁₆ H ₂₀	340.325	23.3	-	No activity reported.
5.	23.37	Estra-1,3,5(10),6-tetraene-3,17-diol, diacetate, (17a')-	-	-	18	Unknown compound	-

Source: Dr. Duke's Phytochemical and Ethnobotanical Databases

Table 5. Phytochemical components identified for ethanolic extract of *Indoneesiella echioides* (L) Nees (GC-MS study).

S.No	RT	Name of the compound	Molecular formula	Molecular weight	Peak area, (%)	Compound Nature	Activity
1.	12.68	O-Himachalene	C ₁₅ H ₂₄	204.3511	4.3	-	Noactivity reported.
2.	14.15	Oxacyclotetradecan-2-one	-	-	15.2	Unknown compound	-
3.	14.5	Ar-tumerone	C ₁₅ H ₂₀ O	216.319	91.8	Sesquiterpenoid	Antivenom. Antidépresseur, Anti-inflammatoire, Neuroprotecteuractivities.
4.	14.9	Curlone	C ₁₅ H ₂₂ O	218.33458	41.4	Ketone	No activity reported.
5.	17.28	Pentadecanoic acid, 14-oxo, methyl ester	C ₁₆ H ₃₀ O ₃	270.40800	7.2	-	Antioxidant, nematocide, pesticide, hypocholesterolemicactivities.
6.	17.93	4'-Methoxy-5,7-dihydroxy isoflavone	C ₁₆ H ₁₂ O ₅	284.2635	6.4	Flavone	Used as a pharmaceutical intermediates.
7.	19.05	E,E,Z-1,3,12-Nonadecatriene-5,14-diol	C ₁₉ H ₃₄ O ₂	294	4.4	-	Antimicrobial
8.	19.55	(Z,Z)-Ethanol,2-(9,12-octadecadienyloxy)-	C ₂₀ H ₃₈ O ₂	310	5.6	Alcoholic compound.	Antimicrobial
9.	21.63	Tricosan-2-ol	-	-	7.8	Unknown compound	-

Source: Dr. Duke's Phytochemical and Ethnobotanical Databases

Table 6. Phytochemical components identified for butanol extract of *Indoneesiella echioides* (L) Nees (GC-MS study).

S.No.	RT	Name of the compound	Molecular formula	Molecular weight	Peak area (%)	Compound nature	Activity
1.	12.12	E-2-Tetradecen-1-ol	C ₁₄ H ₂₈ O	212.3715	3.1	Unsaturated alcohol	No activity reported.
2.	12.67	6,10-Dodecadien-1-ol,3,7,11-trimethyl-,(E)-(n)-	C ₁₅ H ₂₈ O	224.38222	11.9	-	No activity reported.
3.	14.15	E,E-6,8-Tridecadien-2-ol, acetate	-	-	16.3	Unknown compound	-
4.	14.45	Ar-tumerone	C ₁₅ H ₂₀ O	216.319	91.8	Sesquiterpenoid	Antivenom, Antidépresseur, Anti-inflammatoire, Neuroprotecteur
5.	15.93	5-Hexenoic acid,(9-decen-2-yl) ester	-	-	15.7	Unknown compound	-
6.	17.22	4',5,7-Trihydroxy isoflavone	C ₁₅ H ₁₀ O ₅	270.2369	11.7	Flavone	Antitumor agent, antioxidant, antiangiogenic and immunosuppressive activities.
7.	17.88	Ethyl 9-hexadecenoate	C ₁₈ H ₃₄ O ₂	282.4614	6.2	Fatty acid ester	No activity reported.
8.	19.15	16-Octadecenoic acid, methyl ester	C ₁₉ H ₃₆ O ₂	296.49	7.2	Fatty acid ester	Inhibit eukaryotic DNA polymerase activities <i>in vitro</i>
9.	19.5	(Z,Z)-Ethanol,2-(9,12-octadecadienyloxy)-	C ₂₀ H ₃₈ O ₂	310	6.5	Alcoholic compound	Antimicrobial activity.
10	21.63	Eicosanoic acid, 3-methyl-, methyl ester	-	-	7.8	Unknown compound	-

Source: Dr. Duke's Phytochemical and Ethnobotanical Databases

Table 7. Phytochemical components identified for methanolic extract of *Indoneesiella echioides* (L) Nees (GC-MS study).

S.No.	RT	Name of the compound	Molecular formula	Molecular weight	Peak area (%)	Compound nature	Activity
1.	16.5	Methyl 2,8-dimethyltridecanoate	C ₁₆ H ₃₂ O ₂	256.42408	11.1	-	No activity reported.
2.	18.8	4'-Methoxy-5,7-dihydroxy isoflavone	C ₁₆ H ₁₂ O ₅	284.2635	61.7	Flavone	Used as a pharmaceutical intermediates.
3.	19.15	Cyclohexan-1-ol-3-one-1-carboxylic acid, 6-(2,3-dimethoxyphenyl)-	-	-	14	Unknown compound	-
4.	19.72	Ethyl Oleate	C ₂₀ H ₃₈ O ₂	310.52	42.2	Fatty acid ester	It is used for intra-muscular drug delivery
5.	21.78	Elaidic acid, isopropyl ester	C ₂₁ H ₄₀ O ₂	324.541	13.9	-	Anti-inflammatory, hypocholesterolemic, cancer preventive, hepatoprotective
6.	23.38	Isopropyl stearate	C ₂₁ H ₄₂ O ₂	326.568	10.1	Stearic acid	Skin conditioning agent, binder and humectant activities.
7.	25.53	Estra-1,3,5(10)-trien-17a'-ol, 3-methoxy-17-(2-methylallyl)-	-	-	7.2	Unknown compound	-

Source: Dr. Duke's Phytochemical and Ethnobotanical Databases.

Out of the nine phytochemicals obtained from chloroform extract, two (Table 3, S. No. 8 and 9) are unknown compounds.

The mass spectra of unknown compounds isolated from the extracts made by various solvents can be found in the supplementary material.

Analysis of acetone extract

Five phytochemicals were isolated from the acetone extract of *Indoneesiella echioides* (L) Nees plant leaves (Table 4). Out of five components, only one (at S. No. 5) is unknown compound.

Analysis of ethanolic extract

Nine phytochemicals isolated from the ethanolic extract of *Indoneesiella echioides* (L) Nees leaves and are listed in Table 5. Out of these, only one compound (at S. No. 9) is unknown compound.

Analysis of butanol extract

Ten phytochemicals were isolated from the butanol extract of *Indoneesiella echioides* (L) Nees leaves and are listed in Table 6. Out of these three (at S. No. 3, 5 and 10) are unknown compounds.

Analysis of methanolic extract

Seven isolated from the methanolic extract of *Indoneesiella echioides* (L) Nees plant leaves and are listed in Table 7. Out of these compounds, two (at S. No. 3 and 7) are unknown compounds.

Results and Discussion

Shen et al²⁰ reported that the new compounds of androgechside A (5,8,2'-trihydroxy-7-methoxyflavone-5-O-β-D-glucopyranoside), androgechside B (2R)-5,2'-dihydroxy-7-methoxyflavanone-5-O-β-D-glucopyranoside), androechioside A (2-O-β-D-glucopyranosyl-4-methoxy-2,4,6-trihydroxybenzoate), androechioside B (methyl 3-(2-hydroxyphenyl)-3-oxopropanoate 2-O-β-D-glucopyranoside) are isolated and structurally elucidated by spectral analysis and chemical transformation and 37 known compounds were identified to be, 2',6'-dihydroxyacetophenone 2'-O-β-D-glucopyranoside, echioidinin 5-O-β-D-glucopyranoside, echioidinin, pinostrobin, andrographidine C, dihydroechioidinin, tectochrysin 5-glucoside, methyl salicylate glucoside, 7,8-dimethoxy-5-hydroxyflavone, 5,7,8-trimethoxyflavone, skullcapflavone I 2'-methyl ether, acetophenone-2-O-β-D-glucopyranoside, androechin, skullcapflavone I 2'-O-β-D-glucopyranoside, tectochrysin, 5,7,2'-trimethoxyflavone, echioidin, skullcapflavone I, 5,7-dimethoxyflavone, negletein 6-O-β-D-glucopyranoside, andrographidine E, 4-hydroxy-3-methoxy-*trans*-cinnamic acid methyl ester, 4-hydroxybenzaldehyde, 4-hydroxy-*trans*-cinnamic acid methyl ester, *O*-coumaric acid, 2,6-dihydroxybenzoic acid, 132-hydroxy-(132-*R*)-phaeophytin, (*E*)-phytyl-epoxide, phytol, phytene 1,2-diol, (+)-dehydrovomifoliol, 3β-hydroxy-5α, 6α,-epoxy-7-megastigmen-9-one, β-sitosterol, β-sitosterol-3-O-β-glucopyranoside, squalene, 1*H*-indole-3-carbaldehyde, and loliolide by comparison of their physical and spectral data with those reported in the literature.

In the present study preliminary phytochemical analysis of the *Indoneesiella echioides* (L) Nees revealed the presence of flavonoids, alkaloids, terpenoids, triterpenoids saponins, saponins, phenolic compound, sterols and amino acids are qualitatively analysed and the results are listed in table 1. These phytochemicals were found to be dihydroechioidinin, along with four unknown flavones, echioidinin, echioidin, skullcapflavone I 2'-*O*-methyl ester and skullcapflavone I 2'-*O*-glucoside.¹⁹ GC-MS studies indicated the presence of many phytocomponents such as flavones, sesquiterpenoids, fatty acid methyl ester, palmitic acid methyl ester, steroid, fatty acid ester, stearic acid, oleic acid, arachidic acid, myristic acid ester and unsaturated alcoholic compounds in the various extracts of the *Indoneesiella echioides* (L) Nees leaves.

Conclusion

The preliminary phytochemical analysis of *Indoneesiella echioides* (L) Nees leaves showed that they contain many bioactive chemicals like flavonoids, alkaloids, terpenoids, triterpenoids saponins, saponins, phenolic compounds, sterols and amino acids.

The GC-MS studies of *Indoneesiella echioides* (L) Nees leaves clearly indicate that the major compounds are the 4'-Methoxy-5,7-dihydroxy isoflavone (ethanol and methanol fractions), 4',5,7-Trihydroxy isoflavone (butanol fraction), Ar-tumerone (ethanol and butanol fractions), Ethyl Oleate (chloroform, acetone and methanol fractions), Ethanol, 2-(9,12-octadecadienyloxy)-(Z,Z)- (ethanol and butanol fractions) are identified.

Unknown compounds such as 3,5-dicarbethoxy-1-methyl-1,4,5,6,7,8-hexahydropyrrolo (2,3-b)azepin-4,7-dione, butanoic acid, 3-methyl-, hexadecyl ester, estra-1,3,5(10),6-tetraene-3,17-diol, diacetate, (17a)-, tricosan-2-ol, E,E-6,8-tridecadien-2-ol, acetate, 5-hexenoic acid, (9-decen-2-yl) ester, eicosanoic acid, 3-methyl-, methyl ester, 4'-methoxy-5,7-dihydroxy isoflavone, cyclohexan-1-ol-3-one-1-carboxylic acid, 6-(2,3-dimethoxyphenyl)-, estra-1,3,5(10)-trien-17a'-ol, 3-methoxy-17-(2-methylallyl)- are identified.

Minor compounds such as undecanoic acid, 10-methyl-, methyl ester, methyl tetradecanoate, tetradecanoic acid, 12-methyl-, methyl ester, 9-hexadecenoic acid, methyl ester, (Z)-, pentadecanoic acid, 14-methyl-, methyl ester, hexadecanoic acid, 14-methyl-, methyl ester, 10-octadecenoic acid, methyl ester, heptadecanoic acid, 16-methyl-, methyl ester, eicosanoic acid, eicosanoic acid methyl ester, hexadecanoic acid, 1,1-dimethylethyl ester, docosanoic acid methyl ester, benzoic acid, 2,4-dimethoxy-6-methyl-, (8,8-dimethoxy-2-octyl) ester, phenol, 2,4-bis(1,1-dimethylethyl)-, 1,4-dicyano-2-cyclohexylbenzene, flavone, pentadecanoic acid, 13-methyl-, methyl ester, n-hexadecanoic acid, 10-octadecenoic acid, methyl ester, ethyl Oleate, hexadecanoic acid, ethyl ester, 14-hydroxy-15-methylhexadec-15-enoic acid, ethyl ester, 2a,3b,5b,6a-tetramethoxycarbonylbicyclo[2,2,2]oct-7-ene, O-himachalene, oxacyclotetradecan-2-one, curlone, pentadecanoic acid, 14-oxo-, methyl ester, E,E,Z-1,3,12-nonadecatriene-5,14-diol, E-2-tetradecen-1-ol, 6,10-dodecadien-1-ol, 3,7,11-trimethyl-,

(E)-(n)-, ethyl 9-hexadecenoate, 16-octadecenoic acid, methyl ester, methyl 2,8-dimethyltridecanoate, elaidic acid, isopropyl ester, isopropyl stearate, 3-methoxy-17-(2-methylallyl)- were also identified.

These compounds are exhibited activities like antioxidant, cancer-preventive, hypercholesterolemic, nematocide, antifungal, antimicrobial. They are used as skin cancer protein, alpha-glucosidase inhibitors, therapeutic and diagnostic agents, an emollient, skin conditioning agent, binder, humectant, anti-inflammatory, hypocholesterolemic, cancer preventive, hepatoprotective, anticoronary, antieczemic, insectifuge. They are also used for vehicle for intramuscular delivery of drugs such as Progesterone. They selectively inhibit eukaryotic DNA polymerase activities. Some of these compounds are also find use as antitumor agent, antioxidant, antiangiogenic and immunosuppressive, nematocide, pesticide, lubricant, antiandrogenic and flavor agents. Hence *Indoneesiella echioides* (L) Nees is worthy for further investigation in natural drugs developments.

Acknowledgements

I wish to express my deep sense of gratitude and most sincere thanks to Honourable Resource Person Dr. Chandramohan, Principal, Jairams Arts and Science College, Karur-3, Tamilnadu, India for providing support to finish my research work

References

- Nadkarni A. K., Nadkarni K. M., *Indian Materia Medica*, Vol.1, Popular Prakashan, Bombay, **1976**.
- Qadrie, Z. L., Beena, J., Anandan, R., Rajkapoor, B., Rahamathulla, M., *Pak. J. Pharm. Sci.*, **2009**, 22, 123-125.
- Kirtikar, K.R., Basu. B. D., in *Indian medicinal plants*, Vol. 3, Periodical Experts, New Delhi **1975**.
- Kirtikar, K.R., Basu. B. D., in *Indian medicinal plants*, Vol. 3, Periodical Experts, New Delhi **1975**, 1884-1886.
- Chopra, R. N., Nayer, S. L., Chopra, I. C., *Glossary of Indian Medicinal Plants*, Council of Scientific and Industrial Research, New Delhi, **1980**, 18.
- Pandi Kumar P., Ayyanar, M., Ignacimuthu, S., *Indian J. Tredit. Knowl.*, **2007**, 6, 579-582.
- Harbone, J. B., *The Flavonoids: Advances in Research Science 1986*, Chapman and Hall: London, UK, **1994**, 280-290.
- Iinuma, M., Mizuno, M., *Phytochemistry*, **1989**, 28, 681-694.
- Kleipool, R. J. C., *Nature*, **1952**, 169, 33-34.
- Chan, W. R., Taylor, C. R., Willis, R. L., Bodden, R. L., *Tetrahedron*, **1971**, 27, 5081-5091.
- Balmain, A., Connolly, J. D., *J. Chem. Soc., Perkin Trans. I*, **1973**, 1247-1251.
- Fujita, T., Fujitani, R., Takeda, Y., Takaishi, Y., Yamada, T., Kido, M., Miura, I., *Chem. Pharm. Bull.*, **1994**, 42, 1216-1225.
- Matsuda, T., Kuroyanagi, M., Sugiyama, S., Umehara, K., Ueno, A., Nishi, K., *Chem. Pharm. Bull.*, **1994**, 42, 1216-1225.
- Reddy, M. K., Reddy, M. V., Gunasekar, D., Murthy, M. M., Caux, C., Bodo, B. A., *Phytochemistry*, **2003**, 62, 1271-1275.

¹⁵Govindachari, T. R., Parthasarathy P. C., Pai, B. R., Subramaniam, P. S., *Tetrahedron*, **1956**, *21*, 2633-2640.

¹⁶Govindachari, T. R., Parthasarathy P. C., Pai, B. R., Subramaniam, P. S., *Tetrahedron*, **1956**, *21*, 3715-3720.

¹⁷Jayaprakasam, B., Damu, A. G., Gunasekar, D., Blond, A., Bodo, B. *Phytochemistry*, **1999**, *52*, 935-937.

¹⁸Jayaprakasam, B., Gunasekar, D., Rao, K. V., Blond, A., Bodo, B., *J. Asian Nat. Prod. Res.*, **2001**, *3*, 43-48.

¹⁹Sharma, S. K., Ali M., Gupta J., *Phytochem Pharmacol.*, **2002**, *2*, 253-270.

²⁰Shen, D.-Y., Juang, S.-H., Kuo, P.-C., Huang, G.-J., Chan, Y.-Y., Damu, A. G., Wu, T.-S., *J. Mol. Sci.*, **2013**, *14*, 496-514.

Received: 28.08.2016.

Accepted: 05.11.2016.



THE EFFECT OF Hg-POLLUTED DRINKING WATER ON THE LEVEL OF HORMONES IN MALE RATS AND THE POTENTIAL THERAPEUTIC ACTION OF THE THIOSEMICARBAZONE AND ANTIPYRINE LIGANDS AND THEIR COMPLEXES

Samar A. Aly,^[a] Hussien H. Alganzory^{[b]*} and Tarek A. Salem^[c]

Keywords: DTA; Hg(II) complexes; IR; male hormones; oxidative status; TGA.

Novel Hg(II) complexes of d^{10} configuration have been synthesized and characterized by elemental analysis, IR, UV-VIS spectra and thermal analysis. The analytical and spectral data reveal that the ligands (H_2L^1 - HL^3) behave as neutral or mono basic bidentate in nature, coordinating via C=O or C-O and NH or C=N. The harmful effect of Hg-polluted drinking water on male sex hormones, kidney function as well as oxidative status biomarkers of male rats was investigated. Meanwhile, the potential protective effects of synthesized complexes and their ligands were studied. Results showed that orally administration of $HgCl_2$ for 30 days caused a significant disruption of male sex hormones and kidney function. Further, the level of lipid peroxidation was elevated and activities of antioxidant enzymes were markedly declined in kidney and testes homogenates. The co-administration of $HgCl_2$ with antipyrine and thiosemicarbazone as well as their complexes for four weeks led to amelioration in the kidney and testes functions as the levels of male sex hormones and kidney function tests were recovered. Meanwhile, these compounds showed ameliorative effects on the oxidative status of rats. It can be concluded that drinking of Hg-polluted water induces oxidative stress pathways that may lead to deterioration in kidney and testes function. The findings also suggest the curative action of antipyrine and thiosemicarbazone as well as their complexes since they exhibited the ability to resist the harmful action of mercury and to protect the organs from the action of free radicals.

* Corresponding Author: E-Mail: h_ganzory@yahoo.com

[a] Department of Environmental Biotechnology, Genetic Engineering & Biotechnology Research Institute, Sadat University, Egypt.

[b] Department of Chemistry, College of Science, Qassim University, KSA.

[c] Department of Biochemistry, College of Medicine, Qassim University, KSA.

endocrine glands include the hypothalamus, pituitary, thyroid, parathyroid, adrenal gland, pancreas, and gonads (ovary and testis). Hormones are natural secretory products of the endocrine glands and travel via the blood to exert their effects at distant target tissues or organs by binding to specific cell surfaces or nuclear receptors.

Many researchers reported that mercury promotes the formation of reactive oxygen species (ROS) such as hydrogen peroxide. ROS enhance the subsequent iron- and copper-induced production of lipid peroxides and the highly reactive hydroxyl radical.⁶ These lipid peroxides and hydroxyl radical may cause the cell membrane damage and thus destroy the cell. Inorganic mercury also inhibits the activities of the free radical quenching enzymes catalase, superoxide dismutase and glutathione peroxidase.⁷

Thiosemicarbazone is an emerging moiety with wide spectrum of biological activity and having sound scope in research and developing process in pharmaceutical and medicinal chemistry.⁸⁻¹¹ Thiosemicarbazones are of considerable interest because of their chemistry and potentially beneficial biological activity, such as antibacterial antifungal,¹² antiviral,¹³ antiamoebic,¹⁴ antimalarial^{15,16} and antitumor activity.¹⁷ The biological activities of thiosemicarbazones are considered to be due to their ability to form chelates with metals. Biological activities of metal complexes differ from those of either ligands or the metal ions and increase and/or decreased biological activities are reported for several transition metal complexes. Thiosemicarbazone are versatile compounds, two structural isomers (E and Z forms) are possible and they can co-ordinate to the metal either as a neutral ligand or as a

INTRODUCTION

Mercury is one of the oldest chemical elements used in human applications. It is a highly toxic metal that results in a variety of adverse neurological, renal, respiratory, immune, dermatological, reproductive and developmental disorders.¹ Its wide industry-related effects on human and animal biosystems have been well documented² and general exposure to this biologically-active chemical agent has been shown to be exacerbated through contaminated water and food.³

Inorganic mercury is widely used in certain types of batteries and continues to be an essential component of fluorescent light bulbs.⁴ Inorganic mercury is the most common form that is present in drinking water but is not considered to be very harmful to human health, in terms of the levels found in drinking water.⁵

The endocrine system is one of the three important integrating and regulatory systems in the human body. The other two are the nervous and immune systems. The major

deprotonated ligand through the N, S atoms. Thiosemicarbazones have been frequently employed for the quantitative determination of inorganic ions.¹⁸

Pyrazoles is a five-membered heterocyclic system.¹⁹ Many synthetic compounds containing pyrazole moiety are active in the field of medicinal chemistry.²⁰ One of the pyrazole derivatives, 4-aminoantipyrine has played an important role in inorganic chemistry; it forms stable complexes with many transition metal ions. 4-aminoantipyrine and its complexes have found applications in analytical, biological and clinical areas.^{21,22} Antipyrine derivatives are used as anti-inflammatory^{23,24} and chemotherapeutic agents.²⁵ 4-aminoantipyrine is an intermediate in the synthesis of antipyretic and analgesic drugs²⁶ and it is also active against a wide range of microorganisms viz *E.coli*, *Pseudomonas aeruginosa*, *Staphylococcus aureus* and *Candida albicans*.

The target of this work is to synthesis and characterization of new mercury complexes of thiosemicarbazones and antipyrine ligands. The potential protective effects of the synthesized compounds against mercury disruption of male sex hormones in rats were evaluated.

EXPERIMENTAL

All organic compounds and the solvents were purchased from Fluka or Merck (Nasr City, Egypt) and used without further purification.

Synthesis of ligands and Hg(II) complexes

Preparation and characterization of 2-phenyl-aminoacetyl-N-phenylhydrazine-carbothioamide (H_2L^1), 4-formylazohydrazoaniline antipyrine (H_2L^2) and [2-(2-(2,5-dihydro-2,3-dimethyl-1-phenyl-1H-pyrazol-4-yl-5-one)hydrazonemalononitrile] (HL^3) have been reported.²⁷⁻²⁹ The Hg(II) complexes of the ligands were prepared by adding stoichiometric amount of the Hg (II) chloride, sulphate and nitrate in EtOH to the ligands in EtOH in a 1:1 molar ratio. The reaction solution was stirred magnetically at 60°C for 5-9 h. The resulting solids were filtered off, washed several times with EtOH and dried under vacuum over P_4O_{10} .

Physical measurements

Elemental analysis (C, H and Cl) was performed at microanalytical unit of the Cairo University, Egypt. FT-IR measurements were performed (4000–400 cm^{-1}) in KBr with Neneus-Nicolidite-640-MSAFT-IR (Thermo-Electronics Co.) Spectrometer at the Central Lab., Minufiya University, Egypt. ¹HNMR spectra were recorded in DMSO- d_6 using 300 MHz Varian NMR spectrometer (Microanalytical Lab., Cairo University, Egypt). The molar conductivity measurements were made in DMF solution ($10^{-3}M$) using a Tacussel conductometer type CD6N. The electronic spectra were carried out as solution ($10^{-3}M$) in DMF using a Perkin-Elmer Lambda 4B spectrophotometer.

Thermal analysis (DTA/TG) were obtained out by using a Shimadzu DTA/TG-50 Thermal analyzer (Central Lab,

Minufiya University, Egypt) with a heating rate of 10°C min⁻¹ in nitrogen atmosphere with a following rate 20°C min⁻¹, in the temperature range 25 – 600°C using platinum crucibles.

Preparation of compounds and mercury-poisoned water

Newly synthesized derivatives of pyrimidine complexes were dissolved in DMSO to obtain the concentration of 1 mM. These stock solutions were stored at 4°C for further use.

To prepare a stock solution of 1000 ppm of mercury in drinking water, 1.35 g of HgCl₂ was dissolved in 1 litre of water. One milliliter of this solution was mixed with 10 litres of distilled water to obtain water containing mercury at a concentration of 1 ppm.

Animals grouping

Adult male albino rats, weighing about 160 ± 10 g, were housed at 23 ± 2°C and in daily dark/light cycle. They were caged in the animal house of College of Medicine, Qassim University and under standard condition and fed standard chow and water ad libitum.

All experiments were carried out in accordance with protocols approved by the local experimental animal ethics committee. After acclimatization, rats were divided into twelve groups each comprising of eight animals. Normal group (N) in which rats were maintained only on standard pellet diet and water ad libitum. HgCl₂-intoxicated drinking water group, in which, rats were maintained on drinking water intoxicated with 0.5 ppm of HgCl₂ for 30 days. The groups number 3 to 12 include animals co-treated with 0.5 ppm of HgCl₂-poisoned drinking water and 0.1mM of newly synthesized compounds for 30 days. During the course of the 30-day long experiment no animal was died.

Collection of blood and tissues' specimens

At the end of experiments, animals were sacrificed using a sharp razor blade. The blood was collected in prechilled heparinized centrifuge tubes. Plasma specimens were then obtained by centrifugation for 10 minutes at 4000 rpm at 4°C and were kept in clean well-stoppard vials at -20°C until assayed. The kidney and testes were removed and cut into pieces.

Preparation of testes and kidney homogenate

Kidney and testes homogenates were prepared by using a mechanical homogenizer (Potter-Elvehjem) in a 10-fold volume of ice-cold of 20 mM tris-HCl buffer (pH 7.4). The homogenate was centrifuged at 5000 rpm for 30 minutes at 4°C to remove cell debris and nuclei. The supernatant liquid was collected, aliquoted and kept frozen at -20°C for further investigations.

Determination of superoxide dismutase activity

Superoxide dismutase (SOD) activities in kidney and testes homogenates were estimated according to the procedure of Nishikimi et al.³⁰ and by following the manufacturer's procedure (Biodiagnostics, Egypt).

Table 1. Analytical and physical data for the ligands and Hg(II) complexes

No.	Complexes	Color	Yield (%)	Mol. Wt.	Found (Calc.) %					\square_M^a
					C	H	N	M	Cl	
1	[Hg(H ₂ L ¹)Cl ₂ (H ₂ O) ₂]. H ₂ O	Pale brown (60)	625.6	28.6 (28.8)	3.3(3.5)	8.9(9.0)	32.3(32.0)	11(11.3)	24	
2	[Hg(H ₂ L ¹)SO ₄ (H ₂ O)]	Pale yellow (65)	613.6	29.5 (29.3)	3.0(2.8)	9.2 (9.1)	32.8(32.6)	-	15	
3	[Hg(HL ¹) ₂]	Pale yellow (60)	798.6	45.0 (45.1)	3.9(3.8)	13.9(14.0)	25.2(25.1)	-	18	
4	[Hg ₂ (HL ²)(OH) ₂ Cl]	Yellow (70)	870.5	29.2 (29.0)	2.5(2.3)	11.4(11.3)	46.2(46.0)	4.2(4.1)	10	
5	[Hg(HL ²)(NO ₃)(H ₂ O)]	Brown (70)	680.6	37.2 (37.0)	3.0(3.0)	14.4(14.4)	29.7(29.5)	-	20	
6	[Hg(HL ³)(SO ₄)]	Yellow (70)	594.6	28.4 (28.5)	2.2(2.4)	14.3(14.1)	33.6(33.7)	-	Insol.	
7	[Hg(HL ³)(NO ₃) ₂]	Brown (60)	604.6	27.7 (27.8)	1.8(2.0)	14.2(13.9)	33.0(33.2)	-	18	

^a \square_M = molar conductivity ohm⁻¹ cm² mol⁻¹ in 10⁻³ M DMF

Table 2. Fundamental IR spectral bands (cm⁻¹) for the ligands and Hg(II) complexes

Compound	$\nu_{(O-H)}/\nu_{(N4-H)}$	$\nu_{(N1-H)}$	$\nu_{(N2-H)}$	$\nu_{(C=O)^a}$	$\nu_{(C=O)^b}$	$\nu_{(C=N)^c}/\nu_{(C=S)^d}$	$\nu_{(M-O)}$	$\nu_{(M-N)}$
H ₂ L ¹	3463	3340	3250	1677	-	747 ^d	-	-
[Hg(H ₂ L ¹)Cl ₂ (H ₂ O) ₂]. H ₂ O	3393	-	3100	1700	-	752 ^d	614	507
[Hg(H ₂ L ¹)SO ₄ (H ₂ O)]	3390	-	3100	1698	-	751 ^d	615	510
[Hg(HL ¹) ₂]	3402	-	3108	-	-	749 ^d	607	506
H ₂ L ²	3430	-	-	1645	1635	1536 ^c	-	-
[Hg ₂ (HL ²)(OH) ₂ Cl]	3435	-	-	-	1625	1552 ^c	593	536
Hg(HL ²)(NO ₃)(H ₂ O)	3438	-	-	-	1612	1534 ^c	640	454
HL ³	3410	-	-	-	1630	1587	640	477
[Hg(HL ³)(SO ₄)]	3434	-	-	-	1609	1496	574	443
Hg(HL ³)(NO ₃) ₂	3429	-	-	-	1607	1495	582	445

^a (C=O) of side chain, ^b (C=O) of pyrazolone ring, ^c (C=N), ^d (C=S)

Determination of catalase activity

Antioxidant enzyme catalase (CAT) activities in kidney and testes homogenates were determined according to the method of Bergmayer³¹ as described in the manufacturer's procedure (Biodiagnostics, Egypt).

Determination of lipid peroxidation level

The levels of lipid peroxides (LPO) in kidney and testes homogenates were estimated colorimetrically by measuring malondialdehyde (MDA) using the method of Ohkawa et al and by following the manufacturer's procedure (Biodiagnostics, Egypt).³²

Determination of testosterone level

Level of testosterone in testes homogenate was processed by using Fertigenix Testo-ELISA kit (Biosource, Belgium) in accordance with the protocol described by Park et al.³³

Determination of follicle-stimulating hormone level

Follicle stimulating hormone (FSH) concentration was estimated in testes homogenate with IMMULITE analyzer according to the method of Odell et al³⁴ using IMMULITE FSH kit purchased from EURO/DPC Ltd., USA.

Determination of leutinizing hormone level

Leutinizing hormone (LH) concentration was estimated in testes homogenate according to the method of Knobil³⁵ using LH kit purchased from Ameritek (USA) with Vmax ELISA reader

Determination of fructose level

Fructose concentration was estimated in testes homogenate spectrophotometrically according to the method of Karvonen and Malm.³⁶ Briefly, fructose in presence of hydrochloric acid forms a pink colored complex with indole-3-acetic acid. The complex has maximum absorbance at 500-530 nm.

Statistical analysis

Results are expressed as mean \pm S.D. The data for various biochemical parameters were analyzed using analysis of t-test and the group mean was compared by one-way ANOVA. Values were considered statistically significant at $P < 0.05$.

RESULTS AND DISCUSSION

Physical properties

The reaction of the ligands with Hg(II) chloride, sulphate and nitrate give complexes of general formulae $[\text{Hg}(\text{H}_2\text{L}^1)\text{Cl}_2(\text{H}_2\text{O})_2] \cdot \text{H}_2\text{O}$, $[\text{Hg}(\text{H}_2\text{L}^1)\text{SO}_4(\text{H}_2\text{O})]$, $[\text{Hg}(\text{HL}^1)_2]$, $[\text{Hg}_2(\text{HL}^2)(\text{OH})_2\text{Cl}]$, $[\text{Hg}(\text{HL}^2)(\text{NO}_3)(\text{H}_2\text{O})]$ and $[\text{Hg}(\text{HL}^3)\text{XY}]$, where X = SO_4 or NO_3 and Y = O or NO_3 (Table 1). While the reaction of H_2L^2 with Hg(II)sulphate and HL^3 with Hg(II)chloride produce decomposed products. All Hg(II) complexes are freely soluble in DMF and DMSO except complex (6), which is insoluble in DMF and DMSO. The molar conductivity of all Hg(II) complexes in DMF solution (10^{-3} M) at room temperature indicate that all complexes are non-electrolyte.³⁷

FT-IR For H_2L^1 ligand and Hg(II) complexes

The diagnostic IR bands for ligand 2-phenylaminoacetyl-N-phenylhydrazine-carbothioamide (H_2L^1) and Hg(II) complexes (1-3) are listed in Table 2. The most important four bands, exhibited by ligand (H_2L^1) at 3463 cm^{-1} , 3340 cm^{-1} , 1677 cm^{-1} and 747 cm^{-1} are assigned to $\nu(\text{N-H})$, $\nu(\text{N1-H})$, $\nu(\text{N2-H})$, and $\nu(\text{C=S})$ vibrations, respectively. The bands at 1500 cm^{-1} , 1440 cm^{-1} and 1280 cm^{-1} may be due to $\nu(\text{N-C=S})$.³⁸

The bands at 3100 cm^{-1} , 1700 - 1698 cm^{-1} and 752 cm^{-1} seen in the complexes (1) and (2) have been assigned to $\nu(\text{N2-H})$, $\nu(\text{C=O})$ and $\nu(\text{C=S})$ respectively. The IR spectrum of the complex (3) shows that bands due to $\nu(\text{C=O})$ and $\nu(\text{N2-H})$ disappear up on complexation and a new band appeared at 1600 cm^{-1} , which has been assigned to $\nu(\text{C=N})$.

For H_2L^2 , HL^3 and Hg(II) complexes (4-7) the IR data are presented in Table 2. The IR spectra of the free ligands (H_2L^2 and HL^3) show four bands at 3430 cm^{-1} , 3434 cm^{-1} ; 2210 cm^{-1} , 2205 cm^{-1} ; 1645 cm^{-1} , 1630 cm^{-1} ; and 1610 - 1587 cm^{-1} , assigned to $\nu(\text{N-H})$, $\nu(\text{C}\equiv\text{N})$, $\nu(\text{C=O})$ of side chain, $\nu(\text{C=O})$ of pyrazolone ring and $\nu(\text{C=N})$ respectively. The infrared spectra of complexes (6 and 7) show a decrease in the energy of $\nu(\text{C=O})$ of side chain, $\nu(\text{C=O})$ of pyrazolone ring and $\nu(\text{C=N})$ up on complex formation, indicating that carbonyl oxygen of C=O of side chain, C=O of pyrazolone ring and C=N participate in coordination. While in complexes(4 and 5) the bands corresponding to $\nu(\text{C=O})$ of side chain and $\nu(\text{N-H})$ disappear indicating that the ligand is in enolimino form and new bands appears at 1552 cm^{-1} , 1537 cm^{-1} , assigned to $\nu(\text{C=N})$ up on complexation.

The IR spectra of all Hg (II) complexes show new two bands at 640 - 574 cm^{-1} and 536 - 443 cm^{-1} , assigned to $\nu(\text{Hg-O})$ and $\nu(\text{Hg-N})$.^{39,40} However, complexes (1 and 4)

exhibit medium bands at 320 and 325 cm^{-1} due to $\nu(\text{Hg-Cl})$.⁴¹ Also in the complexes (2 and 6) strong band appears at 1110 - 1178 cm^{-1} , assigned to unidentate sulphate moiety.⁴²

The IR spectra of complexes (5 and 7) show strong bands at 1379 - 1390 cm^{-1} , assigned to monodentate of nitrate group. While complexes (1, 2, 4 and 5) reveal broad bands at 3390 - 3435 cm^{-1} and 765 - 878 cm^{-1} assigned to $\nu(\text{Hg-O})$ of coordinated water except in complex (4) only appears a band at 3435 cm^{-1} , assigned to coordination of Hg(II) with the hydroxy group.

Table 3. Electronic spectral bands of the Hg(II) complexes

No.	Complexes	λ_{max} nm
1	$[\text{Hg}(\text{H}_2\text{L}^1)\text{Cl}_2(\text{H}_2\text{O})_2] \cdot \text{H}_2\text{O}$	270
2	$[\text{Hg}(\text{H}_2\text{L}^1)\text{SO}_4(\text{H}_2\text{O})]$	268
3	$[[\text{Hg}(\text{HL}^1)_2]$	267
4	$[\text{Hg}_2(\text{HL}^2)(\text{OH})_2\text{Cl}]$	268, 402
5	$[\text{Hg}(\text{HL}^2)(\text{NO}_3)(\text{H}_2\text{O})]$	266, 401
6	$[\text{Hg}(\text{HL}^3)(\text{SO}_4)]$	268, 389
7	$[\text{Hg}(\text{HL}^3)(\text{NO}_3)_2]$	267, 387

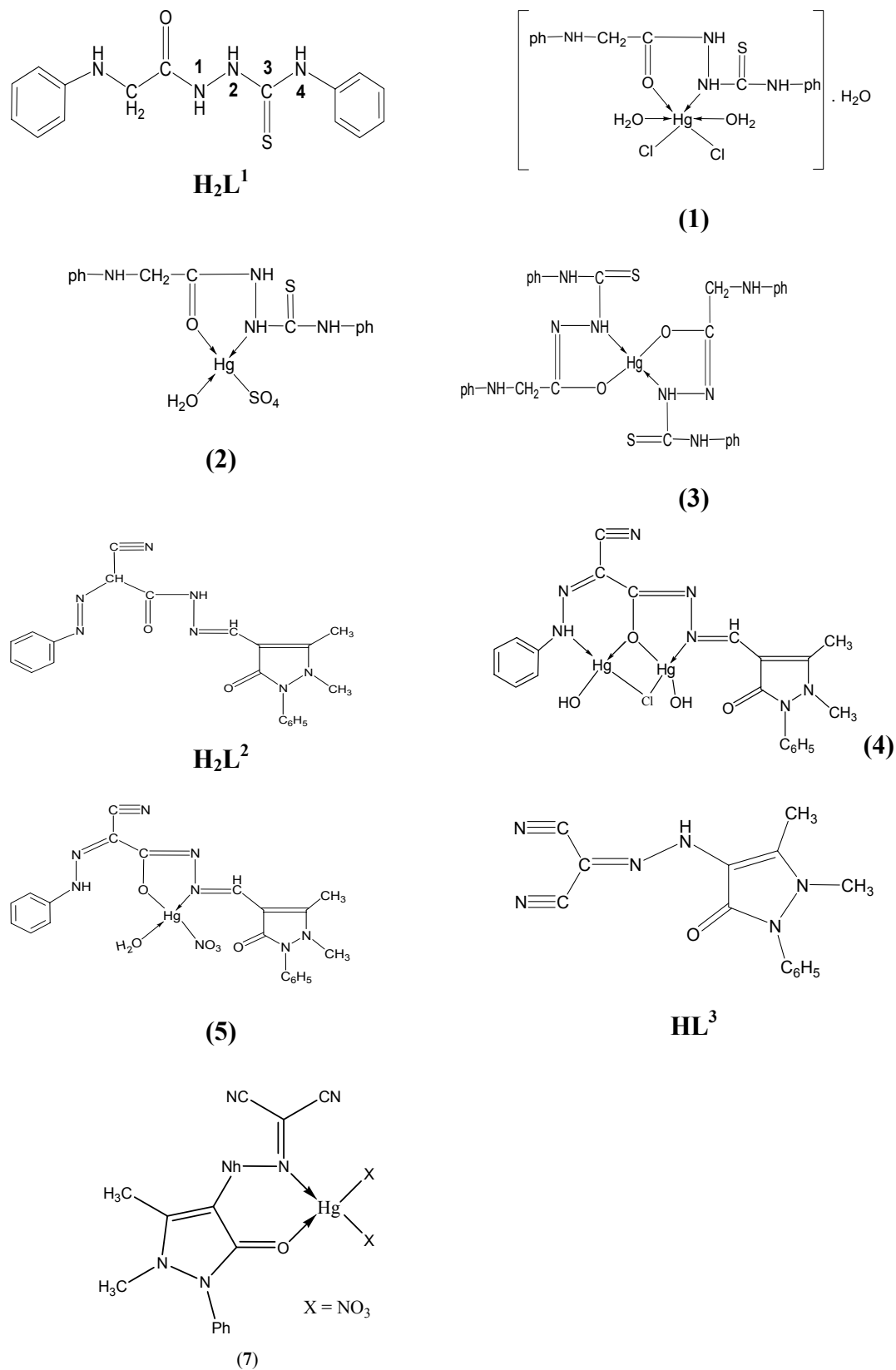
Electronic spectra

The data of electronic spectra of Hg(II) complexes (1-7) are given in Table 3. The absorption spectra of Hg(II) complexes were recorded in DMF solutions (10^{-3} M) in the range 190 - 800 nm using a quartz cuvette of 1 cm path length.

The complexes show only the charge transfer transitions which can be assigned to charge transfer from the ligand to the metal and these ions have the d^{10} configuration and therefore, their complexes should not exhibit any d-d transition. All of complexes of these Hg(II) ions were found to be diamagnetic.⁴³ The absorption bands of Hg(II) complexes observed listed in Table 3. Probable structures of the ligands and complexes are given in Scheme 1.

Thermal studies for Hg(II) complexes

Thermal analyses have been carried out using differential thermal analysis (DTA) and thermogravimetric analysis (TGA) techniques. The thermal behaviour carried out in temperature range 25 - 600°C . DTA and TGA curves recorded for the complexes in an atmosphere of nitrogen and important data are summarized in Table 4. The various steps of the decomposition of the compound with the corresponding mass loss in terms of the proposed formulas for the complexes are given. The Hg(II) complexes (1 and 5) show the three exothermic peaks each. While, complexes (2, 3 and 4) exhibit two broad exothermic and one endothermic DTA peaks.



Scheme 1. Chemical structure of ligands and their Hg(II) complexes

However, in Hg(II) complex (7) one strong exothermic DTA curve in temperature range 200-233°C appears, which has been assigned to loss of ((0.8L + 2HNO₃) and (2CO + 3C),⁴⁴ as shown from TG mass loss in that temperature range. The initial decomposition temperature has been used as an indicator of the thermal stability of the complexes. The results of the thermal analysis of the mercury complexes indicated that complex (3) is thermally more stable compared to the rest of mercury(II) complexes.

Evaluation of kidney function

Serum creatinine level is one of the traditional screening indices for kidney function and renal structure epithelium.⁴⁵ The effects of mercuric chloride on the biochemical tests of renal function in the animals are presented in table 5. After drinking water poisoned with 0.5 ppm of HgCl₂ for 30 days, a statistically significant increase of creatinine and urea concentrations in plasma was observed as compared with control groups. The elevation in creatinine level after exposure to inorganic mercury is accordance with the report of Oriquat et al. in rats.⁴⁶ The rise in creatinine level might be due to damage caused to kidney tubules by inorganic mercury. Co-treatment with different ligands and their complexes caused amelioration on renal function. Results showed that ligands H₂L¹, H₂L² and HL³ and their complexes, except complex (4), significantly reduced (P<0.05) the elevated renal function markers.

Evaluation of oxidative status

The level of malodialdehyde (MDA) is widely used as a marker of free radical mediated lipid peroxidation (LPO). The results of the LPO assays in the kidney and testes homogenates are shown in Table 6. LPO level increased significantly in the kidney and testes homogenates of rats after exposure to 0.5 ppm of mercury for 30 days as

compared to the normal group. The mercuric chloride toxic effect is due to its ability to adhere or to form link with cell enzymes of the respiratory chain and proteins, which alter the metabolism of target cells in organs participating in its elimination. Mercury also provokes a reactive oxygen species (ROS)-dependent vascular damage producing large scale haemorrhage in many organs like kidney. This ROS was significantly reduced when animals were supplemented with various ligands and their complexes showing the ameliorative effects of these compounds.

Results shown in Table 6 revealed that ligands H₂L¹, H₂L² and HL³ significantly reduced the elevated levels of LPO in testes and kidney tissues showing their ability to scavenge free radicals. Meanwhile, their complexes exhibited varied effects on LPO in testes and kidney, where complexes (3, 6 and 7) showed no antioxidative activities as compared to HgCl₂- treated group.

Oxidative stress defines an imbalance between the formation of ROS and antioxidative defence mechanisms. Drinking of HgCl₂-poisoned water for 30 days generated the ROS and caused oxidative stress in intoxicated animals. In oxidative stress, LPO is occurred due to excessive free radical production and is considered a primary mechanism of cell membrane destruction and cell damage. Malondialdehyde (MDA) is the end product of lipid peroxidation.

The toxicity with inorganic mercury increased the testicular MDA and simultaneously decreased the CAT and SOD activities in this study. CAT and SOD were estimated in the kidney and testes homogenates. Results showed that administration of 0.5 ppm of HgCl₂ in drinking water for 30 days significantly decreased the activities of CAT and SOD as compared to those of the normal control group (Table 6).

Table 4. Thermal data of Hg(II) complexes

No.	Complex	DTA ^o C	TGA ^o C	Mass loss %Cal. (F.)	Leaving species
1	[Hg(H ₂ L ¹)Cl ₂ (H ₂ O) ₂]. H ₂ O	97- 201	87 -173	2.8(2.9)	-H ₂ O
		288- 337	193-272	11.5(11.3)	-(2H ₂ O +HCl)
		338-447	294-355	17.8(18.0)	-(HCl+0.25L)
			405- 468	17.0(17.2)	-(C ₆ H ₅ NHCH ₂)
2	[Hg(H ₂ L ¹)SO ₄ (H ₂ O)]	130-180	111- 165	2.9(2.7)	-H ₂ O
		227-274	188-335	39.8(40.3)	-(0.6L+SO ₂)
		293 -329	394-424	9.1(9.5)	-2CO
3	[Hg(HL ¹) ₂]	210-257	111 -117	3.6(3.3)	-(CH ₂ NH)
		413 -450	200-289	14.9 (14.8)	-(C ₆ H ₅ +C ₂ H ₂ O)
		505 -550	340-411	13.3 (13.5)	(C ₆ H ₅ NHCH ₂)
			459-509	14.8 (14.4)	(C ₆ H ₅ NH+ C ₂ H ₂)
4	[Hg ₂ (HL ²)(OH) ₂ Cl]	229- 256	176 -247	16.9(17.0)	(2OH + HCl + C ₆ H ₅)
		280-322	263- 335	50.6(50.3)	(0.6L+Hg)
		504-550	Above 335		Thermal stability
5	Hg(HL ²)(NO ₃)(H ₂ O)	232-271	192-280	18.1 (18.4)	(H ₂ O+
		301- 335	297 -379	40.8 (40.4)	HNO ₃ +C ₂ H ₂ O)
		370-408	Above 379		-(0.5L +C ₆ H ₅)
7	Hg(HL ³)(NO ₃) ₂	200-238	170-238	57.9 (57.7)	- (0.8L+2HNO ₃)
			344 -410	13.9 (13.6)	- (3CO)

On the other hand, rats that were supplemented with ligands and their complexes together with HgCl₂ for 30 days experienced significant increase in CAT and SOD activities when compared to the HgCl₂-treated group. Ligands H₂L¹, H₂L² and HL³ exhibited higher stimulatory effect on the activities of CAT and SOD in testes and kidney tissues as compared to their complexes.

Table 5. Effect of different ligands and their Hg complexes on renal function parameters

Group	Creatinine (mg dL ⁻¹)	BUN (mg dL ⁻¹)
Normal	0.7±0.1	10.4±1.0
HgCl ₂	2.9±1.4	20.8±2.8
HgCl ₂ + H ₂ L ¹	1.6±0.5*	11.0±0.9*
HgCl ₂ + 1	1.9±0.3*	17.6±2.1*
HgCl ₂ + 2	1.3±0.5*	15.2±4.4*
HgCl ₂ + 3	2.1±0.6*	21.8±1.9
HgCl ₂ + H ₂ L ²	0.8±0.2*	11.7±3.1*
HgCl ₂ + 4	2.1±0.6	26.0±5.7
HgCl ₂ + 5	1.7±0.3*	16.8±1.9*
HgCl ₂ + HL ³	0.8±0.3*	10.8±2.8*
HgCl ₂ + 6	1.5±0.4*	15.0±3.8*
HgCl ₂ + 7	2.3±0.9	20.2±2.4

These complexes showed diverse antioxidant actions on the activities of CAT and SOD, where, complexes (3, 6 and 7) did not show ameliorative actions on the activities of CAT and SOD.

Evaluation of some male sex hormones

The mean values of the serum hormones; testosterone, luteinizing hormone (LH) and follicle stimulating hormone (FSH) are shown in Table 7. Results showed that after drinking of 0.5 ppm of HgCl₂-poisoned water for 30 days led to significant decreases ($P < 0.05$) in the levels of testosterone, LH and FSH as compared to the control group. The levels of male sex hormones were restored to control

Table 6. Effect of different ligands and their Hg complexes on the oxidative status in kidney and testes

Group	CAT U g tissue ⁻¹		SOD U g tissue ⁻¹		LPO nmol g tissue ⁻¹	
	Kidney	Testes	Kidney	Testes	Kidney	Testes
Normal	3.5±0.6	5.9±0.7	122.5±11.4	155.2±13.8	135.3±16.7	152.2±9.1
HgCl ₂	1.1±0.3	1.3±0.5	76.8±8.3	92.8±11.1	230.8±23.9*	252.8±16.5
HgCl ₂ + H ₂ L ¹	3.1±0.8*	6.1±0.5*	121.6±10.3*	151.6±12.2*	142.5±21.8*	150.0±12.1*
HgCl ₂ + 1	2.9±0.5*	5.9±0.4*	115.6±9.4*	155.6±10.2*	134.3±13.9*	150.2±21.9*
HgCl ₂ + 2	2.2±0.8*	4.2±0.2*	116.6±12.3*	156.6±15.5*	133.2±14.2*	154.2±4.5*
HgCl ₂ + 3	1.5±1.1	1.8±0.8	72.6±7.7	92.1±9.8	225.0±21.3	248.6±24.5
HgCl ₂ + H ₂ L ²	3.2±0.7*	6.2±0.5*	117.8±10.3*	137.8±11.5*	152.6±15.3*	151.2±14.0*
HgCl ₂ + 4	2.2±0.8*	5.2±0.3*	108.0±13.1*	121.0±15.0*	159.2±14.2*	159.4±13.5
HgCl ₂ + 5	2.1±0.6*	5.1±0.2*	118.4±9.6*	133.4±8.8*	152.6±15.3*	165.7±16.3*
HgCl ₂ + HL ³	4.2±1.4*	6.2±0.4*	119.6±7.7*	159.6±11.8*	142.6±15.3*	153.2±12.4*
HgCl ₂ + 6	1.1±0.3	2.1±0.2	63.2±9.8	83.2±10.8	222.6±18.9	245.6±10.1
HgCl ₂ + 7	0.9±0.1	1.5±0.3	62.5±5.5	92.5±9.9	220.6±17.9	253.3±11.0

values after combination of HgCl₂ with studied ligands and some of their complexes. The tested complexes showed varied effects on the level of male sex hormones. In contrast to their complexes, ligands exhibited potent stimulatory actions on the levels of testosterone, LH and FSH.

Testosterone is essential for spermatogenesis completion because it stimulates the conversion of round spermatids into elongated spermatids between stages VII and VIII of the spermatogenic cycle. Thus, testicular testosterone deficiency as observed in this study after exposure to HgCl₂ for 30 days will impair the spermiation process.⁴⁷

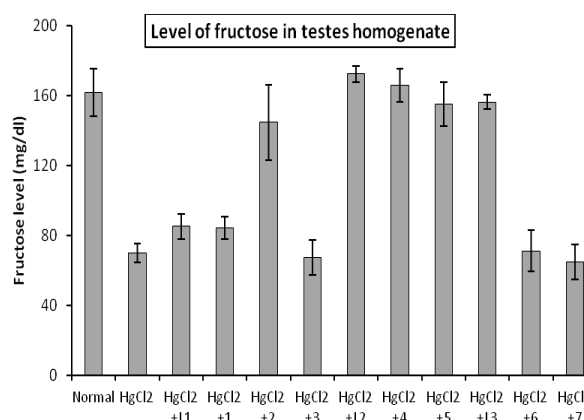


Figure 1. Effect of HgCl₂ and tested compounds on the levels of testicular fructose

Fructose provides energy for sperm motility.⁴⁸ As shown in Figure 1, level of fructose is significantly reduced ($P < 0.05$) in rats after exposure to Hg-intoxicated water for 30 days as compared to that of the control group. Different effects of tested ligands and their complexes on the level of testicular fructose were observed. Results indicate that tested ligands restored the fructose levels to that of the normal animals, while, some complexes did not ameliorate the fructose levels.

Table 7. Levels of testosterone, luteinizing hormone and follicle-stimulating hormone in testes of animals of different studied groups

Groups	Testosterone (ng g ⁻¹)	LH (ng g ⁻¹)	FSH (ng g ⁻¹)
Normal	121.8±2.2	47.2±2.6	34.7±1.5
HgCl ₂	85.6±8.6	20.2±1.9	15.7±1.5
HgCl ₂ + H ₂ L ¹	103.0±5.7*	34.8±7.4*	23.7±1.5*
HgCl ₂ + 1	93.4±9.4*	24.8±0.8	25.3±2.1
HgCl ₂ + 2	102.2±4.5*	20.6±2.4	30.7±4.0*
HgCl ₂ + 3	74.2±10.3	19.8±3.8	17.3±5.0
HgCl ₂ + H ₂ L ²	99.2±7.9*	37.6±6.3*	29.3±1.5*
HgCl ₂ + 4	85.2±9.4	45.2±2.4*	21.3±0.6*
HgCl ₂ + 5	101.4±3.2*	16.4±3.2	32.7±1.5*
HgCl ₂ + HL ³	126.8±4.4*	41.6±2.1*	30.3±2.1*
HgCl ₂ + 6	89.2±3.0	23.2±4.0	13.7±3.2
HgCl ₂ + 7	77.8±9.1	19.6±5.3	15.3±1.5

CONCLUSION

In our study, we characterized mercury(II) complexes of ligands (2-phenylaminoacetyl-N-phenylhydrazine carbothioamide (H₂L¹), 4-formylazohydrazoanilinoantipyrine (H₂L²) and [2-(2-(2,5-dihydro-2,3-dimethyl-1-phenyl-1H-pyrazol-4-yl-5-one)hydrazono)malononitrile] (HL³) using different analytical and spectroscopic methods. The IR spectral show that the ligand of complexes (2) and (5) behave as mono basic bidentate, coordination take place by (C-O) and N(2)H or (C=N). While the ligand of complexes (1, 6 and 7) behave as neutral bidentate and coordination via (C=O) and N(2)H or (C=N) groups. On the other hand, the ligand for complexes (3 and 4) produce mono, dibasic tetradentate and chloro bridge of binuclear complex (4). All complexes are tetrahedral geometry except complex (1) is octahedral geometry and diamagnetic of d¹⁰ of Hg(II) ions. The thermal behavior study showed that complex (3) is more stable as compared of the rest of Hg(II) complexes.

Further it has been shown that mercury causes severe toxic tissue damage in the testis and kidney of rats. This damage may be caused by the ROS produced by mercury within the animals' body. The tested ligands and some of their Hg complexes showed varied effects against mercury toxicity. They interacted with mercury ions, neutralize them and prevent the ROS mediated oxidative damage in testes.

ACKNOWLEDGMENT

The authors would like to thank the Scientific Research Deanship, Qassim University, Saudi Arabia, for financial support of this research project (SR-S-14-16 Sabc).

REFERENCES

¹Risher, J. F., Amler, S. N., *Neurotoxicol.*, **2005**, 26(4), 691–699.

²Sameha, M., Mohamed, L. T., Abdelkader, O., Nadia, B., Bruno, B., Abdelkrim, T., Abdelmadjid, B., *J. Cell Anim. Biol.*, **2009**, 3(12), 222-230.

³Magos, L., Clarkson, T. W., *J. Ann. Clin. Biochem.*, **2006**, 3, 257-268.

⁴Clarkson, T. W., *Crit. Rev. Clin. Lab. Sci.*, **1997**, 34, 369–403.

⁵Dilek, D., Suna, K., Fatma G. U., Filiz, D., Yusuf, K., *Afr. J. Biotechnol.*, **2010**, 9(4), 488-495.

⁶Brandão, R., Santos, F. W., Zeni, G., Rocha, J. B., Nogueira, C. W., *Biomaterials*, **2006**, 19(4), 389-98.

⁷Parekh, A. K., Desai, K. K., *Indian J. Chem.*, **2006**, 45B, 1072.

⁸Chandra S., Gupta L.K., *Spectrochimica Acta Part A*, **2005**, 62, 1089.

⁹Demertzi, D. K., Miller, J. R., Kourkoumelis, N., Hadzikakaou, S. K., Demertzis, M. A., *Polyhedron*, **1999**, 18, 1005.

¹⁰Ferrari, B. M., Fava, G. G., Leperti, E., Pelosi, G., Rossi, R., Tarasconi, P., Albertini, R., Bonati, A., Lunghi, P., Pinelli, S., *J. Inorg. Biochem.*, **1998**, 70, 145.

¹¹Ferrari, M. B., Capacchi, S., Reffo, G., Aelosi, G., Tarasconi, P., Albertini, R., Pinellis, S., Lunghi, P., *J. Inorg. Biochem.*, **2000**, 81, 89.

¹²Sandeep, K., Nitin, K., *Inter. J. Res. Pharm. Biomed. Sci.*, **2013**, 4(1), 305-3011.

¹³Lobana, T. S., Butcher, R. J., Castineiras, A., Bermejo, E., Bharatam, P. V., *J. Inorg. Chem.*, **2006**, 45, 1535.

¹⁴Sharma, S., Athar, F., Maurya, M. R., Azam, A., *Eur. J. Med. Chem.*, **2005**, 40, 1414.

¹⁵Greenbaum, D. C., Mackey, Z., Hansell, E., Doyle, P., Gut, J., Caffrey, C. R., Lehrman, J., Rosenthal, P. J., McKerrow, J. H., Chibale, K., *J. Med. Chem.*, **2004**, 47(12), 3212-9.

¹⁶Lukmantara, A. Y., Kalinowski, D. S., Kumar, N., Richardson, D. R., *Org. Biomol. Chem.*, **2013**, 11(37), 6414-25.

¹⁷Jansson, P. J., Sharpe, P. C., Bernhardt, P. V., Richardson, D. R., *J. Med. Chem.*, **2010**, 53(15), 5759-69.

¹⁸West, D. X., Brain, G. A., Jasinski, J. P., Li, Y., Pozdniakiv, R. Y., Martinez, J. V., Toscano, R. A., Ortega, S. H., *Polyhedron*, **1996**, 15, 665.

¹⁹Acheson, R. M., *An Introduction to Heterocyclic Compounds*, 3rd Edn., John Wiley and Sons, New York, **2009**, 354-364.

²⁰Bansal R. K., *Heterocyclic Chemistry*, 4th Edn., New Age International Publisher, New Delhi, **2010**, 454.

²¹Raman, N., Dhavethuraja, J., Sakthivel, A., *J. Chem. Sci.*, **2007**, 119(4), 303-310.

²²Raman, N., Sakthivel, A., Rajasekaran, K., *J. Mycol.*, **2007**, 35(3), 150-153.

²³Anupama, B., Padmaja, M., Gyana Kumari, C., *E-J. Chem.*, **2012**, 9(1), 389-400.

²⁴Yue, T., Hao, Z., Rutao, L., *J. Mol. Biosyst.*, **2011**, 7(1), 3157-3163.

²⁵Himaja, M., Anish, K. V., Raman, M. A., Karigar, A. A., *J. Pharm. Sci. Innov.*, **2012**, 1(1), 67-70.

²⁶Elemike, E. E., Oviawe, A. P., Otuokere, I. E., *Res. J. Chem. Sci.*, **2011**, 1(8), 6-11.

²⁷Morsy, A. S., Kashar, T., Samar, A., *J. Solid State Sci.*, **2011**, 13, 2080

²⁸El-Sayed, F. A., Ayad, M. I., Issa, R. M., Aly, S. A., *Pol. J. Chem.*, **2000**, 75, 919.

²⁹El-Sayed, F. A., Ayad, M. I., Issa, R. M., Aly, S. A., *Pol. J. Chem.*, **2001**, 75, 773.

³⁰Niskikimi, M., Roa, N.A., Yagi, K., *J. Biophys. Res. Commun.*, **1972**, 46, 849-854.

³¹Bergmayer, H. V., *Methods of Enzymatic Analysis*, 3rd ed., Varly Chem. Weheim, **1983**, 1, 210.

- ³²Ohkawa, H., Wakatsuki, Kaneda, C., *J. Anal. Biochem.*, **1982**, 95, 351–358.
- ³³Park, T. J., Song, K. Y., Sohn, S. H., Lim, I. K., *J. Mol. Carcinog.*, **2002**, 34(3), 151-63.
- ³⁴Odell, W. D., Parlow, A. F., Cargille, C. M., Ross, G. T., *J. Clin. Invest.*, **1968**, 47(12), 2551-2562.
- ³⁵Knobil, E., *Recent Prog. Horm. Res.*, **1980**, 36, 53-88.
- ³⁶Karvonen, M. J., Malm, M., *J. Clin. Lab. Invest.*, **1955**, 7(4), 305.
- ³⁷Hamid G., Maryam, R., *J. Curr. Chem. Lett.*, **2013**, 2, 207.
- ³⁸Rao, C. N., Enkataraghavan, R. V., *Spectrochim. Acta Part A*, **1962**, 18, 541.
- ³⁹Prakash, D., Kumar, C., Prakash, S., Gupta, A. K., Singh, K. R., *J. Indian Chem. Soc.*, **2009**, 86(12), 1257–1261.
- ⁴⁰Raman, N., Esthar, S., Thangaraja, C., *J. Chem. Sci.*, **2004**, 116(4), 209.
- ⁴¹Nakamoto, K., *Infrared Spectra of Inorganic and Coordination Compounds*, 2nd Ed., Wiley Interscience, New York, **1970**.
- ⁴²Nakamoto, K., *Infrared and Raman Spectra of Inorganic and Coordination Compounds*; Wiley Interscience, New York, **1978**.
- ⁴³Ahmed, M., Khalid, W. Y., Zain, A., *J. Pharma. Biol. Sci.*, **2012**, 4, 09
- ⁴⁴El-Boraey, H. A., Serag, A. A., *Spectrochim Acta A*, **2014**, 132, 663–671.
- ⁴⁵Sheikh, T. J., Patel, B. J., Joshi, D. V., Patel, R. B., Jegoda, M. D., *J. Vet. World*, **2013**, 6(8), 563-567.
- ⁴⁶Oriquat, G. A., Saleem, T. H., Naik, R. R., Moussa, S. Z., Al-Gindy, R. M., *Jordan J. Biol. Sci.*, **2012**, 5(2), 141-146.
- ⁴⁷Arikawe, A. P., Oyerinde, A., Olatunji-Bello, I., Obika, L. O., *Niger. J. Physiol. Sci.*, **2012**, 27, 171 – 179.
- ⁴⁸Elzanaty, S., Richthoff, J., Malm, J., Giwereman, A., *Hum. Reprod.*, **2002**, 17(11), 2904 – 2911.

Received: 22.10.2016.

Accepted: 14.11.2016.



ANTIMICROBIAL POTENTIAL OF THIOPHENE DERIVATIVES OF SYNTHETIC ORIGIN: A REVIEW

Raghav Mishra^{[a]*}, Pramod Kumar Sharma^[a], Prabhakar Verma^[b]
and Isha Mishra^[c]

Keywords: Thiophene, thienopyrimidine, antibacterial, antifungal, antitubercular, minimum inhibitory concentration.

Thiophene, a five membered heterocycle is considered as biologically important dynamic scaffold that holds wide range of biological activities. The fruitful application of Cephoxitin as antimicrobial, Thenaldine as anti inflammatory, Ralitrexed as anticancer and Erdosteine as antioxidant proved the potential of thiophene moiety. Diverse biological response profile has pulled in consideration of many researchers to investigate this heterocycle to its multiple potential against several activities. This review is complementary to previous reviews and focuses to review the work reported on antimicrobial activities of thiophene derivatives.

*** Corresponding Authors**

Phone: +919808632494

E-Mail: raghav.mishra92@gmail.com

[a] Department of Pharmacy, School of Medical and Allied Sciences, Galgotias University, Greater Noida, U. P., 201306, India

[b] Department of Pharmaceutical Sciences, Maharishi Dayanand University, Rohtak, Haryana, 124001, India

[c] HMT College of Pharmacy, Greater Noida, U. P., 201306, India

Introduction

As the world's population increases, the health problems expand accordingly and therefore the development of new therapeutics is essentially vital.¹ A steady increase in complexity of the structure and introduction of different molecular functions has been a highlighted feature of pharmaceutical research and development.² Even today only limited repertoires of synthetic transformations are utilized for the construction of simple structures of drug molecules.

As far as antimicrobial activity is concerned, antibiotics were considered as miracle drugs when first became available about 60 years ago, proving to be the major asset in the fight against infectious bacteria.³ Resistance to antibiotics threatens the effectiveness of successful treatment of infection.

Design of new drug molecules arguably offers some of the greatest hopes for success in present and future era. Five membered aromatic rings are the building blocks of many drugs. Amongst the five membered aromatic rings, thiophene has proven to be an alternative isostere, resulting in improved effectiveness of drug molecules. For structures like phenyl, thiophene can serve as biostere which can result in improved pharmacokinetic and pharmacodynamic properties of the drug.⁴

Thiophene comprises of a five membered ring with a sulfur as heteroatom having a molecular formula C₄H₄S. The thiophene ring has been incorporated into a broad range

of known biologically active compounds. It is incorporated as a substituent group or as a substitute of another ring that inspired researchers to synthesize several compounds containing this moiety. Well defined antimicrobial agents bearing thiophene moiety (Figure 1) are cefoxitin (**1a**), cephalothin (**1b**), cephaloridine (**1c**) and temocillin (**1d**).⁵

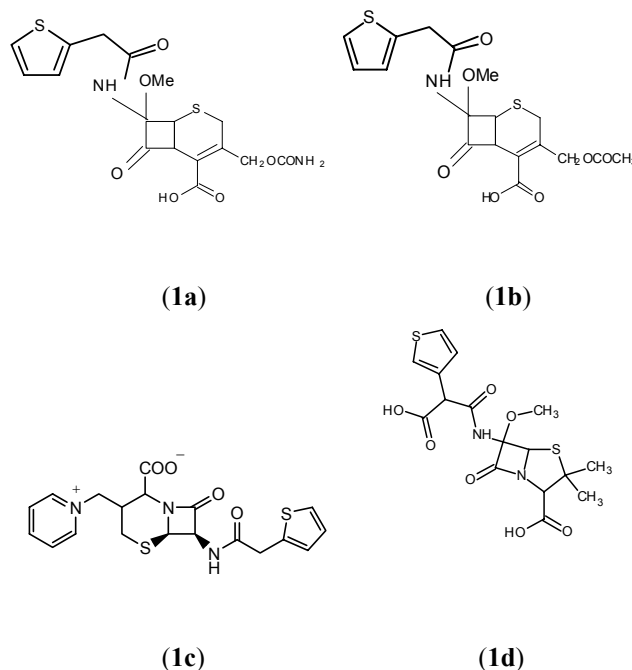


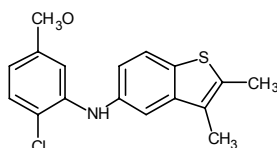
Figure 1. Some antimicrobial agents bearing thiophene moiety.

There are several reports in the literature describing the thiophene derivatives for their antimicrobial activities. The aim of present review is to give emphasis on antimicrobial properties associated with substituted thiophenes and structurally related thiophenes.

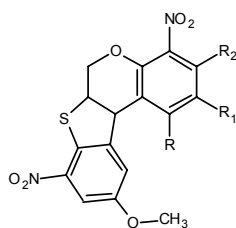
Antimicrobial activity of thiophenes

ortho-Chlorodiarylamines were synthesized from 2,3,7-trimethylbenzo[*b*]thiophene series by Queiroz *et al.*⁶ Cyclisation of these coupling products gave thienocarbazoles and dechlorinated diary amines, which were then evaluated and compared for antimicrobial activity using Ampicillin and Cycloheximide as standard. Compound (2) with methoxy group as a substituent was found active against *E. coli*. The thienocarboline showed lower Minimum Inhibitory Concentration (MICs) for *B. cereus* and *C. albicans* than the corresponding thiocarbazole but for *B. subtilis* both showed the same MIC.⁶

Derivatives of 10-methoxy-4,8-dinitro-6*H*-benzothieno[2,3-*c*]chromen-6-one were reported by Havaladar *et al.* All the synthesized compounds were evaluated for antibacterial activity against *S. aureus*, *B. subtilis*, *E. coli* and *S. typhosa*. The tested compounds (3) exhibited much higher inhibitory effect on the growth of bacteria.⁷



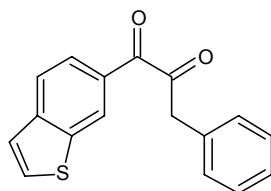
(2)



(3)

R= H, CH₃, OCH₃, Cl; R₁= H, NO₂, CH₃, OCH₃, Cl;
R₂= H, CH₃, Cl

Maurya *et al.* synthesized 4-hydroxy-1-methylindole and benzo[*b*]thiophene-4-ol based unnatural flavanoids as a new class of antimicrobial agents. The majority of the compounds exhibited good antifungal activity against *Trichophyton mentagrophytes*.⁸ It was found that substitution of heterocyclic oxygen by sulfur had produced a marked increase in antifungal activity. Compound (4) exhibited comparable MIC to the known Karanjin.

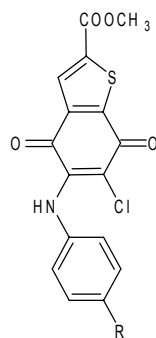


(4)

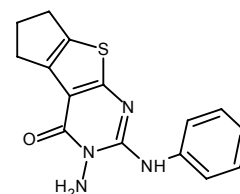
Ryu *et al.* reported synthesis of 5-arylamino-4,7-dioxobenzo[*b*]thiophene derivatives and tested for *in vitro* antifungal activity against *Candida* and *Aspergillus* species. Among the synthesized derivatives, 5-(4-

substitutedphenylamino)-6-chloro-2-(methoxycarbonyl)-4,7-dioxobenzo[*b*]thiophenes (5) exhibited more potent antifungal activity. The 6-chloro moiety had contributed to their antifungal activity significantly.⁹

A series of 2-substituted-amino-3-aminocyclopenteno or cyclohexeno[*b*]thieno[2,3-*d*]-3,4-dihydropyridin-4-ones was synthesized by Sherbeny *et al.* The synthesized derivatives were screened for antimicrobial, antiviral and anticancer activity. Some of the compounds showed promising activity. Compound (6) presented remarkable broad spectrum potency against *Pseudomonas aeruginosa*, *Staphylococcus aureus*, *Bacillus subtilis* and *Candida albicans*.¹⁰

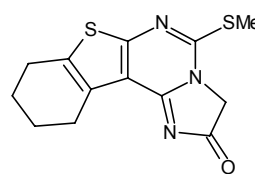


(5)

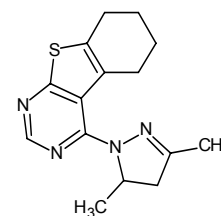


(6)

Bhuiyan *et al.* synthesized various derivatives by treatment of hydrazinothieno[2,3-*d*]pyrimidine with acetyl acetone, benzaldehyde and acetic anhydride. These derivatives were screened for antibacterial and antifungal activity using disc diffusion method and poisoned food techniques. Some of these derivatives showed marked antimicrobial activity. The structure activity relationship study (SAR) depicted that fused pyrimidine containing imidazo (7) and pyrazolo (8) rings showed higher antimicrobial and antifungal activity.¹¹



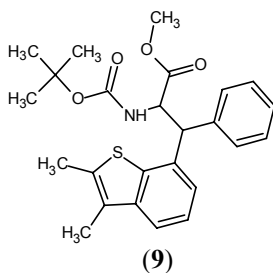
(7)



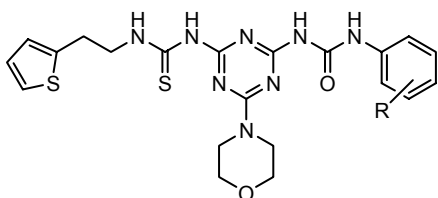
(8)

Ferreira *et al.* reported synthesis of pure stereoisomers of benzo[*b*]thienyl dehydrophenylalanines by Suzuki cross-coupling reaction and evaluation of their antimicrobial activity. It was concluded that the *Z*-isomer (9) was selective and very much active at very low MIC against Gram-positive bacteria: *B. cereus* and *B. subtilis*. Compounds were also active against *Candida albicans* presenting similar MICs.¹²

A new series of aliphatic thiourea derivatives containing S-triazine moiety was synthesized by Chikhalia *et al.* and tested *in vitro* antibacterial activity against different microorganisms using Tetracycline and Chloramphenicol as standard drugs. Some of the synthesized derivatives were tested for antifungal activity using Miconazole as standard drug. Incorporation of ureido linkage showed moderate to good activity. Structural variation such as methyl and halogen group at the *ortho*, *meta* or *para* positions (**10**) to ureido linkage resulted in enhanced antibacterial activity against all the tested microorganisms.¹³



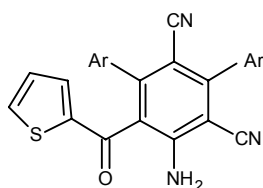
(9)



R= H, 4-Cl, 3-Cl, 2-CH₃, 3-NO₂

(10)

Darwish *et al.* synthesized thiophene and aniline derivatives (**11**) by the reaction of 2-picolinium N-ylide with arylidene derivatives of cyanothioacetamide and malanonitrile. All compounds displayed moderate activity against bacterial species *E.coli* and *S.albus*. Ampicillin and tetracycline were used as references to evaluate the potency of tested compounds.¹⁴

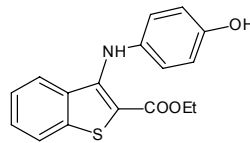


(11)

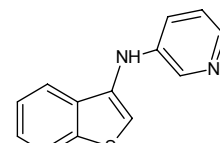
Ar = phenyl,
2-thienyl or
2-furyl

Antifungal activity of diarylamine derivatives of benzo(*b*)thiophene was determined against *Candida*, *Aspergillus* and dermatophyte species employing broth macrodilution test methods by Pinto *et al.* Most active compounds exhibited a broad spectrum activity against all tested fungal strains with particularly low MIC for dermatophyte. It was observed that hydroxyl group is essential for activity in aryl derivatives (**12**). The spectrum of activity in pyridine derivatives was broadened by the absence of ester group on position-2 of benzo[*b*]thiophene system (**13**).¹⁵

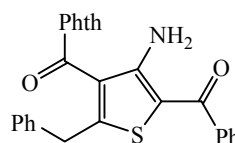
Gouda *et al.* synthesized thiocarbonyl and thioamide derivatives which were utilized as key intermediates for the synthesis of new derivatives of thiazole and thiophene. All the synthesized derivatives were examined for antibacterial activity using ampicillin and chloramphenicol as a standard. Incorporation of phthalazine moiety to thiophene (**14**) resulted in substantial activity against *E.coli* and *B. theringiensis*.¹⁶



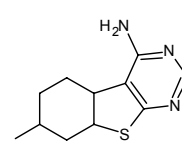
(12)



(13)

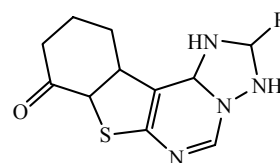


(14)



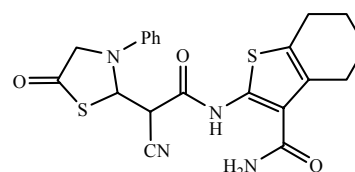
(15)

Khazi *et al.*, by employing Gewald reaction, synthesized tricyclic thienopyrimidines and triazole fused tetracyclicthienopyrimidines and screened them for antimicrobial activity. It was found that tricyclic aminothienopyrimidines (**15**) and tetracyclic triazole fused thienopyrimidine (**16**) exhibited promising antibacterial activity against *B. subtilis*. Some compounds also displayed better antifungal activity against *C. albicans* comparable to the standard fluconazole.¹⁷



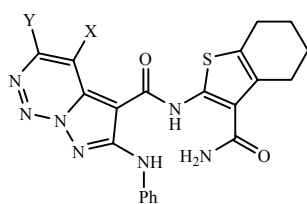
(16)

Gouda *et al.* synthesized thiazole and pyrazole derivatives using 4,5,6,7-tetrahydrobenzothiophene moiety as a base. The synthesized derivatives were evaluated for antimicrobial activity *in vitro*. As an indicator for the activity of the compounds, zone of inhibition was measured and Ampicillin was taken as reference. Most of the synthesized compounds evinced good to moderate antibacterial and antifungal activity. Incorporation of benzothiophene nucleus to thiazole (**17**) or pyrazole (**18**) moieties resulted in remarkable activity against *B. theringiensis*, *K. pneumoniae*, *B. fabae* and *F. oxysporum*.¹⁸



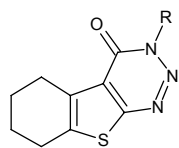
(17)

Antimicrobial activity of series of substituted amino-4,5-tetramethylenethieno[2,3-*d*][1,2,3]-triazine-4(3*H*)-ones was reported by Saravanan *et al.* Compounds with lipophilic groups like chlorophenyl and fluorophenyl groups (**19**) exhibited appreciable antimicrobial activities while substituting with electron donating groups like methyl, ethyl were found less active against all the microbes used.¹⁹



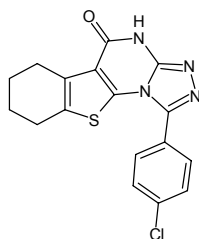
X = NH₂, CH₃; Y = CN, COCH₃

(18)



R = 4-ClC₆H₄, 4-FC₆H₄

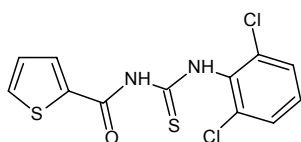
(19)



(20)

Taisan *et al.* synthesized a series of new thienopyrimidin-4-one(thione) derivatives and evaluated their antimicrobial activity against *S. aureus*, *K. monas*, *P. aeruginosa* and *E. coli* employing Vancomycin and Cefazime as standard. Compound (**20**) showed promising antimicrobial activity.²⁰

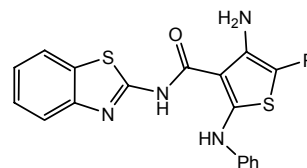
Badiceanu *et al.* prepared new thioureides of 2-thiophene carboxylic acid and evaluated them for antibacterial and antifungal activity. *In vitro* antimicrobial activity assay showed that these derivatives presented significant antimicrobial activity with MIC ranging from 7.8 μg/ml to 500 μg/ml. The majority of the tested compounds showed a broad spectrum of antimicrobial activity at low concentration on Gram-positive, Gram-negative bacteria and fungal strains. Because of the contribution of electron withdrawing group, most effective compound was (**21**) with low MIC value on majority of testing microbial strains.³



(21)

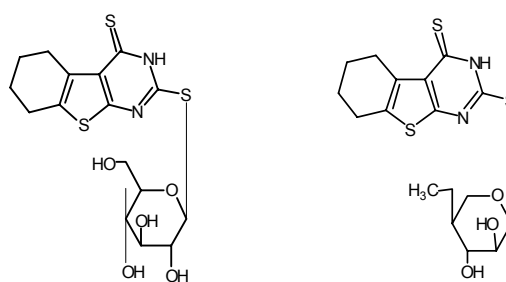
A series of thiazole, pyrazole, thiophene derivatives having benzothiazole moiety in common were reported by Bondock *et al.* by using N-(benzo-thiazol-2-yl)-2-cyanoacetamide as reactant. Synthesized compounds were screened for antimicrobial activity against *S. aureus* and *S. pyogenes* (Gram-positive bacteria), *P. phaseolicola* and *P. fluorescens* (Gram-negative bacteria), *F. oxysporum* and *A. fumigates* (fungal strains). It was noticed that compounds belonging to thiophene and pyrazole series exhibited better antibacterial potential than thiazole series. Incorporation of

thiophene nucleus to benzothiazole at position-3 via carboxamide linker produced high antimicrobial activity. Also thiophenes with electron withdrawing groups like -COOEt (**22**) or -COPh (**23**) recorded higher activity.²¹



(22): R = CO₂Et; (23): R = COPh

Hafez *et al.* synthesized thieno[2,3-*d*]pyrimidine-2,4-dithione derivatives by using 3-(2-amino-thiophene)-carbonitrile derivative precursor as a synthon. The compounds were designed in such a way so that the heterocyclic substituents are straight away linked to thienopyrimidine nucleus at C-2. Triazolo[4,3-*a*]benzothieno[2,3-*d*]pyrimidines were also derived from 2-thioxothienopyrimidine as isosteres. All the compounds were screened for antiviral and antibacterial activity. Some of the compounds showed complete inhibition at 128 mg mL⁻¹ or less while the rest of the compounds showed incomplete inhibition using ampicillin as the standard drug. Introduction of diphenyl-triazolo group at C-2-C-3 ring resulted in ineffectiveness towards *E. coli* but found to be effective against *S. aureus* and *P. putida*. Any other substitution at position C-2-N-3 of pyrimidine ring and C-4-C-5 of the thiophene ring system resulted in a decrease in efficacy of resulting compounds. Substitution of acylated arabino-furanosyl group at C-2 in pyrimidine ring on thieno[2,3-*d*]pyrimidine ensued in potent compounds when compared to other compounds. Deacylated S-glycoside group incorporation in thienopyrimidine resulted in compounds (**24**) and (**25**) which were active against *P. putida*.²²



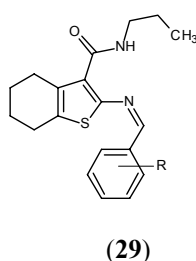
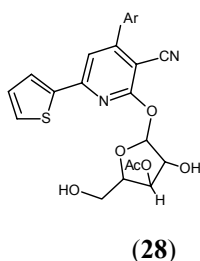
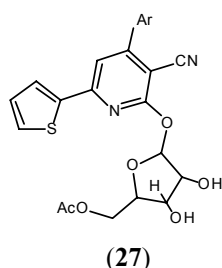
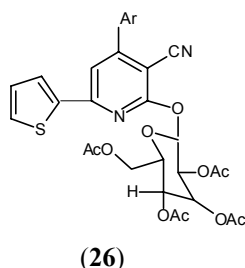
(24)

(25)

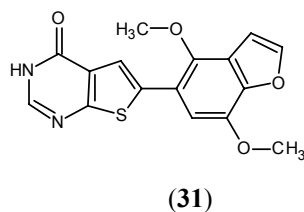
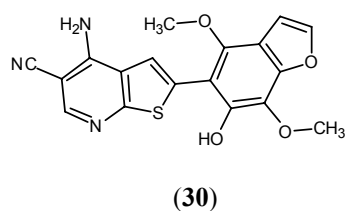
El-Sayed *et al.* reported the synthesis of glycoxyloxy derivatives by glycosylation of pyridine-2-(1*H*)-one. The initial material was obtained by the reaction of 2-acetyl thiophene with 4-chlorobenzaldehyde and ethylcyanoacetate or by reaction of α, β-unsaturated compounds with ethylcyanoacetate in the presence of ammonium acetate. The derivatives were screened for antibacterial activity. The compounds (**26**), (**27**) and (**28**) exhibited higher activity than Ampicillin while other derivative showed moderate activity.²³

Srivastava *et al.* synthesized a series of tetrahydrobenzothiophene as potential antibacterial and mycolytic agents. The antibacterial activity was screened against *Staphylococcus aureus*, *Bacillus subtilis*,

Escherichia coli and *Klebsiella pneumoniae* using Ampicillin as a reference. Miconazole nitrate was used as standard for evaluation of antifungal activity against *Aspergillus niger* and *Candida albicans*. The derivatives showed moderate to significant activity. It was concluded that electron donating and withdrawing groups on aldehydic phenyl ring influenced the activity. Aldehydic phenyl group containing electron withdrawing group like 2-Cl and 2-NO₂ (**29**) showed promising activity.²⁴

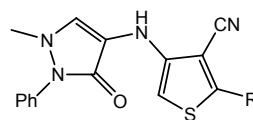


New thienopyridine and thienopyrimidine derivatives were synthesized by Ahmed *et al.*²⁵ from 2-aminothiophen-3-carbonitriles. The carbonitrile derivatives were synthesized via Gewald reaction using visnaginone and khellinone as initial reactant. Antibacterial screening was done against *P. aeruginosa*, *E. coli*, *S. aureus* and *B. subtilis* while for antifungal screening *A. fumigates*, *P. italicum*, *S. racemosum* and *C. albicans* were used. The antimicrobial activity of the synthesized derivatives was measured in comparison to chloramphenicol and terbatiin as standard drugs. Most of the compounds were active and showed moderate activity. From the synthesized series, the most active compounds were compounds (**30**) and (**31**).²⁵



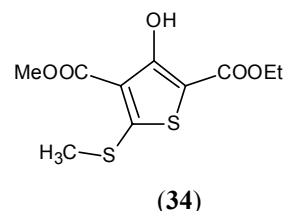
Synthesis and antimicrobial screening of new derivatives of acetamide, oxaloacetyl, acetohydrazide, thiophene and thiophenacrylamide was reported by Aly *et al.* For antifungal activity, four fungal strains: *A. fumigates*, *G. candidum*, *C. albicans* and *S. racemosum* were used.

Clotrimazole and Itraconazole were taken as reference. For antibacterial activity, four bacterial strains: *S. aureus*, *B. subtilis*, *P. aeruginosa* and *E. coli* were used. As a standard drug, Penicillin G and Streptomycin were used as reference to evaluate the potency of tested compounds. All the synthesized compounds exhibited moderate to good activity. From the study, it was observed that synthesized compounds substituted with -OC₂H₅, -COCH₂, -CH₃, -Cl group showed potent activity. Compounds (**32**) and (**33**) were found to have strong antifungal activity.²⁶

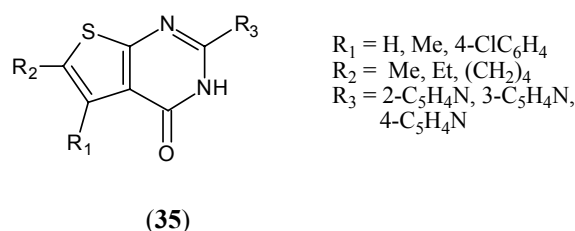


(32) R = -N = CH-OC₂H₅; (33) R = -NHCOCH₂Cl

A series of highly functionalized thiophene and thieno[3,2-*c*]pyran-4-one derivatives was designed by Ram *et al.* These derivatives were screened for antileishmanial and antifungal activities. SAR study revealed that position and nature of substituents at positions 3 and 4 of the thiophene ring are crucial for the activity. Compounds with a carboxymethoxy group at C-4 and hydroxyl group at C-3 (**34**) exhibited significant antifungal activity against all the fungal strain used. Increase in size of ester function from carboxymethoxy to carboxyethoxy resulted in a loss of efficacy. Change of substituent from carboxymethoxy to cyano group resulted in retention of activity. Some of the compounds also showed antileishmanial activity which may be due to the presence of the ester group.²⁷



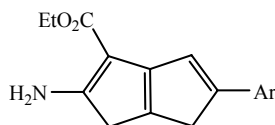
Newly synthesized 2-(pyridin-2-yl)thieno[2,3-*d*]pyrimidin-4(3*H*)-ones derivatives (**35**) were screened for antimicrobial activities against six bacterial strains and two fungal species by Bari *et al.* The presence of long chain aliphatic substituents at C-2 of thiophene ring and presence of the aromatic substituent at position-1 increases the antifungal and antibacterial activity.²⁸



R₁ = H, Me, 4-ClC₆H₄
 R₂ = Me, Et, (CH₂)₄
 R₃ = 2-C₅H₄N, 3-C₅H₄N,
 4-C₅H₄N

Balamurugun *et al.* synthesized a series of novel 2-amino-5-arylthieno[2,3-*b*]thiophene under thermal as well as microwave irradiation conditions employing Gewald dehydrogenation reaction. The synthesized compounds were screened for *in vitro* for antitubercular activity against *M. tuberculosis* (MTB) and multidrug resistant *M. tuberculosis*

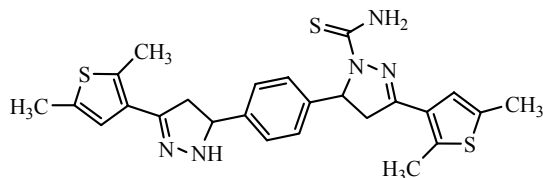
(MDR-TB). Compound (36) was found to be most active compound with MIC of 1.1 μM against MTB and MDR-TB. Compounds with $-\text{CN}$ group were found to be less active than $-\text{COOEt}$ group. It was also reported that lipophilicity is an important factor for antitubercular activity.²⁹



Ar = 1-naphthyl, C_6H_5

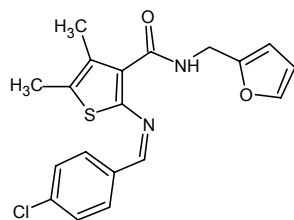
(36)

Khan *et al.* prepared pyrazoline, pyrazole and pyrimidine derivatives from chalcones previously obtained from the reaction of terephthalaldehyde with 3-acetyl-2,5-dimethyl thiophene and evaluated antibacterial activity *in vitro* by disc diffusion assay against *S. aureus*, *S. pyogenes*, *S. typhimurium* and *E. coli*. Results showed that pyrazoline derivative (37) bearing thiophene moiety were better at inhibiting growth of both types of bacteria compared to Chloramphenicol.³⁰



(37)

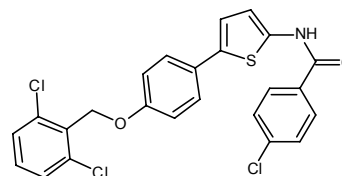
Various Schiff bases were synthesized by Iqbal *et al.* by reaction of substituted aromatic aldehydes with 2-amino-3-(N-furfurylamido)-4,5-dimethyl thiophene. The Schiff bases were screened for antibacterial and antifungal activity using Ampicillin and Miconazole nitrate as standard. Most of the compounds showed mild to moderate antimicrobial activity and some of them were found to be equipotent to the standard drug used. It was concluded that compounds having electron withdrawing group (38) on aldehydic phenyl ring showed better antibacterial and antifungal activity as compared to compounds having electron donating groups.³¹



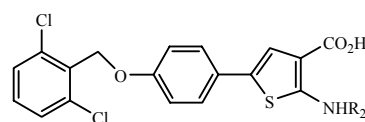
(38)

Lu *et al.* developed a series of acylated and alkylated amino-5-(4-(benzyloxy)phenyl)thiophene-3-carboxylic acid derivatives and evaluated them for anti-tubercular activity. Some of these derivatives inhibited *Mycobacterium tuberculosis* growth with MIC value between 1.9 and 7.7 μM and low toxicity against VERO cells. Compounds were found to show moderate activity against multidrug resistant tuberculosis and drug-resistant tuberculosis clinical strains. SAR studies of these derivatives indicated that 2,6-

dichlorobenzyloxy group (39) is supposed to play a significant role in the activity. Amide derivatives were found to display superior anti-tubercular activity than amine derivatives. The data also suggested that compounds with C-3, C-4 alkyls showed best anti-tubercular activity (40). A further increase in the carbon chain resulted in decrease in potency.³²



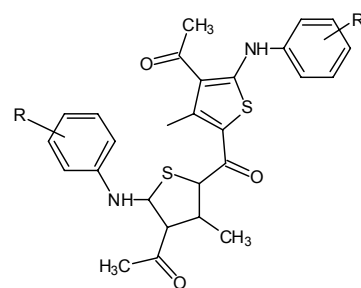
(39)



$\text{R}_2 = \text{n-butyl}$, carboxymethyl

(40)

Sable *et al.* synthesized ethyl 2-(4-acetyl-3-methyl-5-(phenylamino)thiophen-2-yl)-2-oxoacetate derivatives, ethyl 3-(4-acetyl-3-methyl-5-(phenylamino)thiophen-2-yl)-3-oxopropanoate derivatives and di((4-acetyl-3-methyl-5-(phenylamino)thiophen-2-yl)ketone derivatives under mild conditions from acetyl acetone, phenyl isothiocyanates and 2-chloromethyl derivatives. All the synthesized compounds exhibited good to moderate activity. Compounds having $\text{R} = \text{H/Cl}$ (41) were found to be more potent against Gram-positive bacteria with moderate potential against fungal strains. With $\text{R} = \text{CH}_3/\text{OCH}_3$, compounds were more active against *B. subtilis*, *P. aeruginosa* and *E. coli*.³³

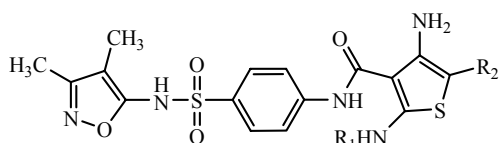


$\text{R} = \text{H}$, 4- OCH_3 , 4- Cl

(41)

A new series of thiophene, acrylamide, pyrazole and pyridine derivatives tagged with sulfoxazole moieties were synthesized by Nasr *et al.* *In vitro* antimicrobial activity screening was done against Gram-positive bacteria *S. pneumoniae*, *B. subtilis* and *S. Epidermidis*, Gram-negative bacteria *E. coli*, *P. vulgaris* and *K. pneumoniae* and fungal strain *A. fumigates*, *S. racemosum* and *G. candidum* using agar diffusion method and Ampicillin, Gentamycin, Sulfoxazole and Amphotericin B as reference drugs. Most of the newly synthesized compounds (42) were found to be more potent than sulfoxazole. The synthesized compounds had higher lipophilic character than sulfoxazole, and therefore had more intracellular concentration due to their

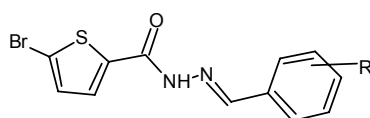
improved cellular penetration. Molecular docking simulations represented that the synthesized compounds can be accommodated in p-aminobenzoic acid pocket of dihydropteroate synthase thereby acting in a similar way as that of sulfa drugs. Therefore, thiophene derivatives bearing larger N-alkyl substituent exhibited better antimicrobial activity.³⁴



$R_1 = -CH_3, -C_2H_5, -CH_2-CH=CH_2, -C_6H_5; R_2 = -COCH_3, -CN$

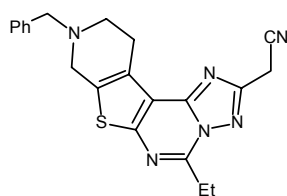
(42)

Naliapara *et al.* prepared a convenient method for the synthesis of Schiff bases of 5-bromothiophene-2-carbohydrazide having good to moderate yield. All the compounds were evaluated for antimicrobial activity by well-diffusion method against bacterial strains (*E. coli*, *P. aeruginosa*, *S. aureus* and *S. pyogenus*) and fungal strains (*C. albicans*, *A. niger* and *A. clavatus*). Compounds like (43), having electron withdrawing groups, exhibited good antibacterial and antifungal activity.³⁵



$R = 4-F, 4-Cl, 4-Br, 3-Cl, 4-CN$ (43)

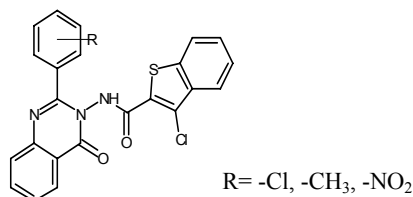
Jabli *et al.* designed a new series of 2-cyano-methylthieno-triazolopyrimidines using substituted aminothiophene-3-carbonitrile and cyanoacetic acid hydrazide as starting material. All the compounds were screened for antibacterial activity using Tetracycline as reference. The strains used were *S. typhimurium*, *P. aeruginosa*, *E. coli* and *S. aureus*. All the synthesized compounds showed moderate antibacterial activity. Among these, compound (44) exhibited highest antibacterial activity. It may be attributed because of the presence of dihydronaphtho and benzyl moiety.³⁶



(44)

Analogs of 3-chloro-N-(4-oxo-2-arylquinazolin-3(4H)-yl)-1-benzothiophene-2-carboxamide were prepared from 3-amino-2-arylquinazolin-4(3H)-one by Rao *et al.* These compounds were evaluated for *in vitro* antibacterial activity against Gram-positive bacteria and Gram-negative bacteria using Ciprofloxacin as standard. Compound with 3-methyl substitution on phenyl ring (45) at position-2 of quinazoline moiety showed significant activity against *S. aureus* while

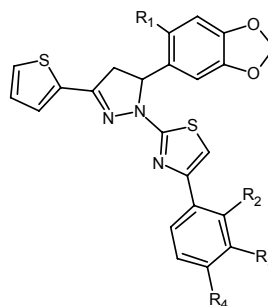
compound with -Cl, -CH₃ and -NO₂ group substitution showed moderate activity against both Gram-positive microorganisms. Most of the compounds showed moderate activity against Gram-negative bacteria.³⁷



$R = -Cl, -CH_3, -NO_2$

(45)

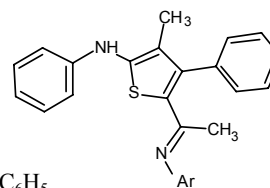
Series of thiophene and benzodioxole appended thiazolopyrazoline derivatives (46) were synthesized and screened for antimicrobial activity by Antony *et al.* Some of the compounds presented good antimicrobial activity against bacterial and fungal strain used. Docking study revealed that all synthesized derivatives showed good binding energy toward target receptor DNA topoisomerase IV, ranging from -10.42 to -11.66 kcal mol⁻¹. Substitution of -Br at R₁ position and -CN group at R₃ position resulted in a marked increase in antimicrobial activity.³⁸



$R_1 = H, Br; R_2 = H, Cl; R_3 = H, CN; R_4 = H, F$

(46)

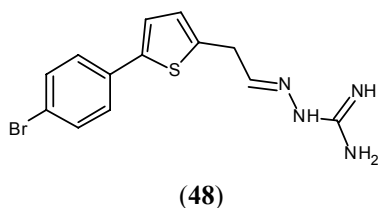
Mabkhot *et al.* synthesized derivatives of thiophene using 5-acyl-4-phenyl-2-(phenyl-amino)thiophene-3-carboxylate as precursor. These derivatives were screened for antibacterial activity against Gram-positive bacteria (*B. subtilis* and *S. pneumoniae*) and Gram-negative bacteria (*E. coli* and *P. aeruginosa*) using disc diffusion method with Ampicillin and Gentamycin as standard drugs. For antifungal activity, four fungal strains (*A. fumigates*, *S. racemosum*, *G. cardium*, *C. albicans*) were used and Amphotericin B was taken as standard drug. All the compounds exhibited moderate to good antimicrobial activity. SAR studies suggested that introduction of appropriate substituent at position-5 of thiophene ring (47) enhanced antibacterial activity.³⁹



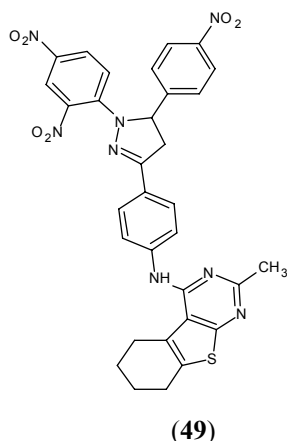
$Ar = -C_6H_5, 4-ClC_6H_5$

(47)

Ajdacic *et al.* designed a series of new thiophene-based guanylhydrazones and evaluated antifungal activity against broad ambit of medically valued fungal strains including yeast, moulds and dermatophytes in comparison to drug Voriconazole. All guanylhydrazones showed significant activity against *Candida* spp., *A. fumigates*, *F. oxysporum*, *M. canis* and *T. mentagrophytes*. Some of the compounds exhibited excellent activity against voriconazole resistant *Candida albicans* with very low MIC value $< 2 \mu\text{g mL}^{-1}$. Compound (48) having -Br group on phenyl ring was found to be most effective with MIC ranging from 0.25-6.25 $\mu\text{g mL}^{-1}$. It was concluded that thiophene based guanynyl hydrazone showed higher inhibitory activity than corresponding furan.⁴⁰



Various chalcones were used as building block for the synthesis of various thieno[2,3-d]pyrimidine derivatives by Elissa *et al.* These derivatives were screened for antimicrobial activity against Gram-positive, Gram-negative and fungal strains. MIC was determined by the paper disc diffusion method. It was observed that substitution with a methyl group at position-2 of tetrahydrothienopyrimidine derivative of enone series decreased the activity against Gram-positive bacteria and removed the activity against *C. albicans*. A terminal amino group of the hydrazine group when unsubstituted, together with the presence of methyl group position-2 showed broad spectrum activity. The presence of phenyl group at N¹ and dinitrophenyl group of dihydropyrazol ring (49) yielded derivative with broad spectrum activity.⁴¹



Conclusion

Considerable attention has been given to compounds which possess thiophene rings in order to search for drugs with a higher degree of potency and fewer toxic side effects. The analytical and other informational data, available in literature so far, have lightened thiophene as a significantly important class of heterocyclic compounds and their

applications in the ever challenging chemotherapy of various ailments/ infections since last two decades. A large number of thiophene derivatives have been discovered and reflected significant antimicrobial activity with appreciably wider spectrum.

Thiophene can be fused with various heterocyclic systems, resulting in various new heterocyclic systems with enhanced biological activity. Thienopyrimidine and benzothiophene occupy a special position among these compounds. Most of the positions were explored to improve the antimicrobial profile of thiophene analogs. Derivatives with C-2 and C-4 substituted positions and compoment of electron-withdrawing group on the aromatic ring on C-2 position of thiophene presents varied degrees of inhibition against Gram-positive bacteria, Gram-negative bacteria and fungal strains, showing inhibition as good as to the standard drugs used. The versatile synthetic applicability and biological activity of this heterocyclic moiety will help the medicinal chemists to plan, organize and implement new approaches towards discovery of novel drugs. Further combinatorial libraries of these compounds can be generated which can be screened optimal pharmacological activities by optimization techniques using 2D and 3D QSAR investigation.

Acknowledgement

The author would like to extend sincere appreciation to the Department of Pharmacy, Galgotias University, Greater Noida for providing literature survey facility to carry out the work.

References

- Mishra, R., Jha, K. K., Kumar, S., Tomer, I., *Pharm. Chem.*, **2011**, 3, 38.
- Baumann, M., Barendale, I. R., Ley, S. V., Nikbin, N., *Beilstein J. Org. Chem.*, **2011**, 7, 442.
- Badiceanu, C. D., Missir, A. V., Chifiriuc, M. C., Dracea, O., Raut, J., Larion, C., Dity, L. M., Mihaescu, G., *Rom. Biotech. Lett.*, **2010**, 15, 5545.
- Dalvie, D. K., Kalgutkar, A. S., Khojasteh-Bakht, S. C., Obach, R. S., O'Donnell, J. P., *Chem. Res. Toxicol.*, **2002**, 15, 269.
- Jha, K. K., Tomer, I., Mishra, R., *J. Pharm. Res.*, **2010**, 5, 560.
- Queiroz, M. R. P., Ferreira, I. C. F. R., Goetano, Y. D., Kirsch, G., Calhelha, R. C., Estevinho, L. M., *Bioorg. Med. Chem. Lett.*, **2006**, 14, 6827.
- Havaldar, F. H., Bhise, S., Burudkar, S., *J. Serb. Chem. Soc.*, **2004**, 69, 527.
- Yadav, P. P., Gupta, P., Chaturvedi, A. K., Shukla, P. K., Maurya, R., *Bioorg. Med. Chem.*, **2005**, 13, 1497.
- Ryu, C. K., Lee, S. K., Hen, J. Y., Jung, O. J., Lee, J. Y., Jeong, S. H., *Bioorg. Med. Chem. Lett.*, **2005**, 15, 2617.
- Sherbeny, M. A., El-Ashmawy, M. B., Subbagh, H. I., El-Emam, A. A., Badria, F. A., *Eur. J. Med. Chem.*, **1995**, 30, 445.
- Bhuiyan, M. H., Rahman, K. M. M., Hussain K., Rahim, A., Hussain, I., Naser, A., *Acta. Pharm.*, **2006**, 56, 441.
- Abreu, A. S., Ferreira, P. M. T., Monterio, L. S., Queiroz, M. J. R. P., Ferreira, I. L. F. R., Calhelha, R. C., Estevinha, L. M., *Tetrahedron*, **2004**, 60, 11821.

- ¹³Desai, A. D., Mahajan, D. H., Chikhalia, K. H., *Indian J. Chem.*, **2007**, *46B*, 1169.
- ¹⁴Darwish, E. S., *Molecules*, **2008**, *13*, 1066.
- ¹⁵Pinto, E., Queiroz, M. J. R. P., Vale-Silva, L. A., Oliveira, J. F., Begowin, A., Begowin, J. M., Kirsch, G., *Bioorg. Med. Chem.*, **2008**, *16*, 8172.
- ¹⁶Khalil, A. M., Berghot, M. A., Gouda, M. A., *Eur. J. Med. Chem.*, **2006**, *44*, 4434.
- ¹⁷Shetty, N. K. S., Lamani, R. S., Khazi, I. A. M., *J. Chem. Sci.*, **2009**, *121*, 301.
- ¹⁸Gouda, M. A., Berghot, M. A., Abd El-Ghani, G. E., Khalil, A. M., *Eur. J. Med. Chem.*, **2010**, *45*, 1338.
- ¹⁹Saravanan, J., Mohan, S., Roy, J. J., *Eur. J. Med. Chem.*, **2010**, *45*, 4365.
- ²⁰Al-Taisan, K. M., Al-Hazimi, H. M. A., Al-Shihry, S. S., *Molecules*, **2010**, *15*, 3932.
- ²¹Bondock, S., Fadaly, W., Mefwally, M. A., *Eur. J. Med. Chem.*, **2010**, *45*, 3692.
- ²²Hafez, H. N., Hussein, H. A. R., El-Gazzar, A. B. B. A., *Eur. J. Med. Chem.*, **2010**, *45*, 4026.
- ²³El-Sayed, H. A., Moustafa, A. H., Haikal, A. E. Z., El-Halawa, R. A., El-Ashry, E. H., *Eur. J. Med. Chem.*, **2011**, *46*, 2948.
- ²⁴Srivastava, S., Das, B., *Der Pharm. Chemica*, **2011**, *3*, 103.
- ²⁵Ahmed, E. M., Marzouk, N. A., Hessein, S. A., Ali, A. M., *World J. Chem.*, **2011**, *6*, 25.
- ²⁶Aly, H. M., Saleh, N. M., Elhady, H. A., *Eur. J. Med. Chem.*, **2011**, *46*, 4566.
- ²⁷Ram, V. J., Goel, A., Shukla, P. K., Kapil, A., *Bioorg. Med. Chem. Lett.*, **1997**, *7*, 3101.
- ²⁸Haswani, N. G., Bari, S. B., *Turk. J. Chem.*, **2011**, *35*, 915.
- ²⁹Balamurugan, K., Perumal, S., Reddy, A. S. K., Yogeewari, P., Sriram, D., *Tetrahedron Lett.*, **2009**, *50*, 6191.
- ³⁰Asiri, A. M., Khan, S. A., *Molecules*, **2011**, *16*, 523.
- ³¹Iqbal, M. I. C., Satyendra, D., Apurba, T., Patel, M., Monica, K., Girish, K., Mohan, S., Saravanan, J., *Hygeia. J. D. Med.*, **2012**, *4*, 116.
- ³²Lu, X., Wan, B., Franzblau, S. G., You, Q., *Eur. J. Med. Chem.*, **2011**, *46*, 3551.
- ³³Sable, P. N., Ganguly, S., Chaudhari, P. D., *Chin. Chem. Lett.*, **2014**, *25*, 1099.
- ³⁴Nasr, T., Bondock, S., Eid, S., *Eur. J. Med. Chem.*, **2014**, *84*, 491.
- ³⁵Makwana, H., Naliapara, Y. T., *Inter. J. Chem. Phy. Astro.*, **2014**, *14*, 99.
- ³⁶Jabli, D., Lahbib, K., Dridi, K., Efrif, M. L., *J. Pharm. Chem. Biol. Sci.*, **2015**, *3*, 178.
- ³⁷Rao, G. K., Subramaniam, R., *Chem. Sci. J.*, **2015**, *6*, 1.
- ³⁸Sulthana, S. S., Antony, S. A., Balachandran, C., *Bioorg. Med. Chem. Lett.*, **2015**, *25*, 2753.
- ³⁹Mabkhot, Y. N., Alatibi, F., El-Sayed, N. N. E., Al-Showiman, S., Kheder, N. A., Wadood, A., Rauf, A., Bawazeer, S., Handa, T. B., *Molecules*, **2016**, *21*, 01.
- ⁴⁰Ajdacic, V., Senerovic, L., Vranic, M., Pehnezovic, M., Arsnijevic, V. A., Veselinovic, A., Veselinovic, J., Solaja, B. A., Runic, J. N., Opsenica, I. M., *Bioorg. Med. Chem.*, **2016**, *24*, 1277.
- ⁴¹Elissa, A. A. H. M., Moneer, A. A., *Arch. Res. Pharm.*, **2004**, *27*, 885.

Received: 20.10.2016.

Accepted: 15.11.2016.



OPTIMIZATION OF EXTRACTION CONDITIONS FOR LIQUID-LIQUID EXTRACTION OF PERSIPEPTIDES FROM *STREPTOMYCES ZAGROSENSIS* FERMENTATION BROTH

Hamed Kazemi Shariat Panahi^[a], Fatemeh Mohammadipناه^{[a]*} and Mona Dehghani^[a]

Keywords: Anti-MRSA; drug discovery; enhanced-production; experimental design; HPLC; liquid-liquid extraction; pentapeptide.

Generally, during drug discovery programs, after identification of new antibiotic metabolite, its high quantity production is obtained by various approaches, including production or extraction improvement or even strain genetic manipulation. To provide enough amounts of two novel non-toxic anti-MRSA pentapeptides named persipeptides (A and B) required for drug discovery programs, seven different fermentation broths examined. CM1 medium considerably enhanced the biosynthesis of persipeptides up to 219.63 ± 2.48 , compared with ISP2 medium (36.31 ± 1.37), showing a six-fold increase. Additionally, at the extraction level, results of experimental design indicated that liquid-liquid extraction (LLE) of persipeptides by 34 % BuOH at 228 rpm (Stirrer speed), temperature 28 °C, and pH 9-9.5 for 78 min (stirring time) was equal to $264 \pm 9.85 \mu\text{g mL}^{-1}$, which was the most favorable combination for their extraction. Compared with un-optimized extraction process ($219.63 \pm 2.48 \mu\text{g mL}^{-1}$), the optimized conditions improved the yield of the extraction by 20.20 %, while saving both time and solvent usage up to 67 % (162 min) and 16 %, respectively. The total sum of persipeptides enhancements resulted from the replacement of fermentation broth and subsequent optimization of their extraction by LLE reached almost seven-time, compared to conventional method ($36.31 \pm 1.37 \mu\text{g mL}^{-1}$). Therefore, relatively large amounts of persipeptides can be economically produced and extracted for various future experiments.

* Corresponding Authors

Fax: +982166415081

E-Mail: fmoammadipناه@ut.ac.ir

[a] Department of Microbial Biotechnology, School of Biology and Center of Excellence in Phylogeny of Living Organisms, College of Science, University of Tehran, 14155-6455, Tehran, Iran

Introduction

The treatment of drug-resistant bacteria, including MRSA, in terms of their resistance to the current antibiotics is among major challenges worldwide.¹ New cyclo-pentapeptides, named as persipeptides, consist of two types of amino acids repetition of valine and phenylalanine, two of which are *N*-methylated. So far; two isomers, A and B, has been produced² by *Streptomyces zagrosensis* UTM 1154 with bioactivity against methicillin resistance *Staphylococcus aureus* (MRSA) DSM 23622 (UTMC 1401).³ Existence of *N*-methylated residues in peptides usually led to higher interesting therapeutic profiles⁴ and consequently improved pharmacokinetic properties such as enzymatic stability,⁵ receptor selectivity,⁶ enhanced potency,⁷ membrane permeability,⁸ and bioavailability.⁹

The development and the validation of analytical methods play vital roles in discoveries, developments and manufactures of pharmaceuticals. High-performance liquid chromatography (HPLC) is extensively applied as a versatile analytical technology for quantitative analysis of target biomolecules and other compounds in biological matrixes as well as fermentation culture media of microorganisms producing them.¹⁰ HPLC-based methods has previously been developed and validated for persipeptides determination from fermentation broth of *S. zagrosensis* UTM 1154. The reported assay method requires sample pretreatment using LLE with the aid of *n*-butanol (*n*-BuOH).³ This pretreatment

is required for separating and concentrating of the target analyte and removing interferences, or even increasing the life of HPLC column by the elimination of damaging compounds.¹¹ However, the LLE method used for sample pretreatment or extraction of persipeptides has not been optimized yet; therefore, has some drawbacks, including lower efficiency and time consumption. These drawbacks directly affect the extraction yield and expenses, including materials usage and equipment depreciation. Improvement of a system performance or a process in order to maximize the exploitation from it is referred as optimization. Process optimization will obtain conditions that produce the best possible response when applied to a production/extraction procedure.¹² Traditional optimization of analytical chemistry are accomplished by one-variable-at-a-time, in which at any given time, influence of only one factor has been examined while all other factors have been kept at a constant level.¹³ An alternative to this is response surface methodology (RSM), which decreases the number of experiments while increases the effectiveness for responses that are confounded by many factors and their interactions.¹³ Additionally, analysis of variance (ANOVA) provides the statistical results and diagnostic checking tests, which enable researchers to evaluate the adequacy of the models.¹⁴ Although, RSM has been successfully applied in the optimization of culture media to enhance the production of *Streptomyces* secondary metabolites, including streptolydigin,¹⁵ virginiamycin,¹⁶ daptomycin,¹⁷ clavulanic acid,¹⁸ streptomycin,¹⁹ and neomycin,²⁰ RSM in the optimization of solvent extraction of antibiotics produced by *Streptomyces* has been rarely exploited and the only example is the optimization of extractive fermentation of clavulanic acid.²¹

In the present study, six culture media consisting of novel complex carbon sources and insoluble nitrogen sources were examined and compared with ISP2 medium. After determination of the most productive medium, the

optimization of parameters in the process of LLE, including volume percentage of extraction solvent, stirring rate, sample pH, extraction temperature, and process time for LLE of persipeptides from fermentation culture medium samples of *S. zagrosensis* UTMC 1154³ were done in two steps. In the first step, primary evaluation of mentioned factors using half-fraction of factorial design was performed and striking factors were screened. In the second step, selected factors were investigated by RSM using central composite rotatable design (CCRD) in order to maximize the extraction efficiency of persipeptides.

Experimentals

HPLC grade acetonitrile was purchased from Merck (Darmstadt, Germany). All other organic solvent used for LLE of persipeptides, including *n*-butanol (*n*-BuOH), 1-propanol, 2-propanol, cyclohexane, dichloromethane, methanol, and chloroform were extra-pure grade and obtained from Merck (Darmstadt, Germany). HPLC grade water was produced by Barnstead/Thermolyne, USA (Model: d8992-33 Nanopure infinity).

Strain and culture conditions

The commonly used ISP2 medium (consisted of (g L⁻¹): glucose (4); yeast extract (4); and malt (10), pH 7.2) was used as growth and maintenance (supplemented with 2 g L⁻¹) and seeding media. Persipeptides were produced by the inoculation of spore suspension (1 mL of 1 × 10⁷ CFU mL⁻¹) of *S. zagrosensis* UTMC 1154 in 100-mL Erlenmeyer flasks containing 9 mL of ISP2 liquid medium, followed by 36 h of shaking (220 rpm) at 28 °C to develop seeding culture. This pre-culture was used for the subsequent inoculation of various fermentation media (50 mL) in 250-mL Erlenmeyer flasks with inoculant size of 10 % (5 mL). The inoculated production media were incubated at 28 °C on shaker incubator with 220 rpm for seven days.³ In order to examine persipeptides production, seven different media, named as candidate media (CM) 1-6 were investigated (Table 1). The optimization was done using the most productive medium.

Experimental designs and statistical analyses

In the previously reported method, the effect of critical parameters, including pH of the fermentation broth, extraction temperature, percentage of organic solvent, stirring rate, and extraction time on extraction process has not been determined.³ Therefore, an experimental design using half fraction of factorial design was employed to screen significant variables with the minimum required number of experiments. After the determination of variables with significant effect on extraction process, a three factors CCRD was employed to determine optimal conditions for critical factors. Design-Expert Version® 7.0.0 was used to fit the quadratic response surface model to the experimental information as well as to generate response surfaces, analysis of data, and contour plots diagrams, while keeping a variable constant in the second-order polynomial model. The statistical significance of an effect was evaluated by *p*-values <0.05.

The response was persipeptides peak area and actual values of independent variables (X_i) were coded to x_i according to Eqn. (1).

Table 1. Compositions of seven different production media used for enhancing persipeptides production.

Medium	C-source, g L ⁻¹	N-source, g L ⁻¹	Salt g L ⁻¹	pH
CM1	Starch (20)	Soybean (30)	MgSO ₄ ·7H ₂ O (1) and CaCO ₃ (10)	7.0
CM2	Acorn (20)	Yeast Extract (4)	-	7.0
CM3	Rape seed (10)	Malt (10)	-	7.0
CM4	Cotton seed (10)	Malt (10)	-	7.0
CM5	Sesame (20)	Malt (10)	-	7.0
CM6	Glycerol (15)	Soybean (10)	CaCO ₃ (1), NaCl (5), and COCl ₂ ·7H ₂ O (1)	7.0
ISP2	Glucose (4)	Yeast extract (4)	-	7.4

$$x_i = \frac{X_i - \bar{X}_i}{(X_{iHi} - X_{iLow})/2}, i = 1, 2, 3 \dots k \quad (1)$$

where,

x_i = coded value of independent variable;

$X_{iHi/Low}$ = real values of the independent variable;

\bar{X}_i = real values of the independent variable at the center point of the domain; and

x_1 (coded value of percentage of organic solvent),

x_2 (coded value of stirring rate), and

x_3 (coded value of extraction time) were given in Eqn. (2), (3) and (4).

$$x_1 = \frac{X_1 - 50}{25} \quad (2)$$

$$x_2 = \frac{X_2 - 225}{75} \quad (3)$$

$$x_3 = \frac{X_3 - 49}{29} \quad (4)$$

Response surface analysis of a five coded level CCRD for three factors, 20 runs (Table 2), was done using the generalized second-order polynomial model of Eqn. (5), and economically optimum conditions for LLE of persipeptides was determined by same equation.

$$Y = \beta_0 + \sum_{i=1}^k \beta_i X_i + \sum_{i=1}^k \beta_{ii} X_i^2 + \sum_{ij=1(i \neq j)}^k \beta_{ij} X_i X_j$$

(5)

where,

Y = the experimental response;

β_0 , β_i , β_{ii} , and β_{ij} = the constant (intercept) coefficient, the linear coefficient, the quadratic coefficient, and the coefficient of interaction effect, respectively; and

X_i and X_j = independent variables

The quality of the fitted model was evaluated through analysis of variance (ANOVA). Additionally, the statistical analysis of the result, the evaluation of model and factors involved, and the determination of the influence of individual factors and their interaction with other factors on persipeptides extraction from the fermentation culture matrix by LLE were performed by determination of the coefficients from eqn. (5).

Table 2. Experimental sheet for five coded level CCRD of significant factors selected by screening design.

Run	Factor 1 x_1 : BuOH %	Factor 2 x_2 : stirring rate	Factor 3 x_3 : stirring time
1	50	225	49
2	50	225	0.23
3	92	225	49
4	8	225	49
5	50	225	49
6	50	352	49
7	75	300	20
8	50	99	49
9	50	225	49
10	50	225	98
11	50	225	49
12	25	150	78
13	25	300	20
14	75	300	78
15	25	300	78
16	75	150	78
17	25	150	20
18	50	225	49
19	75	150	20
20	50	225	49

Sample preparation

The fermentation medium was harvested and divided for further experiments. Samples were prepared based on experimental conditions defined by experimental designs, then butanol containing fermentation broths were centrifuged at 2937 ×g for 10 min. One-hundred-fifty-μL of each supernatants was separated and the solvent was removed using N₂ gas. The obtained precipitate was dissolved in 150 μL acetonitrile-water (1:1 v/v) and analyzed by HPLC method.

HPLC instrument and analysis

A Cecil instrument with in-line-degasser (CE 4040) consisted of manual Rheodyne (Rohnert Park, CA, USA) injector with 20 μL loop was employed. The sample was retained on an ACE (Aberdeen, UK) LiChrosob C18 column (250 × 4.6 mm ID, particle size 5 μm, ACE-121-2546) protected by Hichrom (Reading, UK) C18 column (NC100-5C18) and thermostated at 27 °C. The analytes were eluted by water (A) and acetonitrile (B) as mobile phase using a gradient elution, in which B was 50 % at start point, increased to 64 % in 5.5 min, then to 95 % within 1.5 min, followed by 5 min isocratic at 95 % (purge time), finally decreased to 50 % within 3 min and kept at this B % for as long as 10 min to equilibrate the column to prepare the system for next injection. Measurements were held at 210 nm and data was collected and processed by chromatography system manager and power stream software version 3.1, respectively.³

Results and discussion

The core aim of current study was the enhancement of persipeptides retrieval. At the production step, the most effective medium basis for persipeptides biosynthesis was chosen amongst seven candidate media listed in Table 1. After cultivation, persipeptides were separately isolated from them using un-optimized LLE method previously provided.³ Results, in Table 3, indicate the CM1 medium as the most productive fermentation culture medium for persipeptides biosynthesis, which enhances its production by more than six times, reaching to 219.63 ± 2.48, compared with ISP2 medium (36.31 ± 1.37). All other examined novel carbon sources; including acorn, sesame, cotton seed, and rape seed failed to increase the persipeptides production, compared with ISP2 and the production was in range of 33 to 39 μg mL⁻¹. The second most promising medium after CM1 was CM6, which composed of glycerol and soybean as carbon and nitrogen sources, respectively. CM6 considerably enhanced persipeptides production (159.69 ± 27.36), and four times increased in their production was resulted, compared to that of ISP2 medium (36.31 ± 1.37). Therefore, CM1 medium was selected as the final production medium and used for further optimization of LLE.

In this study, the LLE followed by HPLC-UV was applied for the extraction and the quantification of persipeptides in fermentation broth samples, respectively. Effects of multiple factors, including volume ratio of extraction solvent, stirring rate, sample pH, extraction temperature and process time were investigated. Optimized conditions were obtained by

screening design, and subsequently, CCRD was applied for the evaluation of significant factors along with their interactions thereof.

Table 3. Production of persipeptides in different fermentation media tested.

Name	1 st trial	2 nd trial	3 rd trial	Average
CM1	220.36	216.86	221.66	219.63 ± 2.48
CM2	38.39	35.258	37.93	37.93 ± 1.69
CM3	33.65	33.57	33.97	33.73 ± 0.21
CM4	42.42	33.62	39.14	38.39 ± 4.45
CM5	36.84	37.14	37.31	37.10 ± 0.24
CM6	132.27	159.81	186.99	159.69 ± 27.36
ISP2	34.93	36.33	37.68	36.31 ± 1.37

Before starting optimization procedures, broad range of solvents, including ethyl acetate, 1-propanol, 2-propanol, cyclohexane, dichloromethane, methanol, *n*-BuOH, and chloroform were examined for obtaining maximum extraction (Data not shown). Among them, *n*-butanol was selected as the extracting solvent, as it has a high boiling point, which prevent solvent loss during extraction, and low melting point (less than -89 °C); is immiscible with aqueous solution and its density is lower than water; and is compatible with the RP-HPLC used in the quantification of persipeptides.

Screening design

Half fraction of factorial (resolution V) design is useful for preliminary purposes or in initial optimization steps owing to its great power in estimation of effects as well as considerable reduction in the number of experimental runs to be performed. Applying this design allows the estimation of all the main effects and two-factor interactions (2 FI) with the assumption that no three-factor or/and higher interactions occur/s. Therefore, half fraction factorial design was used for the screening step. Major factors, which are assumed to influence the LLE of persipeptides, include volume percentage of extraction solvent, stirring rate, sample pH, extraction temperature and process time. Levels of factors for the screening design were selected according to our knowledge, and are presented in Table 4. The overall design matrix, consisted of 20 runs of which four of them were center runs, was randomly performed in order to minimize unexplained variability effects in obtained responses due to systematic errors. Half-normal probability plot was used to choose significant effects, which were further analyzed by ANOVA and obtained results were evaluated to determine main effects (Table 5).

The standard effect was estimated for calculating a *t*-statistic for each effect. Normalized results of the performed experimental design were investigated at a 5 % of significance and analyzed by standardized Pareto chart (Figure 1). On this plot (Figure 1), effects that are now above the second vertical line, Bonferroni limit, and those between second and first vertical lines, *t*-value limit, are almost certainly and possibly significant parameters, respectively.

Table 4. Levels of factors for the screening design.

Independent Factors	CS	Levels and Ranges		
		-1 (L)	0 (M)	+1 (H)
Broth pH	A	7	9	11
Temperature (°C)	B	20	40	60
BuOH % (v/v)	C	50	63	75
Stirring rate (rpm)	D	100	200	300
Process time (min)	E	20	70	120

CS, L, M, and H stand for Coded Symbol, Low, Middle, and High, respectively.

The model F-value of 10.25 implies the significance of the model. There is only a 0.05 % chance that the model F-value of this large could have been occurred due to noise. The measured curvature F-value of 37.33 as the difference between the average of the center points and that of the factorial points implies that the curvature in the design space is significant, and there is a 0.01 % probability that it could occur due to noise. Therefore, there was a need for higher resolution design (RSM) to optimize the significant factors. Furthermore, the lack of fit F-value of 0.35 implies that it is not significant relative to the pure error, and there is an 89.72 % chance that it could occur due to noise, therefore, the model can fit. The model had the predicted R-square of 0.74, which is in reasonable agreement with the adjusted R-square of 0.78. Moreover, model adequate precision measuring the signal to noise ratio had the value of 10.217 being considerably greater than 4, and therefore, the model can be used to navigate the designed space.

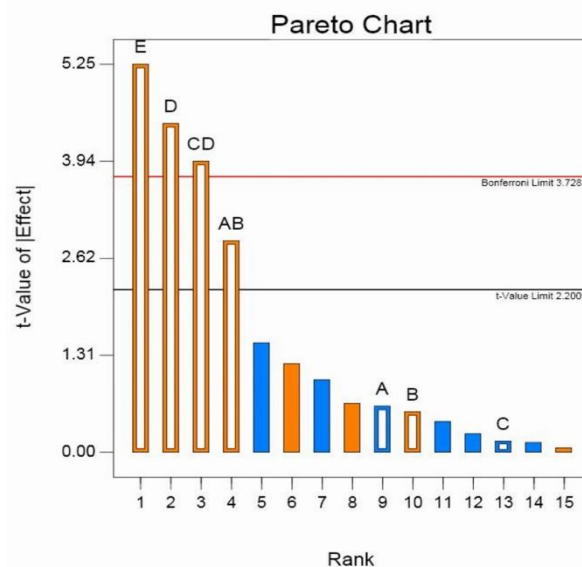


Figure 1. Pareto chart with selected main effects obtained from the half fraction of factorial design for LLE of persipeptides; A: sample pH; B: extraction temperature; C: percentage of BuOH; D: stirring rate; E: extraction time; AB and CD are 2FI between sample pH and extraction temperature, and percentage of BuOH and stirring time, respectively; 1: extraction time; 2: stirring rate; 3: 2FI between percentage of BuOH and extraction time; 4: 2FI between sample pH and extraction temperature; 5: 2FI between sample pH and extraction time; 6: 2FI between extraction temperature and stirring rate; 7: 2FI between extraction temperature and percentage of BuOH; 8: sample pH; 9: 2FI between sample pH and percentage of BuOH; 10: 2FI between sample pH and stirring rate; 11: 2FI between percentage of BuOH and extraction time; 12: 2FI between extraction temperature and percentage of BuOH; 13: 2FI between extraction temperature and extraction time; 14: extraction temperature; and 15: percentage of BuOH.

Table 5. Estimated ANOVA for half fraction of factorial design relationship between response variable (extraction yield) and independent variables (A, B, C, D, and E) in determination of significant factors to be optimized by RSM.

Source	SST	df	MS	F-Value	p-value Prob > F
Model	2438730	7	348390	10.24817	0.0005
A-pH	13219.25	1	13219.25	0.388855	0.5456
B-Temperature	10287.03	1	10287.03	0.302601	0.5933
C- BuOH %	771.4506	1	771.4506	0.022693	0.8830
D-Stirring rate	672359	1	672359	19.77798	0.0010
E-Stirring time	936685.2	1	936685.2	27.55335	0.0003
AB	278440.9	1	278440.9	8.190562	0.0155
CD	526967.1	1	526967.1	15.50116	0.0023
Curvature	1268896	1	1268896	37.32559	<0.0001
Residual	373948.7	11	33995.33		
Lack of Fit	179699.1	8	22462.39	0.34691	0.8972
Pure error	194249.6	3	64749.85		
Cor total	4081575	19			

SST, MS, and df stand for Sum of Squares, Mean Square, and Degree of Freedom, respectively.

According to Figure 1 and Table 5, duration of stirring time was the most significant factor with a negative effect on the extraction efficiency of persipeptides. The second most important negative-effect variable was the rate of stirring. Interestingly, 2 FI between percentage of BuOH and stirring rate was significant with a negative effect on the extraction process. In contrast, both pH and temperature were non-significant factors with positive and negative effect, respectively. In low temperatures, extraction is slow process with lower yield, whereas at higher temperature, solvent is more soluble in aqueous phase, and therefore its separation from aqueous solution is more complicated. Additionally, persipeptides degradation is apparent at high temperatures;³ therefore, temperature for their extraction was set at 28 °C. Moreover, the pH of the extraction process was kept the same as the pH of fermentation broth of *S. zagrosensis* (9 and 9.5).

Optimization of significant factors

In the next step, a CCRD design was applied to optimize the values of three factors (percentage of BuOH, stirring rate, and extraction time), selected from the prior screening design. The process variable of LLE of persipeptides examined using CCRD presented in Table 6. The number of experiments is determined by the expression: $(2^n + 2n + C)$, where n represents the number of factors (6) and C denoted the number of center points (3). The design of CCRD consisted of a factorial design (2^n) augmented with $(2n)$ run per axial points, which is the number of times each axial run will be performed and located at $+1.682\alpha$ and -1.682α from the center of the experiment domain to satisfy the rotatability condition of the CCRD, and central points (C). Center runs with six repetitions were employed to estimate pure error for the lack of fit test as well as provides rather uniform precision designs. This means that the error inside a sphere that has a radius equal to ± 1 level is nearly uniform. Thus, predictions in this region are equally good.

Table 6. The significant variables and the level of the central composite response design used in the optimization of the persipeptides extraction.

Factor	Level			Star points*	
	-1 (L)	0 (C)	+1 (H)	- α	+ α
x_1 : BuOH %	25	50	75	8	92
x_2 : Stirring rate	150	225	300	99	351
x_3 : Stirring time	20	49	78	0.3	98

*The value is ($\alpha = 1.682$). L, C, and H stand for Low, Central, and High, respectively

The data obtained were analyzed by ANOVA (Table 7) and then backward elimination regression, with alpha to exit equal to 0.100, was employed to improve the ANOVA results, in which the quadratic response was reduced by the elimination of x_1x_2 (2FI) and x_3^2 (Table 8).

Fitting the model

A regression evaluation (Table 8) was performed for fitting mathematical models to the experimental data aiming at an optimal area, and a quadratic model was suggested according to the results. The predicted model of the regression equation for the peak area of persipeptides was expressed as eqn. (6) in terms of coded factors.

$$Y_1 = 1604.08 - 18.95x_1 + 231.51x_2 + 267.34x_3 - 225.41x_1x_3 - 220.52x_2x_3 - 183.06x_1^2 - 138.61x_2^2 \quad (6)$$

The F-test and p -value (Table 8) were used to determine the significance of each coefficient. If the p -value becomes smaller and the absolute F-value becomes higher, the corresponding variable would be of more significant.²²

Table 7. Estimated ANOVA of relationship between response variables (extraction yield) and independent variables (x_1 , x_2 and x_3) for response surface quadratic model.

Source	SST	df	MS	F-Value	p-value Prob >F
Model	3301366	9	366818.5	3.606939	0.029
x_1	4902.709	1	4902.709	0.048209	0.8306
x_2	731993.3	1	731993.3	7.197717	<u>0.023</u>
x_3	976072.3	1	976072.3	9.597755	<u>0.0113</u>
x_1x_2	2266.328	1	2266.328	0.022285	0.8843
x_1x_3	406463.8	1	406463.8	3.996774	<u>0.0735</u>
x_2x_3	389028.2	1	389028.2	3.825328	<u>0.079</u>
x_1^2	443707	1	443707	4.362988	0.0633
x_2^2	247389.7	1	247389.7	2.432592	0.1499
x_3^2	84216.33	1	84216.33	0.828102	0.3842
Residual	1016980	10	101698		
Lack of fit	789641.9	5	157928.4	3.473428	0.099
Pure error	227337.9	5	45467.59		
Cor. total	4318346	19			

SST, MS, and df stand for Sum of Squares, Mean Square, and Degree of Freedom, respectively.

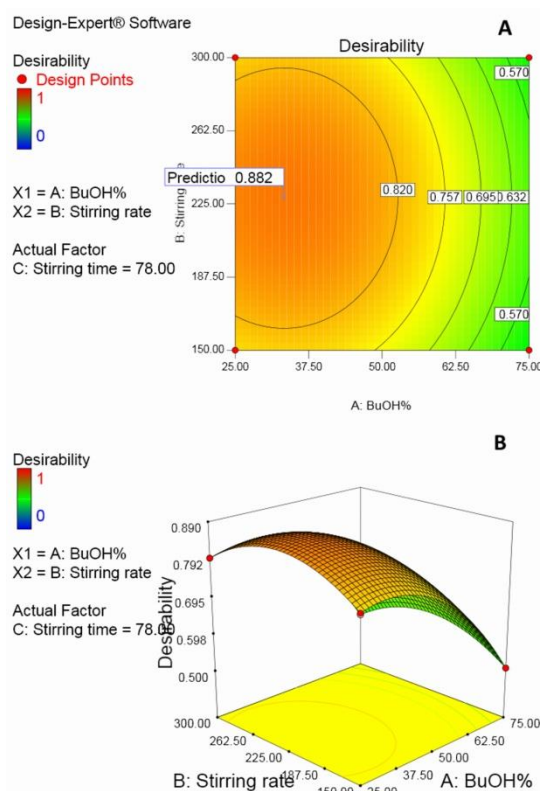
Table 8. ANOVA of relationship between response variables (extraction yield) and independent variables (x_1 , x_2 and x_3) in response surface reduced quadratic model.

Source	SST	df	MS	F-Value	p-value
Model	3214883	7	459269.1	4.994487	0.0075
x_1	4902.709	1	4902.709	0.053316	0.8213
x_2	731993.3	1	731993.3	7.960324	0.0154
x_3	976072.3	1	976072.3	10.61465	0.0069
x_1x_3	406463.8	1	406463.8	4.420237	0.0573
x_2x_3	389028.2	1	389028.2	4.230627	0.0621
x_1^2	487734.6	1	487734.6	5.304045	0.0400
x_2^2	279641.6	1	279641.6	3.041063	0.1067
Residual	1103462	12	91955.21		
Lack of fit	876124.5	7	125160.6	2.752744	0.1413
Pure error	227337.9	5	45467.59		
Cor. total	4318346	19			

It was observed that most significant variables were the linear terms of extraction time (x_3) and stirring rate (x_2).

The result suggested that the change in extraction time ($p < 0.0069$) and stirring rate ($p < 0.0154$) had considerable effects on the LLE of persipeptides. Indeed, extraction time (x_3) had a pivotal effect in LLE method and was required to be optimized in order to achieve high efficiency in extraction of the persipeptides. The procedure time was the driving force

for transportation of the persipeptides from aqueous solution to organic solvent as a result of the increase in compounds interaction with organic solvent until the extraction equilibrium has been reached. However, if the time is set erroneously high, then persipeptides will be degraded³ and in turn, the extraction efficiency will decrease. Persipeptides degradation may reach up to 21 % when fermentation broth is kept at room temperature for 24 h prior to extraction or its concentration may be decreased by up to 13 % when the broth is preserved at 4 °C in BuOH for same period of time.³ Results showed that the extraction time is in reverse relationship with the percentage of organic solvent used, justifying the existence of significant interaction between two factors, which was found in the screening design. In high percentage of organic solvent, the time of extraction could be diminished to as low as 33 min. Nevertheless, increasing the rate of stirring as high as possible (up to 300 rpm), which was the second most important factor in this process, enhanced the extraction capability. These are in accordance with other studies conducted on the effect of stirring rate, solvent amount, and hold-up on efficiency of a typical extraction process, which have reported that when stirring speed and solvent amount were increased, the efficiency increased. Additionally, it has been proposed that the efficiency of the compounds extraction increased monotonously with speeding up stirring rate.²³ Following the mathematical model fitting, multiple response method, called the desirability function (D), was employed to optimize the studied parameters.

**Figure 2.** Contour plot (A) and 3D surface graph (B) of desirability versus ratio of BuOH and stirring rate. Stirring time was 78 min, pH was 9, and temperature was 28 °C were the experiment condition.

This method was applied to meet the requirement for increasing the yield of extraction in as shortest process as possible to both decrease the expenses and prevent persipeptides degradation. The most desired value for the responses is a desirability value of one, whereas a value equal to zero represents an unacceptable value for responses.

The aim of the optimization was to improve the LLE efficiency of persipeptides. In this approach, a process with desired characteristics is obtained by combining process parameters, which has been evaluated by RSM, into a single variable for the prediction of the optimal levels of the independent variables. To achieve the highest desirability, all factors were set to within range, except the concentration of persipeptides that was set to maximum level. Figures 2A and 2B, respectively, illustrate the contour plot and 3D surface graph of desirability for LLE of persipeptides generated from 15 optimum points through numerical optimization.

Among 30 starting points, the best local maximum for LLE of persipeptides ($264 \pm 9.85 \mu\text{g mL}^{-1}$) was resulting in 34 % BuOH, 228 rpm (stirrer speed), and 78 min (stirring time) with the value of desirability of 0.88. Compared with un-optimized process (persipeptides concentration of $219.63 \pm 2.48 \mu\text{g mL}^{-1}$), the optimized conditions increased the extraction of persipeptides by 20.20 %, while decreased both time and percentage of BuOH by 67 % (162 min) and 16 %, respectively. Therefore, using optimized LLE method and suggested fermentation broth, a total of seven times increased in persipeptides production was reached. Nevertheless, from large scale prospect, the final reaction conditions *i.e.* broth pH, 9-9.5; temperature, 28 °C; stirrer speed, 228 rpm; percentage of BuOH; 34 %; and process time, 78 min have industrial compatibility.

This is because of no pre-pH adjustment requirement for LLE of persipeptides as the ambient pH of *S. zagrosensis* CM1 broth is within the mentioned range. It is worth to note that as pH increased and temperature decreased the corrosion rate of steel from different parts of extraction plants decreased, which is an astonishing feature of this optimized process. Moreover, minimum facilities and energy consumption are required for adjusting temperature at 28 °C; therefore, greatly decreases the expense of extraction. The percentage of BuOH was decreased in expense of increasing time from 33 to 78 min to minimize instrument corrosion and solvent usage and its subsequent evaporation expenses. However; despite great effort, the agitation could not be decreased and indeed increased from 150 rpm in un-optimized process to 228 rpm in further optimized method, which is inevitably still not considered as an improving step.

Conclusions

The direct impact of this optimization is on decreasing the cost of extraction as well as the time of process, whereas increasing the yield of extraction. This in turn, facilitates further clinical trial investigations, which require several of grams of purified persipeptides. This was the first attempt reported on retrieval of persipeptides from fermentation broth that has been optimized. It has been previously shown that presence of glucose plus a more slowly utilized carbon source such as malt result in production of higher secondary

metabolites, as glucose utilization results in good growth of bacteria and complex carbon source is used for antibiotic synthesis.²⁴ However, rapid catabolism of glucose has been shown to decrease the rate of antibiotic production.^{25, 26} In practice, ISP2 medium, which have been tested on the basis of this assumption failed to increase the production of persipeptides. In contrast, both CM1 and CM6 increased the production of persipeptides. These increases may be due to the fact that application of low solubility carbon sources, such as insoluble starch in CM1 and glycerol in CM6, prevents carbon catabolite regulation.²⁶ Despite the advantage of utilization of glycerol in fermentation, which contains more energy than starch and glucose on a weight-to-weight basis, it has some disadvantages, including higher oxygen requirement, increased medium viscosity, and more problematic downstream processing.²⁶ Interestingly, both CM1 and CM6, considerably enhanced persipeptides production by six and four times, respectively, compared to ISP2 medium. CM1 and CM6 contain soybean, which is a rich source of valine and phenylalanine amino acids with percentage of total weight on dry basis of 2.06 ± 0.19 and 2.16 ± 0.21 , respectively.²⁷ These amino acids are present in core structure of persipeptides with repetitions as the only utilized amino acids. CM1 contains three times more soybean than CM6, which may explain its 37 % (approximately $60 \mu\text{g L}^{-1}$) more persipeptides production, compared to CM6 by means of providing more valine and phenylalanine. It has been observed that increase in amount of CaCO_3 from 2 to 10 g L^{-1} improves the production of persipeptides (Data not shown); however, there is little knowledge on effects of various salts in biosynthesis of persipeptides. Therefore, a systematic study using a number of techniques such as labeled precursors for the study of various media components and its further optimization for exploiting the best result are required.

References

- 1 Brown, E.D., Wright G. D., *Nature*, **2016**; 529(7586), 336.
- 2 Mohammadpanah, F., Matasyoh, J., Hamed, J., Klenk, H. P., Laatsch, H., *Bioorg. Med. Chem.*, **2012**; 20(1), 335.
- 3 Mohammadpanah, F., Panahi, H. K. S., Imanparast, F., Hamed, J., *Chromatographia*, **2016**, 79(19-20), 1325.
- 4 Davidson, B. S., *Chem. Rev.*, **1993**, 93(5), 1771.
- 5 Cody, W. L., He, J. X., Reily, M. D., Haleen, S. J., Walker, D., M., Reyner, E. L., Stewart, B. H., Doherty, A. M., *J. Med. Chem.*, **1997**, 40(14), 2228.
- 6 Rajeswaran, W., Hocart, S. J., Murphy, W. A., Taylor, J. E., Coy, D. H., *J. Med. Chem.*, **2001**, 44(8), 1305.
- 7 Dechantsreiter, M. A., Planker, E., Mathä, B., Lohof, E., Hölzemann, G., Jonczyk, A., Goodman, S.L., Kessler, H., *J. Med. Chem.*, **1999**, 42(16), 3033.
- 8 Hess, S., Ovidia, O., Shalev, D., E., Senderovich, H., Qadri, B., Yehezkel, T., Salitra, Y., Sheynis, T., Jelinek, R., Gilon, C., Hoffman, A., *J. Med. Chem.*, **2007**, 50(24), 6201.
- 9 Barker, P., L., Bullens, S., Bunting, S., Burdick, D., J., Chan, K., S., Deisher, T., Eigenbrot, C., Gadek T., R., Gantz, R., *J. Med. Chem.*, **1992**, 35(11), 2040.
- 10 Dong, M. W., *Modern HPLC for Practicing Scientists*, Wiley, Hoboken, **2006**.
- 11 Snyder, L., R., Kirkland, J., J., Dolan, J., W., *Basic Concepts and the Control of Separation. Introduction to Modern Liquid Chromatography*, 3rd ed., Wiley, Hoboken, **2010**.

- ¹²Araujo, P. W., Brereton, R. G., *Trends Anal. Chem.*, **1996**, 15(2), 63.
- ¹³Bezerra, M. A., Santelli, R. E., Oliveira, E. P., Villar, L. S., Escalera, L. A., *Talanta*, **2008**, 76(5), 965.
- ¹⁴Ghafari, S., Aziz, H. A., Isa, M. H., Zinatizadeh, A. A., *J. Hazard. Mater.*, **2009**, 163(2), 650.
- ¹⁵Li L.Z., Zheng H., Xian M., *J. Taiwan Inst. Chem. Eng.*, **2010**, 41(3), 252.
- ¹⁶Shioya, S., Morikawa, M., Kajihara, Y., Shimizu, H., *Appl. Microbiol. Biotechnol.*, **1999**, 51 (2) 164.
- ¹⁷Zhu, Y., Chen, G., Wu, M., Miao, X., Xu, J., Wang, M., *Chin. J. Pharm.*, **2010**, 3, 014.
- ¹⁸Marques, D. A. V., Cunha, M. N. C., Araújo, J. M., Lima Filho, J. L., Converti, A., Pessoa, J. R. A., Porto, A. L., *Braz. J. Microbiol.*, **2011**, 42 (2), 658.
- ¹⁹Saval, S., Pablos, L., Sanchez, S., *Bioresour. Technol.*, **1993**, 43 (1), 19.
- ²⁰Adinarayana, K., Ellaiah, P., Srinivasulu, B., Devi, R. B., Adinarayana, G., *Process Biochem.*, **2003**, 38 (11), 1565.
- ²¹Viana Marques, D., Pessoa Júnior, A., Lima Filho, J., Converti, A., Perego, P., Porto, A., *Biotechnol. Prog.*, **2011**, 27 (1), 95.
- ²²Atkinso, A., Donev, A., *Technometrics*, **1996**, 38 (4), 333.
- ²³Abolghasemi, H., Moosavian, M., Bahmanyar, H., Maragheh, M. G., *Iran J. Chem. Eng.*, **2005**, 2 (1), 11.
- ²⁴Martín, J. F., Demain, A. L., *Microbiol. Rev.*, **1980**, 44 (2), 230.
- ²⁵Revila, G., Lopez Nieto, M. J., Luengo, J. M., Martin, J. F., *J. Antibiot.*, **1984**, 37 (7), 781.
- ²⁶Saudagar, P. S., Survase, S. A., Singhal, R. S., *Biotechnol. Adv.*, **2008**, 26 (4), 335.
- ²⁷Kovalenko, I. V., Rippke, G. R., Hurburgh, C. R., *J. Agric. Food Chem.*, **2006**, 54 (10), 3485.

Received: 21.10.2016.

Accepted: 25.11.2016,



ATTEMPTS ON PREPARATION OF ELASTIC ABSORBENT FROM WASTE RUBBER TYRES FOR RECOVERY OF BIOBUTANOL FROM FERMENT LIQUORS

László Kótai,^[a, b] István Somogyi,^[c] Li Zhibin,^[d] Baiquan Chen,^[d] Kalyan K. Banerji,^[e] R. P. Pawar,^[f] Rajni Kant^[g] and Tünde Kocsis^[b]

Keywords: Biobutanol, extractive fermentation, superabsorbent, solid sponge, sulphonated rubber, tyre wastes.

Attempts on the preparation of elastic sorbents from waste rubber tyres, for removal of biobutanol from ferment liquor extracts, using low-distribution apolar solvent like n-heptane have been discussed. The main factors in preparation of useful sorbents are the type of the waste tyre, the type of the sulphonating agent, and the reaction conditions. The waste tyres containing large amount of styrene proved to be useful base material for preparation of elastic sorbent with concentrated sulphuric acid as sulphonation agent. The common mixed waste tyres resulted in elastic sorbents with lower absorbing capacities. Therefore, the styrene containing ones were studied over a wide range of the sulphonation conditions.

* Corresponding Authors

E-Mail: kotai.laszlo@ttk.mta.hu

- [a] Institute of Materials and Environmental Chemistry, Research Centre for Natural Sciences, Hungarian Academy of Science, H-1117, Magyar Tudósok krt. 2., Budapest, Hungary
- [b] Deuton-X Ltd., H-2030, Selmeci út 89, Érd, Hungary.
- [c] Iontech Ltd., 8196, Árpád utca 38, Litér, Hungary
- [d] China New Energy Co., Room 210, Floor 2 Integration Service Building Guangzhou Science and Technology Innovation Base, 80 Lanyue Road, Guangzhou, China.
- [e] Faculty of Science, National Law University, Jodhpur, India
- [f] Department of Chemistry, Deogiri College, Aurangabad-431005, Maharashtra, INDIA.
- [g] X-ray Crystallography Laboratory, Post-Graduate Department of Physics & Electronics, University of Jammu, Jammu, India.

aliphatic hydrocarbon extractants used in the extractive biobutanol fermentation processes are described starting from waste rubber tyres.

Experimentals

Sulphonation of the soft waste rubber tyres

A waste soft rubber tyre granulate (sample made from a cross motor tyre cubes with putting that into liquid nitrogen and grinding the cooled inelastic form with selecting a fraction with 2.5 mm average equivalent diameter) (4.1 g) was mixed with 4 ml 1,2-dichloroethane and 50 ml of 96 % sulphuric acid at room temperature. The reaction mixture was heated until 90 °C in 2 h then kept at this temperature for 3 h, and cooled left to cool to room temperature (roughly 1.5 h). The sample was thoroughly washed with water until acid-free and the ion-exchange and salt-splitting capacities were measured with a standard method.⁶

The water content was measured with drying the samples in an oven at 105 °C. Solvent absorbing capacities were measured with gravimetrically after keeping the sample in the appropriate solvent for an hour. Both the salt-splitting and the ion-exchange capacity were found to be 0.50 mequiv mL⁻¹. The binding capacity for n-BuOH and some other solvents including water is given in Table 1.

Sulphonation of the hard waste rubber tyres at high temperature

A waste hard rubber tyre granulate (made from a hard tyre cubes with putting that into liquid nitrogen and grinding the cooled inelastic form with selecting a fraction with 2.5 mm average equivalent diameter) (4.4 g) was mixed with 1,2-dichloroethane (4 mL) and 90 g of 96 % sulphuric acid at room temperature. The reaction mixture was heated until 90 °C in 2 h then kept at this temperature for 3 h, and cooled left to cool to room temperature (roughly 1.5 h). The sample was thoroughly washed with water until acid-free. The n-butanol and water absorbing capacities were found to be 21.6 and 147.0 %, respectively. The salt-splitting capacity was found to be 0.31 mequiv mL⁻¹.

Introduction

Biobutanol, one of the most promising biofuel of the near-future, is produced in fermentative processes from agricultural products and wastes.^{1,2} In order to improve the effectiveness and decreasing the process costs, the so-called extractive fermentation processes are favoured in order to avoid the accumulation of the toxic biobutanol during the fermentation process.²⁻⁴ The most effective extractants like heptanal, however, are toxic, and the non-toxic solvents like aliphatic hydrocarbons such as n-heptane have very low distribution coefficients. Combining the extractive fermentation in the presence of aliphatic hydrocarbon extractants by removing of biobutanol from the low hydrocarbon solvent with a solid phase regenerable super absorbent before recycling that to the fermentation process, is a potential way to solve this problem.⁵

In order to regenerate of the solid sponges with heat treatment (both the absorption and regeneration processes initiate large volume changes of the absorbents due to swelling and drying) in order to prevent the cracking and mechanical destroying, the supersorbents used for recovery of butanol and similar polar solvents should be elastic.

In this communication the preliminary results on attempts on preparing a cheap, elastic and regenerable solid supersorbents for recovery of biobutanol from apolar

Sulphonation of the hard waste rubber tyres at room temperature

The common waste tyre granulate (30 g) removed from car tyres prepared in a method given previously was swelled with 20 mL of 1,2-dichloroethane for 30 min, the excess of solvent was decanted and the sulphonation was performed with 120 g of 96 % sulphuric acid at room temperature for 3 h. The same methods as previously described were used to isolate and characterize the product. The salt splitting/ion exchange capacity was found to be 0.21 mequiv. mL⁻¹.

Effect of sulphuric acid on the sulphonation of the hard waste rubber tyres at room temperature

The common waste tyre granulate (25 g) removed from waste tyres prepared in a method given previously was swelled with 47.7 mL of 1,2-dichloroethane for 30 min, the excess of solvent was decanted and the sulphonation was performed with 500 g of 96 % sulphuric acid at room temperature for 3 h. The same method was used to isolate and characterize the product as earlier. The salt splitting/ion exchange capacities were found to be the same, namely 0.09 mequiv mL⁻¹.

Attempts on sulphonation of waste hard rubber tyres with chlorosulphonic acid

Waste tyre granulates (5 g, 2.5 mm fraction) were swelled in 25 mL of 1,2-dichloroethane for 30 min, the solvent was removed by decantation, then 40 g of chlorosulphonic acid was added at room temperature with stirring. The reaction mixture was heated until 40 °C in 30 min, when a weak gas evolution was started with strong H₂S smell. The gas evolution was decreased after 1.5 h and the reaction mixture was allowed to cool for 30 min. The product was a strong tar-like substance which could not be removed and processed.

Attempt on sulphonation of waste rubber tyres with chlorosulphonic acid without outer heating

Another portion of (20 g) of waste tyre granules ($d = 2.5$ mm) was mixed with 175 g of chlorosulphonic acid, when the reaction mixture was warmed up to 35 °C. After 10 min stirring, the granulates were disintegrated into powder.

Attempt on sulphonation of waste rubber tyres with chlorosulphonic acid with ice-cooling

Five gram of waste tyre granules (2.5 mm in average equivalent diameter) were swelled for 15 min in 25 mL of 1,2-dichloroethane, the mixture was cooled to 5 °C with ice and 10 mL of chlorosulphonic acid was added dropwise in an hour. The maximal temperature was observed due to reaction heat at half of the acid adding (~14 °C). The mixture was stirred for 10 min at 5 °C, and the mixture was poured into ice cubes. No further reaction (evolution of HCl gas) was observed with the residual chlorosulphonic acid.

The solvent was removed by distillation, the residue was washed five times of 400 mL of distilled water. The product was inelastic.

Swelling experiment with α -methylstyrene

Common waste rubber tyre granulate (2.5 mm in diameter in average, 7.14 gram) was mixed with 11.95 g of α -methylstyrene as swelling and copolymerizing agent, and the mixture was polymerized with 0.5 % dibenzoyl peroxide. The polymer product was a sticky material which could not be isolated from the reactor.

Results and Discussions

Extractive fermentation with using non-toxic extractants like aliphatic hydrocarbons results only low distribution coefficients. For example, this value is 0.21, 0.056 and 0.16 for n-BuOH, ethanol and acetone (ABE fermentation products) with 0.031 water equilibrium ratio.⁷ In order to remove these solvents, especially the most toxic n-butanol, a solid absorbent is needed, which is in contact with the non-toxic extractant^{5,8} before recycling that into the extractive fermentation.

There are known some polar solid absorbents which can absorb butanol and the secondary solvents of butanol production as well,^{5,8} together with the small amount of water which exists in the n-heptane in contact with the aqueous ferment liquor. The two most promising ones among them are the sulphonated⁵ and nitrated⁸ styrene-divinylbenzene copolymers. The sulphonated styrene-divinylbenzene copolymers are commercialized as microporous sulphonated cation exchangers.⁶

The main problem is with using these polymers are, that during absorption of the n-BuOH and other solvents a strong swelling and volume increasing can be observed, and during removal of the solvents from the solid sorbents (regeneration and solvent collection with thermal treatment), a strong volume contraction takes place. Alternate volume changes during the repeated use and regeneration cause formation of cracks and mechanical powdering of the solid absorbent granules.

This is a strong disadvantage due to material loss and technological problems caused by the powder formation. Since the sulphonated polymers are more polar and bound less with aliphatic hydrocarbon solvents than the nitrated ones, our efforts were focused on preparation an elastic type sulphonated type polymer material.

From economic point of view, the best choice as elastic polymer materials for sulphonation experiments was different kinds of waste rubber tyres. Two series of waste rubber tyre materials, namely a soft rubber with high styrene content and a hard rubber (average mixture of waste car rubber tyre processing) were used.

Table 1. Solvent absorbing capacity of the raw waste tyres granulates and the sulphonated soft rubber tyres*

Solvent	Raw soft waste tyre		Dry sulphonated soft tyre		69.5 % water contg. sulphonated rubber
	Absorbed amount, g/100 g	Swelling in vol. %	Absorbed amount, g/100 g	Swelling, vol. %	Absorbed amount, g/100 g
n-Butanol	7	7	63	87	27
n-BuOH-H ₂ O=82:12, v/v	-	-	12	-	-
Ethanol	5	5	73	102	-
Ethanol:water, 1:1, v/v	-	-	37	-	-
Methanol	10	10	75	105	-
Methanol:water, 1:1 (v/v)	-	-	39	-	-
1,2-Dichloroethane	292	200	92	87	39
n-Heptane	24	28	37	60	6
Water	0	-	87	97	-

*Prepared from a soft rubber (removed from a cross-motor) tyre

Since the sulphonation of polystyrene-butadiene rubbers with chlorosulphonic acid was not thermodynamically favourable (ΔH^0 , ΔS^0 , and ΔG^0 were found to be 40.708 kJ, 64.22 J K⁻¹, and 22.916 kJ, respectively),⁹ the sulphonation of styrene-based rubbers was tested only with sulphuric acid, while the common waste tyre rubber mixtures were tested with both cc. sulphuric acid and chlorosulphonic acid.

Preparation and properties of the high-styrene content sulphonated (soft) waste tyres

Sulphonation of soft waste tyres containing high amount of styrene (2.5 mm equivalent diameter) and swelled in 1,2-dichloroethane with concentrated sulphuric acid at 90 °C led to black coloured granulates having the expected elastic properties. The prepared air-dried sample contained 69.5 % water which was transformed to dry at 105 °C in an oven. The bulk density of the water-containing and the dry samples was 1.1762 g mL⁻¹ and 0.4761 g mL⁻¹, respectively. This shows highly porous structure of the formed resins. The ion-exchange capacity is the same as the salt-splitting capacity, so the all active groups proved to be strongly acidic sulphonic groups in the resin.

The solvent absorbing capacities and the volume changes during swelling in the given solvent are presented in Table 1. The pure butanol absorbing capacity of the dry resin was found to be 63 % with 87 % of volume changes. The resin without drying can absorb 27 % butanol. Taking into consideration the water content of the wet resin, the absorbing capacity of the dry material content in the wet resin is close to the result get in case of the oven-dried sample.

Comparing the absorption of other polar solvents such as ethanol, methanol, 1,2-dichloroethane and water with the dry resin, the absorbing capacities correlate with the polarity of the solvents. The more polar solvent the more solvent can be absorbed, which unambiguously support the assumption that the active sites of sorption are located in the environment of the polar sulphonic groups. The apolar n-heptane was absorbed only in 37 % and 6 % amount in case of dry and wet resin, respectively. The swelling of dry resin was found to be 39 %. It shows that only the pores play role in absorption of heptane.

The distribution coefficient of the water between the ferment liquor and the extractant selected is a key parameter in the design of biobutanol production technology, because

the presence of water decreases the absorption of polar solvents in a large extent. The butanol absorbing capacity decreases to 12 % in the case of 88 % BuOH-12 % H₂O mixture (v/v), while in case of 1:1 (v/v) mixtures of ethanol or methanol the absorbing capacity roughly decreases to the half of their original values.

The elastic sulphonated rubbers are promising candidates for recovery of the solvent mixtures from n-heptane before recycling that in the extractive ABE (acetone-butanol-ethanol) or IBE (isopropanol-butanol-ethanol) fermentation processes due to two reasons. First, the distribution coefficient values of n-butanol and other polar solvents between n-heptane and water. Secondly, the low solubility of water in n-heptane, butanol and other polar or less polar solvent containing n-heptane mixtures at low polar solvent concentration.

Preparation and properties of the sulphonated common (hard) waste tyres

The sulphonation of a rubber mixture (2.5 mm in average diameter) prepared from common waste tyres were studied in detail both with cc. sulphuric acid and chlorosulphonic acid in a wide range of reaction conditions. In the case of chlorosulphonic acid the efforts failed, because tar-like or powdered material formed in every case, even if the reaction was proceeded with strong cooling. If the reaction proceeded with gentle heating, malodorous gas (H₂S or mercaptans) were formed which strongly suggests that the disulphide bridges decomposes under the action of chlorosulphonic acid which can explain the formation of tar-like products.

Using concentrated sulphuric acid, the ion-exchange/salt-splitting capacities are the same, but these values are lower than in case of styrene-containing soft rubbers. The more drastic conditions (excess of acid, higher temperature) were used, the less sulphonic acid groups were built into the structure, and there were no elastic products formed in any of the cases. The ion-exchange capacity values decreased from 0.31 mequiv mL⁻¹ to 0.09 mequiv. mL⁻¹, which suggest that the sulphuric acid decomposes the sites where the sulphonyl groups could be attached. Similarly, loss of the elastic properties of the starting rubbers shows that the disulphide bridges are also decomposed during the sulphonation process. Since the chemical environment of disulphide bridges in case of styrene containing starting polymer chain might be

different, the favoured reaction was the sulphonation of aromatic ring and not the decomposition of disulphide bridges in the case of soft rubber tyres.

In order to introduce aromatic ring content into the waste common rubber tyres, to mimic the styrene-based rubbers, the swelling of common rubbers was done with α -methylstyrene before sulphonation. We expected that the aromatic ring containing product will be more advantageous for preparation of products with sulphonated group, keeping the elasticity of the starting rubber. The polymerization was started with 0.5 % dibenzoyl peroxide, however, the polymers formed cannot be removed from the reactor, a tar-like sticky material was only formed, so the sulphonation tests could not be performed. .

Further studies on usage of the sulphonated elastic soft-rubber tyre based resins as biobutanol supersorbents in ABE and IBE extractive fermentation in the presence of aliphatic hydrocarbons as extractants are in progress.

Conclusions

The styrene-containing waste rubber tyres are valuable raw materials to prepare sulphonated elastic superabsorbent butanol sponges. The sulphonation of rubber tyres was performed with concentrated sulphuric acid, chlorosulphonic acid led to useless tar-like products at various reaction conditions. The common waste tyres resulted products with lower biobutanol absorbing ability and non-elastic properties led to limited applicability in extractive biobutanol fermentations.

References

- ¹Liu, H., Wang, G., Zhang, Y., "The promising fuel -Biobutanol", in: *Liquid, Gaseous and solid biofuels*, Ed. Z. Fang, INTEC, **2013**, Chapter 6, p. 175-198., Rijeka, Croatia.
- ²Kótai, L., Szépvölgyi, J., Szilágyi, M., Zhibin, L., Baiquan, C., Sharma, V., Sharma, P. K., "Biobutanol from renewable agricultural and lignocellulose resources and its perspectives as alternative of liquid fuels", in: *Liquid, Gaseous and solid biofuels*, Ed. Z. Fang, INTEC, **2013**, Chapter 6, p. 199-262., Rijeka, Croatia.
- ³Kótai, L., Sharma, P. K., *Int. J. Chem. (Mumbai)*, **2012**,1(4), 480-485
- ⁴Kótai, L., Gács, I., *Eur. Chem. Bull.*, **2012**, 1, 1-3.
- ⁵Kótai, L., Szépvölgyi, J., Bozi, J., Gács, I., Bálint, Sz., Gömör, Á., Angyal, A., Balogh, J., Li, Z., Chen, M., Wang, C., Chen, B., *An integrated waste free biomass utilization system for an increased productivity of biofuel and bioenergy*, in: *Biodiesel: Feedstock and processing technologies*, ed. Stoytcheva, M., Montero, G., INTECH, **2011**, 201-228, Rijeka, Croatia.
- ⁶Inczédy, J., *Ioncserélők és analitikai alkalmazásai*, Budapest, **1978**.
- ⁷Dadgar, A. M., Foutch, G.L., *Biotechnol. Bioeng. Symp.*, **1985**, 15, 611-620.
- ⁸Larsson, M., Mattiasson, B. *Chem. Industry (London, United Kingdom)*, **1984**(12), 428-31.
- ⁹Idibie, C. A., Abdulkareem, A. S., Pienaar, H. C. Z., Iyuke, S. E., Van Dyk, L., *J. Appl. Polym. Sci.*, **2010**, 117, 1766-1771.

Received: 13.10.2016

Accepted: 20.10.2016.



SELECTIVE SENSORS FOR POTENTIOMETRIC ASSESSMENT OF IODIDE BASED ON ANION RECOGNITION THROUGH COPPER (II) [DIPEPTIDE DERIVATIVE] COMPLEX

Ayman H. Kamel^{[a]*}, Magdi E. Khalifa^[b], S. A. Abd El-Maksoud^[c] and Fadl A. Elgendy^[c]

Keywords: iodide; copper (II) [dipeptide derivative] complex; anion recognition; PVC membrane sensors; potentiometry.

New selective sensors based on potentiometric transduction for iodide assessment are described. The sensors based on the use of a newly synthesized copper (II) [N,N-bis-(1-carboxy-2-(p-hydroxybenzyl))-2,6-di(aminocarbonyl)pyridine] complex (CuL) as neutral ionophore in plasticized poly(vinyl chloride) (PVC) membranes. The influence of lipophilic cationic and anionic additives on the response properties of the sensors was evaluated. The fabricated sensors exhibited enhanced response towards iodide ions over the concentration range 6.3×10^{-6} to 1.0×10^{-2} mol L⁻¹ with a detection limit of $0.33 \mu\text{g mL}^{-1}$ and a slope of -63.6 ± 0.2 mV per decade. These sensors showed a fast and stable response, good reproducibility, and long-term stability. The sensors showed a stable potential over a wide pH range (4.5–9) and exhibited high selectivity for I⁻ ion in the presence of many common anions. The sensors were applied for direct potentiometric measurements of iodide ions over the concentration range 0.8–1270 $\mu\text{g mL}^{-1}$ and also for the titration of some metal ions (e.g. Ag⁺, Hg²⁺) and MnO₄⁻ through sequential monitoring. The sequential binding of these ions with I⁻ ensured share stepwise titration curves with consecutive end point breaks at the equivalent points.

* Corresponding Authors

Tel.: +201000361328

E-Mail: ahkamel76@sci.asu.edu.eg

[a] Chemistry Department, Faculty of Science, Ain Shams University, Abbasia, Cairo, Egypt.

[b] Chemistry Department, Faculty of Science, Mansoura University, Mansoura, Egypt.

[c] Chemistry Department, Faculty of Science, Port Said University, Port Said, Egypt.

suffer from the need for expensive instrumentation, well controlled experimental conditions, frequent maintenance and sample pretreatment. Therefore, development of analytical techniques for iodide assessment that do not require expensive or complicated equipment has become increasingly important.

On the other hand, potentiometric sensors offer an inexpensive and convenient method for fast analysis with high sensitivity and selectivity.¹⁴⁻¹⁷ They can be considered as one of the promising tools used for direct determination of various species in the biological and industrial analysis.¹⁸⁻²²

Ion selective electrodes (ISEs) for anions, based on ion exchangers such as lipophilic quaternary ammonium or phosphonium salts, displayed classical Hofmeister selectivity behavior in which membrane selectivity is controlled by the free energy of hydration of ions involved.²³ The anti-Hofmeister anion selectivity is obtained in the case of membrane electrodes incorporated with an organometallic complex,²⁴ metalloporphyrins,²⁵ metal phthalocyanines²⁶ and Schiff base metallic complexes.²⁷ This deviation arises from the steric effects coming from the structure of the ionophore and from the binding affinity of the central atom in the ionophore with the anion. Therefore, the focus of this research is on the anion-sensitive materials with anti-Hofmeister behavior.

Several iodide sensors based on a variety of ion carriers have also been reported in the literature.²⁸⁻⁵⁰ Some of these sensors showed narrow linear range^{28,30,31,41,43,44,49,50} narrow pH range,^{31-33,36,43} high detection limit,^{31,49,50} long response time.^{28,49} Others showed a serious interference from some anions such as SCN⁻,^{30,33,34,36,41-43,46,49,50} NO₂⁻,^{39,43,48} Br⁻,^{36,49} CN⁻,^{42,46} and Sal⁻.^{29,30,49,50}

In this study, we have synthesized copper(II) [N,N-bis-(1-carboxy-2-(p-hydroxybenzyl))-2,6-di(aminocarbonyl)pyri-

Introduction

Anions play an important role in biology, medicine, and environmental chemistry, so there is a constantly increasing need for their online monitoring. Among them, iodide is of particular interest because of its presence in food, drug compounds and in drinking water. Moreover, it is often added to table salt for preventing iodine deficiency disorders.¹ It is also used as a catalyst and stabilizer in the production of polymers and as a disinfectant. Iodine is an essential micronutrient that are required for the biosynthesis of the thyroid hormones thyroxine and triiodothyronine by the thyroid gland. Iodine deficiency is widely known as a global problem because 30% of the world's population lives in an environment where the soil has low iodine content. Also, its deficiency in human causes hypothyroidism and formation of goiter in adults or cretinism in children.² An excess of iodine or iodide ingestion can produce goiter and hypothyroidism as well as hyperthyroidism.^{3,4} Therefore, determination of iodide and other iodine species is an important analytical task in a variety of fields such as food, clinical, biological and environmental samples. Numerous analytical methods have been reported in the literature for iodide determination at trace levels. These include gas chromatography (GC-MS),⁵ neutron activation analysis,⁶ polarography,⁷ spectrophotometry,⁸ chemiluminescence,⁹ pulse stripping analysis,¹⁰ inductively coupled plasma-atomic emission spectrometry¹¹ and capillary electrophoresis.^{12,13} These approaches, although sensitive,

dine] complex (CuL) as a new ionophore in the fabrication of polymeric membrane sensors for iodide ion assessment. The performance characteristics of the sensors were evaluated and satisfactorily used for accurate determination of μg quantities of iodide. Sequential monitoring of Ag^+ , Hg^{2+} , Bi^{3+} and MnO_4^- in single or binary mixtures via the titration with iodide was also performed. The sequential binding of these ions with I^- shared stepwise titration curves with consecutive breaks at the equivalent points.

Experimental

Reagents and solutions

All chemicals were of analytical-reagent grade. Twice-distilled water was used to prepare all solution and in all experiments. Dioctyl phthalate (DOP), *p*-chlorotetrakis-tetraphenyl borate (*p*CITPB) and high molecular weight polyvinylchloride (PVC) were obtained from Sigma-Aldrich (Steinheim, Germany). Tridodecylmethylammonium chloride (TDMAC) and THF were purchased from Fluka (S.A.G. Buchs, Switzerland). All anions used were in their sodium salts and purchased from Merck [Dermsdat, Germany]. The ligand [N,N-bis-(1-carboxy-2-(*p*-hydroxybenzyl))-2,6-di(aminocarbonyl)pyridine] (Figure 1) was synthesized as described before.⁵¹ Standard iodide solution, 0.1 mol L^{-1} , was prepared by dissolving accurately weighed NaI in 100 mL twice-distilled water. Iodide solutions used for the sensor characterization (1×10^{-6} – $1 \times 10^{-2} \text{ mol L}^{-1}$) were prepared daily from the stock solution. The ionic strength (IS) was adjusted to 0.01 mol L^{-1} by means of a $3.5 \times 10^{-3} \text{ mol L}^{-1} \text{ Na}_2\text{SO}_4$ solution. The pH adjustment was carried out with 0.01 mol L^{-1} phosphate buffer solutions of pH 6 in addition to 0.01 mol L^{-1} IS.

Equipment

All potentiometric measurements were made at $25 \pm 0.1 \text{ }^\circ\text{C}$ with a Cole-Parmer pH/mV meter (USA model 59003-05) and iodide-PVC membrane sensors in conjunction with a Sentek, Ag/AgCl double junction reference electrode (UK model R2/2MM) filled with $1.0 \text{ mol L}^{-1} \text{ KNO}_3$ in the outer compartment. A combination glass pH electrode (Schott blue line 25, Germany) was used for all pH measurements. The IR spectra were measured on Prestige-21 FT-IR instrument (SHIMADZU, Japan). The thermal studies were carried out using DTG 60 AH (SHIMADZU, Japan) under the following conditions: temperature ranges 25–1000 $^\circ\text{C}$, heating rate $25 \text{ }^\circ\text{C min}^{-1}$ and sample weight 6.0 mg. Elemental analyzes were carried out on Elementar Vario EL cube, Germany. Cu-content was determined by Perkin Elmer Atomic Absorption Spectrometer (Model 3100 USA). The molar conductivity of the complex was measured by using OAKTON (Model CON510 USA) conductivity meter.

Syntheses of the complexes

A 20 mL of a methanolic solution containing 2.77 g (10 mmol) of $\text{Cu}(\text{NO}_3)_2 \cdot 5\text{H}_2\text{O}$ was added to a hot 20 mL methanolic solution containing 10 mmol of the ligand. After stirring for 1 h, the formed green precipitate complex was filtered, collected and then washed for several times with

hot methanol until the filtrate became colorless. The complex was dried in a desiccator over anhydrous CaCl_2 under vacuum. The dried ligands and complex were subjected to IR, elemental and thermal gravimetric analysis. The complex is air-stable, nonhygroscopic, insoluble in H_2O , slightly soluble in ethanol. The elemental analysis of the free ligand [L] ($\text{C}_{25}\text{H}_{23}\text{N}_3\text{O}_8$) was found: C, 60.84; H, 4.69; N, 8.51. Characteristics of the complex were as follows: $[\text{CuL} \cdot \text{H}_2\text{O}]$ ($\text{C}_{25}\text{H}_{25}\text{N}_3\text{O}_9\text{Cu}$): Yield 85%. Color: green. M.P. $>300 \text{ }^\circ\text{C}$. $\Lambda_m(\Omega^{-1} \text{ cm}^{-1} \text{ mol}^{-1})$ 4.2. Elemental analysis: Found (%): C 52.358; H 4.014; N 7.3302; Cu 11.082. Calcd: C 52.21; H 4.35; N 7.31; Cu 11.05.

Sensors preparation and EMF measurement

The procedure to prepare the PVC membrane was based on mixing 190 mg of powdered PVC, 10 mg of the ionophore, 2 mg of cationic additive TMDAC and 350 mg of plasticizer DOP. The mixture was dissolved in 3 mL of dry THF. The membrane solutions were cast into conductive supports of tubular shapes and left overnight for drying. The sensors were then conditioned before use by soaking in 0.01 mol L^{-1} NaI solution (for at least 24 h) and stored in the same solution when not in use. Calibration was made by immersing the membrane sensor in conjunction with a double junction Ag/AgCl reference electrode in 25 mL beakers containing 10 mL aliquots of standard 1.0×10^{-6} – $1.0 \times 10^{-2} \text{ mol L}^{-1}$ NaI solution. The pH of the solutions was adjusted to 6 using 0.01 mol L^{-1} phosphate buffer. Potential readings were carried out for iodide until stabilization occurred. The calibration plot was constructed by plotting the measured potential as a function of the logarithm of iodide concentrations. This calibration plot was used for subsequent measurements of unknown iodide samples.

Direct potentiometric determination of iodide

Iodide / iodine in pharmaceutical samples was analyzed using $[\text{CuL} + \text{TDMAC}]$ membrane sensor. Vaginal douche and mouthwash (1–10 % w/v), collected from the local market, were diluted with de-ionized water. For total iodide + iodine measurement, the iodide sensor and a Sentek Ag/AgCl double junction reference electrode were immersed in a 25 mL beaker containing 10 mL of $1.0 \times 10^{-2} \text{ mol L}^{-1}$ phosphate buffer of pH 6 and ascorbic acid 0.1 mol L^{-1} for reduction of iodine into iodide. Aliquots (200 μL) of the diluted samples were successively added and the potential response of each sample was measured after potential stabilization. Other aliquots (200 μL) of the diluted samples were successively added to a 25 mL beaker containing 10 mL of a 0.1 mol L^{-1} resorcinol of pH 8.0. The potential response is equivalent to $\frac{1}{2} \text{ I}_2$ and I^- .

The calibration plot was constructed by plotting the potential change against the logarithm of the I^- concentration. The plot was then used for subsequent determination of unknown I^- samples.

Potentiometric titration of metal ions

A series of potentiometric precipitation titrations was performed in which the sensor was used as an indicator electrode to locate the equivalence point. Sample solutions

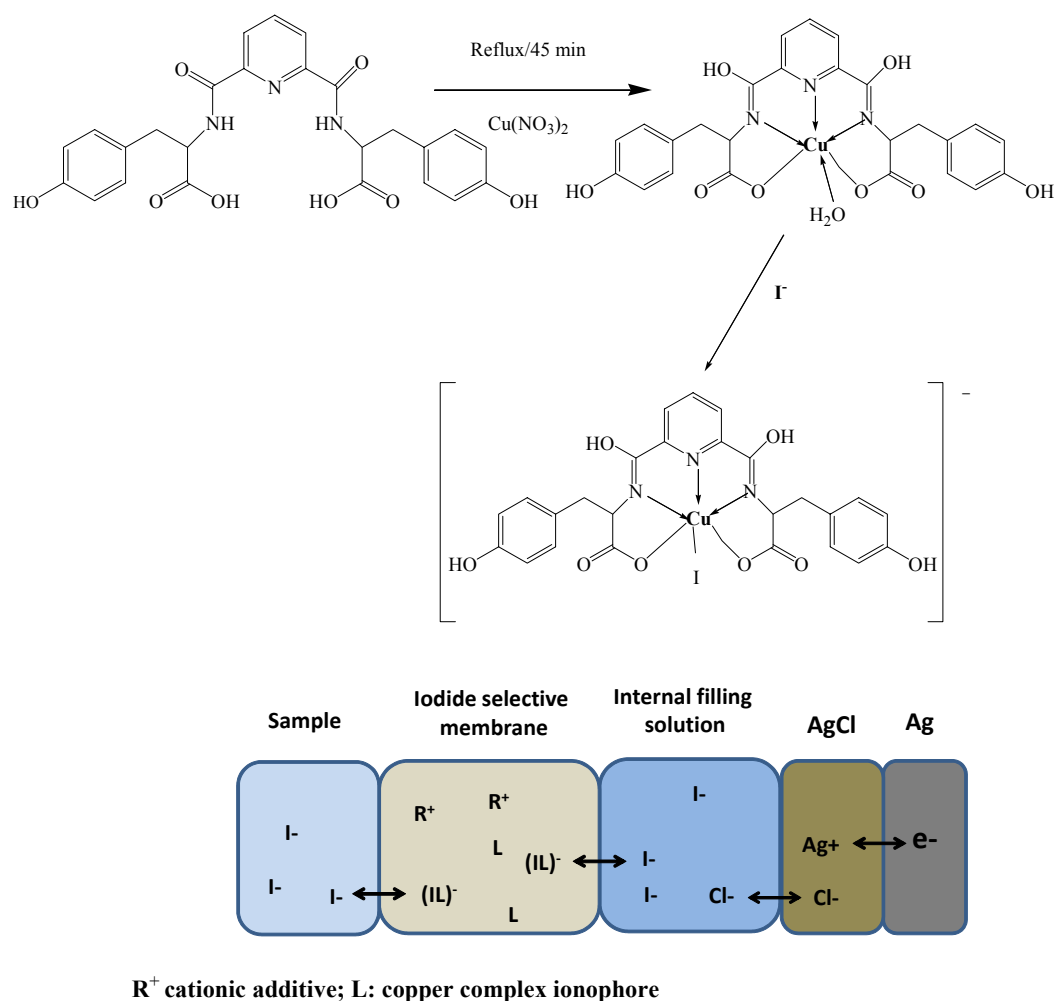


Figure 1. Chemical structure of the ionophore and an illustrative scheme describing the measuring instrument.

containing a single ion (e.g. Ag^+ , Hg^{2+} , MnO_4^-) were then titrated with $0.01 \text{ mol L}^{-1} \text{I}^-$. The equivalence points at each inflection break were determined and the concentration of each ion was assessed ($1 \text{ mol I}^- = 0.5 \text{ mol Hg}^{2+} = 1 \text{ mol Ag}^+ = 0.33 \text{ mol MnO}_4^-$).

Results and discussion

All applied ionophore in the ISE field must be able to bind the target ion via a selective (pattern) reversible reaction in order to generate a stable response in a short time.⁵² The potentiometric sensor containing the CuL ionophore significantly responded to iodide ion according to Nernstian response over other common anions. Therefore, the detailed characteristic performance of the membrane sensor based on the application of this carrier has been evaluated. In a preliminary experiment, membranes with/without the ionophore were constructed. Blank membranes showed poor selectivity toward iodide and their response was not reliable. However, the addition of the proposed ionophore to the membrane leads to the generation of a Nernstian response and remarkable response to iodide ions over several common anions. The preferential response toward iodide anion is believed to be associated with its selective coordination as a carrier to the copper center in the complex.

Structural properties

Pyridine carboxamides can be considered as a burgeoning class of multidentate ligands containing carboxamide [-CONH-] linkage. It can be prepared from condensation reactions between pyridyl-bearing amine or carboxylic acid precursors, promoted by coupling agents such as 1,1'-carbonyldiimidazole, diphenoxy phosphoryl azide or triphenyl phosphite.⁵³⁻⁵⁵ The behavior of pyridine carboxamides towards biologically relevant d-block metals has been widely investigated. These ligands support a range of coordination numbers, geometries, and nuclearities for copper (II).⁵⁶⁻⁶⁰

Elemental analysis and magnetic susceptibility data of the ligand and complex indicated the formation of 1:1 [Cu:L]. The molar conductance values of the synthesized complex determined using $1 \times 10^{-3} \text{ mol L}^{-1}$ DMF solution were in the range of $4.5\text{--}6.8 \Omega^{-1} \text{cm}^2 \text{mol}^{-1}$. These results suggested the presence of a non-electrolytic nature in the same solvent.⁶¹ These values also indicated that there were no anions in the outer coordination sphere.

The IR spectrum of the complex, in comparison with that of the free ligand, displayed significant changes that could be indicative of the type of coordination (Figure 2). The FTIR spectrum of free ligand showed characteristic bands at

3600 – 2617 (broadband, OH, and NH), 1728.2 (C=O, acid), 1662.6, 1516, 1230.5 (amide I, II and III) cm^{-1} . In the IR spectra of metal complexes, characteristic bands at 3600 – 2750 (broadband, OH phenolic, and OH iminol), 1627 (C=N, iminol), and 1384.8 (C=N, bending). The peaks at 1732, 1657, 1533 and 1225 were completely disappeared. In addition to these bands, the complex also showed weak bands at 837.1, 759.9 and 660-640 Cm^{-1} due to coordinated water. On the basis of the physical and spectral data of the free ligand and the complex discussed above, one can assume that the two imide groups coordinate to copper ion forming iminol groups in addition to (nitrogen) from pyridine and the two carboxylic groups present in the free ligand as illustrated in Figure 1.

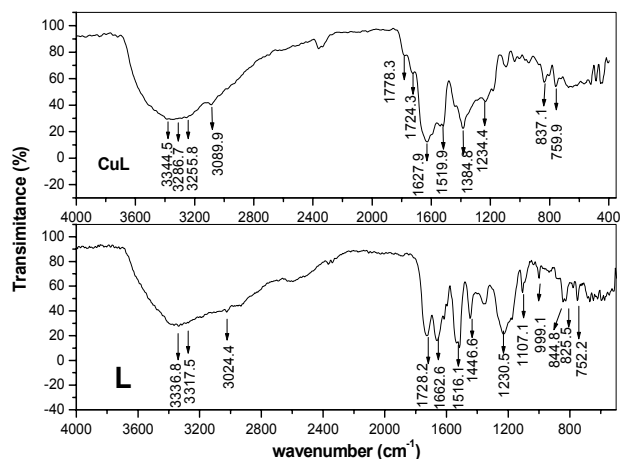


Figure 2. FTIR spectrum for the free ligand and its copper complex.

The thermal gravimetric analysis of the complex was shown in figure 3. The dehydration step in the complex occurred in the 60-120 °C range. The weight losses correspond to the loss of one water molecule and the complex decomposed in three steps via the formation of unstable intermediates. The decomposition started at 173-445 °C and ended at 450-1000 °C (oxides formation). The metal percentages of the complex were calculated from the residual metal oxide % formed in the final step and were in good agreement with data obtained by the elemental analysis. On the basis of the above observations, the following general scheme for thermal decomposition may be proposed for the metal complex.

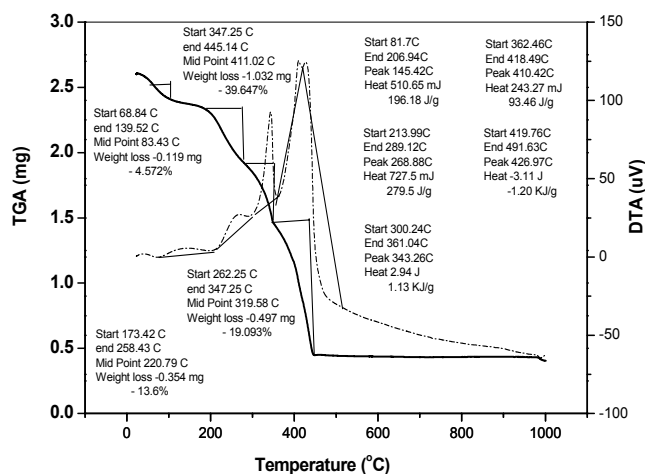


Figure 3. TG and DTG-plots of the Cu (1:1) complex.

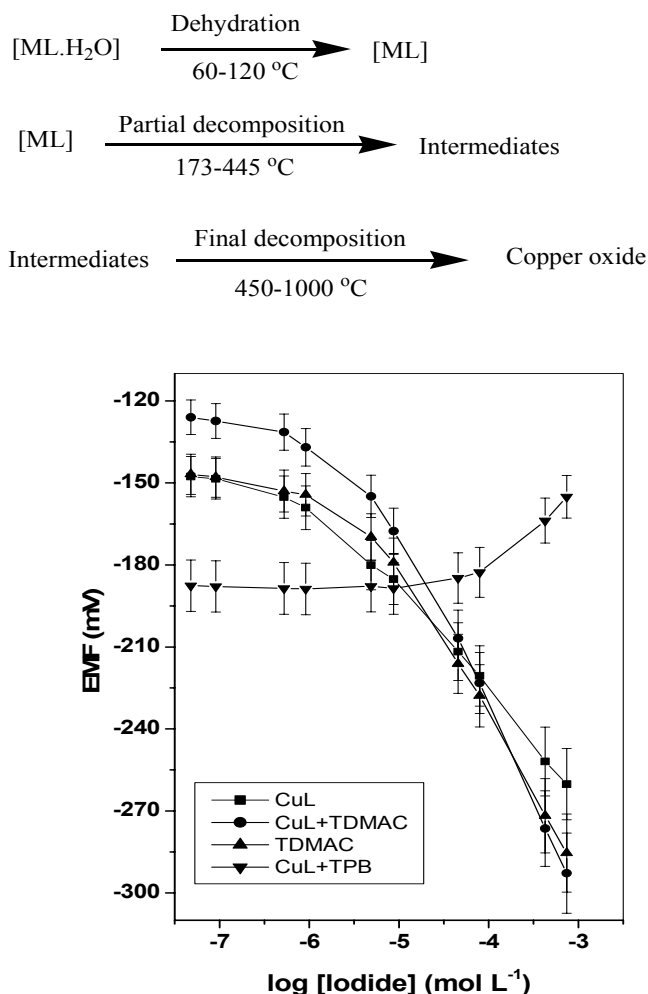


Figure 4. Potentiometric plot of iodide membrane sensors in 0.01 mol L^{-1} phosphate buffer (pH 6.0).

Response characteristics of iodide sensors

The potentiometric response characteristics of the sensors assembled with the different membranes were shown in Figure 4. The sensor based on [copper complex] showed a linear response towards iodide over the concentration range of 4.1×10^{-6} – 1.0×10^{-3} mol L^{-1} in a 0.01 mol L^{-1} phosphate buffer solution of pH 6 with a slope of -35.5 ± 2.3 mV decade $^{-1}$ and a detection limit of 0.13 $\mu\text{g mL}^{-1}$. On the other hand, the addition of 5 mg of TDMAC relative to the ionophore to the membranes showed an enhancement of the potentiometric response characteristics. These membrane electrodes exhibited a slope of -63.6 ± 0.2 mV decade $^{-1}$ over the concentration range of 6.3×10^{-6} – 1.0×10^{-3} mol L^{-1} and detection limit of 0.32 mol L^{-1} . However, the sensor based on cationic additive alone showed a linear response towards iodide over the concentration range of 6.1×10^{-6} – 1.0×10^{-3} mol L^{-1} with a slope of -53.6 ± 0.3 mV decade $^{-1}$ and detection limit 8.9 $\mu\text{g mL}^{-1}$ (Table 1). This is in accordance with the results reported previously that the cationic sites in neutral carrier-based electrodes can stabilize the formation of the negatively charged product (iodide copper complex) in the membrane phase as well as lowering the electrical membrane resistance and improving the potentiometric response characteristics of the membrane electrodes.⁶²⁻⁶⁴

Table 1. Response characteristics of [CuL] membrane based sensors at pH 6.

Parameter	CuL	CuL+TDMAC	TDMAC
Slope, mV decade ⁻¹	-35.5±2.3	-63.6±0.2	-53.6±0.3
coefficient, r	-0.996	-0.997	0.999
Detection limit, µg mL ⁻¹	1.0 × 10 ⁻⁶	2.5 × 10 ⁻⁶	6.1 × 10 ⁻⁶
Linear range, mol L ⁻¹	4.1 × 10 ⁻⁶ - 1.0 × 10 ⁻³	6.3 × 10 ⁻⁶ - 1.0 × 10 ⁻³	7.0 × 10 ⁻⁵ - 1.0 × 10 ⁻²
Response time, s	10 - 20	10 - 20	10 - 20
Working pH range	4.5 - 9	4.5 - 9	4 - 10
SD (%)	1.3	1.5	1.5
Accuracy (%)	99.3	98.8	98.7
Precision, C _v w(%)	0.9	0.7	1.1
Between-day variability, C _v b (%)	1.1	0.9	0.9

The robustness of the method was also evaluated via testing the effect of pH and the measuring time on the potentiometric response. The influence of the pH was tested using 10⁻⁴ and 10⁻³ mol L⁻¹ iodide solutions over the pH range 2–10. Adjustment of pH values was carried out using NaOH and/or HCl. From pH-potential profiles, it was apparent that there is no change in potential response within the pH range 4.5–9 for all sensors. At high pH values (> 9), the sensor response increased, probably due to the ability of hydroxide ions to be coordinated on the axial coordination site of the central metal. At pH < 3, the response towards iodide decreased probably due to the oxidation of iodide into iodine by molecular oxygen which was stabilized in acidic medium.

The response time of the electrodes was obtained by measuring the time required to achieve a steady state potential (within ± 1mV) after successive immersion of the electrodes in a series of iodide ions solutions, each having a 10-fold increase in concentration from 1.0 × 10⁻⁶ to 1.0 × 10⁻³ mol L⁻¹. The actual potential versus time trace showed, all concentrations ranges, that the sensors reach the equilibrium response in a very short time (<10 s). These results indicate that all sensors were amenable to be used with the automated system.

Selectivity

Potentiometric selectivity coefficients ($K^{pot}_{I,B}$) were evaluated according to IUPAC guidelines using the separate solutions method^{65,66} in which the potential of a cell comprising the membrane electrode and a reference electrode is measured with two separate solutions, one containing the iodide ion *A* at the activity a_A (but no *B*), the other containing the interfering ion *B* at the same activity $a_A = a_B$ (but no *A*) and E_A and E_B are the measured values, respectively. Different interfering anions at a concentration of 1 × 10⁻³ mol L⁻¹ at pH 6 were utilized and the results were obtained using the equation:

$$\log K^{pot}_{A,B} = (E_B - E_A)/S + (1 - Z_A/Z_B) \log a_A \quad (1)$$

where

$K^{pot}_{A,B}$ is the potentiometric selectivity coefficient, *S* the slope of the calibration plot, a_A the activity of iodide and Z_A and Z_B are the charges on I^- and the interfering anion, respectively.

The selectivity coefficient values were shown in Table 2. The selectivity coefficients of [CuL] membrane sensor without membrane additive were in the order: $I^- > SCN^- > ClO_4^- > IO_4^- > IO_3^- > Asco^- > Cl^- > Br^- > NO_2^- > NO_3^- > F^- > SO_4^{2-} > CH_3COO^- > PO_4^{3-}$. For [CuL] based membrane sensor doped with TDMAC as a cationic additive, the selectivity behavior of the sensor was in the order: $I^- > ClO_4^- > IO_4^- \sim SCN^- > NO_3^- > Br^- > IO_3^- > NO_2^- \sim Cl^- > Asco^- > SO_4^{2-} > F^- > PO_4^{3-} > CH_3COO^-$ which is almost identical with the Hofmeister pattern. Membrane sensors incorporating [CuL] without additives exhibited enhanced selectivity towards iodide ions but the selectivity pattern was anti-Hofmeister. This selectivity order clarified that the response mechanism is a neutral carrier mechanism that showed a non-Hofmeister selectivity pattern. This explanation is based on the strong coordination affinity between the metal center in the ionophore and the iodide ion.

Table 2. Selectivity coefficients ($K^{pot}_{I,i}$) of iodide PVC membrane sensors.

Ion	[CuL]	[CuL]+TDMAC	TDMAC
I^-	0	0	0
IO_4^-	-2.60	-0.8	+1.1
IO_3^-	-3.12	-2.21	-2.85
SCN^-	-1.80	-0.88	+1.0
Ascorbate	-3.40	-3.27	-3.21
ClO_4^-	-2.10	-0.75	+1.7
NO_3^-	-3.81	-1.41	-1.2
NO_2^-	-3.73	-2.66	-2.3
Cl^-	-3.42	-2.70	-2.5
Br^-	-3.51	-2.06	-2.1
F^-	-4.22	-3.61	-3.5
SO_4^{2-}	-4.30	-3.42	-3.3
PO_4^{3-}	-4.32	-3.92	-4.1
CH_3COO^-	-4.31	-4.01	-3.9

Determination of iodide and iodine in pharmaceutical formulations

Vaginal douche and mouthwash and vaginal douche collected from local market containing iodide/iodine in pharmaceutical samples were analyzed using [CuL+TDMAC] membrane sensor. Determination of iodine in the presence of iodide ions required two potentiometric measurements. The first involved measurement of total iodine and iodide (I_2 & I^-) after treatment with a suitable reducing agent such as 0.1 mol L⁻¹ ascorbic acid. The second measurement is done by measuring the remained iodide ions ($1/2 I_2$ & I^-) after reaction with resorcinol at pH 8.0 via iodination.⁶⁷ The results obtained for determining iodide and iodine in povidone iodine was in good agreement with data obtained using the titrimetric method recommended by British Pharmacopoeia⁶⁷ (Table 3).

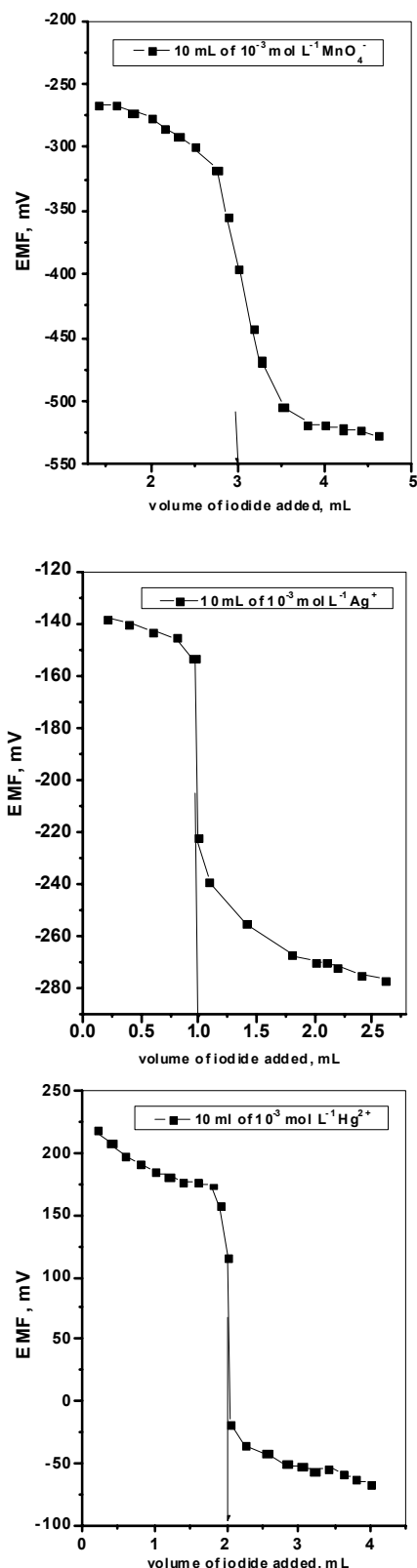


Figure 5. Potentiometric titration plot of Ag⁺, Hg²⁺ and MnO₄⁻ with 0.01 mol L⁻¹ I⁻ using an iodide membrane sensor.

Table 3. Potentiometric determination of povidone iodine using [CuL+TDMAC] PVC membrane based sensor.

Sample*	This work	BP ⁶⁶	Recovery, %
Betadine mouth wash	1.87±0.5 mg I ₂ mL ⁻¹	1.91±0.7 mg I ₂ mL ⁻¹	97.9
Betadine vaginal douch	10.23±0.6 mg I ₂ mL ⁻¹	10.12±0.2 mg I ₂ mL ⁻¹	101.1

*Obtained from the Nile pharm. chem., Egypt

Potentiometric titration of metal ions

The iodide membrane sensor based on ionophore (I) was also used for monitoring some ions (e.g. Ag⁺, Hg²⁺, and MnO₄⁻), single or in binary mixtures, with a standardized iodide solution. The titration curves obtained showed sharp inflection breaks (~ 80 mV) at 1:1 for I/Ag⁺ and (~ 200 & 180 mV) at 1:2 and 1:3 reactions for I/Hg²⁺ and I/MnO₄⁻, respectively. Typical potentiometric titration curves were shown in figure 5.

Conclusion

Novel potentiometric iodide sensors based on copper complex of [N,N- bis-(1carboxy-2-(p-hydroxy benzyl))-2,6-(diaminocarbonyl)-pyridine] were constructed and evaluated. The performance characteristics of the sensors showed stable and selective potential responses towards iodide ions over the concentration range of 6.3 x 10⁻⁶ - 1.0 x 10⁻² mol L⁻¹ with a limit of detection 2.5x10⁻⁶ mol L⁻¹ and a slope of -63.6±0.3 mV decade⁻¹. The addition of a cationic additive to the membranes showed a slope of -63.6±0.2 mV decade⁻¹ over the concentration range of 6.3x10⁻⁶-1.0x10⁻³ mol L⁻¹ and detection limit of 0.32 mol L⁻¹. The iodide PVC-based membrane sensor was satisfactorily used for potentiometric determination of iodide under the static mode of operation in pharmaceutical formulations. Sequential monitoring via potentiometric titration of some ions (e.g. Hg²⁺, Ag⁺ and MnO₄⁻) was determined using the iodide sensor to locate the equivalent points. The sequential binding of these ions with I⁻ ensured share stepwise titration curves with consecutive end point breaks at their equivalent points. It is interesting to note that a comparison of the selectivity and working of the proposed iodide electrode along with those reported before clearly indicate a good enhancement in the behavior of the proposed iodide sensors.

Acknowledgments

The authors are gratefully acknowledging Dr. Abd El-Galil E. Amr (Prof. of Organic Chemistry, National Research Centre, Dokki, Cairo, Egypt) for preparing and supporting the ligand [N,N- bis-(1carboxy-2-(p-hydroxy benzyl))-2,6-(diaminocarbonyl)-pyridine] used in this work.

References

- ¹Lind, P. Kunning, G. Heinich, M. Igerc, I. Mikosch, P. Gallowitsch, H.J. Kresnik, E. Gomez, I. Unterwegen, O. Aigner, H., *Thyroid*, **2002**, *12*, 903-907.
- ²WHO, UNICEF, ICCIDD, WHO Publication, Geneva, **1994**.
- ³Azizi, F. Hedayati, M. Rahmani, M. Sheikholeslam, R. Allahverdian, S. Salarkia, N., *J. Endocrinol. Invest.*, **2005**, *28*, 23-25.
- ⁴Reid, J. R. Wheeler, S. F., *Am. Fam. Phys.*, **2005**, *72*, 623-630.
- ⁵Bichsel, Y. Von-Gunten, U., *Anal. Chem.*, **1999**, *71*, 34-38.
- ⁶Hou, X. Dahlgaard, H. Rietz, B. Jacobsen U., Nielsen, S. P. Aarkrog, A., *Anal. Chem.*, **1999**, *71*, 2745-2750.
- ⁷Turner, J. A. Abel, R. H. Osteryoung, R. A., *Anal. Chem.*, **1975**, *47*, 1343.
- ⁸Schwehr, K. A. Santschi, P. H., *Anal. Chim. Acta*, **2003**, *482*, 59-71.
- ⁹Ratanawimarnwong, N., Amornthammarong, N., Choengchan, N., Chaisuwan, P., Amatatongchai, M., Wilairat, P., McKelvie, I. D., Nacapricha, D., *Talanta*, **2005**, *65*, 756-761.
- ¹⁰Propst, R. C., *Anal. Chem.*, **1977**, *49*, 1199-1205.
- ¹¹Larsen, E. H., Ludwigsen, M. B., *J. Anal. Atom. Spectrom.*, **1997**, *72*, 435-439.
- ¹²Ito, K. Ichihara, T. Zhuo, H. Kumamoto, K. Timerbaev, A. R. Hirokawa, T., *Anal. Chim. Acta*, **2003**, *497*, 67-74.
- ¹³Yokota, K., Fukushi, K., Takeda, S., Wakida, S. I., *J. Chromatogr. A*, **2004**, *1035*, 145-150.
- ¹⁴Kamel, A. H. Soror, T. Y. Al-Romian, F. M., *Anal. Meth.*, **2012**, *4*, 3007-3012.
- ¹⁵Kamel, A. H. Al-Romian, F. M., *Int. J. Chem. Mat. Sci.*, **2013**, *1*, 1-12.
- ¹⁶Abd-Rabboh, H. S. M., Kamel, A. H., *Electroanalysis*, **2012**, *24*, 1409-1415.
- ¹⁷Gupta, V. K. Ganjali, M. R. Norouzi, P. Khani, H. Nayak, A. Agarwal, S., *Crit. Rev. Anal. Chem.*, **2011**, *41*, 282-313.
- ¹⁸Hassan, S. S. M. Badr, I. H. A. Kamel, A. H. Mohamed, M. S., *Electroanalysis*, **2013**, *25*, 1-9.
- ¹⁹Hassan, S. S. M. Kamel, A. H. Abd El-Naby, H., *Eur. Chem. Bull.*, **2013**, *2*, 232-237.
- ²⁰Kamel, A. H., Al Romian, F. M., Amr, A. E., *Eur. Chem. Bull.*, **2013**, *2*, 687-693.
- ²¹Gupta, V. K., Singh, L. P., Singh, R., Upadhyay, N., Kaur, S. P., Sethi, B., *J. Mol. Liq.*, **2012**, *174*, 11-16.
- ²²Hassan, S. S. M. Sayour, H. E. M. Kamel, A. H., *Anal. Chim. Acta*, **2009**, *640*, 75-81.
- ²³Sollner, K., Shean, G. M., *J. Am. Chem. Soc.*, **1964**, *86*, 1901-1902.
- ²⁴Zanjanchi, M. A. Arvand, M. Akbari, M., *Sens. Act. B*, **2006**, *113*, 304-309.
- ²⁵Pietrzak, M., Meyerhoff M. E., Malinowska, E., *Anal. Chim. Acta*, **2007**, *596*, 201-209.
- ²⁶Xu, W. J., Yuan, R., Chai, Y. Q., *Anal. Bioanal. Chem.*, **2008**, *392*, 297-303.
- ²⁷Xu, W. J., Zhang, Y., Chai, Y. Q., Yuan, R., *Desalination*, **2009**, *249*, 139-142.
- ²⁸Benvidi, A. Alizadeh, M. Zare, H. R. Vafazadeh, R., *J. Iran. Chem. Res.*, **2008**, *2*, 103-111.
- ²⁹Farhadi, K. Maleki, R. Yamchi, R. H., *Anal. Sci.*, **2004**, *20*, 805-809.
- ³⁰Jeong, D. C. Lee, H. K. Jeon, S., *Bull. Korean Chem. Soc.*, **2006**, *27*, 1985-1988.
- ³¹Lizondo-Sabater, J. Martynez-Manez, R. Sancenon, F., *Anal. Chim. Acta*, **2002**, *459*, 229-234.
- ³²Song, Y. Q. Yuan, R. Ying, M., *Fres. J. Anal. Chem.*, **1998**, *360*, 47-51.
- ³³Xu, W. J., Chai, Y. Q. Yuan, R., *Anal. Sci.*, **2006**, *22*, 1345-1349.
- ³⁴Pouretedal, H. R. Keshavarz, M. H., *Talanta*, **2004**, *62*, 221-225.
- ³⁵Ying, M. Yuan, R. Song, Y. Q. Li, Z. Q., *Analyst*, **1997**, *122*, 1143-1146.
- ³⁶Daunert, S., Florido, A., Bricker, J., Dunaway, W., Bachas, L. G., Valiente, M., *Electroanalysis*, **1993**, *5*, 839-843.
- ³⁷El Aamrani, F. Z., Sastre, A., Aguliar, M., Beyer, L., Florido, A., *Anal. Chim. Acta*, **1996**, *329*, 247-252.
- ³⁸Yuan, R., Chai, Y. Q., Liu, D., Gao, D., Li, J. Z., Yu, R. Q., *Anal. Chem.*, **1993**, *65*, 2572-2575.
- ³⁹Li, Z. Q., Yuan, R., Ying, M., Song, Y. Q., Shen, G. L., Yu, R. Q., *Anal. Lett.*, **1997**, *30*, 1455-1464.
- ⁴⁰Singh, A. K. Mehtab, S., *Talanta*, **2008**, *74*, 806.
- ⁴¹Shamsipur, M. Sadeghi, S. Naeimi, H. Sharghi, H., *Polish J. Chem.*, **2000**, *74*, 231-238.
- ⁴²Shamsipur, M. Soleymannpour, A. Akhond, M. Sharghi, H. Naseri, M. A., *Anal. Chim. Acta*, **2001**, *450*, 37-44.
- ⁴³Sanchez-Pedreno, C. Ortuno, J. A. Martinez, D., *Talanta*, **1998**, *47*, 305-310.
- ⁴⁴Benvidi, A. Ghanbarzadeh, M.T. Mazloum-Ardakani, M. Vafazadeh, R., *Chin. Chem. Lett.*, **2011**, *22*, 1087-1090.
- ⁴⁵Poursaberi, T. Hosseini, M. Taghizadeh, M. Pirelahi, H. Shamsipur, M., Ganjali, M. R., *Microchem. J.*, **2002**, *72*, 77.
- ⁴⁶Karimipour, G., Gharghani, S., Ahmadpour, R., *E-J. Chem.*, **2012**, *9*, 2565-2574.
- ⁴⁷Ghanei-Motlagh, M. Taher, M. A. Ahmadi, K. Sheikhshoae, I., *Mat. Sci. Eng.*, **2011**, *C31*, 1625-1631.
- ⁴⁸Ghaedi, M., Montazerzohori, M., Mousavi, A., Khodadoust, S., Mansouri, M., *Mat. Sci. Eng.*, **2012**, *C32*, 523-529.
- ⁴⁹Shvedene, N. V., Avramenko, O. A., Baulin, V. E., Tomilova, L. G., Pletnev, I. V., *Electroanalysis*, **2011**, *23*, 1067-1072.
- ⁵⁰Shvedene, N. V., Rzhavskaia, A. V., Pletnev, I. V., *Talanta*, **2012**, *102*, 123-127.
- ⁵¹Amr, A. E., Abo-Ghalia, M., Abdalah, M. M., *Z. Naturforsch.*, **2006**, *61b*, 1335-1345.
- ⁵²Bakker, E., Buhlmann, P., Pretsch, E., *Chem. Rev.*, **1997**, *97*, 3083-3132.
- ⁵³Lin, J., Zhang, J. Y., Xu, Y., Ke, X. K. and Guo, Z., *Acta Crystallogr.*, **2001**, *C57*, 192-194.
- ⁵⁴Conlon D. A. and Yasuda, N., *Adv. Synth. Catal.*, **2001**, *343*, 137-138.
- ⁵⁵Kurosaki, H., Sharma, R. K., Aoki, S., Inoue, T., Okamoto, Y., Sugiura, Y., Doi, M., Ishida, T., Otsuka M. and Goto, M., *J. Chem. Soc., Dalton Trans.*, **2001**, 441-442.
- ⁵⁶Jain, S. L., Bhattacharyya, P., Milton, H. L., Slawin, A. M. Z., Crayston, J. A., Woollins, J. D., *Dalton Trans.*, **2004**, 862-871.
- ⁵⁷Marlin, D. S. Olmstead, M. M. Mascharak, P. K., *Inorg. Chim. Acta*, **2001**, *323*, 1-4.
- ⁵⁸Rowland, J. M., Olmstead, M. M., Mascharak, P. K., *Inorg. Chem.*, **2000**, *39*, 5326-5332.
- ⁵⁹Chavez, F. A., Olmstead, M. M., Mascharak, P. K., *Inorg. Chem.*, **1996**, *35*, 1410-1412.

- ⁶⁰Rowland, J. M., Thornton, M. L., Olmstead, M. M., Mascharak, P. K., *Inorg. Chem.*, **2001**, *40*, 1069-1073.
- ⁶¹Abdel-Aziz, A. A., Kamel, A. H., *Talanta*, **2010**, *80*, 1356–1363
- ⁶²Bakker, E., Malinowska, E., Schiller, R. D., Meyerhoff, M. E., *Talanta*, **1994**, *41*, 881-890.
- ⁶³Eugster, R., Gehrig, P. M., Morf, W. E., Spichiger, U. E., Simon, W., *Anal. Chem.*, **1991**, *63*, 2285-2289.
- ⁶⁴Schaller, U., Bakker, E., Spichiger, U. E., Pretsch, E., *Anal. Chem.*, **1994**, *66*, 391-398.
- ⁶⁵Umezawa, Y., Umezawa, K. Sato, H., *Pure Appl. Chem.*, **1995**, *67*, 507-518.
- ⁶⁶Bakker, E. Pretsch, E. Buhlmann, P., *Anal. Chem.*, **2000**, *72*, 1127-1133.
- ⁶⁷British Pharmacopoeia, Her Majesty's Stationary Office, London, **2003**.

Received: 17.07.2016.

Accepted: 03.11.2016.



STUDIES ON EFFECTIVE SEGREGATION COEFFICIENTS OF IMPURITIES IN SILICON PULLED FROM MG-Si MELT

N. Kekelidze^[a], G. Tavadze^[a], E. Khutsishvili^{[a]*}, L. Gabrichidze^[a] and G. Mikaberidze^[a]

Keywords: Silicon, segregation, impurity, crystallization, purification.

Minimization of impurities content in Si, necessary for its application as semiconductor material, was performed by using directional crystallization of metallurgical grade Si (*n*-MG-Si) with 98 wt. % Si purity without intermediate stages. After pulling from melt, *n*-MG-Si goes into *p*-type Si with current carriers concentration (*p*) $\sim 10^{16} \text{ cm}^{-3}$ and Si has been purified practically from most of the impurities. The possibility of uncontrolled impurities removal from Si depends on impurities effective coefficient of segregation in Si. Therefore we have investigated the effective coefficient of segregation of unwanted impurities in Si crystals, obtained by pulling directly from MG-Si melt. In the presented article the effective segregation coefficient of major impurities in Si has been calculated and analysed in the dependence on the crystallization conditions. Effective coefficient of segregation makes possible estimate the capacity and efficiency of Si purification from impurities during crystallization from melt.

* Corresponding Author:

E-Mail: elzakhutsishvili@yahoo.com

[a] Laboratory of Semiconductor Materials Science, Ferdinand Tavadze Institute of Metallurgy and Materials Science, Tbilisi, Georgia

presented in Si. Effective coefficient of segregation makes possible estimate the capacity and efficiency of Si purification from impurities during crystallization from melt. So the objective of the presented article is the investigation of effective coefficient of segregation of unwanted impurities in Si crystals, obtained by pulling directly from metallurgical grade Si (MG-Si) melt.

Introduction

Silicon technology has had a strong influence on the world economy over the past few decades, and presently is the driving force behind the revolution in semiconductor engineering applications. Silicon has advantages over other semiconductor materials because of its abundance on the earth, meeting most required criteria and having a number of better properties.^{1, 2} It is predicted to remain the prevailing semiconductor technology for the near future. The continual reduction of the size of Si devices has led to exponential increase in their quality together with an exponential decrease in the cost per function. The size reduction of bulk crystalline Si to the nanometre dimension expands the scope of silicon application. For example, nano crystalline Si becomes light emitting. Silicon technology is gradually moving into new applications as novel silicon-base nanotechnology. However further development of Si application requires further investigations in the direction of identification of behaviour of uncontrolled impurities in Si. The main criterion of Si suitability for application in semiconductor devices is its chemical purity. Therefore the problems connected with uncontrolled impurities removal from Si are very important.

Minimization of impurity contents of Si, intended for application as semiconductor material, is achieved by using many known traditional refinement methods, among them is crystallization from the melt. As a rule, it is applied on the final stage of technological process of purification of substances. However in given work a directional crystallization is used for direct purification of metallurgical Si without any intermediate stages. The possibility of removal of unintended impurities from Si depends on effective coefficient of segregation (*k*) of impurities

Experimental

The first step product of Si obtained by restoration from quartzite with reaction to carbon is metallurgical Si. *n*-MG-Si with ~ 98 wt. % Si has been taken as initial material. Ample quantity (~ 2 wt. %) of unwanted impurities Fe, Al, P, Ca, Cu, Mg, Mn, Ni, Ti has fallen one after the other into MG-Si from quartzite and restoring materials in time of restoration process. Carbon and oxygen has been presented in MG-Si too. The known Czochralski growth method of pulling crystals has been used for obtaining Si directly from MG-Si melt. Crystals have been grown from 48 mm diameter quartz crucible. Si crystalline rods with the length of 50 mm were used as the seeds. During the process of the crystal pulling the crucible with the mother melt revolved with the rate of rotation 45 and 10 revolutions per minute in opposite directions. The optimal effect of Si purification has been achieved at $\sim 0.25 - 0.30$ mm per minute rate of crystal growth. Such conditions provide the symmetry of temperature field at the crystallization front.

First the melting camera has been pumped off up to 10^{-4} mm Hg, and then washed by flow of argon. The fusion has been carried out in the argon atmosphere at a pressure of not more than 50 kPa. *n*-type MG-Si ($n \approx 10^{18} \text{ cm}^{-3}$) have been charged into the crucible. The volatile impurities actively evaporated from the surface of MG-Si have been removed from melting camera with equipped special apparatus for gas removing (gas-extracting arrangement). An argon supply and discharge of the working chamber was regulated so, that the pressure in the chamber remained constant at the level of 50 kPa.

The content of contaminating impurities in Si before and after the directional crystallization has been defined by X-ray diffraction method, micro X-ray spectral and emissive spectral analyses. Electrical properties and microstructure analysis of Si experimental samples have been implemented too. Effective segregation coefficient of detrimental impurities in Si at the crystal pulling from MG-Si has been determined on the base of established content of unwanted impurities in Si. *n*-MG-Si after pulling goes into *p*-type Si.

Results and Discussion

Mechanisms of impurity removal

At initial step of melting at low temperatures Si has been purified from mixture of those impurities which are more volatile than basic component. The melt had sufficiently large surface. So volatile impurities actively evaporated from the surface of Si melt at low temperatures and 10^{-3} mm Hg pressure. Their content is defined by pressure and composition of atmosphere in a processing chamber. At temperatures lower than Si melting temperature (1450 °C) impurities with less fusion temperature have evaporated too. On the next step of process temperature has increased by 50–70 °C higher than 1450 °C and Si melt stayed in liquid state certain time for removal (evaporation) of uneasily meltable impurities like Fe and Ti. Under the conditions of low pressure and high temperatures those impurities, which vapor tension is higher than one of Si (P, Al, etc.), have evaporated too.

It is known,³ that quantity of impurity (m), which vaporizes from open unit area of the melt (reflection of molecules from crucible walls is taken into account) is defined by:

$$m = \beta P \sqrt{\frac{M}{2\pi RT}} \quad (1)$$

where

P is the equilibrium pressure of impurity steam,

M is the molecular weight of impurity,

R is the gas constant,

T is the melting temperature,

and the coefficient β can be written as

$$\beta = \frac{156.6\alpha}{1 + \alpha ld^{-1}} \quad (2)$$

where

α is the condensing coefficient,

d is the crucible diameter, and

l is the height of walls of crucible above the melt.

Purification by evaporation has been effective for those impurities, which equilibrium pressure of steam exceeds one for Si. Those impurities which equilibrium pressure of steam

is higher than for the rest of the impurities vaporized easier at the identical conditions. The ratio of equilibrium pressure of steam for impurities and Si defines the degree of their partition. It follows from expression (1) that the vaporizability or ability to be removed of easy vaporable impurities from Si melt reduces in the row of $Mg > Ca > Mn > Al > Cu > Fe > Ni > Ti$.

Among a great number of foreign unforeseen electrically neutral impurities carbon and oxygen in Si attract attention. They get into semiconductors because of technology equipment (quartz crucible, heated graphite). Gaseous carbon and oxygen compounds products of the reaction have been removed by gas-extracting arrangement. At the same time refractory products have precipitated at the end of crystal. IR spectroscopy measurements of carbon distribution in Si have confirmed that carbon concentration increases at the end of a crystal. It indicates the enrichment of the melt with carbon due to segregation of carbon during the growth of the crystal. This cannot be explained only by the low distribution coefficient of carbon in silicon. It is also caused by collection of carbon in the melt in the result of chemical reactions of silicon with quartz and quartz with graphite. At the melt cooling carbide compounds are in isolated state. So, it is clear, that the carbon segregation process in silicon and the enrichment of the melt with carbon depend on the time of crystal growth process. Finally carbon has been removed with cut off part of Si crystal. It is remarkable, that Fe, Ca and oxygen promote the reduction of carbon solubility in Si.

MG-Si after pulling became *p*-type with current carriers concentration $\sim 10^{16}$ cm⁻³ and has been purified practically from majority of impurities. Incidentally the impurities in MG-Si have obeyed to the procedure of purification in a variety of mechanisms because of different physical properties of impurities. During the execution of the metallurgical silicon purification process the quantity of Ca, Mn, Ni out of the whole collection of unwanted impurities has reduced so much (< 0.001 wt. %), that their concentration has been less of detection limit of applied methods of impurities determination.

The purification of silicon from Mg, Mn, Cu, Fe, Ni, Ti impurities have occurred mainly by segregation because of their small segregation coefficient in Si (10^{-4} – 10^{-6}). Equilibrium coefficients of distribution of Al and Ca impurities (k_0) in Si ($2.0 \cdot 10^{-3}$ and $8.0 \cdot 10^{-3}$ accordingly) are not sufficiently small for being removed from Si by directional crystallization. But saturation vapor pressure of Al and Ca is much more than one for Si. Thus their removal from melt surface into gaseous phase at high temperatures and afterwards by gas-extracting arrangement has been possible.

Effective coefficient of distribution of harmful impurities in Si at crystal withdrawal

It is known, that at the pulling of Si from melt impurities have redistributed between solid and liquid phases with certain ratio as mentioned above and this process is characterised by effective coefficient of segregation of impurity. k of impurities in Si for experimental samples has

been calculated on the base of experimentally established data of impurity composition. The dependence of k of impurities in Si on the pulling speed of crystals is shown in the Figure 1.

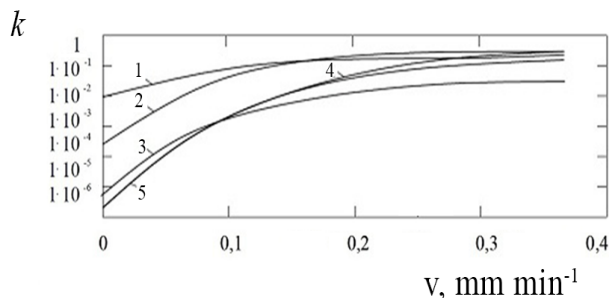


Figure 1. The dependence of effective distribution coefficients (k) of impurities in Si crystals on the pulling speed from melt. Impurities: 1 – Al; 2 – Cu; 3 – Fe; 4 – Mg; 5 – Ti.

The crystal Si pulling speed 0 mm min^{-1} belongs to the state of “equilibrium”, i.e. practically to very low pulling speed of crystal. For certain finite pulling speed magnitudes, k depends on the crystal pulling rate. It is remarkable, that equilibrium coefficient of distribution of majority of impurities in Si $k_0 < 1$. So as expected an increase in rate of crystal pulling results in k and at high pulling rates verge towards 1 (when quickly migrating separating phase is included) independently of magnitude of equilibrium coefficient of distribution of impurities k_0 .⁴ Data of effective coefficient of distribution of major impurities in Si corresponds to $k_0 \leq k \leq 1$ inequality. This result is in a good agreement with theory of Barton–Prima–Slichter.⁵ According to Barton–Prima–Slichter theory relationship between k and k_0 is defined by eqn. (3), at diffused transport of mass in δ layer (depth of melt near crystallization front-diffusion layer).

$$k = \frac{k_0}{k_0 + (1 - k_0)e^{-\Delta}} \quad (3)$$

where

$\Delta = v\delta/D$ is a dimensionless quantity, so called reduced velocity,

v is the solidification rate,

D is the diffusion coefficient of impurity

δ value depends on rate of rotation of crystal and changes in the range of $0.1\text{--}0.001 \text{ cm}$.

It can be seen from Eqn. (3), that in the first approximation k depends on the conditions of crystal growth processes i.e., solidification rate and rate of rotation of crystal (conditions of melt mixing). According to this theory when equilibrium distribution coefficient of impurities $k_0 < 1$, k increases at the growth of crystal pulling rate. While crystal is pulling from melt impurities with $k_0 < 1$ accumulate little by little in the melt because of they get into melt from crystallization front.

Accordingly impurities concentration at the surface exceeds their concentration in the melt. So $k > k_0$ and during the process of crystal growth the melt is progressively

enriched by impurities because of their bad solubility in solid phase. Therefore the end of crystal, where all residual impurities are concentrated, has always been cut off.

Impurity distribution along the ingot at crystal withdrawal

It is remarkable, that impurities are mainly concentrated at the end of Si crystal. Fig. 2 shows clearly that contaminated dark end parts of Si crystal.

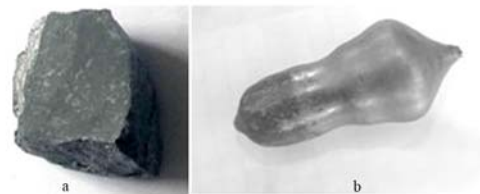


Figure 2. (a) Metallurgical Si and (b) Si crystal obtained by pulling from melt with 0.3 mm min^{-1} velocity.

The size of impure section reduces at the increase of the velocity pulling speed of crystal. It means that the effect of co-location of impurities at the end of crystal intensifies with growth of crystal pulling velocity. Impurity distribution along the crystal length during the crystal pulling from the melt is described by the following formula of Scheil.⁶

$$C = k C_0 (1 - g)^{k-1}, \quad (4)$$

where

$g = V_m/V_0$, g is the crystallized part of initial volume of melt;

V_m is the volume of crystallized phase,

V_0 is the initial volume of liquid phase,

when $g = 0$, impurity concentration in the melt C equates to its initial magnitude in the melt C_0 .

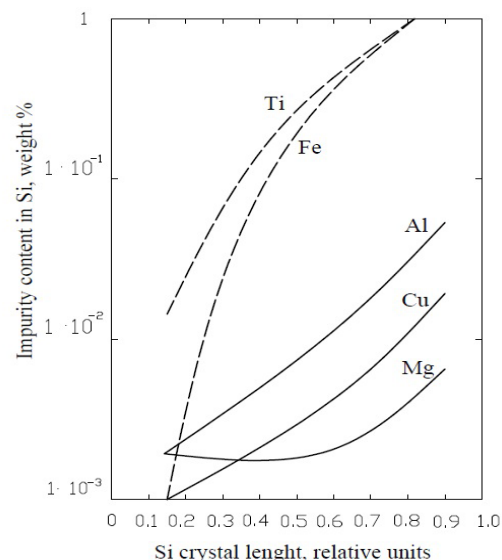


Figure 3. Dependence of impurities concentration in Si solid phase on the crystallized part of melt.

According to Eqn. (4) when $k < 1$ (at equilibrium during the process of crystal pulling, $k = \text{const}$) impurities concentration increases along the crystal length.

For majority of impurities in Si, $k \ll 1$, so Eqn. (4) can be written as Eqn. (5).

$$C \cong \frac{kC_0}{1-g} \quad (5)$$

where kC_0 is a constant. Eqn. (5) shows, that C is inversely proportional to the remaining part of melt. Dependence of impurity concentration in Si solid phase on crystallized part of melt is shown in the Figure 3.

Typical X-ray diffraction spectra have shown that obtained Si is single-phase. Consequently, there is only Si diffraction maxima on the diffractogram. Microstructure investigations has confirmed, that the tracks of different phase inclusions observed in initial microstructure of MG-Si almost disappeared after pulling Si crystal out of the melt. So crystal phase of Si is purer than liquid phase with irregular impurity distribution along length.

Conclusion

Thus Si and two or more liquid layers of slags, which differ by density, originate at Si melting and the purification of Si of impurities like Fe, Al, P, Ca, Cu, Mg, Mn, Ni, Ti take place by different mechanisms or their combination.

Concrete mechanisms processing at Si purification are defined by impurity-Si interactions and depend on impurity distribution coefficient between solid and liquid phases, degree of volatility, steam tension, melting temperature, specific weight, and other chemical properties of impurities. Because virtually all basic impurities in Si have distribution coefficient $k < 1$, their effective removal is carried out by pushing aside impurities into liquid phase.

Acknowledgement

This paper has been presented at the 4th International Conference "Nanotechnologies", October 24 – 27, 2016, Tbilisi, Georgia (Nano – 2016).

References

- ¹Green, M. A., Emery, K., Hishikawa, Y., Warta, W., Dunlop, E. D., *Progr. Photovoltaics: Res. Appl.*, **2015**, *23*, 1.
- ²Khutsishvili, E., Khutsishvili, N., Kvirkevelia, B., Kekelidze, G., Nadiradze, L., Kekelidze, N., *J. Electr. Eng.*, **2015**, *3*, 53.
- ³Sing, K. S. W., Everett, D. H. R., Haul, A. W., Moscou, I., Pierotti, R. A., Rouquerol, J., Siemieniewska, T., *Pure Appl. Chem.*, **1985**, *57*, 603
- ⁴Martorano, M. A., Neto, J. B. F., Oliveira, T. S., Tsubaki, T. O., *Mater. Sci. Eng. B*, **2011**, *76(3)*, 217.
- ⁵Burton, J. A., Prim, R. S., Slichter, W. P., *J. Chem. Phys.*, **1953**, *21*, 1987.
- ⁶Pfann, W. G., *Trans. AIME*, **1952**, *194*, 747.

Received: 30.07.2016.

Accepted: 03.11.2016.



PECULIARITIES OF “ALLOY” SCATTERING IN SEMICONDUCTORS

N. Kekelidze,^[a] E. Khutsishvili,^{[a]*} D. Kekelidze,^[a] B. Kvirkvelia,^[a] L. Nadiradze^[b] and K. Sadradze^[b]

Keywords: Semiconductor Alloys, disorders, charge carriers mobility.

The effect of nanometer size disordered regions in $\text{Si}_x\text{Ge}_{1-x}$ and $\text{InP}_x\text{As}_{1-x}$ semiconductor alloys on the mobility of charge carriers has been investigated. The investigation has shown, that the composition dependence of the mobility appears as a result of contribution of main processes of current carriers scattering on phonons, ionized impurities and “alloy” disorders in $\text{Si}_x\text{Ge}_{1-x}$ and $\text{InP}_x\text{As}_{1-x}$ alloys. We have calculated the contribution of these scattering processes towards total scattering. Share of contribution of “alloy” disorders into the total mobility is different for $\text{Si}_x\text{Ge}_{1-x}$ and $\text{InP}_x\text{As}_{1-x}$ solid solutions. Unlike $\text{Si}_x\text{Ge}_{1-x}$ alloys, the “alloy” disorders in $\text{InP}_x\text{As}_{1-x}$ practically do not disturb the crystal lattice in a tangible way at temperatures in the range of 4.2 – 300 K because of sublattices of InP and InAs retain certain individuality in $\text{InP}_x\text{As}_{1-x}$ alloys.

* Corresponding Author

E-Mail: elzakhutsishvili@yahoo.com

- [a] Laboratory of Semiconductor Materials Science, Ferdinand Tavadze Institute of Metallurgy and Materials Science, Tbilisi, 0186, Georgia
 [b] Department of Engineering Physics, Georgian Technical University, Tbilisi, 0175, Georgia

Introduction

Studies of semiconductors have shown that there might be various types of heterogeneity, which have independent scientific and practical interest in terms of materials with nanometer size disordered regions. The presence of such regions may seriously alter the transport and other properties of semiconductors. These disorders are of different origin, associated with a non-uniform distribution of impurity ions in doped and compensated semiconductors,¹ arisen at irradiation² and at the growth of crystals,³ related to the presence of crystalline boundaries in polycrystals.⁴ Independently of semiconductor crystals growth methods there always exist these or those disordered areas, which are an accompanying appearance in semiconductor technology and cannot be ignored, because may contribute to the electrical,⁵ optical⁶ properties, etc. in a greater or lesser extent. All types of the heterogeneity listed above are caused by random space distribution of impurity ions and electrons and have electrostatic nature. The main peculiarity of these kinds of heterogeneity is that they modulate the semiconductors energy bands in a way, so that the optical energy gap remains invariable.

There may be another type of heterogeneity connected with random space fluctuations of the composition⁷ so-called “alloy” disorders. This type of heterogeneity is one of the most interesting for semiconductor technology because semiconductor alloys (or so-called solid solutions) of elementary semiconductors or III–V compounds may extend the functionality and operational parameters of electronic devices based on them. Changes in the composition of these solutions allow monitoring of important physicochemical properties of the obtained materials, thereby are more widely used in modern semiconductor devices than their pure initial components. Many of semiconductor alloys devices offer higher

performance compared to silicon devices and are competitive with GaAs-based products. Presently, experimental knowledge concerning “alloy” disorders in such materials is rudimentary with a few exceptions.

This paper is devoted mainly to review the influence of “alloy disorders” on the base of electrical properties in semiconductor alloys of elementary semiconductors and III–V compounds, $\text{Si}_x\text{Ge}_{1-x}$ and $\text{InP}_x\text{As}_{1-x}$. Among the solid solutions, these systems are of great interest for engineering. In this paper, we have focused on the influence of “alloy” disorders on the mobility of charge carriers, the key parameter determining thermoelectric and microelectronic applications of semiconductors.

Experimental

The *p*-type $\text{Si}_x\text{Ge}_{1-x}$ ($0 \leq x \leq 1$) crystals were grown by the Czochralski technique. Experimental *n*-type samples of $\text{InP}_x\text{As}_{1-x}$ solid solutions were grown by the horizontal zone melting method. High degree of homogeneity of solid solutions was confirmed by several methods, among which the most important are X-ray microanalysis and application of Vegard law. Charge carriers mobility was evaluated from Hall-effect and conductivity measurements by a standard dc bridge technique. The standard deviation in the carriers' concentration was 8 – 10 % and that in the conductivity was 4 – 5%.

Results and discussion

$\text{Si}_x\text{Ge}_{1-x}$ Alloys

“Alloy” disorder scattering was observed for the first time in $\text{Si}_x\text{Ge}_{1-x}$ semiconductor alloys.⁸ Our data of current carriers mobility (μ_{exp}) for $\text{Si}_x\text{Ge}_{1-x}$ solid solutions with nearly the same carriers concentration $n \sim 10^{16}$, 10^{17} and 10^{19} cm^{-3} are presented in Figure 1. Composition dependence of the charge carriers mobility of $\text{Si}_x\text{Ge}_{1-x}$ solid solutions at 300 K with the carriers concentrations $n \sim 10^{16}$ and 10^{17} cm^{-3} (Figure 1) reveals strong minimum in the middle of solid solutions system.

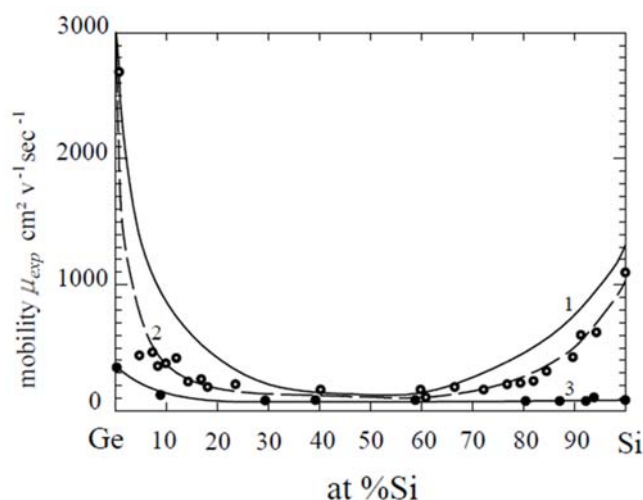


Figure 1. Composition dependence of the mobility charge carriers (μ_{exp}) at 300 K for $\text{Si}_x\text{Ge}_{1-x}$ alloys with charge concentration: 1 = $1 \times 10^{16} \text{ cm}^{-3}$, 2 = $1 \times 10^{17} \text{ cm}^{-3}$ and 3 = $2 \times 10^{19} \text{ cm}^{-3}$.

The presence of minimum in composition dependence of mobility is defined by “alloy” scattering.^{5,7} To achieve complete agreement between experimental results and the theory, it is necessary to assume the existence of an additional mechanisms of the current carriers scattering due to the disordered arrangement of solid solution atoms. Hence, we considered simultaneous action of different kinds of carriers scattering in $\text{Si}_x\text{Ge}_{1-x}$ alloys viz., the alloy disorder scattering, the scattering on acoustic lattice vibrations and the scattering on impurity ions. The individual share of contribution of these scattering mechanisms to the total varies with the compositions of $\text{Si}_x\text{Ge}_{1-x}$ solid solutions. To compare the experimental results with the theory in impurity-doped $\text{Si}_x\text{Ge}_{1-x}$ alloys, a relationship (eqn. 1), which takes into account simultaneous presence of scattering processes with different energetic dependences, was used.^{9,10} The net mobility (μ) depends on the various mobility components, associated with each scattering mechanism.

$$\frac{1}{\mu} = \frac{1}{\mu_{\text{dis}}} + \frac{1}{F} \left(\frac{1}{\mu_{\text{L}}} + \frac{1}{\mu_{\text{I}}} \right) \quad (1)$$

where,

μ_{L} , and μ_{I} are the components related to the lattice vibrations and ionized impurity scattering respectively, μ_{dis} is the component related to disorder scattering and F is a correction factor, which takes into account the combined effect of different scattering processes.⁹

Comparison of experimental and theoretical mobility showed that component of mobility related to alloy disorders scattering follows the law predicted by theory^{5,7} in $\text{Si}_x\text{Ge}_{1-x}$ alloys.

Calculation of this contribution has been made by using an expression originally derived by Brooks.⁷

$$\mu_{\text{dis}} = \frac{(2\pi)^{1/2} e \hbar^4 N_0}{3(m^*)^{5/2} (kT)^{1/2} c(1-c)(E_a - E_b)^2} \quad (2)$$

where

N_0 is the number of atoms per unit volume,

c is the composition of one of the component of alloy,

E_a and E_b are energy-positions of edges of bands for two components of alloy.

According to Brooks⁷ in alloy with disorders regions the composition changes from one region to other one at the expense of statistical fluctuations. This causes energy bands deformation, peaks and dips at the edge of bands, which looks like deformation potential in theory of scattering by thermal vibration of lattice atoms. So “alloy” scattering can be considered as “frozen” scattering by thermal vibration of lattice.⁵ At low level of carriers concentration “alloy” scattering contribution to the mobility increases with increase of alloy components content. At high level of carriers concentration the mobility does not depend on alloy components content and scattering is defined by ionized impurities (Figure 1).¹⁰

The “alloy” scattering of current carriers is very important for creating of effective thermoelements on the base of $\text{Si}_x\text{Ge}_{1-x}$. The perfect combination of properties connected with “alloy” disorders and thermoelectric properties in $\text{Si}_x\text{Ge}_{1-x}$ alloys makes them high effective thermoelectric materials for use at high temperatures.¹⁰

$\text{InP}_x\text{As}_{1-x}$ alloys

Contribution of disorder scattering to the electrons mobility has been revealed also for a number of III-V compound alloys, particularly for $\text{InP}_x\text{As}_{1-x}$ solid solutions. Mobility data of current carriers for $\text{InP}_x\text{As}_{1-x}$ solid solutions with nearly the same carriers concentration $n \sim 10^{16}$ and 10^{18} cm^{-3} are presented in Figure 2.

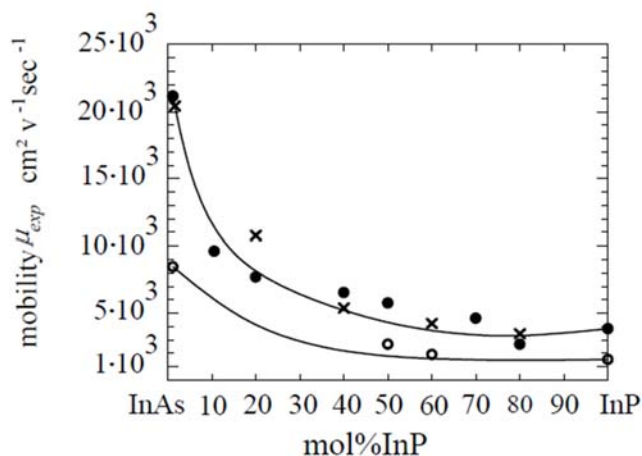


Figure 2. Composition dependence of the mobility of charge carriers (μ_{exp}) at 300 K for $\text{InP}_x\text{As}_{1-x}$ alloys with charge concentration = 10^{16} cm^{-3} (• – our data, × – data from ref. 11) and 10^{18} cm^{-3} (○ – our data).

Composition dependence of electrons mobility at 300 K for $\text{InP}_x\text{As}_{1-x}$ solid solutions with the carriers concentrations $n \sim 10^{16}$ and 10^{18} cm^{-3} (Figure 2) reveals weak minimum on the InP-rich side of solid solutions system. Such character of composition dependence of mobility is connected with the change of contribution of scattering mechanisms of separate components into the total scattering at the alteration of composition. We carried out appropriate analysis of the mobility on the basis of reasonable theories.^{7,9,12,13} Comparison with theoretical predictions in $\text{InP}_x\text{As}_{1-x}$ solid solutions with $n \sim 10^{16} \text{ cm}^{-3}$ has shown that at temperatures near 300 K the prevailing mechanism is the scattering on optical phonons.¹⁴ Contribution of the disorder scattering increases with increasing of InP composition in solid solutions system at fixed temperatures and weakens with lowering of temperature in the range of 4.2-300 K and never dominates.¹⁵ Assumption of the existence of an additional mechanism of the current carriers scattering due to the disordered arrangement of solid solution atoms allows achieving the full agreement of experimental mobility with the theory.

The composition dependence of the mobility of current carriers for $\text{InP}_x\text{As}_{1-x}$ alloys (Figure 2) differs from the similar dependence for $\text{Si}_x\text{Ge}_{1-x}$ alloys (Figure 1) with well-defined minimum in the middle of alloys system. The data for alloy scattering in $\text{InP}_x\text{As}_{1-x}$ solid solutions do not reveal such tendency.

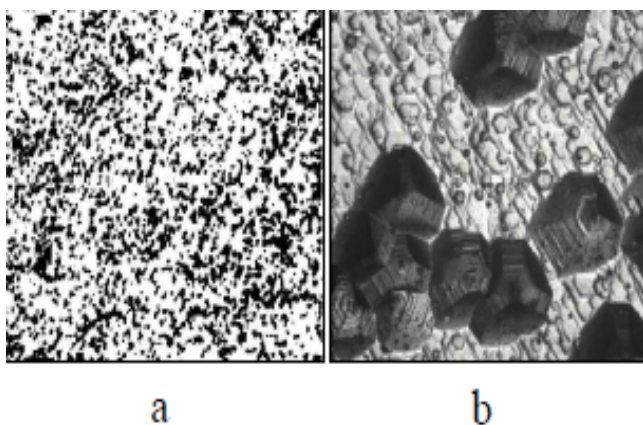


Figure 3. Dislocation structure of single crystals of semiconductor alloys on the plane (111) (a) $\text{Si}_x\text{Ge}_{1-x}$ ($\times 1000$) and (b) $\text{InP}_x\text{As}_{1-x}$ ($\times 250$).

An estimate of maximal share of disorder scattering in $\text{InP}_x\text{As}_{1-x}$ solid solutions results in the value which does not exceed $\sim 20\%$ of total magnitude of determinative scattering at 300 K and $\sim 10\%$ at lower temperatures. The reason of absence of clear minimum in the composition dependence of mobility for $\text{InP}_x\text{As}_{1-x}$ solid solutions may be apparently connected with the specific properties of $\text{InP}_x\text{As}_{1-x}$ caused by fact, that sublattices of InP and InAs retain a certain natural properties in contrast to Si and Ge in $\text{Si}_x\text{Ge}_{1-x}$ alloys. The preservation of individuality of sublattices of InP and InAs in their alloys has been previously found by us at optical properties research,¹⁴ where has been discovered two mode behavior of lattice vibrations in $\text{InP}_x\text{As}_{1-x}$ alloys.

The retention of individuality of sublattices of InP and InAs in $\text{InP}_x\text{As}_{1-x}$ alloys is confirmed by microstructural studies (see Figure 3).

This image clearly show, that InP and InAs sublattices in $\text{InP}_x\text{As}_{1-x}$ alloys retain their identity as distinct from $\text{Si}_x\text{Ge}_{1-x}$ where Si and Ge do not preserve their identity.

Conclusion

Unlike $\text{Si}_x\text{Ge}_{1-x}$, the “alloy” scattering in $\text{InP}_x\text{As}_{1-x}$ never dominates. In contrast to $\text{Si}_x\text{Ge}_{1-x}$, solid solutions InP and InAs retain a certain individuality in $\text{InP}_x\text{As}_{1-x}$ alloys. This result means, that mobility in $\text{InP}_x\text{As}_{1-x}$ solid solutions is mainly defined by the factors determining III–V compounds. A relative small contribution of disorder scattering is important for devices designed on the base of $\text{InP}_x\text{As}_{1-x}$ system.

Acknowledgement

This paper has been presented at the 4th International Conference “Nanotechnologies”, October 24 – 27, 2016, Tbilisi, Georgia (Nano – 2016).

References

- ¹Shklovski, B., Efros, A., *Electronic Properties of Doped Semiconductors*, 1984, Berlin: Springer-Verlag, 136.
- ²Gossick, B.R., *J. Appl. Phys.*, **1959**, 30, 1214.
- ³Kekelidze, N., Kekelidze, D., Milovanova, L., Khutsishvili, E., Davitaya, Z., Kvirkvelia, B., Khomasuridze, D., *Acta Phys. Pol. A*, **2012**, 121, 27.
- ⁴Khutsishvili, E., Kekua, M., *Phys. Stat. Sol. (a)*, **1980**, 61, K1.
- ⁵Shik, A. Y., *Electronic Properties of Inhomogeneous Semiconductors*, Electro Component Science Monographs, Gordon & Breach Science Pub., **1995**, 153.
- ⁶Humlicek, J., Lukes, F., Schmidt, E., Kekua, M., Khutsishvili, E., *Solid State Comm.*, **1983**, 47, 387.
- ⁷Makowski, L., Glicksman, M., *J. Phys. Chem. Solids*, **1973**, 34, 487.
- ⁸Levitas, A., *Phys. Rev.*, **1955**, 99, 1810.
- ⁹Mansfield, R., *Proc. Phys. Soc.*, **1956**, B69, 76.
- ¹⁰Kekua, M., Khutsishvili, E., *Germanium–Silicon Semiconductor Solid Solutions*, Tbilisi, Metsniereba, **1985**.
- ¹¹Weiss, H., *Zeitschrift Naturforschung Teil A*, **1956**, 11, 430.
- ¹²Ehrenreich, H., *J. Phys. Chem. Solids*, **1959**, 12, 1297.
- ¹³Anselm, A. I., *Introduction to the Theory of Semiconductors*, **1978**, Moscow: Nauka, 615.
- ¹⁴Kekelidze, N., Khutsishvili, E., Kvirkvelia, B., Kekelidze, G., *J. Electr. Eng.*, **2014**, 2, 207.
- ¹⁵Kekelidze, N., Kekelidze, G., Makharadze, Z., *J. Phys. Chem. Sol.*, **1973**, 34, 117.

Received: 09.08.2016.

Accepted: 03.11.2016.



COMPARATIVE PHYTOCHEMICAL PROFILE OF *INDONEESIELLA ECHIOIDES* (L.) NEES LEAVES

A. Elaiyaraja^{[a]*} and G. Chandramohan^[b]

Keywords: *Indoneesiella echioides* (L) Nees, phytochemical screening, separation and identification of compounds, GC-MS studies, spectral analysis.

Indoneesiella echioides (or) *Andrographis echioides* (L) Nees is an important herb widely distributed in south India. This is commonly known as False water willow. *Indoneesiella echioides* (L) Nees is used as in traditional Indian medicine. The leaf juice of this plant is used to cure fever. Different pharmacological properties of *Indoneesiella echioides* have already been reported. Thus, the present study was performed to investigate the preliminary phytochemical screening, separation, identification of compounds and compare the phytochemical composition of various fraction of *Indoneesiella echioides* using gas chromatography-mass spectrometry. The plant was extracted for various solvents in increasing order of polarity from using n-hexane, chloroform, ethyl acetate, acetone, ethanol, butanol and methanol. The result obtained after GC-MS studies were confirmed by spectral analysis.

* Corresponding Authors

Tel: +919043571103

E-Mail: raja_mscchem@rediffmail.com

[a] Department of Chemistry, A.V.V.M. Sri Pushpam College, Poondi, Thanjavur 613 503, Tamilnadu, India.

[b] Department of Chemistry, Jairams Arts and Science College, Karur-3, Tamilnadu, India.

Introduction

Indoneesiella echioides (L) Nees (Acanthaceae), also known as *Andrographis echioides* (L) Nees, is commonly known as False Water Willow and grows abundantly in south India. *Indoneesiella echioides* (L) Nees is medicinally highly important. The plants of genus *Indoneesiella* is used in goiter, liver diseases,¹ fertility problems, bacterial infection and malarial and fungal disorders.² The leaf juice of this plant is used to treating fever.³ Several *Indoneesiella* species (about 40 species) has been used in treatment of influenza, malaria, dyspepsia and respiratory diseases. The plants of *Indoneesiella* species are also used as antidote for poisonous stings of some insects.^{4,5} The leaf juice is mixed and boiled with coconut oil used to control falling and greying of hair.⁶ Phytochemistry of *Indoneesiella echioides* has been investigated and reported to contain several flavonoids^{7,8} and labdane diterpenoids.⁹⁻¹⁴

In previous literatures only flavonoids are reported as a major component in *Indoneesiella echioides* (L) Nees extracts.¹⁵⁻¹⁸ It has been reported that variety of phytoconstituents like phenols, coumarins, lignans, essential oil, monoterpenes, carotenoids, glycosides, flavonoids, organic acids, lipids, alkaloids and xanthenes are also present.¹⁹

Hence the present investigation was carried out to determine the possible phytochemical compounds of *Indoneesiella echioides* by GC-MS studies.

Experimental

Collection of plant materials

The leaves of *Indoneesiella echioides* was collected from Poondi village, Thanjavur District, Tamilnadu, India. The botanical identity (Voucher No: A.A.R 001 on 04-02-2015) of the plant was confirmed by Dr. S. John Britto, Rapinat Herbarium, St. Joseph's College, Tiruchirappalli, India.

Preparation of extracts

The fine powder (5 kg) was extracted with 95% ethanol at room temperature for ten days. The extract were filtered and concentrated under reduced pressure in a rotary evaporator and extracted with various solvents in increasing order of polarity, starting from n-hexane, chloroform, acetone, ethanol, butanol and methanol. The extract was taken in a beaker and kept in a water bath and heated at 30-40 °C till all the solvent is evaporated. The dried extracts were subjected to preliminary phytochemicals and GC-MS studies. All the extracts were tested for the presence bioactive compounds by using standard methods.

Phytochemical screening

The preliminary phytochemical analysis of *Indoneesiella echioides* (L) Nees was carried out as per standard methods (Table 1).

Identification of phytocompounds by GC-MS

GC-MS, one of the most reliable biophysical method for its specificity and repeatability, was utilized for the phytochemical profiling of *Indoneesiella echioides* (L) Nees leaves.

Table 1. Preliminary phytochemical constituents of *Indoneesiella echioides* (L) Nees leaves.

S. No.	Phytochemicals	Hexane extract	Chloroform extract	Acetone extract	Ethanol extract	Butanol extract	Methanol extract
1.	Alkaloids	-	-	Present	Present	-	-
2.	Flavonoids	-	Present	Present	Present	Present	Present
3.	Terpenes	Present	Present	-	-	-	-
4.	Triterpenoid saponins	-	Present	Present	-	-	-
5.	Saponins	-	Present	Present	Present	Present	Present
6.	Glycosides	-	-	-	-	-	-
7.	Steroids	Present	Present	Present	-	-	-
8.	Carbohydrates	-	-	-	-	-	-
9.	Phenolic compounds	Present	Present	Present	-	Present	Present
10.	Tannins	-	-	-	-	-	-
11.	Amino acids	-	-	Present	Present	-	Present

Table 2. Phytochemical components identified for n-hexane extract of *Indoneesiella echioides* (L) Nees (GC-MS study).

S.N	RT	Name of the compound	Molecular formula	Molecular weight	Peak area (%)	Compound nature	Activity
1.	12.85	Undecanoic acid, 10-methyl-, methyl ester	C ₁₃ H ₂₆ O ₂	214.3443	87	-	No activity reported.
2.	15.07	Methyl tetradecanoate	C ₁₅ H ₃₀ O ₂	242.3975	100	Myristic acid ester	Antioxidant, cancer-preventive, hypercholesterolemic, nematicide activities.
3.	15.72	Tetradecanoic acid, 12-methyl-, methyl ester	C ₁₆ H ₃₂ O ₂	256.4241	100	Fatty acid methyl ester	No activity reported.
4.	16.95	(Z)-9-Hexadecenoic acid, methyl ester,	C ₁₇ H ₃₂ O ₂	268.4348	63.9	Fatty acid methyl ester	No activity reported.
5.	17.17	Pentadecanoic acid, 14-methyl-, methyl ester	C ₁₇ H ₃₄ O ₂	270.4507	100	Palmitic acid methyl ester	Antioxidant, antifungal, antimicrobial activities.
6.	18.15	Hexadecanoic acid, 14-methyl-, methyl ester	C ₁₈ H ₃₆ O ₂	284.4772	100	-	No activity reported.
7.	18.93	10-Octadecenoic acid, methyl ester	C ₁₉ H ₃₆ O ₂	296.4879	100	Fatty acid ester	antioxidant, antimicrobial activities.
8.	19.1	Heptadecanoic acid, 16-methyl-, methyl ester	C ₁₉ H ₃₈ O ₂	298.5038	100	Stearic acid	Used against skin cancer protein.
9.	19.72	Eicosanoic acid	C ₂₀ H ₄₀ O ₂	312.5304	74.7	Fatty acid	No activity reported.
10.	20.92	Eicosanoic acid, methyl ester	C ₂₁ H ₄₂ O ₂	326.5570	100	Arachidic acid	α-Glucosidase inhibitors activity.
11.	21.18	Hexadecanoic acid, 1,1-dimethylethyl ester	C ₂₀ H ₄₀ O ₂	312.5304	54.5	-	No activity reported.
12.	22.95	Docosanoic acid, methyl ester	C ₂₃ H ₄₆ O ₂	354.6101	98.4	Fatty acid	Therapeutic, diagnostic activities.
13.	23.28	Benzoic acid, 2,4-dimethoxy-6-methyl-, (8,8-dimethoxy-2-octyl) ester	C ₂₀ H ₃₂ O ₆	368.46448	94.4	-	No activity reported.

Source: Dr. Duke's Phytochemical and Ethnobotanical Databases

Interpretation on Mass-Spectra GC-MS was conducted using the database of National Institute Standard and Technology (NIST) having more 62,000 patterns. The spectrum of the unknown components was compared with the spectrum of known components stored in the NIST library.

The name, molecular weight and structure of the components of the test materials were ascertained. In the present study many phytochemical constituents have been identified from various fractions of *Indoneesiella echioides*(L) Nees leaves by GC-MS analysis.

Analysis of n-hexane extract

Thirteen phytocomponents which appeared in the n-hexane extract of *Indoneesiella echioides* (L) Nees leaves are listed in Table 2. All these compounds were known compounds.

Analysis of chloroform extract

Nine phytocomponents were identified from the chloroform extract of *Indoneesiella echioides* (L) Nees leaves and are listed in Table 3.

Table 3. Phytochemical components identified for chloroform extract of *Indoneesiella echioides* (L) Nees (GC-MS study).

S.No.	RT	Name of the compound	Molecular formula	Molecular weight	Peak area (%)	Compound nature	Activity
1.	12.63	Phenol, 2,4-bis(1,1-dimethylethyl)-	C ₁₄ H ₂₂ O	206.3239	27	-	Antifungal, antimicrobial, antioxidant, antimalarial activities.
2.	14.52	1,4-Dicyano-2-cyclohexylbenzene	C ₁₄ H ₁₄ N ₂	210.27436	3.5	-	-
3.	15.7	Flavone	C ₁₅ H ₁₀	222.239	6.4	-	-
4.	17.15	Pentadecanoic acid, 13-methyl-, methyl ester	C ₁₇ H ₃₄ O ₂	270.4507	15.5	-	-
5.	18.03	n-Hexadecanoic acid	C ₁₆ H ₃₂ O ₂	256.4241	12.5	Fatty acid	Antioxidant, hypocholesterolemic, nematocidal, pesticide, lubricant, Antiandrogenic, flavor, hemolytic, 5- α -reductase inhibitor activities.
6.	18.83	10-Octadecenoic acid, methyl ester	C ₁₉ H ₃₆ O ₂	296.4879	13.1	Fatty acid ester	Antioxidant, antimicrobial activities.
7.	19.45	Ethyl Oleate	C ₂₀ H ₃₈ O ₂	310.52	24.9	Fatty acid ester	It is used as a vehicle for intramuscular drug delivery.
8.	21.4	3,5-Dicarbethoxy-1-methyl-1,4,5,6,7,8-hexahydropyrrolo[2,3-b]azepin-4,7-dione	-	-	7.3	Unknown compound	-
9.	23.18	Butanoic acid, 3-methyl-, hexadecyl ester.	-	-	25.8	Unknown compound	-

Source: Dr. Duke's Phytochemical and Ethnobotanical Databases

Table 4. Phytochemical components identified for acetone extract of *Indoneesiella echioides* (L) Nees (GC-MS study).

S.N o.	RT	Name of the compound	Molecular formula	Molecular weight	Peak Area (%)	Compound nature	Activity
1.	17.97	Hexadecanoic acid, ethyl ester	C ₁₈ H ₃₆ O ₂	284	100	Fatty acid	Antioxidant, Hypocholesterolemic, Nematocidal, Pesticide, Lubricant, Antiandrogenic, Flavor activities.
2.	19.57	Ethyl Oleate	C ₂₀ H ₃₈ O ₂	310.52	100	Fatty acid ethyl ester	It is used for vehicle for intramuscular drug delivery.
3.	19.8	14-Hydroxy-15-methylhexadec-15-enoic acid, ethyl ester	C ₁₉ H ₃₆ O ₃	312.48734	91.2	-	No activity reported.
4.	21.75	2a,3b,5b,6a-Tetramethoxy carbonyl-bicyclo(2,2,2)oct-7-ene	C ₁₆ H ₂₀	340.325	23.3	-	No activity reported.
5.	23.37	Estra-1,3,5(10),6-tetraene-3,17-diol, diacetate, (17a')-	-	-	18	Unknown compound	-

Source: Dr. Duke's Phytochemical and Ethnobotanical Databases

Table 5. Phytochemical components identified for ethanolic extract of *Indoneesiella echioides* (L) Nees (GC-MS study).

S.No	RT	Name of the compound	Molecular formula	Molecular weight	Peak area, (%)	Compound Nature	Activity
1.	12.68	O-Himachalene	C ₁₅ H ₂₄	204.3511	4.3	-	Noactivity reported.
2.	14.15	Oxacyclotetradecan-2-one	-	-	15.2	Unknown compound	-
3.	14.5	Ar-tumerone	C ₁₅ H ₂₀ O	216.319	91.8	Sesquiterpenoid	Antivenom. Antidépresseur, Anti-inflammatoire, Neuroprotecteuractivities.
4.	14.9	Curlone	C ₁₅ H ₂₂ O	218.33458	41.4	Ketone	No activity reported.
5.	17.28	Pentadecanoic acid, 14-oxo, methyl ester	C ₁₆ H ₃₀ O ₃	270.40800	7.2	-	Antioxidant, nematocide, pesticide, hypocholesterolemicactivities.
6.	17.93	4'-Methoxy-5,7-dihydroxy isoflavone	C ₁₆ H ₁₂ O ₅	284.2635	6.4	Flavone	Used as a pharmaceutical intermediates.
7.	19.05	E,E,Z-1,3,12-Nonadecatriene-5,14-diol	C ₁₉ H ₃₄ O ₂	294	4.4	-	Antimicrobial
8.	19.55	(Z,Z)-Ethanol,2-(9,12-octadecadienyloxy)-	C ₂₀ H ₃₈ O ₂	310	5.6	Alcoholic compound.	Antimicrobial
9.	21.63	Tricosan-2-ol	-	-	7.8	Unknown compound	-

Source: Dr. Duke's Phytochemical and Ethnobotanical Databases

Table 6. Phytochemical components identified for butanol extract of *Indoneesiella echioides* (L) Nees (GC-MS study).

S.No.	RT	Name of the compound	Molecular formula	Molecular weight	Peak area (%)	Compound nature	Activity
1.	12.12	E-2-Tetradecen-1-ol	C ₁₄ H ₂₈ O	212.3715	3.1	Unsaturated alcohol	No activity reported.
2.	12.67	6,10-Dodecadien-1-ol,3,7,11-trimethyl-,(E)-(n)-	C ₁₅ H ₂₈ O	224.38222	11.9	-	No activity reported.
3.	14.15	E,E-6,8-Tridecadien-2-ol, acetate	-	-	16.3	Unknown compound	-
4.	14.45	Ar-tumerone	C ₁₅ H ₂₀ O	216.319	91.8	Sesquiterpenoid	Antivenom, Antidépresseur, Anti-inflammatoire, Neuroprotecteur
5.	15.93	5-Hexenoic acid,(9-decen-2-yl) ester	-	-	15.7	Unknown compound	-
6.	17.22	4',5,7-Trihydroxy isoflavone	C ₁₅ H ₁₀ O ₅	270.2369	11.7	Flavone	Antitumor agent, antioxidant, antiangiogenic and immunosuppressive activities.
7.	17.88	Ethyl 9-hexadecenoate	C ₁₈ H ₃₄ O ₂	282.4614	6.2	Fatty acid ester	No activity reported.
8.	19.15	16-Octadecenoic acid, methyl ester	C ₁₉ H ₃₆ O ₂	296.49	7.2	Fatty acid ester	Inhibit eukaryotic DNA polymerase activities <i>in vitro</i>
9.	19.5	(Z,Z)-Ethanol,2-(9,12-octadecadienyloxy)-	C ₂₀ H ₃₈ O ₂	310	6.5	Alcoholic compound	Antimicrobial activity.
10	21.63	Eicosanoic acid, 3-methyl-, methyl ester	-	-	7.8	Unknown compound	-

Source: Dr. Duke's Phytochemical and Ethnobotanical Databases

Table 7. Phytochemical components identified for methanolic extract of *Indoneesiella echioides* (L) Nees (GC-MS study).

S.No.	RT	Name of the compound	Molecular formula	Molecular weight	Peak area (%)	Compound nature	Activity
1.	16.5	Methyl 2,8-dimethyltridecanoate	C ₁₆ H ₃₂ O ₂	256.42408	11.1	-	No activity reported.
2.	18.8	4'-Methoxy-5,7-dihydroxy isoflavone	C ₁₆ H ₁₂ O ₅	284.2635	61.7	Flavone	Used as a pharmaceutical intermediates.
3.	19.15	Cyclohexan-1-ol-3-one-1-carboxylic acid, 6-(2,3-dimethoxyphenyl)-	-	-	14	Unknown compound	-
4.	19.72	Ethyl Oleate	C ₂₀ H ₃₈ O ₂	310.52	42.2	Fatty acid ester	It is used for intra-muscular drug delivery
5.	21.78	Elaidic acid, isopropyl ester	C ₂₁ H ₄₀ O ₂	324.541	13.9	-	Anti-inflammatory, hypocholesterolemic, cancer preventive, hepatoprotective
6.	23.38	Isopropyl stearate	C ₂₁ H ₄₂ O ₂	326.568	10.1	Stearic acid	Skin conditioning agent, binder and humectant activities.
7.	25.53	Estra-1,3,5(10)-trien-17a'-ol, 3-methoxy-17-(2-methylallyl)-	-	-	7.2	Unknown compound	-

Source: Dr. Duke's Phytochemical and Ethnobotanical Databases.

Out of the nine phytochemicals obtained from chloroform extract, two (Table 3, S. No. 8 and 9) are unknown compounds.

The mass spectra of unknown compounds isolated from the extracts made by various solvents can be found in the supplementary material.

Analysis of acetone extract

Five phytochemicals were isolated from the acetone extract of *Indoneesiella echioides* (L) Nees plant leaves (Table 4). Out of five components, only one (at S. No. 5) is unknown compound.

Analysis of ethanolic extract

Nine phytochemicals isolated from the ethanolic extract of *Indoneesiella echioides* (L) Nees leaves and are listed in Table 5. Out of these, only one compound (at S. No. 9) is unknown compound.

Analysis of butanol extract

Ten phytochemicals were isolated from the butanol extract of *Indoneesiella echioides* (L) Nees leaves and are listed in Table 6. Out of these three (at S. No. 3, 5 and 10) are unknown compounds.

Analysis of methanolic extract

Seven isolated from the methanolic extract of *Indoneesiella echioides* (L) Nees plant leaves and are listed in Table 7. Out of these compounds, two (at S. No. 3 and 7) are unknown compounds.

Results and Discussion

Shen et al²⁰ reported that the new compounds of androgechside A (5,8,2'-trihydroxy-7-methoxyflavone-5-O-β-D-glucopyranoside), androgechside B (2R)-5,2'-dihydroxy-7-methoxyflavanone-5-O-β-D-glucopyranoside), androechioside A (2-O-β-D-glucopyranosyl-4-methoxy-2,4,6-trihydroxybenzoate), androechioside B (methyl 3-(2-hydroxyphenyl)-3-oxopropanoate 2-O-β-D-glucopyranoside) are isolated and structurally elucidated by spectral analysis and chemical transformation and 37 known compounds were identified to be, 2',6'-dihydroxyacetophenone 2'-O-β-D-glucopyranoside, echioidinin 5-O-β-D-glucopyranoside, echioidinin, pinostrobin, andrographidine C, dihydroechioidinin, tectochrysin 5-glucoside, methyl salicylate glucoside, 7,8-dimethoxy-5-hydroxyflavone, 5,7,8-trimethoxyflavone, skullcapflavone I 2'-methyl ether, acetophenone-2-O-β-D-glucopyranoside, androechin, skullcapflavone I 2'-O-β-D-glucopyranoside, tectochrysin, 5,7,2'-trimethoxyflavone, echioidin, skullcapflavone I, 5,7-dimethoxyflavone, negletein 6-O-β-D-glucopyranoside, andrographidine E, 4-hydroxy-3-methoxy-trans-cinnamic acid methyl ester, 4-hydroxybenzaldehyde, 4-hydroxy-trans-cinnamic acid methyl ester, O-coumaric acid, 2,6-dihydroxybenzoic acid, 132-hydroxy-(132-R)-phaeophytin, (E)-phytyl-epoxide, phytol, phytene 1,2-diol, (+)-dehydrovomifoliol, 3β-hydroxy-5α, 6α,-epoxy-7-megastigmen-9-one, β-sitosterol, β-sitosterol-3-O-β-D-glucopyranoside, squalene, 1H-indole-3-carbaldehyde, and loliolide by comparison of their physical and spectral data with those reported in the literature.

In the present study preliminary phytochemical analysis of the *Indoneesiella echioides* (L) Nees revealed the presence of flavonoids, alkaloids, terpenoids, triterpenoids saponins, saponins, phenolic compound, sterols and amino acids are qualitatively analysed and the results are listed in table 1. These phytochemicals were found to be dihydroechioidinin, along with four unknown flavones, echioidinin, echioidin, skullcapflavone I 2'-*O*-methyl ester and skullcapflavone I 2'-*O*-glucoside.¹⁹ GC-MS studies indicated the presence of many phytocomponents such as flavones, sesquiterpenoids, fatty acid methyl ester, palmitic acid methyl ester, steroid, fatty acid ester, stearic acid, oleic acid, arachidic acid, myristic acid ester and unsaturated alcoholic compounds in the various extracts of the *Indoneesiella echioides* (L) Nees leaves.

Conclusion

The preliminary phytochemical analysis of *Indoneesiella echioides* (L) Nees leaves showed that they contain many bioactive chemicals like flavonoids, alkaloids, terpenoids, triterpenoids saponins, saponins, phenolic compounds, sterols and amino acids.

The GC-MS studies of *Indoneesiella echioides* (L) Nees leaves clearly indicate that the major compounds are the 4'-Methoxy-5,7-dihydroxy isoflavone (ethanol and methanol fractions), 4',5,7-Trihydroxy isoflavone (butanol fraction), Ar-tumerone (ethanol and butanol fractions), Ethyl Oleate (chloroform, acetone and methanol fractions), Ethanol, 2-(9,12-octadecadienyloxy)-(Z,Z)- (ethanol and butanol fractions) are identified.

Unknown compounds such as 3,5-dicarbethoxy-1-methyl-1,4,5,6,7,8-hexahydropyrrolo (2,3-b)azepin-4,7-dione, butanoic acid, 3-methyl-, hexadecyl ester, estra-1,3,5(10),6-tetraene-3,17-diol, diacetate, (17a)-, tricosan-2-ol, E,E-6,8-tridecadien-2-ol, acetate, 5-hexenoic acid, (9-decen-2-yl) ester, eicosanoic acid, 3-methyl-, methyl ester, 4'-methoxy-5,7-dihydroxy isoflavone, cyclohexan-1-ol-3-one-1-carboxylic acid, 6-(2,3-dimethoxyphenyl)-, estra-1,3,5(10)-trien-17a'-ol, 3-methoxy-17-(2-methylallyl)- are identified.

Minor compounds such as undecanoic acid, 10-methyl-, methyl ester, methyl tetradecanoate, tetradecanoic acid, 12-methyl-, methyl ester, 9-hexadecenoic acid, methyl ester, (Z)-, pentadecanoic acid, 14-methyl-, methyl ester, hexadecanoic acid, 14-methyl-, methyl ester, 10-octadecenoic acid, methyl ester, heptadecanoic acid, 16-methyl-, methyl ester, eicosanoic acid, eicosanoic acid methyl ester, hexadecanoic acid, 1,1-dimethylethyl ester, docosanoic acid methyl ester, benzoic acid, 2,4-dimethoxy-6-methyl-, (8,8-dimethoxy-2-octyl) ester, phenol, 2,4-bis(1,1-dimethylethyl)-, 1,4-dicyano-2-cyclohexylbenzene, flavone, pentadecanoic acid, 13-methyl-, methyl ester, n-hexadecanoic acid, 10-octadecenoic acid, methyl ester, ethyl Oleate, hexadecanoic acid, ethyl ester, 14-hydroxy-15-methylhexadec-15-enoic acid, ethyl ester, 2a,3b,5b,6a-tetramethoxycarbonylbicyclo[2,2,2]oct-7-ene, O-himachalene, oxacyclotetradecan-2-one, curlone, pentadecanoic acid, 14-oxo-, methyl ester, E,E,Z-1,3,12-nonadecatriene-5,14-diol, E-2-tetradecen-1-ol, 6,10-dodecadien-1-ol, 3,7,11-trimethyl-,

(E)-(n)-, ethyl 9-hexadecenoate, 16-octadecenoic acid, methyl ester, methyl 2,8-dimethyltridecanoate, elaidic acid, isopropyl ester, isopropyl stearate, 3-methoxy-17-(2-methylallyl)- were also identified.

These compounds are exhibited activities like antioxidant, cancer-preventive, hypercholesterolemic, nematocide, antifungal, antimicrobial. They are used as skin cancer protein, alpha-glucosidase inhibitors, therapeutic and diagnostic agents, an emollient, skin conditioning agent, binder, humectant, anti-inflammatory, hypocholesterolemic, cancer preventive, hepatoprotective, anticoronary, antieczemic, insectifuge. They are also used for vehicle for intramuscular delivery of drugs such as Progesterone. They selectively inhibit eukaryotic DNA polymerase activities. Some of these compounds are also find use as antitumor agent, antioxidant, antiangiogenic and immunosuppressive, nematocide, pesticide, lubricant, antiandrogenic and flavor agents. Hence *Indoneesiella echioides* (L) Nees is worthy for further investigation in natural drugs developments.

Acknowledgements

I wish to express my deep sense of gratitude and most sincere thanks to Honourable Resource Person Dr. Chandramohan, Principal, Jairams Arts and Science College, Karur-3, Tamilnadu, India for providing support to finish my research work

References

- Nadkarni A. K., Nadkarni K. M., *Indian Materia Medica*, Vol.1, Popular Prakashan, Bombay, **1976**.
- Qadrie, Z. L., Beena, J., Anandan, R., Rajkapoor, B., Rahamathulla, M., *Pak. J. Pharm. Sci.*, **2009**, *22*, 123-125.
- Kirtikar, K.R., Basu. B. D., in *Indian medicinal plants*, Vol. 3, Periodical Experts, New Delhi **1975**.
- Kirtikar, K.R., Basu. B. D., in *Indian medicinal plants*, Vol. 3, Periodical Experts, New Delhi **1975**, 1884-1886.
- Chopra, R. N., Nayer, S. L., Chopra, I. C., *Glossary of Indian Medicinal Plants*, Council of Scientific and Industrial Research, New Delhi, **1980**, 18.
- Pandi Kumar P., Ayyanar, M., Ignacimuthu, S., *Indian J. Tredit. Knowl.*, **2007**, *6*, 579-582.
- Harbone, J. B., *The Flavonoids: Advances in Research Science 1986*, Chapman and Hall: London, UK, **1994**, 280-290.
- Iinuma, M., Mizuno, M., *Phytochemistry*, **1989**, *28*, 681-694.
- Kleipool, R. J. C., *Nature*, **1952**, *169*, 33-34.
- Chan, W. R., Taylor, C. R., Willis, R. L., Bodden, R. L., *Tetrahedron*, **1971**, *27*, 5081-5091.
- Balmain, A., Connolly, J. D., *J. Chem. Soc., Perkin Trans. I*, **1973**, 1247-1251.
- Fujita, T., Fujitani, R., Takeda, Y., Takaishi, Y., Yamada, T., Kido, M., Miura, I., *Chem. Pharm. Bull.*, **1994**, *42*, 1216-1225.
- Matsuda, T., Kuroyanagi, M., Sugiyama, S., Umehara, K., Ueno, A., Nishi, K., *Chem. Pharm. Bull.*, **1994**, *42*, 1216-1225.
- Reddy, M. K., Reddy, M. V., Gunasekar, D., Murthy, M. M., Caux, C., Bodo, B. A., *Phytochemistry*, **2003**, *62*, 1271-1275.

¹⁵Govindachari, T. R., Parthasarathy P. C., Pai, B. R., Subramaniam, P. S., *Tetrahedron*, **1956**, *21*, 2633-2640.

¹⁶Govindachari, T. R., Parthasarathy P. C., Pai, B. R., Subramaniam, P. S., *Tetrahedron*, **1956**, *21*, 3715-3720.

¹⁷Jayaprakasam, B., Damu, A. G., Gunasekar, D., Blond, A., Bodo, B. *Phytochemistry*, **1999**, *52*, 935-937.

¹⁸Jayaprakasam, B., Gunasekar, D., Rao, K. V., Blond, A., Bodo, B., *J. Asian Nat. Prod. Res.*, **2001**, *3*, 43-48.

¹⁹Sharma, S. K., Ali M., Gupta J., *Phytochem Pharmacol.*, **2002**, *2*, 253-270.

²⁰Shen, D.-Y., Juang, S.-H., Kuo, P.-C., Huang, G.-J., Chan, Y.-Y., Damu, A. G., Wu, T.-S., *J. Mol. Sci.*, **2013**, *14*, 496-514.

Received: 28.08.2016.

Accepted: 05.11.2016.



THE EFFECT OF Hg-POLLUTED DRINKING WATER ON THE LEVEL OF HORMONES IN MALE RATS AND THE POTENTIAL THERAPEUTIC ACTION OF THE THIOSEMICARBAZONE AND ANTIPYRINE LIGANDS AND THEIR COMPLEXES

Samar A. Aly,^[a] Hussien H. Alganzory^{[b]*} and Tarek A. Salem^[c]

Keywords: DTA; Hg(II) complexes; IR; male hormones; oxidative status; TGA.

Novel Hg(II) complexes of d^{10} configuration have been synthesized and characterized by elemental analysis, IR, UV-VIS spectra and thermal analysis. The analytical and spectral data reveal that the ligands (H_2L^1 - HL^3) behave as neutral or mono basic bidentate in nature, coordinating via C=O or C-O and NH or C=N. The harmful effect of Hg-polluted drinking water on male sex hormones, kidney function as well as oxidative status biomarkers of male rats was investigated. Meanwhile, the potential protective effects of synthesized complexes and their ligands were studied. Results showed that orally administration of $HgCl_2$ for 30 days caused a significant disruption of male sex hormones and kidney function. Further, the level of lipid peroxidation was elevated and activities of antioxidant enzymes were markedly declined in kidney and testes homogenates. The co-administration of $HgCl_2$ with antipyrine and thiosemicarbazone as well as their complexes for four weeks led to amelioration in the kidney and testes functions as the levels of male sex hormones and kidney function tests were recovered. Meanwhile, these compounds showed ameliorative effects on the oxidative status of rats. It can be concluded that drinking of Hg-polluted water induces oxidative stress pathways that may lead to deterioration in kidney and testes function. The findings also suggest the curative action of antipyrine and thiosemicarbazone as well as their complexes since they exhibited the ability to resist the harmful action of mercury and to protect the organs from the action of free radicals.

* Corresponding Author: E-Mail: h_ganzory@yahoo.com

[a] Department of Environmental Biotechnology, Genetic Engineering & Biotechnology Research Institute, Sadat University, Egypt.

[b] Department of Chemistry, College of Science, Qassim University, KSA.

[c] Department of Biochemistry, College of Medicine, Qassim University, KSA.

endocrine glands include the hypothalamus, pituitary, thyroid, parathyroid, adrenal gland, pancreas, and gonads (ovary and testis). Hormones are natural secretory products of the endocrine glands and travel via the blood to exert their effects at distant target tissues or organs by binding to specific cell surfaces or nuclear receptors.

Many researchers reported that mercury promotes the formation of reactive oxygen species (ROS) such as hydrogen peroxide. ROS enhance the subsequent iron- and copper-induced production of lipid peroxides and the highly reactive hydroxyl radical.⁶ These lipid peroxides and hydroxyl radical may cause the cell membrane damage and thus destroy the cell. Inorganic mercury also inhibits the activities of the free radical quenching enzymes catalase, superoxide dismutase and glutathione peroxidase.⁷

Thiosemicarbazone is an emerging moiety with wide spectrum of biological activity and having sound scope in research and developing process in pharmaceutical and medicinal chemistry.⁸⁻¹¹ Thiosemicarbazones are of considerable interest because of their chemistry and potentially beneficial biological activity, such as antibacterial antifungal,¹² antiviral,¹³ antiamebic,¹⁴ antimalarial^{15,16} and antitumor activity.¹⁷ The biological activities of thiosemicarbazones are considered to be due to their ability to form chelates with metals. Biological activities of metal complexes differ from those of either ligands or the metal ions and increase and/or decreased biological activities are reported for several transition metal complexes. Thiosemicarbazone are versatile compounds, two structural isomers (E and Z forms) are possible and they can co-ordinate to the metal either as a neutral ligand or as a

INTRODUCTION

Mercury is one of the oldest chemical elements used in human applications. It is a highly toxic metal that results in a variety of adverse neurological, renal, respiratory, immune, dermatological, reproductive and developmental disorders.¹ Its wide industry-related effects on human and animal biosystems have been well documented² and general exposure to this biologically-active chemical agent has been shown to be exacerbated through contaminated water and food.³

Inorganic mercury is widely used in certain types of batteries and continues to be an essential component of fluorescent light bulbs.⁴ Inorganic mercury is the most common form that is present in drinking water but is not considered to be very harmful to human health, in terms of the levels found in drinking water.⁵

The endocrine system is one of the three important integrating and regulatory systems in the human body. The other two are the nervous and immune systems. The major

deprotonated ligand through the N, S atoms. Thiosemicarbazones have been frequently employed for the quantitative determination of inorganic ions.¹⁸

Pyrazoles is a five-membered heterocyclic system.¹⁹ Many synthetic compounds containing pyrazole moiety are active in the field of medicinal chemistry.²⁰ One of the pyrazole derivatives, 4-aminoantipyrine has played an important role in inorganic chemistry; it forms stable complexes with many transition metal ions. 4-aminoantipyrine and its complexes have found applications in analytical, biological and clinical areas.^{21,22} Antipyrine derivatives are used as anti-inflammatory^{23,24} and chemotherapeutic agents.²⁵ 4-aminoantipyrine is an intermediate in the synthesis of antipyretic and analgesic drugs²⁶ and it is also active against a wide range of microorganisms viz *E.coli*, *Pseudomonas aeruginosa*, *Staphylococcus aureus* and *Candida albicans*.

The target of this work is to synthesis and characterization of new mercury complexes of thiosemicarbazones and antipyrine ligands. The potential protective effects of the synthesized compounds against mercury disruption of male sex hormones in rats were evaluated.

EXPERIMENTAL

All organic compounds and the solvents were purchased from Fluka or Merck (Nasr City, Egypt) and used without further purification.

Synthesis of ligands and Hg(II) complexes

Preparation and characterization of 2-phenyl-aminoacetyl-N-phenylhydrazine-carbothioamide (H_2L^1), 4-formylazohydrazoaniline antipyrine (H_2L^2) and [2-(2-(2,5-dihydro-2,3-dimethyl-1-phenyl-1H-pyrazol-4-yl-5-one)hydrazon)malononitrile] (HL^3) have been reported.²⁷⁻²⁹ The Hg(II) complexes of the ligands were prepared by adding stoichiometric amount of the Hg (II) chloride, sulphate and nitrate in EtOH to the ligands in EtOH in a 1:1 molar ratio. The reaction solution was stirred magnetically at 60°C for 5-9 h. The resulting solids were filtered off, washed several times with EtOH and dried under vacuum over P_4O_{10} .

Physical measurements

Elemental analysis (C, H and Cl) was performed at microanalytical unit of the Cairo University, Egypt. FT-IR measurements were performed (4000–400 cm^{-1}) in KBr with Neneus-Nicolidite-640-MSAFT-IR (Thermo-Electronics Co.) Spectrometer at the Central Lab., Minufiya University, Egypt. ¹HNMR spectra were recorded in DMSO- d_6 using 300 MHz Varian NMR spectrometer (Microanalytical Lab., Cairo University, Egypt). The molar conductivity measurements were made in DMF solution ($10^{-3}M$) using a Tacussel conductometer type CD6N. The electronic spectra were carried out as solution ($10^{-3}M$) in DMF using a Perkin-Elmer Lambda 4B spectrophotometer.

Thermal analysis (DTA/TG) were obtained out by using a Shimadzu DTA/TG-50 Thermal analyzer (Central Lab,

Minufiya University, Egypt) with a heating rate of 10°C min⁻¹ in nitrogen atmosphere with a following rate 20°C min⁻¹, in the temperature range 25 – 600°C using platinum crucibles.

Preparation of compounds and mercury-poisoned water

Newly synthesized derivatives of pyrimidine complexes were dissolved in DMSO to obtain the concentration of 1 mM. These stock solutions were stored at 4°C for further use.

To prepare a stock solution of 1000 ppm of mercury in drinking water, 1.35 g of HgCl₂ was dissolved in 1 litre of water. One milliliter of this solution was mixed with 10 litres of distilled water to obtain water containing mercury at a concentration of 1 ppm.

Animals grouping

Adult male albino rats, weighing about 160 ± 10 g, were housed at 23 ± 2°C and in daily dark/light cycle. They were caged in the animal house of College of Medicine, Qassim University and under standard condition and fed standard chow and water ad libitum.

All experiments were carried out in accordance with protocols approved by the local experimental animal ethics committee. After acclimatization, rats were divided into twelve groups each comprising of eight animals. Normal group (N) in which rats were maintained only on standard pellet diet and water ad libitum. HgCl₂-intoxicated drinking water group, in which, rats were maintained on drinking water intoxicated with 0.5 ppm of HgCl₂ for 30 days. The groups number 3 to 12 include animals co-treated with 0.5 ppm of HgCl₂-poisoned drinking water and 0.1mM of newly synthesized compounds for 30 days. During the course of the 30-day long experiment no animal was died.

Collection of blood and tissues' specimens

At the end of experiments, animals were sacrificed using a sharp razor blade. The blood was collected in prechilled heparinized centrifuge tubes. Plasma specimens were then obtained by centrifugation for 10 minutes at 4000 rpm at 4°C and were kept in clean well-stoppard vials at -20°C until assayed. The kidney and testes were removed and cut into pieces.

Preparation of testes and kidney homogenate

Kidney and testes homogenates were prepared by using a mechanical homogenizer (Potter-Elvehjem) in a 10-fold volume of ice-cold of 20 mM tris-HCl buffer (pH 7.4). The homogenate was centrifuged at 5000 rpm for 30 minutes at 4°C to remove cell debris and nuclei. The supernatant liquid was collected, aliquoted and kept frozen at -20°C for further investigations.

Determination of superoxide dismutase activity

Superoxide dismutase (SOD) activities in kidney and testes homogenates were estimated according to the procedure of Nishikimi et al.³⁰ and by following the manufacturer's procedure (Biodiagnostics, Egypt).

Table 1. Analytical and physical data for the ligands and Hg(II) complexes

No.	Complexes	Color	Yield (%)	Mol. Wt.	Found (Calc.) %					\square_M^a
					C	H	N	M	Cl	
1	[Hg(H ₂ L ¹)Cl ₂ (H ₂ O) ₂]. H ₂ O	Pale brown (60)	625.6	28.6 (28.8)	3.3(3.5)	8.9(9.0)	32.3(32.0)	11(11.3)	24	
2	[Hg(H ₂ L ¹)SO ₄ (H ₂ O)]	Pale yellow (65)	613.6	29.5 (29.3)	3.0(2.8)	9.2 (9.1)	32.8(32.6)	-	15	
3	[Hg(HL ¹) ₂]	Pale yellow (60)	798.6	45.0 (45.1)	3.9(3.8)	13.9(14.0)	25.2(25.1)	-	18	
4	[Hg ₂ (HL ²)(OH) ₂ Cl]	Yellow (70)	870.5	29.2 (29.0)	2.5(2.3)	11.4(11.3)	46.2(46.0)	4.2(4.1)	10	
5	[Hg(HL ²)(NO ₃)(H ₂ O)]	Brown (70)	680.6	37.2 (37.0)	3.0(3.0)	14.4(14.4)	29.7(29.5)	-	20	
6	[Hg(HL ³)(SO ₄)]	Yellow (70)	594.6	28.4 (28.5)	2.2(2.4)	14.3(14.1)	33.6(33.7)	-	Insol.	
7	[Hg(HL ³)(NO ₃) ₂]	Brown (60)	604.6	27.7 (27.8)	1.8(2.0)	14.2(13.9)	33.0(33.2)	-	18	

^a \square_M = molar conductivity ohm⁻¹ cm² mol⁻¹ in 10⁻³ M DMF

Table 2. Fundamental IR spectral bands (cm⁻¹) for the ligands and Hg(II) complexes

Compound	$\nu_{(O-H)}/\nu_{(N4-H)}$	$\nu_{(N1-H)}$	$\nu_{(N2-H)}$	$\nu_{(C=O)}^a$	$\nu_{(C=O)}^b$	$\nu_{(C=N)}^c / \nu_{(C=S)}^d$	$\nu_{(M-O)}$	$\nu_{(M-N)}$
H ₂ L ¹	3463	3340	3250	1677	-	747 ^d	-	-
[Hg(H ₂ L ¹)Cl ₂ (H ₂ O) ₂]. H ₂ O	3393	-	3100	1700	-	752 ^d	614	507
[Hg(H ₂ L ¹)SO ₄ (H ₂ O)]	3390	-	3100	1698	-	751 ^d	615	510
[Hg(HL ¹) ₂]	3402	-	3108	-	-	749 ^d	607	506
H ₂ L ²	3430	-	-	1645	1635	1536 ^c	-	-
[Hg ₂ (HL ²)(OH) ₂ Cl]	3435	-	-	-	1625	1552 ^c	593	536
Hg(HL ²)(NO ₃)(H ₂ O)	3438	-	-	-	1612	1534 ^c	640	454
HL ³	3410	-	-	-	1630	1587	640	477
[Hg(HL ³)(SO ₄)]	3434	-	-	-	1609	1496	574	443
Hg(HL ³)(NO ₃) ₂	3429	-	-	-	1607	1495	582	445

^a (C=O) of side chain, ^b (C=O) of pyrazolone ring, ^c (C=N), ^d (C=S)

Determination of catalase activity

Antioxidant enzyme catalase (CAT) activities in kidney and testes homogenates were determined according to the method of Bergmayer³¹ as described in the manufacturer's procedure (Biodiagnostics, Egypt).

Determination of lipid peroxidation level

The levels of lipid peroxides (LPO) in kidney and testes homogenates were estimated colorimetrically by measuring malondialdehyde (MDA) using the method of Ohkawa et al and by following the manufacturer's procedure (Biodiagnostics, Egypt).³²

Determination of testosterone level

Level of testosterone in testes homogenate was processed by using Fertigenix Testo-ELISA kit (Biosource, Belgium) in accordance with the protocol described by Park et al.³³

Determination of follicle-stimulating hormone level

Follicle stimulating hormone (FSH) concentration was estimated in testes homogenate with IMMULITE analyzer according to the method of Odell et al³⁴ using IMMULITE FSH kit purchased from EURO/DPC Ltd., USA.

Determination of leutinizing hormone level

Leutinizing hormone (LH) concentration was estimated in testes homogenate according to the method of Knobil³⁵ using LH kit purchased from Ameritek (USA) with Vmax ELISA reader

Determination of fructose level

Fructose concentration was estimated in testes homogenate spectrophotometrically according to the method of Karvonen and Malm.³⁶ Briefly, fructose in presence of hydrochloric acid forms a pink colored complex with indole-3-acetic acid. The complex has maximum absorbance at 500-530 nm.

Statistical analysis

Results are expressed as mean \pm S.D. The data for various biochemical parameters were analyzed using analysis of t-test and the group mean was compared by one-way ANOVA. Values were considered statistically significant at $P < 0.05$.

RESULTS AND DISCUSSION

Physical properties

The reaction of the ligands with Hg(II) chloride, sulphate and nitrate give complexes of general formulae $[\text{Hg}(\text{H}_2\text{L}^1)\text{Cl}_2(\text{H}_2\text{O})_2] \cdot \text{H}_2\text{O}$, $[\text{Hg}(\text{H}_2\text{L}^1)\text{SO}_4(\text{H}_2\text{O})]$, $[\text{Hg}(\text{HL}^1)_2]$, $[\text{Hg}_2(\text{HL}^2)(\text{OH})_2\text{Cl}]$, $[\text{Hg}(\text{HL}^2)(\text{NO}_3)(\text{H}_2\text{O})]$ and $[\text{Hg}(\text{HL}^3)\text{XY}]$, where X = SO_4 or NO_3 and Y = O or NO_3 (Table 1). While the reaction of H_2L^2 with Hg(II)sulphate and HL^3 with Hg(II)chloride produce decomposed products. All Hg(II) complexes are freely soluble in DMF and DMSO except complex (6), which is insoluble in DMF and DMSO. The molar conductivity of all Hg(II) complexes in DMF solution (10^{-3} M) at room temperature indicate that all complexes are non-electrolyte.³⁷

FT-IR For H_2L^1 ligand and Hg(II) complexes

The diagnostic IR bands for ligand 2-phenylaminoacetyl-N-phenylhydrazine-carbothioamide (H_2L^1) and Hg(II) complexes (1-3) are listed in Table 2. The most important four bands, exhibited by ligand (H_2L^1) at 3463 cm^{-1} , 3340 cm^{-1} , 1677 cm^{-1} and 747 cm^{-1} are assigned to $\nu(\text{N-H})$, $\nu(\text{N1-H})$, $\nu(\text{N2-H})$, and $\nu(\text{C=S})$ vibrations, respectively. The bands at 1500 cm^{-1} , 1440 cm^{-1} and 1280 cm^{-1} may be due to $\nu(\text{N-C=S})$.³⁸

The bands at 3100 cm^{-1} , $1700-1698\text{ cm}^{-1}$ and 752 cm^{-1} seen in the complexes (1) and (2) have been assigned to $\nu(\text{N2-H})$, $\nu(\text{C=O})$ and $\nu(\text{C=S})$ respectively. The IR spectrum of the complex (3) shows that bands due to $\nu(\text{C=O})$ and $\nu(\text{N2-H})$ disappear up on complexation and a new band appeared at 1600 cm^{-1} , which has been assigned to $\nu(\text{C=N})$.

For H_2L^2 , HL^3 and Hg(II) complexes (4-7) the IR data are presented in Table 2. The IR spectra of the free ligands (H_2L^2 and HL^3) show four bands at 3430 cm^{-1} , 3434 cm^{-1} , 2210 cm^{-1} , 2205 cm^{-1} , 1645 cm^{-1} , 1630 cm^{-1} ; and $1610-1587\text{ cm}^{-1}$, assigned to $\nu(\text{N-H})$, $\nu(\text{C}\equiv\text{N})$, $\nu(\text{C=O})$ of side chain, $\nu(\text{C=O})$ of pyrazolone ring and $\nu(\text{C=N})$ respectively. The infrared spectra of complexes (6 and 7) show a decrease in the energy of $\nu(\text{C=O})$ of side chain, $\nu(\text{C=O})$ of pyrazolone ring and $\nu(\text{C=N})$ up on complex formation, indicating that carbonyl oxygen of C=O of side chain, C=O of pyrazolone ring and C=N participate in coordination. While in complexes(4 and 5) the bands corresponding to $\nu(\text{C=O})$ of side chain and $\nu(\text{N-H})$ disappear indicating that the ligand is in enolimino form and new bands appears at 1552 cm^{-1} , 1537 cm^{-1} , assigned to $\nu(\text{C=N})$ up on complexation.

The IR spectra of all Hg(II) complexes show new two bands at $640-574\text{ cm}^{-1}$ and $536-443\text{ cm}^{-1}$, assigned to $\nu(\text{Hg-O})$ and $\nu(\text{Hg-N})$.^{39,40} However, complexes (1 and 4)

exhibit medium bands at 320 and 325 cm^{-1} due to $\nu(\text{Hg-Cl})$.⁴¹ Also in the complexes (2 and 6) strong band appears at $1110-1178\text{ cm}^{-1}$, assigned to unidentate sulphate moiety.⁴²

The IR spectra of complexes (5 and 7) show strong bands at $1379-1390\text{ cm}^{-1}$, assigned to monodentate of nitrate group. While complexes (1, 2, 4 and 5) reveal broad bands at $3390-3435\text{ cm}^{-1}$ and $765-878\text{ cm}^{-1}$ assigned to $\nu(\text{Hg-O})$ of coordinated water except in complex (4) only appears a band at 3435 cm^{-1} , assigned to coordination of Hg(II) with the hydroxy group.

Table 3. Electronic spectral bands of the Hg(II) complexes

No.	Complexes	λ_{max} nm
1	$[\text{Hg}(\text{H}_2\text{L}^1)\text{Cl}_2(\text{H}_2\text{O})_2] \cdot \text{H}_2\text{O}$	270
2	$[\text{Hg}(\text{H}_2\text{L}^1)\text{SO}_4(\text{H}_2\text{O})]$	268
3	$[[\text{Hg}(\text{HL}^1)_2]$	267
4	$[\text{Hg}_2(\text{HL}^2)(\text{OH})_2\text{Cl}]$	268, 402
5	$[\text{Hg}(\text{HL}^2)(\text{NO}_3)(\text{H}_2\text{O})]$	266, 401
6	$[\text{Hg}(\text{HL}^3)(\text{SO}_4)]$	268, 389
7	$[\text{Hg}(\text{HL}^3)(\text{NO}_3)_2]$	267, 387

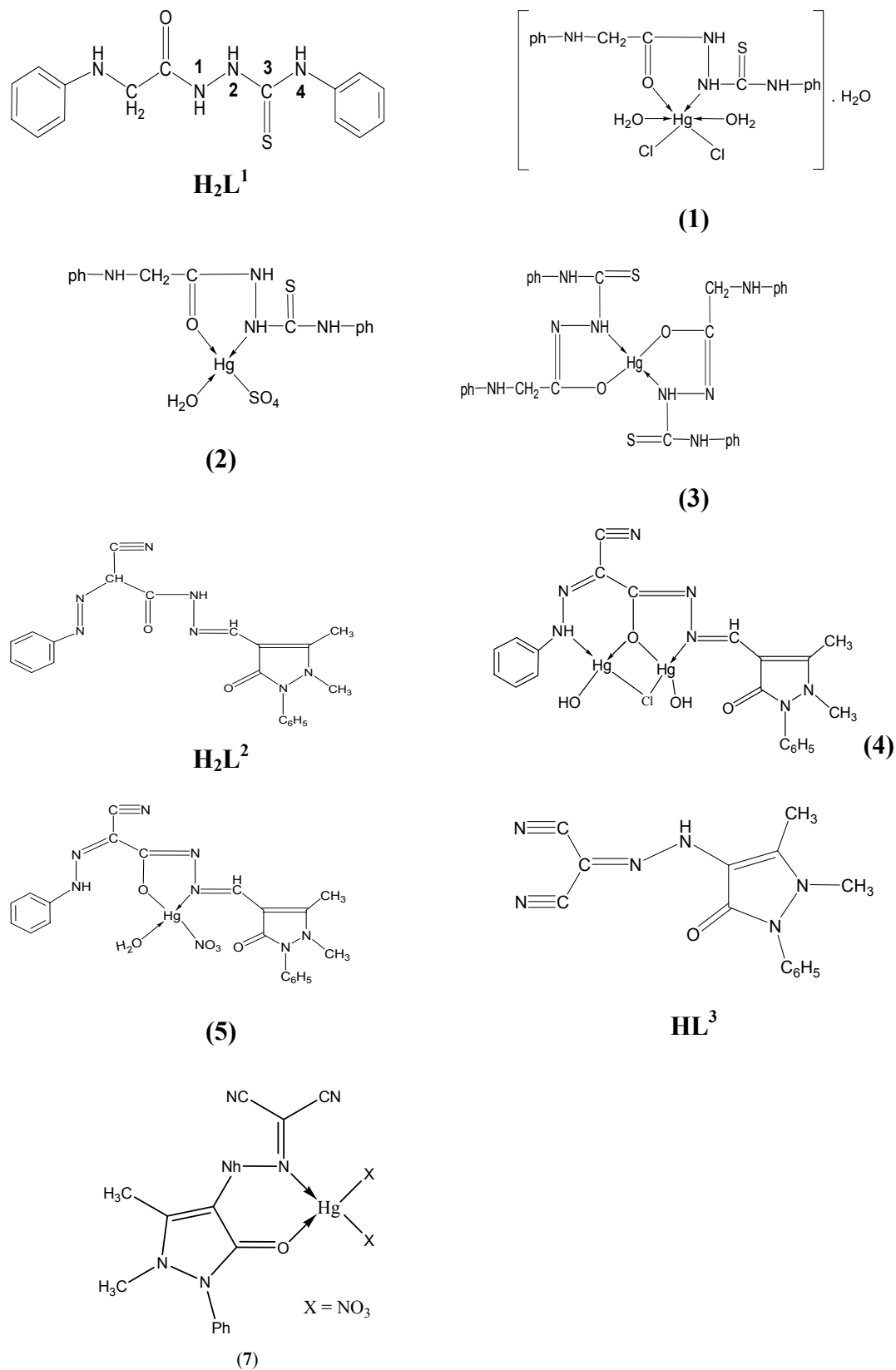
Electronic spectra

The data of electronic spectra of Hg(II) complexes (1-7) are given in Table 3. The absorption spectra of Hg(II) complexes were recorded in DMF solutions (10^{-3} M) in the range $190-800\text{ nm}$ using a quartz cuvette of 1 cm path length.

The complexes show only the charge transfer transitions which can be assigned to charge transfer from the ligand to the metal and these ions have the d^{10} configuration and therefore, their complexes should not exhibit any d-d transition. All of complexes of these Hg(II) ions were found to be diamagnetic.⁴³ The absorption bands of Hg(II) complexes observed listed in Table 3. Probable structures of the ligands and complexes are given in Scheme 1.

Thermal studies for Hg(II) complexes

Thermal analyses have been carried out using differential thermal analysis (DTA) and thermogravimetric analysis (TGA) techniques. The thermal behaviour carried out in temperature range $25-600^\circ\text{C}$. DTA and TGA curves recorded for the complexes in an atmosphere of nitrogen and important data are summarized in Table 4. The various steps of the decomposition of the compound with the corresponding mass loss in terms of the proposed formulas for the complexes are given. The Hg(II) complexes (1 and 5) show the three exothermic peaks each. While, complexes (2, 3 and 4) exhibit two broad exothermic and one endothermic DTA peaks.



Scheme 1. Chemical structure of ligands and their Hg(II) complexes

However, in Hg(II) complex (7) one strong exothermic DTA curve in temperature range 200-233°C appears, which has been assigned to loss of ((0.8L + 2HNO₃) and (2CO + 3C),⁴⁴ as shown from TG mass loss in that temperature range. The initial decomposition temperature has been used as an indicator of the thermal stability of the complexes. The results of the thermal analysis of the mercury complexes indicated that complex (3) is thermally more stable compared to the rest of mercury(II) complexes.

Evaluation of kidney function

Serum creatinine level is one of the traditional screening indices for kidney function and renal structure epithelium.⁴⁵ The effects of mercuric chloride on the biochemical tests of renal function in the animals are presented in table 5. After drinking water poisoned with 0.5 ppm of HgCl₂ for 30 days, a statistically significant increase of creatinine and urea concentrations in plasma was observed as compared with control groups. The elevation in creatinine level after exposure to inorganic mercury is accordance with the report of Oriquat et al. in rats.⁴⁶ The rise in creatinine level might be due to damage caused to kidney tubules by inorganic mercury. Co-treatment with different ligands and their complexes caused amelioration on renal function. Results showed that ligands H₂L¹, H₂L² and HL³ and their complexes, except complex (4), significantly reduced (P<0.05) the elevated renal function markers.

Evaluation of oxidative status

The level of malodialdehyde (MDA) is widely used as a marker of free radical mediated lipid peroxidation (LPO). The results of the LPO assays in the kidney and testes homogenates are shown in Table 6. LPO level increased significantly in the kidney and testes homogenates of rats after exposure to 0.5 ppm of mercury for 30 days as

compared to the normal group. The mercuric chloride toxic effect is due to its ability to adhere or to form link with cell enzymes of the respiratory chain and proteins, which alter the metabolism of target cells in organs participating in its elimination. Mercury also provokes a reactive oxygen species (ROS)-dependent vascular damage producing large scale haemorrhage in many organs like kidney. This ROS was significantly reduced when animals were supplemented with various ligands and their complexes showing the ameliorative effects of these compounds.

Results shown in Table 6 revealed that ligands H₂L¹, H₂L² and HL³ significantly reduced the elevated levels of LPO in testes and kidney tissues showing their ability to scavenge free radicals. Meanwhile, their complexes exhibited varied effects on LPO in testes and kidney, where complexes (3, 6 and 7) showed no antioxidative activities as compared to HgCl₂- treated group.

Oxidative stress defines an imbalance between the formation of ROS and antioxidative defence mechanisms. Drinking of HgCl₂-poisoned water for 30 days generated the ROS and caused oxidative stress in intoxicated animals. In oxidative stress, LPO is occurred due to excessive free radical production and is considered a primary mechanism of cell membrane destruction and cell damage. Malondialdehyde (MDA) is the end product of lipid peroxidation.

The toxicity with inorganic mercury increased the testicular MDA and simultaneously decreased the CAT and SOD activities in this study. CAT and SOD were estimated in the kidney and testes homogenates. Results showed that administration of 0.5 ppm of HgCl₂ in drinking water for 30 days significantly decreased the activities of CAT and SOD as compared to those of the normal control group (Table 6).

Table 4. Thermal data of Hg(II) complexes

No.	Complex	DTA ^o C	TGA ^o C	Mass loss %Cal. (F.)	Leaving species
1	[Hg(H ₂ L ¹)Cl ₂ (H ₂ O) ₂]. H ₂ O	97- 201	87 -173	2.8(2.9)	-H ₂ O
		288- 337	193-272	11.5(11.3)	-(2H ₂ O +HCl)
		338-447	294-355	17.8(18.0)	-(HCl+0.25L)
			405- 468	17.0(17.2)	-(C ₆ H ₅ NHCH ₂)
2	[Hg(H ₂ L ¹)SO ₄ (H ₂ O)]	130-180	111- 165	2.9(2.7)	-H ₂ O
		227-274	188-335	39.8(40.3)	-(0.6L+SO ₂)
		293 -329	394-424	9.1(9.5)	-2CO
3	[Hg(HL ¹) ₂]	210-257	111 -117	3.6(3.3)	-(CH ₂ NH)
		413 -450	200-289	14.9 (14.8)	-(C ₆ H ₅ +C ₂ H ₂ O)
		505 -550	340-411	13.3 (13.5)	(C ₆ H ₅ NHCH ₂)
			459-509	14.8 (14.4)	(C ₆ H ₅ NH+ C ₂ H ₂)
4	[Hg ₂ (HL ²)(OH) ₂ Cl]	229- 256	176 -247	16.9(17.0)	(2OH + HCl + C ₆ H ₅)
		280-322	263- 335	50.6(50.3)	(0.6L+Hg)
		504-550	Above 335		Thermal stability
5	Hg(HL ²)(NO ₃)(H ₂ O)	232-271	192-280	18.1 (18.4)	(H ₂ O+
		301- 335	297 -379	40.8 (40.4)	HNO ₃ +C ₂ H ₂ O)
		370-408	Above 379		-(0.5L +C ₆ H ₅)
7	Hg(HL ³)(NO ₃) ₂	200-238	170-238	57.9 (57.7)	- (0.8L+2HNO ₃)
			344 -410	13.9 (13.6)	- (3CO)

On the other hand, rats that were supplemented with ligands and their complexes together with HgCl₂ for 30 days experienced significant increase in CAT and SOD activities when compared to the HgCl₂-treated group. Ligands H₂L¹, H₂L² and HL³ exhibited higher stimulatory effect on the activities of CAT and SOD in testes and kidney tissues as compared to their complexes.

Table 5. Effect of different ligands and their Hg complexes on renal function parameters

Group	Creatinine (mg dL ⁻¹)	BUN (mg dL ⁻¹)
Normal	0.7±0.1	10.4±1.0
HgCl ₂	2.9±1.4	20.8±2.8
HgCl ₂ + H ₂ L ¹	1.6±0.5*	11.0±0.9*
HgCl ₂ + 1	1.9±0.3*	17.6±2.1*
HgCl ₂ + 2	1.3±0.5*	15.2±4.4*
HgCl ₂ + 3	2.1±0.6*	21.8±1.9
HgCl ₂ + H ₂ L ²	0.8±0.2*	11.7±3.1*
HgCl ₂ + 4	2.1±0.6	26.0±5.7
HgCl ₂ + 5	1.7±0.3*	16.8±1.9*
HgCl ₂ + HL ³	0.8±0.3*	10.8±2.8*
HgCl ₂ + 6	1.5±0.4*	15.0±3.8*
HgCl ₂ + 7	2.3±0.9	20.2±2.4

These complexes showed diverse antioxidant actions on the activities of CAT and SOD, where, complexes (3, 6 and 7) did not show ameliorative actions on the activities of CAT and SOD.

Evaluation of some male sex hormones

The mean values of the serum hormones; testosterone, luteinizing hormone (LH) and follicle stimulating hormone (FSH) are shown in Table 7. Results showed that after drinking of 0.5 ppm of HgCl₂-poisoned water for 30 days led to significant decreases ($P < 0.05$) in the levels of testosterone, LH and FSH as compared to the control group. The levels of male sex hormones were restored to control

Table 6. Effect of different ligands and their Hg complexes on the oxidative status in kidney and testes

Group	CAT U g tissue ⁻¹		SOD U g tissue ⁻¹		LPO nmol g tissue ⁻¹	
	Kidney	Testes	Kidney	Testes	Kidney	Testes
Normal	3.5±0.6	5.9±0.7	122.5±11.4	155.2±13.8	135.3±16.7	152.2±9.1
HgCl ₂	1.1±0.3	1.3±0.5	76.8±8.3	92.8±11.1	230.8±23.9*	252.8±16.5
HgCl ₂ + H ₂ L ¹	3.1±0.8*	6.1±0.5*	121.6±10.3*	151.6±12.2*	142.5±21.8*	150.0±12.1*
HgCl ₂ + 1	2.9±0.5*	5.9±0.4*	115.6±9.4*	155.6±10.2*	134.3±13.9*	150.2±21.9*
HgCl ₂ + 2	2.2±0.8*	4.2±0.2*	116.6±12.3*	156.6±15.5*	133.2±14.2*	154.2±4.5*
HgCl ₂ + 3	1.5±1.1	1.8±0.8	72.6±7.7	92.1±9.8	225.0±21.3	248.6±24.5
HgCl ₂ + H ₂ L ²	3.2±0.7*	6.2±0.5*	117.8±10.3*	137.8±11.5*	152.6±15.3*	151.2±14.0*
HgCl ₂ + 4	2.2±0.8*	5.2±0.3*	108.0±13.1*	121.0±15.0*	159.2±14.2*	159.4±13.5
HgCl ₂ + 5	2.1±0.6*	5.1±0.2*	118.4±9.6*	133.4±8.8*	152.6±15.3*	165.7±16.3*
HgCl ₂ + HL ³	4.2±1.4*	6.2±0.4*	119.6±7.7*	159.6±11.8*	142.6±15.3*	153.2±12.4*
HgCl ₂ + 6	1.1±0.3	2.1±0.2	63.2±9.8	83.2±10.8	222.6±18.9	245.6±10.1
HgCl ₂ + 7	0.9±0.1	1.5±0.3	62.5±5.5	92.5±9.9	220.6±17.9	253.3±11.0

values after combination of HgCl₂ with studied ligands and some of their complexes. The tested complexes showed varied effects on the level of male sex hormones. In contrast to their complexes, ligands exhibited potent stimulatory actions on the levels of testosterone, LH and FSH.

Testosterone is essential for spermatogenesis completion because it stimulates the conversion of round spermatids into elongated spermatids between stages VII and VIII of the spermatogenic cycle. Thus, testicular testosterone deficiency as observed in this study after exposure to HgCl₂ for 30 days will impair the spermiation process.⁴⁷

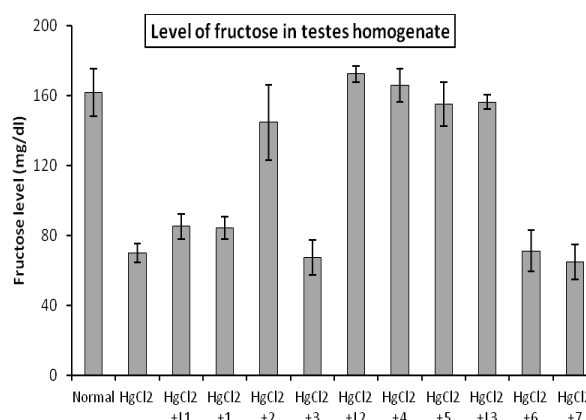


Figure 1. Effect of HgCl₂ and tested compounds on the levels of testicular fructose

Fructose provides energy for sperm motility.⁴⁸ As shown in Figure 1, level of fructose is significantly reduced ($P < 0.05$) in rats after exposure to Hg-intoxicated water for 30 days as compared to that of the control group. Different effects of tested ligands and their complexes on the level of testicular fructose were observed. Results indicate that tested ligands restored the fructose levels to that of the normal animals, while, some complexes did not ameliorate the fructose levels.

Table 7. Levels of testosterone, luteinizing hormone and follicle-stimulating hormone in testes of animals of different studied groups

Groups	Testosterone (ng g ⁻¹)	LH (ng g ⁻¹)	FSH (ng g ⁻¹)
Normal	121.8±2.2	47.2±2.6	34.7±1.5
HgCl ₂	85.6±8.6	20.2±1.9	15.7±1.5
HgCl ₂ + H ₂ L ¹	103.0±5.7*	34.8±7.4*	23.7±1.5*
HgCl ₂ + 1	93.4±9.4*	24.8±0.8	25.3±2.1
HgCl ₂ + 2	102.2±4.5*	20.6±2.4	30.7±4.0*
HgCl ₂ + 3	74.2±10.3	19.8±3.8	17.3±5.0
HgCl ₂ + H ₂ L ²	99.2±7.9*	37.6±6.3*	29.3±1.5*
HgCl ₂ + 4	85.2±9.4	45.2±2.4*	21.3±0.6*
HgCl ₂ + 5	101.4±3.2*	16.4±3.2	32.7±1.5*
HgCl ₂ + HL ³	126.8±4.4*	41.6±2.1*	30.3±2.1*
HgCl ₂ + 6	89.2±3.0	23.2±4.0	13.7±3.2
HgCl ₂ + 7	77.8±9.1	19.6±5.3	15.3±1.5

CONCLUSION

In our study, we characterized mercury(II) complexes of ligands (2-phenylaminoacetyl-N-phenylhydrazine carbothioamide (H₂L¹), 4-formylazohydrazoneanilinoantipyrine (H₂L²) and [2-(2-(2,5-dihydro-2,3-dimethyl-1-phenyl-1H-pyrazol-4-yl-5-one)hydrazono)malononitrile] (HL³) using different analytical and spectroscopic methods. The IR spectral show that the ligand of complexes (2) and (5) behave as mono basic bidentate, coordination take place by (C-O) and N(2)H or (C=N). While the ligand of complexes (1, 6 and 7) behave as neutral bidentate and coordination via (C=O) and N(2)H or (C=N) groups. On the other hand, the ligand for complexes (3 and 4) produce mono, dibasic tetradentate and chloro bridge of binuclear complex (4). All complexes are tetrahedral geometry except complex (1) is octahedral geometry and diamagnetic of d¹⁰ of Hg(II) ions. The thermal behavior study showed that complex (3) is more stable as compared of the rest of Hg(II) complexes.

Further it has been shown that mercury causes severe toxic tissue damage in the testis and kidney of rats. This damage may be caused by the ROS produced by mercury within the animals' body. The tested ligands and some of their Hg complexes showed varied effects against mercury toxicity. They interacted with mercury ions, neutralize them and prevent the ROS mediated oxidative damage in testes.

ACKNOWLEDGMENT

The authors would like to thank the Scientific Research Deanship, Qassim University, Saudi Arabia, for financial support of this research project (SR-S-14-16 Sabc).

REFERENCES

¹Risher, J. F., Amler, S. N., *Neurotoxicol.*, **2005**, 26(4), 691–699.

²Sameha, M., Mohamed, L. T., Abdelkader, O., Nadia, B., Bruno, B., Abdelkrim, T., Abdelmadjid, B., *J. Cell Anim. Biol.*, **2009**, 3(12), 222-230.

³Magos, L., Clarkson, T. W., *J. Ann. Clin. Biochem.*, **2006**, 3, 257-268.

⁴Clarkson, T. W., *Crit. Rev. Clin. Lab. Sci.*, **1997**, 34, 369–403.

⁵Dilek, D., Suna, K., Fatma G. U., Filiz, D., Yusuf, K., *Afr. J. Biotechnol.*, **2010**, 9(4), 488-495.

⁶Brandão, R., Santos, F. W., Zeni, G., Rocha, J. B., Nogueira, C. W., *Biomaterials*, **2006**, 19(4), 389-98.

⁷Parekh, A. K., Desai, K. K., *Indian J. Chem.*, **2006**, 45B, 1072.

⁸Chandra S., Gupta L.K., *Spectrochimica Acta Part A*, **2005**, 62, 1089.

⁹Demertzi, D. K., Miller, J. R., Kourkoumelis, N., Hadzikakaou, S. K., Demertzis, M. A., *Polyhedron*, **1999**, 18, 1005.

¹⁰Ferrari, B. M., Fava, G. G., Leperti, E., Pelosi, G., Rossi, R., Tarasconi, P., Albertini, R., Bonati, A., Lunghi, P., Pinelli, S., *J. Inorg. Biochem.*, **1998**, 70, 145.

¹¹Ferrari, M. B., Capacchi, S., Reffo, G., Aelosi, G., Tarasconi, P., Albertini, R., Pinellis, S., Lunghi, P., *J. Inorg. Biochem.*, **2000**, 81, 89.

¹²Sandeep, K., Nitin, K., *Inter. J. Res. Pharm. Biomed. Sci.*, **2013**, 4(1), 305-3011.

¹³Lobana, T. S., Butcher, R. J., Castineiras, A., Bermejo, E., Bharatam, P. V., *J. Inorg. Chem.*, **2006**, 45, 1535.

¹⁴Sharma, S., Athar, F., Maurya, M. R., Azam, A., *Eur. J. Med. Chem.*, **2005**, 40, 1414.

¹⁵Greenbaum, D. C., Mackey, Z., Hansell, E., Doyle, P., Gut, J., Caffrey, C. R., Lehrman, J., Rosenthal, P. J., McKerrow, J. H., Chibale, K., *J. Med. Chem.*, **2004**, 47(12), 3212-9.

¹⁶Lukmantara, A. Y., Kalinowski, D. S., Kumar, N., Richardson, D. R., *Org. Biomol. Chem.*, **2013**, 11(37), 6414-25.

¹⁷Jansson, P. J., Sharpe, P. C., Bernhardt, P. V., Richardson, D. R., *J. Med. Chem.*, **2010**, 53(15), 5759-69.

¹⁸West, D. X., Brain, G. A., Jasinski, J. P., Li, Y., Pozdniakiv, R. Y., Martinez, J. V., Toscano, R. A., Ortega, S. H., *Polyhedron*, **1996**, 15, 665.

¹⁹Acheson, R. M., *An Introduction to Heterocyclic Compounds*, 3rd Edn., John Wiley and Sons, New York, **2009**, 354-364.

²⁰Bansal R. K., *Heterocyclic Chemistry*, 4th Edn., New Age International Publisher, New Delhi, **2010**, 454.

²¹Raman, N., Dhavethuraja, J., Sakthivel, A., *J. Chem. Sci.*, **2007**, 119(4), 303-310.

²²Raman, N., Sakthivel, A., Rajasekaran, K., *J. Mycol.*, **2007**, 35(3), 150-153.

²³Anupama, B., Padmaja, M., Gyana Kumari, C., *E-J. Chem.*, **2012**, 9(1), 389-400.

²⁴Yue, T., Hao, Z., Rutao, L., *J. Mol. Biosyst.*, **2011**, 7(1), 3157-3163.

²⁵Himaja, M., Anish, K. V., Raman, M. A., Karigar, A. A., *J. Pharm. Sci. Innov.*, **2012**, 1(1), 67-70.

²⁶Elemike, E. E., Oviawe, A. P., Otuokere, I. E., *Res. J. Chem. Sci.*, **2011**, 1(8), 6-11.

²⁷Morsy, A. S., Kashar, T., Samar, A., *J. Solid State Sci.*, **2011**, 13, 2080

²⁸El-Sayed, F. A., Ayad, M. I., Issa, R. M., Aly, S. A., *Pol. J. Chem.*, **2000**, 75, 919.

²⁹El-Sayed, F. A., Ayad, M. I., Issa, R. M., Aly, S. A., *Pol. J. Chem.*, **2001**, 75, 773.

³⁰Niskikimi, M., Roa, N.A., Yagi, K., *J. Biophys. Res. Commun.*, **1972**, 46, 849-854.

³¹Bergmayer, H. V., *Methods of Enzymatic Analysis*, 3rd ed., Varly Chem. Weheim, **1983**, 1, 210.

- ³²Ohkawa, H., Wakatsuki, Kaneda, C., *J. Anal. Biochem.*, **1982**, 95, 351–358.
- ³³Park, T. J., Song, K. Y., Sohn, S. H., Lim, I. K., *J. Mol. Carcinog.*, **2002**, 34(3), 151-63.
- ³⁴Odell, W. D., Parlow, A. F., Cargille, C. M., Ross, G. T., *J. Clin. Invest.*, **1968**, 47(12), 2551-2562.
- ³⁵Knobil, E., *Recent Prog. Horm. Res.*, **1980**, 36, 53-88.
- ³⁶Karvonen, M. J., Malm, M., *J. Clin. Lab. Invest.*, **1955**, 7(4), 305.
- ³⁷Hamid G., Maryam, R., *J. Curr. Chem. Lett.*, **2013**, 2, 207.
- ³⁸Rao, C. N., Enkataraghavan, R. V., *Spectrochim. Acta Part A*, **1962**, 18, 541.
- ³⁹Prakash, D., Kumar, C., Prakash, S., Gupta, A. K., Singh, K. R., *J. Indian Chem. Soc.*, **2009**, 86(12), 1257–1261.
- ⁴⁰Raman, N., Esthar, S., Thangaraja, C., *J. Chem. Sci.*, **2004**, 116(4), 209.
- ⁴¹Nakamoto, K., *Infrared Spectra of Inorganic and Coordination Compounds*, 2nd Ed., Wiley Interscience, New York, **1970**.
- ⁴²Nakamoto, K., *Infrared and Raman Spectra of Inorganic and Coordination Compounds*; Wiley Interscience, New York, **1978**.
- ⁴³Ahmed, M., Khalid, W. Y., Zain, A., *J. Pharma. Biol. Sci.*, **2012**, 4, 09
- ⁴⁴El-Boraey, H. A., Serag, A. A., *Spectrochim Acta A*, **2014**, 132, 663–671.
- ⁴⁵Sheikh, T. J., Patel, B. J., Joshi, D. V., Patel, R. B., Jegoda, M. D., *J. Vet. World*, **2013**, 6(8), 563-567.
- ⁴⁶Oriquat, G. A., Saleem, T. H., Naik, R. R., Moussa, S. Z., Al-Gindy, R. M., *Jordan J. Biol. Sci.*, **2012**, 5(2), 141-146.
- ⁴⁷Arikawe, A. P., Oyerinde, A., Olatunji-Bello, I., Obika, L. O., *Niger. J. Physiol. Sci.*, **2012**, 27, 171 – 179.
- ⁴⁸Elzanaty, S., Richthoff, J., Malm, J., Giwereman, A., *Hum. Reprod.*, **2002**, 17(11), 2904 – 2911.

Received: 22.10.2016.

Accepted: 14.11.2016.



ANTIMICROBIAL POTENTIAL OF THIOPHENE DERIVATIVES OF SYNTHETIC ORIGIN: A REVIEW

Raghav Mishra^{[a]*}, Pramod Kumar Sharma^[a], Prabhakar Verma^[b]
and Isha Mishra^[c]

Keywords: Thiophene, thienopyrimidine, antibacterial, antifungal, antitubercular, minimum inhibitory concentration.

Thiophene, a five membered heterocycle is considered as biologically important dynamic scaffold that holds wide range of biological activities. The fruitful application of Cephoxitin as antimicrobial, Thenaldine as anti inflammatory, Ralitrexed as anticancer and Erdosteine as antioxidant proved the potential of thiophene moiety. Diverse biological response profile has pulled in consideration of many researchers to investigate this heterocycle to its multiple potential against several activities. This review is complementary to previous reviews and focuses to review the work reported on antimicrobial activities of thiophene derivatives.

* Corresponding Authors

Phone: +919808632494

E-Mail: raghav.mishra92@gmail.com

[a] Department of Pharmacy, School of Medical and Allied Sciences, Galgotias University, Greater Noida, U. P., 201306, India

[b] Department of Pharmaceutical Sciences, Maharishi Dayanand University, Rohtak, Haryana, 124001, India

[c] IIMT College of Pharmacy, Greater Noida, U. P., 201306, India

Introduction

As the world's population increases, the health problems expand accordingly and therefore the development of new therapeutics is essentially vital.¹ A steady increase in complexity of the structure and introduction of different molecular functions has been a highlighted feature of pharmaceutical research and development.² Even today only limited repertoires of synthetic transformations are utilized for the construction of simple structures of drug molecules.

As far as antimicrobial activity is concerned, antibiotics were considered as miracle drugs when first became available about 60 years ago, proving to be the major asset in the fight against infectious bacteria.³ Resistance to antibiotics threatens the effectiveness of successful treatment of infection.

Design of new drug molecules arguably offers some of the greatest hopes for success in present and future era. Five membered aromatic rings are the building blocks of many drugs. Amongst the five membered aromatic rings, thiophene has proven to be an alternative isostere, resulting in improved effectiveness of drug molecules. For structures like phenyl, thiophene can serve as biostere which can result in improved pharmacokinetic and pharmacodynamic properties of the drug.⁴

Thiophene comprises of a five membered ring with a sulfur as heteroatom having a molecular formula C₄H₄S. The thiophene ring has been incorporated into a broad range

of known biologically active compounds. It is incorporated as a substituent group or as a substitute of another ring that inspired researchers to synthesize several compounds containing this moiety. Well defined antimicrobial agents bearing thiophene moiety (Figure 1) are cefoxitin (**1a**), cephalothin (**1b**), cephaloridine (**1c**) and temocillin (**1d**).⁵

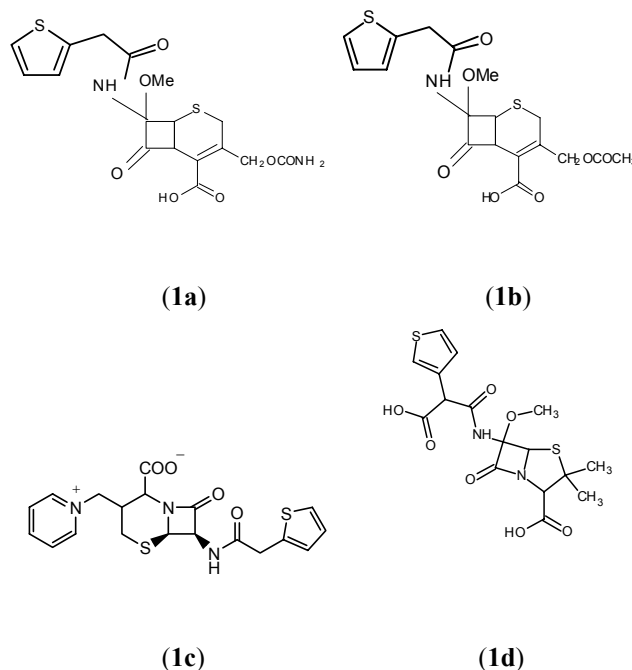


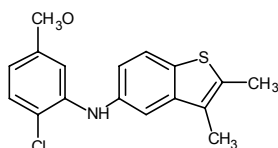
Figure 1. Some antimicrobial agents bearing thiophene moiety.

There are several reports in the literature describing the thiophene derivatives for their antimicrobial activities. The aim of present review is to give emphasis on antimicrobial properties associated with substituted thiophenes and structurally related thiophenes.

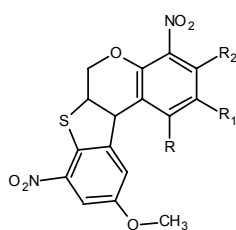
Antimicrobial activity of thiophenes

ortho-Chlorodiarylamines were synthesized from 2,3,7-trimethylbenzo[*b*]thiophene series by Queiroz *et al.*⁶ Cyclisation of these coupling products gave thienocarbazoles and dechlorinated diary amines, which were then evaluated and compared for antimicrobial activity using Ampicillin and Cycloheximide as standard. Compound (2) with methoxy group as a substituent was found active against *E. coli*. The thienocarboline showed lower Minimum Inhibitory Concentration (MICs) for *B. cereus* and *C. albicans* than the corresponding thiocarbazole but for *B. subtilis* both showed the same MIC.⁶

Derivatives of 10-methoxy-4,8-dinitro-6*H*-benzothieno[2,3-*c*]chromen-6-one were reported by Havaladar *et al.* All the synthesized compounds were evaluated for antibacterial activity against *S. aureus*, *B. subtilis*, *E. coli* and *S. typhosa*. The tested compounds (3) exhibited much higher inhibitory effect on the growth of bacteria.⁷



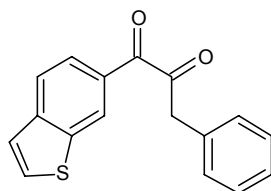
(2)



(3)

R= H, CH₃, OCH₃, Cl; R₁= H, NO₂, CH₃, OCH₃, Cl;
R₂= H, CH₃, Cl

Maurya *et al.* synthesized 4-hydroxy-1-methylindole and benzo[*b*]thiophene-4-ol based unnatural flavanoids as a new class of antimicrobial agents. The majority of the compounds exhibited good antifungal activity against *Trichophyton mentagrophytes*.⁸ It was found that substitution of heterocyclic oxygen by sulfur had produced a marked increase in antifungal activity. Compound (4) exhibited comparable MIC to the known Karanjin.

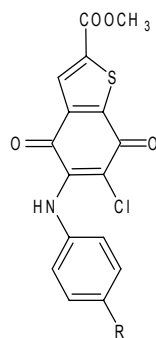


(4)

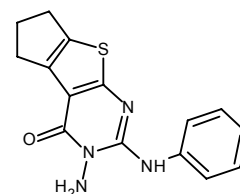
Ryu *et al.* reported synthesis of 5-arylamino-4,7-dioxobenzo[*b*]thiophene derivatives and tested for *in vitro* antifungal activity against *Candida* and *Aspergillus* species. Among the synthesized derivatives, 5-(4-

substitutedphenylamino)-6-chloro-2-(methoxycarbonyl)-4,7-dioxobenzo[*b*]thiophenes (5) exhibited more potent antifungal activity. The 6-chloro moiety had contributed to their antifungal activity significantly.⁹

A series of 2-substituted-amino-3-aminocyclopenteno or cyclohexeno[*b*]thieno[2,3-*d*]-3,4-dihydropyridin-4-ones was synthesized by Sherbeny *et al.* The synthesized derivatives were screened for antimicrobial, antiviral and anticancer activity. Some of the compounds showed promising activity. Compound (6) presented remarkable broad spectrum potency against *Pseudomonas aeruginosa*, *Staphylococcus aureus*, *Bacillus subtilis* and *Candida albicans*.¹⁰

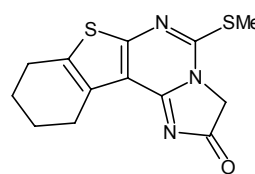


(5)

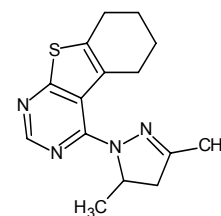


(6)

Bhuiyan *et al.* synthesized various derivatives by treatment of hydrazinothieno[2,3-*d*]pyrimidine with acetyl acetone, benzaldehyde and acetic anhydride. These derivatives were screened for antibacterial and antifungal activity using disc diffusion method and poisoned food techniques. Some of these derivatives showed marked antimicrobial activity. The structure activity relationship study (SAR) depicted that fused pyrimidine containing imidazo (7) and pyrazolo (8) rings showed higher antimicrobial and antifungal activity.¹¹



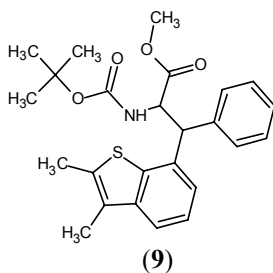
(7)



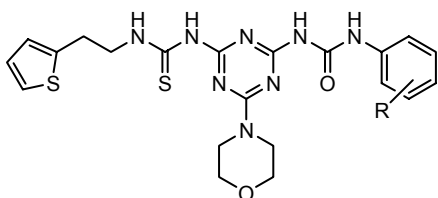
(8)

Ferreira *et al.* reported synthesis of pure stereoisomers of benzo[*b*]thienyl dehydrophenylalanines by Suzuki cross-coupling reaction and evaluation of their antimicrobial activity. It was concluded that the *Z*-isomer (9) was selective and very much active at very low MIC against Gram-positive bacteria: *B. cereus* and *B. subtilis*. Compounds were also active against *Candida albicans* presenting similar MICs.¹²

A new series of aliphatic thiourea derivatives containing S-triazine moiety was synthesized by Chikhalia *et al.* and tested *in vitro* antibacterial activity against different microorganisms using Tetracycline and Chloramphenicol as standard drugs. Some of the synthesized derivatives were tested for antifungal activity using Miconazole as standard drug. Incorporation of ureido linkage showed moderate to good activity. Structural variation such as methyl and halogen group at the *ortho*, *meta* or *para* positions (**10**) to ureido linkage resulted in enhanced antibacterial activity against all the tested microorganisms.¹³



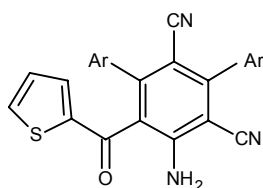
(9)



R= H, 4-Cl, 3-Cl, 2-CH₃, 3-NO₂

(10)

Darwish *et al.* synthesized thiophene and aniline derivatives (**11**) by the reaction of 2-picolinium N-ylide with arylidene derivatives of cyanothioacetamide and malanonitrile. All compounds displayed moderate activity against bacterial species *E.coli* and *S.albus*. Ampicillin and tetracycline were used as references to evaluate the potency of tested compounds.¹⁴

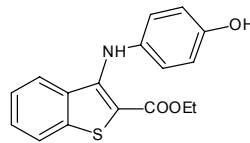


(11)

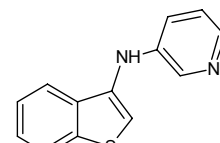
Ar = phenyl,
2-thienyl or
2-furyl

Antifungal activity of diarylamine derivatives of benzo(*b*)thiophene was determined against *Candida*, *Aspergillus* and dermatophyte species employing broth macrodilution test methods by Pinto *et al.* Most active compounds exhibited a broad spectrum activity against all tested fungal strains with particularly low MIC for dermatophyte. It was observed that hydroxyl group is essential for activity in aryl derivatives (**12**). The spectrum of activity in pyridine derivatives was broadened by the absence of ester group on position-2 of benzo[*b*]thiophene system (**13**).¹⁵

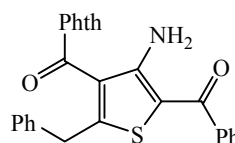
Gouda *et al.* synthesized thiocarbonyl and thioamide derivatives which were utilized as key intermediates for the synthesis of new derivatives of thiazole and thiophene. All the synthesized derivatives were examined for antibacterial activity using ampicillin and chloramphenicol as a standard. Incorporation of phthalazine moiety to thiophene (**14**) resulted in substantial activity against *E.coli* and *B. theringiensis*.¹⁶



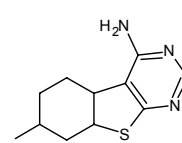
(12)



(13)

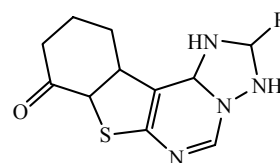


(14)



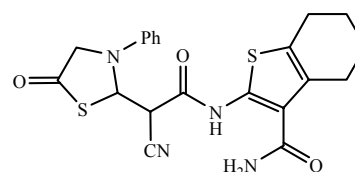
(15)

Khazi *et al.*, by employing Gewald reaction, synthesized tricyclic thienopyrimidines and triazole fused tetracyclicthienopyrimidines and screened them for antimicrobial activity. It was found that tricyclic aminothienopyrimidines (**15**) and tetracyclic triazole fused thienopyrimidine (**16**) exhibited promising antibacterial activity against *B. subtilis*. Some compounds also displayed better antifungal activity against *C. albicans* comparable to the standard fluconazole.¹⁷



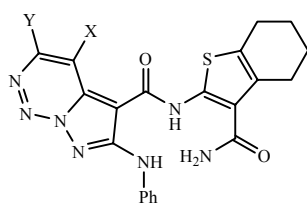
(16)

Gouda *et al.* synthesized thiazole and pyrazole derivatives using 4,5,6,7-tetrahydrobenzothiophene moiety as a base. The synthesized derivatives were evaluated for antimicrobial activity *in vitro*. As an indicator for the activity of the compounds, zone of inhibition was measured and Ampicillin was taken as reference. Most of the synthesized compounds evinced good to moderate antibacterial and antifungal activity. Incorporation of benzothiophene nucleus to thiazole (**17**) or pyrazole (**18**) moieties resulted in remarkable activity against *B. theringiensis*, *K. pneumoniae*, *B. fabae* and *F. oxysporum*.¹⁸



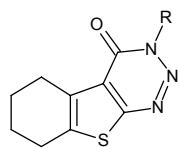
(17)

Antimicrobial activity of series of substituted amino-4,5-tetramethylenethieno[2,3-*d*][1,2,3]-triazine-4(3*H*)-ones was reported by Saravanan *et al.* Compounds with lipophilic groups like chlorophenyl and fluorophenyl groups (**19**) exhibited appreciable antimicrobial activities while substituting with electron donating groups like methyl, ethyl were found less active against all the microbes used.¹⁹



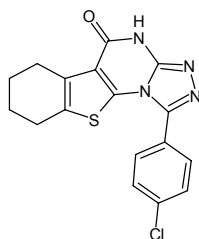
X = NH₂, CH₃; Y = CN, COCH₃

(18)



R = 4-ClC₆H₄, 4-FC₆H₄

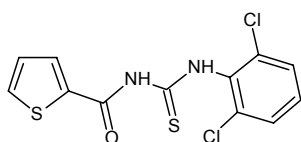
(19)



(20)

Taisan *et al.* synthesized a series of new thienopyrimidin-4-one(thione) derivatives and evaluated their antimicrobial activity against *S. aureus*, *K. monas*, *P. aeruginosa* and *E. coli* employing Vancomycin and Cefazime as standard. Compound (**20**) showed promising antimicrobial activity.²⁰

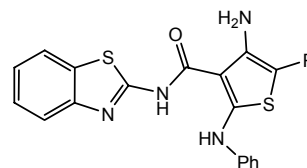
Badiceanu *et al.* prepared new thioureides of 2-thiophene carboxylic acid and evaluated them for antibacterial and antifungal activity. *In vitro* antimicrobial activity assay showed that these derivatives presented significant antimicrobial activity with MIC ranging from 7.8 μg/ml to 500 μg/ml. The majority of the tested compounds showed a broad spectrum of antimicrobial activity at low concentration on Gram-positive, Gram-negative bacteria and fungal strains. Because of the contribution of electron withdrawing group, most effective compound was (**21**) with low MIC value on majority of testing microbial strains.³



(21)

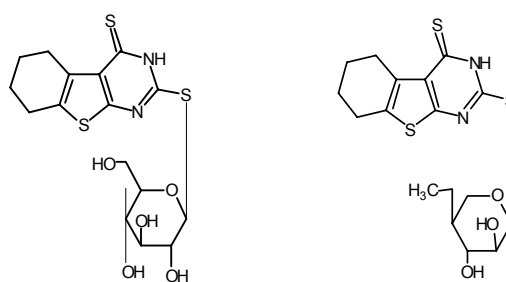
A series of thiazole, pyrazole, thiophene derivatives having benzothiazole moiety in common were reported by Bondock *et al.* by using N-(benzo-thiazol-2-yl)-2-cyanoacetamide as reactant. Synthesized compounds were screened for antimicrobial activity against *S. aureus* and *S. pyogenes* (Gram-positive bacteria), *P. phaseolicola* and *P. fluorescens* (Gram-negative bacteria), *F. oxysporum* and *A. fumigates* (fungal strains). It was noticed that compounds belonging to thiophene and pyrazole series exhibited better antibacterial potential than thiazole series. Incorporation of

thiophene nucleus to benzothiazole at position-3 via carboxamide linker produced high antimicrobial activity. Also thiophenes with electron withdrawing groups like -COOEt (**22**) or -COPh (**23**) recorded higher activity.²¹



(22): R = CO₂Et; (23): R = COPh

Hafez *et al.* synthesized thieno[2,3-*d*]pyrimidine-2,4-dithione derivatives by using 3-(2-amino-thiophene)-carbonitrile derivative precursor as a synthon. The compounds were designed in such a way so that the heterocyclic substituents are straight away linked to thienopyrimidine nucleus at C-2. Triazolo[4,3-*a*]benzothieno[2,3-*d*]pyrimidines were also derived from 2-thioxothienopyrimidine as isosteres. All the compounds were screened for antiviral and antibacterial activity. Some of the compounds showed complete inhibition at 128 mg mL⁻¹ or less while the rest of the compounds showed incomplete inhibition using ampicillin as the standard drug. Introduction of diphenyl-triazolo group at C-2-C-3 ring resulted in ineffectiveness towards *E. coli* but found to be effective against *S. aureus* and *P. putida*. Any other substitution at position C-2-N-3 of pyrimidine ring and C-4-C-5 of the thiophene ring system resulted in a decrease in efficacy of resulting compounds. Substitution of acylated arabino-furanosyl group at C-2 in pyrimidine ring on thieno[2,3-*d*]pyrimidine ensued in potent compounds when compared to other compounds. Deacylated S-glycoside group incorporation in thienopyrimidine resulted in compounds (**24**) and (**25**) which were active against *P. putida*.²²



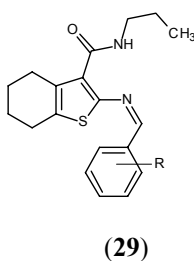
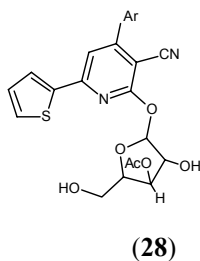
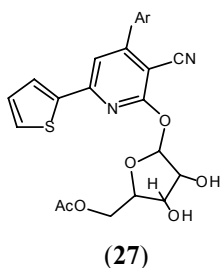
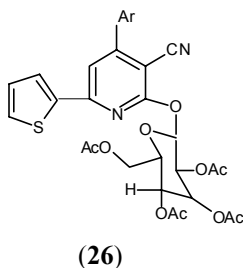
(24)

(25)

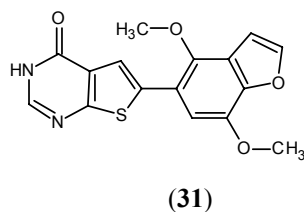
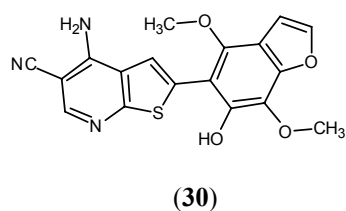
El-Sayed *et al.* reported the synthesis of glycoxyloxy derivatives by glycosylation of pyridine-2-(1*H*)-one. The initial material was obtained by the reaction of 2-acetyl thiophene with 4-chlorobenzaldehyde and ethylcyanoacetate or by reaction of α, β-unsaturated compounds with ethylcyanoacetate in the presence of ammonium acetate. The derivatives were screened for antibacterial activity. The compounds (**26**), (**27**) and (**28**) exhibited higher activity than Ampicillin while other derivative showed moderate activity.²³

Srivastava *et al.* synthesized a series of tetrahydrobenzothiophene as potential antibacterial and mycolytic agents. The antibacterial activity was screened against *Staphylococcus aureus*, *Bacillus subtilis*,

Escherichia coli and *Klebsiella pneumoniae* using Ampicillin as a reference. Miconazole nitrate was used as standard for evaluation of antifungal activity against *Aspergillus niger* and *Candida albicans*. The derivatives showed moderate to significant activity. It was concluded that electron donating and withdrawing groups on aldehydic phenyl ring influenced the activity. Aldehydic phenyl group containing electron withdrawing group like 2-Cl and 2-NO₂ (**29**) showed promising activity.²⁴

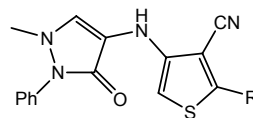


New thienopyridine and thienopyrimidine derivatives were synthesized by Ahmed *et al.*²⁵ from 2-aminothiophen-3-carbonitriles. The carbonitrile derivatives were synthesized via Gewald reaction using visnaginone and khellinone as initial reactant. Antibacterial screening was done against *P. aeruginosa*, *E. coli*, *S. aureus* and *B. subtilis* while for antifungal screening *A. fumigates*, *P. italicum*, *S. racemosum* and *C. albicans* were used. The antimicrobial activity of the synthesized derivatives was measured in comparison to chloramphenicol and terbinafin as standard drugs. Most of the compounds were active and showed moderate activity. From the synthesized series, the most active compounds were compounds (**30**) and (**31**).²⁵



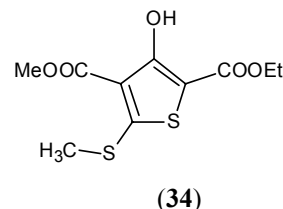
Synthesis and antimicrobial screening of new derivatives of acetamide, oxaloacetyl, acetohydrazide, thiophene and thiophenacrylamide was reported by Aly *et al.* For antifungal activity, four fungal strains: *A. fumigates*, *G. candidum*, *C. albicans* and *S. racemosum* were used.

Clotrimazole and Itraconazole were taken as reference. For antibacterial activity, four bacterial strains: *S. aureus*, *B. subtilis*, *P. aeruginosa* and *E. coli* were used. As a standard drug, Penicillin G and Streptomycin were used as reference to evaluate the potency of tested compounds. All the synthesized compounds exhibited moderate to good activity. From the study, it was observed that synthesized compounds substituted with -OC₂H₅, -COCH₂, -CH₃, -Cl group showed potent activity. Compounds (**32**) and (**33**) were found to have strong antifungal activity.²⁶

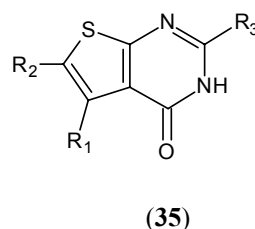


(32) R = -N = CH-OC₂H₅; (33) R = -NHCOCH₂Cl

A series of highly functionalized thiophene and thieno[3,2-*c*]pyran-4-one derivatives was designed by Ram *et al.* These derivatives were screened for antileishmanial and antifungal activities. SAR study revealed that position and nature of substituents at positions 3 and 4 of the thiophene ring are crucial for the activity. Compounds with a carboxymethoxy group at C-4 and hydroxyl group at C-3 (**34**) exhibited significant antifungal activity against all the fungal strain used. Increase in size of ester function from carboxymethoxy to carboxyethoxy resulted in a loss of efficacy. Change of substituent from carboxymethoxy to cyano group resulted in retention of activity. Some of the compounds also showed antileishmanial activity which may be due to the presence of the ester group.²⁷



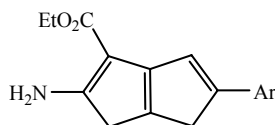
Newly synthesized 2-(pyridin-2-yl)thieno[2,3-*d*]pyrimidin-4(3*H*)-ones derivatives (**35**) were screened for antimicrobial activities against six bacterial strains and two fungal species by Bari *et al.* The presence of long chain aliphatic substituents at C-2 of thiophene ring and presence of the aromatic substituent at position-1 increases the antifungal and antibacterial activity.²⁸



R₁ = H, Me, 4-ClC₆H₄
R₂ = Me, Et, (CH₂)₄
R₃ = 2-C₅H₄N, 3-C₅H₄N,
4-C₅H₄N

Balamurugun *et al.* synthesized a series of novel 2-amino-5-arylthieno[2,3-*b*]thiophene under thermal as well as microwave irradiation conditions employing Gewald dehydrogenation reaction. The synthesized compounds were screened for *in vitro* for antitubercular activity against *M. tuberculosis* (MTB) and multidrug resistant *M. tuberculosis*

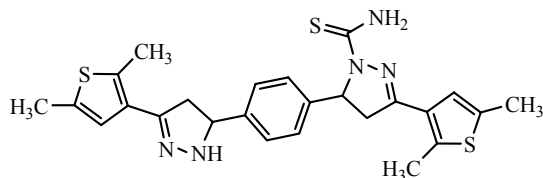
(MDR-TB). Compound (36) was found to be most active compound with MIC of 1.1 μM against MTB and MDR-TB. Compounds with $-\text{CN}$ group were found to be less active than $-\text{COOEt}$ group. It was also reported that lipophilicity is an important factor for antitubercular activity.²⁹



Ar = 1-naphthyl, C_6H_5

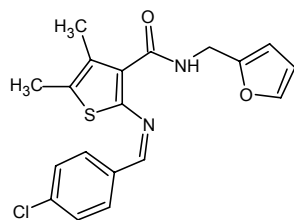
(36)

Khan *et al.* prepared pyrazoline, pyrazole and pyrimidine derivatives from chalcones previously obtained from the reaction of terephthalaldehyde with 3-acetyl-2,5-dimethyl thiophene and evaluated antibacterial activity *in vitro* by disc diffusion assay against *S. aureus*, *S. pyogenes*, *S. typhimurium* and *E. coli*. Results showed that pyrazoline derivative (37) bearing thiophene moiety were better at inhibiting growth of both types of bacteria compared to Chloramphenicol.³⁰



(37)

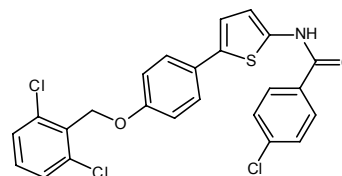
Various Schiff bases were synthesized by Iqbal *et al.* by reaction of substituted aromatic aldehydes with 2-amino-3-(N-furfurylamido)-4,5-dimethyl thiophene. The Schiff bases were screened for antibacterial and antifungal activity using Ampicillin and Miconazole nitrate as standard. Most of the compounds showed mild to moderate antimicrobial activity and some of them were found to be equipotent to the standard drug used. It was concluded that compounds having electron withdrawing group (38) on aldehydic phenyl ring showed better antibacterial and antifungal activity as compared to compounds having electron donating groups.³¹



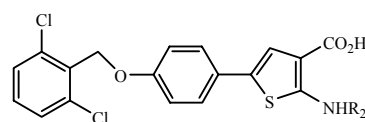
(38)

Lu *et al.* developed a series of acylated and alkylated amino-5-(4-(benzyloxy)phenyl)thiophene-3-carboxylic acid derivatives and evaluated them for anti-tubercular activity. Some of these derivatives inhibited *Mycobacterium tuberculosis* growth with MIC value between 1.9 and 7.7 μM and low toxicity against VERO cells. Compounds were found to show moderate activity against multidrug resistant tuberculosis and drug-resistant tuberculosis clinical strains. SAR studies of these derivatives indicated that 2,6-

dichlorobenzyloxy group (39) is supposed to play a significant role in the activity. Amide derivatives were found to display superior anti-tubercular activity than amine derivatives. The data also suggested that compounds with C-3, C-4 alkyls showed best anti-tubercular activity (40). A further increase in the carbon chain resulted in decrease in potency.³²



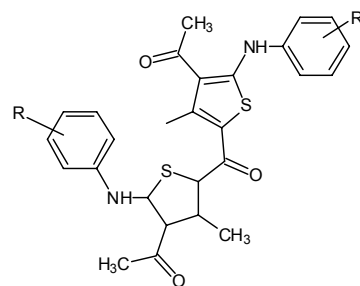
(39)



$\text{R}_2 = \text{n-butyl}$, carboxymethyl

(40)

Sable *et al.* synthesized ethyl 2-(4-acetyl-3-methyl-5-(phenylamino)thiophen-2-yl)-2-oxoacetate derivatives, ethyl 3-(4-acetyl-3-methyl-5-(phenylamino)thiophen-2-yl)-3-oxopropanoate derivatives and di((4-acetyl-3-methyl-5-(phenylamino)thiophen-2-yl)ketone derivatives under mild conditions from acetyl acetone, phenyl isothiocyanates and 2-chloromethyl derivatives. All the synthesized compounds exhibited good to moderate activity. Compounds having R = H/Cl (41) were found to be more potent against Gram-positive bacteria with moderate potential against fungal strains. With R = CH_3/OCH_3 , compounds were more active against *B. subtilis*, *P. aeruginosa* and *E. coli*.³³

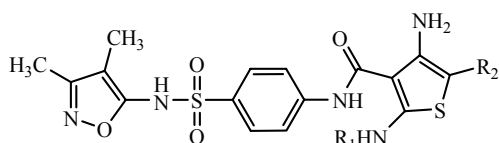


R = H, 4-OCH₃, 4-Cl

(41)

A new series of thiophene, acrylamide, pyrazole and pyridine derivatives tagged with sulfoxazole moieties were synthesized by Nasr *et al.* *In vitro* antimicrobial activity screening was done against Gram-positive bacteria *S. pneumoniae*, *B. subtilis* and *S. Epidermidis*, Gram-negative bacteria *E. coli*, *P. vulgaris* and *K. pneumoniae* and fungal strain *A. fumigates*, *S. racemosum* and *G. candidum* using agar diffusion method and Ampicillin, Gentamycin, Sulfoxazole and Amphotericin B as reference drugs. Most of the newly synthesized compounds (42) were found to be more potent than sulfoxazole. The synthesized compounds had higher lipophilic character than sulfoxazole, and therefore had more intracellular concentration due to their

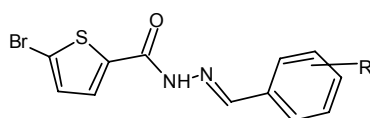
improved cellular penetration. Molecular docking simulations represented that the synthesized compounds can be accommodated in p-aminobenzoic acid pocket of dihydropteroate synthase thereby acting in a similar way as that of sulfa drugs. Therefore, thiophene derivatives bearing larger N-alkyl substituent exhibited better antimicrobial activity.³⁴



$R_1 = -CH_3, -C_2H_5, -CH_2-CH=CH_2, -C_6H_5; R_2 = -COCH_3, -CN$

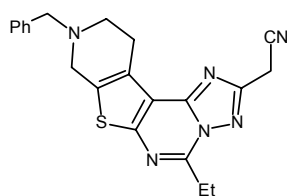
(42)

Naliapara *et al.* prepared a convenient method for the synthesis of Schiff bases of 5-bromothiophene-2-carbohydrazide having good to moderate yield. All the compounds were evaluated for antimicrobial activity by well-diffusion method against bacterial strains (*E. coli*, *P. aeruginosa*, *S. aureus* and *S. pyogenus*) and fungal strains (*C. albicans*, *A. niger* and *A. clavatus*). Compounds like (43), having electron withdrawing groups, exhibited good antibacterial and antifungal activity.³⁵



$R = 4-F, 4-Cl, 4-Br, 3-Cl, 4-CN$ (43)

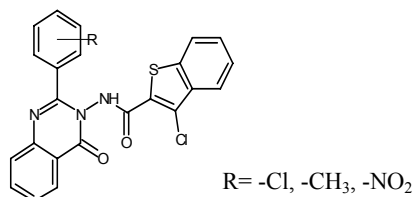
Jabli *et al.* designed a new series of 2-cyano-methylthieno-triazolopyrimidines using substituted aminothiophene-3-carbonitrile and cyanoacetic acid hydrazide as starting material. All the compounds were screened for antibacterial activity using Tetracycline as reference. The strains used were *S. typhimurium*, *P. aeruginosa*, *E. coli* and *S. aureus*. All the synthesized compounds showed moderate antibacterial activity. Among these, compound (44) exhibited highest antibacterial activity. It may be attributed because of the presence of dihydronaphtho and benzyl moiety.³⁶



(44)

Analogs of 3-chloro-N-(4-oxo-2-arylquinazolin-3(4H)-yl)-1-benzothiophene-2-carboxamide were prepared from 3-amino-2-arylquinazolin-4(3H)-one by Rao *et al.* These compounds were evaluated for *in vitro* antibacterial activity against Gram-positive bacteria and Gram-negative bacteria using Ciprofloxacin as standard. Compound with 3-methyl substitution on phenyl ring (45) at position-2 of quinazoline moiety showed significant activity against *S. aureus* while

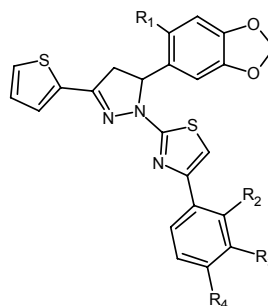
compound with -Cl, -CH₃ and -NO₂ group substitution showed moderate activity against both Gram-positive microorganisms. Most of the compounds showed moderate activity against Gram-negative bacteria.³⁷



$R = -Cl, -CH_3, -NO_2$

(45)

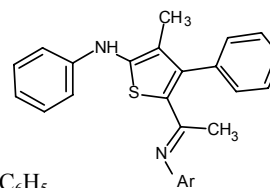
Series of thiophene and benzodioxole appended thiazolopyrazoline derivatives (46) were synthesized and screened for antimicrobial activity by Antony *et al.* Some of the compounds presented good antimicrobial activity against bacterial and fungal strain used. Docking study revealed that all synthesized derivatives showed good binding energy toward target receptor DNA topoisomerase IV, ranging from -10.42 to -11.66 kcal mol⁻¹. Substitution of -Br at R₁ position and -CN group at R₃ position resulted in a marked increase in antimicrobial activity.³⁸



$R_1 = H, Br; R_2 = H, Cl; R_3 = H, CN; R_4 = H, F$

(46)

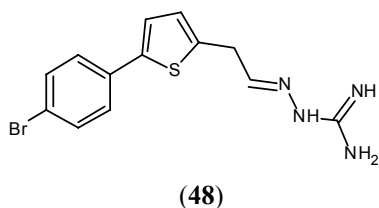
Mabkhot *et al.* synthesized derivatives of thiophene using 5-acyl-4-phenyl-2-(phenyl-amino)thiophene-3-carboxylate as precursor. These derivatives were screened for antibacterial activity against Gram-positive bacteria (*B. subtilis* and *S. pneumoniae*) and Gram-negative bacteria (*E. coli* and *P. aeruginosa*) using disc diffusion method with Ampicillin and Gentamycin as standard drugs. For antifungal activity, four fungal strains (*A. fumigates*, *S. racemosum*, *G. cardium*, *C. albicans*) were used and Amphotericin B was taken as standard drug. All the compounds exhibited moderate to good antimicrobial activity. SAR studies suggested that introduction of appropriate substituent at position-5 of thiophene ring (47) enhanced antibacterial activity.³⁹



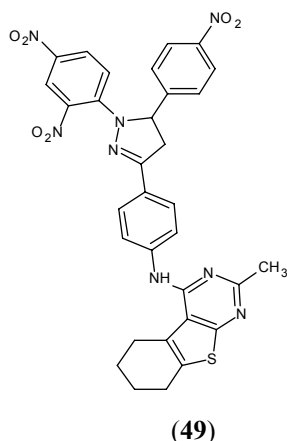
$Ar = -C_6H_5, 4-ClC_6H_5$

(47)

Ajdacic *et al.* designed a series of new thiophene-based guanylhydrazones and evaluated antifungal activity against broad ambit of medically valued fungal strains including yeast, moulds and dermatophytes in comparison to drug Voriconazole. All guanylhydrazones showed significant activity against *Candida* spp., *A. fumigates*, *F. oxysporum*, *M. canis* and *T. mentagrophytes*. Some of the compounds exhibited excellent activity against voriconazole resistant *Candida albicans* with very low MIC value $< 2 \mu\text{g mL}^{-1}$. Compound (48) having -Br group on phenyl ring was found to be most effective with MIC ranging from 0.25-6.25 $\mu\text{g mL}^{-1}$. It was concluded that thiophene based guanynyl hydrazone showed higher inhibitory activity than corresponding furan.⁴⁰



Various chalcones were used as building block for the synthesis of various thieno[2,3-d]pyrimidine derivatives by Elissa *et al.* These derivatives were screened for antimicrobial activity against Gram-positive, Gram-negative and fungal strains. MIC was determined by the paper disc diffusion method. It was observed that substitution with a methyl group at position-2 of tetrahydrothienopyrimidine derivative of enone series decreased the activity against Gram-positive bacteria and removed the activity against *C. albicans*. A terminal amino group of the hydrazine group when unsubstituted, together with the presence of methyl group position-2 showed broad spectrum activity. The presence of phenyl group at N¹ and dinitrophenyl group of dihydropyrazol ring (49) yielded derivative with broad spectrum activity.⁴¹



Conclusion

Considerable attention has been given to compounds which possess thiophene rings in order to search for drugs with a higher degree of potency and fewer toxic side effects. The analytical and other informational data, available in literature so far, have lightened thiophene as a significantly important class of heterocyclic compounds and their

applications in the ever challenging chemotherapy of various ailments/ infections since last two decades. A large number of thiophene derivatives have been discovered and reflected significant antimicrobial activity with appreciably wider spectrum.

Thiophene can be fused with various heterocyclic systems, resulting in various new heterocyclic systems with enhanced biological activity. Thienopyrimidine and benzothiophene occupy a special position among these compounds. Most of the positions were explored to improve the antimicrobial profile of thiophene analogs. Derivatives with C-2 and C-4 substituted positions and compoment of electron-withdrawing group on the aromatic ring on C-2 position of thiophene presents varied degrees of inhibition against Gram-positive bacteria, Gram-negative bacteria and fungal strains, showing inhibition as good as to the standard drugs used. The versatile synthetic applicability and biological activity of this heterocyclic moiety will help the medicinal chemists to plan, organize and implement new approaches towards discovery of novel drugs. Further combinatorial libraries of these compounds can be generated which can be screened optimal pharmacological activities by optimization techniques using 2D and 3D QSAR investigation.

Acknowledgement

The author would like to extend sincere appreciation to the Department of Pharmacy, Galgotias University, Greater Noida for providing literature survey facility to carry out the work.

References

- Mishra, R., Jha, K. K., Kumar, S., Tomer, I., *Pharm. Chem.*, **2011**, 3, 38.
- Baumann, M., Barendale, I. R., Ley, S. V., Nikbin, N., *Beilstein J. Org. Chem.*, **2011**, 7, 442.
- Badiceanu, C. D., Missir, A. V., Chifiriuc, M. C., Dracea, O., Raut, J., Larion, C., Dity, L. M., Mihaescu, G., *Rom. Biotech. Lett.*, **2010**, 15, 5545.
- Dalvie, D. K., Kalgutkar, A. S., Khojasteh-Bakht, S. C., Obach, R. S., O'Donnell, J. P., *Chem. Res. Toxicol.*, **2002**, 15, 269.
- Jha, K. K., Tomer, I., Mishra, R., *J. Pharm. Res.*, **2010**, 5, 560.
- Queiroz, M. R. P., Ferreira, I. C. F. R., Goetano, Y. D., Kirsch, G., Calhelha, R. C., Estevinho, L. M., *Bioorg. Med. Chem. Lett.*, **2006**, 14, 6827.
- Havaldar, F. H., Bhise, S., Burudkar, S., *J. Serb. Chem. Soc.*, **2004**, 69, 527.
- Yadav, P. P., Gupta, P., Chaturvedi, A. K., Shukla, P. K., Maurya, R., *Bioorg. Med. Chem.*, **2005**, 13, 1497.
- Ryu, C. K., Lee, S. K., Hen, J. Y., Jung, O. J., Lee, J. Y., Jeong, S. H., *Bioorg. Med. Chem. Lett.*, **2005**, 15, 2617.
- Sherbeny, M. A., El-Ashrawy, M. B., Subbagh, H. I., El-Emam, A. A., Badria, F. A., *Eur. J. Med. Chem.*, **1995**, 30, 445.
- Bhuiyan, M. H., Rahman, K. M. M., Hussain K., Rahim, A., Hussain, I., Naser, A., *Acta. Pharm.*, **2006**, 56, 441.
- Abreu, A. S., Ferreira, P. M. T., Monterio, L. S., Queiroz, M. J. R. P., Ferreira, I. L. F. R., Calhelha, R. C., Estevinha, L. M., *Tetrahedron*, **2004**, 60, 11821.

- ¹³Desai, A. D., Mahajan, D. H., Chikhaliya, K. H., *Indian J. Chem.*, **2007**, *46B*, 1169.
- ¹⁴Darwish, E. S., *Molecules*, **2008**, *13*, 1066.
- ¹⁵Pinto, E., Queiroz, M. J. R. P., Vale-Silva, L. A., Oliveira, J. F., Begowin, A., Begowin, J. M., Kirsch, G., *Bioorg. Med. Chem.*, **2008**, *16*, 8172.
- ¹⁶Khalil, A. M., Berghot, M. A., Gouda, M. A., *Eur. J. Med. Chem.*, **2006**, *44*, 4434.
- ¹⁷Shetty, N. K. S., Lamani, R. S., Khazi, I. A. M., *J. Chem. Sci.*, **2009**, *121*, 301.
- ¹⁸Gouda, M. A., Berghot, M. A., Abd El-Ghani, G. E., Khalil, A. M., *Eur. J. Med. Chem.*, **2010**, *45*, 1338.
- ¹⁹Saravanan, J., Mohan, S., Roy, J. J., *Eur. J. Med. Chem.*, **2010**, *45*, 4365.
- ²⁰Al-Taisan, K. M., Al-Hazimi, H. M. A., Al-Shihry, S. S., *Molecules*, **2010**, *15*, 3932.
- ²¹Bondock, S., Fadaly, W., Mefwally, M. A., *Eur. J. Med. Chem.*, **2010**, *45*, 3692.
- ²²Hafez, H. N., Hussein, H. A. R., El-Gazzar, A. B. B. A., *Eur. J. Med. Chem.*, **2010**, *45*, 4026.
- ²³El-Sayed, H. A., Moustafa, A. H., Haikal, A. E. Z., El-Halawa, R. A., El-Ashry, E. H., *Eur. J. Med. Chem.*, **2011**, *46*, 2948.
- ²⁴Srivastava, S., Das, B., *Der Pharm. Chemica*, **2011**, *3*, 103.
- ²⁵Ahmed, E. M., Marzouk, N. A., Hessein, S. A., Ali, A. M., *World J. Chem.*, **2011**, *6*, 25.
- ²⁶Aly, H. M., Saleh, N. M., Elhady, H. A., *Eur. J. Med. Chem.*, **2011**, *46*, 4566.
- ²⁷Ram, V. J., Goel, A., Shukla, P. K., Kapil, A., *Bioorg. Med. Chem. Lett.*, **1997**, *7*, 3101.
- ²⁸Haswani, N. G., Bari, S. B., *Turk. J. Chem.*, **2011**, *35*, 915.
- ²⁹Balamurugan, K., Perumal, S., Reddy, A. S. K., Yogeeswari, P., Sriram, D., *Tetrahedron Lett.*, **2009**, *50*, 6191.
- ³⁰Asiri, A. M., Khan, S. A., *Molecules*, **2011**, *16*, 523.
- ³¹Iqbal, M. I. C., Satyendra, D., Apurba, T., Patel, M., Monica, K., Girish, K., Mohan, S., Saravanan, J., *Hygeia. J. D. Med.*, **2012**, *4*, 116.
- ³²Lu, X., Wan, B., Franzblau, S. G., You, Q., *Eur. J. Med. Chem.*, **2011**, *46*, 3551.
- ³³Sable, P. N., Ganguly, S., Chaudhari, P. D., *Chin. Chem. Lett.*, **2014**, *25*, 1099.
- ³⁴Nasr, T., Bondock, S., Eid, S., *Eur. J. Med. Chem.*, **2014**, *84*, 491.
- ³⁵Makwana, H., Naliapara, Y. T., *Inter. J. Chem. Phy. Astro.*, **2014**, *14*, 99.
- ³⁶Jabli, D., Lahbib, K., Dridi, K., Efrif, M. L., *J. Pharm. Chem. Biol. Sci.*, **2015**, *3*, 178.
- ³⁷Rao, G. K., Subramaniam, R., *Chem. Sci. J.*, **2015**, *6*, 1.
- ³⁸Sulthana, S. S., Antony, S. A., Balachandran, C., *Bioorg. Med. Chem. Lett.*, **2015**, *25*, 2753.
- ³⁹Mabkhot, Y. N., Alatibi, F., El-Sayed, N. N. E., Al-Showiman, S., Kheder, N. A., Wadood, A., Rauf, A., Bawazeer, S., Handa, T. B., *Molecules*, **2016**, *21*, 01.
- ⁴⁰Ajdacic, V., Senerovic, L., Vranic, M., Pehnezovic, M., Arsnijevic, V. A., Veselinovic, A., Veselinovic, J., Solaja, B. A., Runic, J. N., Opsenica, I. M., *Bioorg. Med. Chem.*, **2016**, *24*, 1277.
- ⁴¹Elissa, A. A. H. M., Moneer, A. A., *Arch. Res. Pharm.*, **2004**, *27*, 885.

Received: 20.10.2016.

Accepted: 15.11.2016.



OPTIMIZATION OF EXTRACTION CONDITIONS FOR LIQUID-LIQUID EXTRACTION OF PERSIPEPTIDES FROM *STREPTOMYCES ZAGROSENSIS* FERMENTATION BROTH

Hamed Kazemi Shariat Panahi^[a], Fatemeh Mohammadipناه^{[a]*} and Mona Dehghani^[a]

Keywords: Anti-MRSA; drug discovery; enhanced-production; experimental design; HPLC; liquid-liquid extraction; pentapeptide.

Generally, during drug discovery programs, after identification of new antibiotic metabolite, its high quantity production is obtained by various approaches, including production or extraction improvement or even strain genetic manipulation. To provide enough amounts of two novel non-toxic anti-MRSA pentapeptides named persipeptides (A and B) required for drug discovery programs, seven different fermentation broths examined. CM1 medium considerably enhanced the biosynthesis of persipeptides up to 219.63 ± 2.48 , compared with ISP2 medium (36.31 ± 1.37), showing a six-fold increase. Additionally, at the extraction level, results of experimental design indicated that liquid-liquid extraction (LLE) of persipeptides by 34 % BuOH at 228 rpm (Stirrer speed), temperature 28 °C, and pH 9-9.5 for 78 min (stirring time) was equal to $264 \pm 9.85 \mu\text{g mL}^{-1}$, which was the most favorable combination for their extraction. Compared with un-optimized extraction process ($219.63 \pm 2.48 \mu\text{g mL}^{-1}$), the optimized conditions improved the yield of the extraction by 20.20 %, while saving both time and solvent usage up to 67 % (162 min) and 16 %, respectively. The total sum of persipeptides enhancements resulted from the replacement of fermentation broth and subsequent optimization of their extraction by LLE reached almost seven-time, compared to conventional method ($36.31 \pm 1.37 \mu\text{g mL}^{-1}$). Therefore, relatively large amounts of persipeptides can be economically produced and extracted for various future experiments.

* Corresponding Authors

Fax: +982166415081

E-Mail: fmoammadipناه@ut.ac.ir

[a] Department of Microbial Biotechnology, School of Biology and Center of Excellence in Phylogeny of Living Organisms, College of Science, University of Tehran, 14155-6455, Tehran, Iran

Introduction

The treatment of drug-resistant bacteria, including MRSA, in terms of their resistance to the current antibiotics is among major challenges worldwide.¹ New cyclo-pentapeptides, named as persipeptides, consist of two types of amino acids repetition of valine and phenylalanine, two of which are *N*-methylated. So far; two isomers, A and B, has been produced² by *Streptomyces zagrosensis* UTM 1154 with bioactivity against methicillin resistance *Staphylococcus aureus* (MRSA) DSM 23622 (UTMC 1401).³ Existence of *N*-methylated residues in peptides usually led to higher interesting therapeutic profiles⁴ and consequently improved pharmacokinetic properties such as enzymatic stability,⁵ receptor selectivity,⁶ enhanced potency,⁷ membrane permeability,⁸ and bioavailability.⁹

The development and the validation of analytical methods play vital roles in discoveries, developments and manufactures of pharmaceuticals. High-performance liquid chromatography (HPLC) is extensively applied as a versatile analytical technology for quantitative analysis of target biomolecules and other compounds in biological matrixes as well as fermentation culture media of microorganisms producing them.¹⁰ HPLC-based methods has previously been developed and validated for persipeptides determination from fermentation broth of *S. zagrosensis* UTM 1154. The reported assay method requires sample pretreatment using LLE with the aid of *n*-butanol (*n*-BuOH).³ This pretreatment

is required for separating and concentrating of the target analyte and removing interferences, or even increasing the life of HPLC column by the elimination of damaging compounds.¹¹ However, the LLE method used for sample pretreatment or extraction of persipeptides has not been optimized yet; therefore, has some drawbacks, including lower efficiency and time consumption. These drawbacks directly affect the extraction yield and expenses, including materials usage and equipment depreciation. Improvement of a system performance or a process in order to maximize the exploitation from it is referred as optimization. Process optimization will obtain conditions that produce the best possible response when applied to a production/extraction procedure.¹² Traditional optimization of analytical chemistry are accomplished by one-variable-at-a-time, in which at any given time, influence of only one factor has been examined while all other factors have been kept at a constant level.¹³ An alternative to this is response surface methodology (RSM), which decreases the number of experiments while increases the effectiveness for responses that are confounded by many factors and their interactions.¹³ Additionally, analysis of variance (ANOVA) provides the statistical results and diagnostic checking tests, which enable researchers to evaluate the adequacy of the models.¹⁴ Although, RSM has been successfully applied in the optimization of culture media to enhance the production of *Streptomyces* secondary metabolites, including streptolydigin,¹⁵ virginiamycin,¹⁶ daptomycin,¹⁷ clavulanic acid,¹⁸ streptomycin,¹⁹ and neomycin,²⁰ RSM in the optimization of solvent extraction of antibiotics produced by *Streptomyces* has been rarely exploited and the only example is the optimization of extractive fermentation of clavulanic acid.²¹

In the present study, six culture media consisting of novel complex carbon sources and insoluble nitrogen sources were examined and compared with ISP2 medium. After determination of the most productive medium, the

optimization of parameters in the process of LLE, including volume percentage of extraction solvent, stirring rate, sample pH, extraction temperature, and process time for LLE of persipeptides from fermentation culture medium samples of *S. zagrosensis* UTMC 1154³ were done in two steps. In the first step, primary evaluation of mentioned factors using half-fraction of factorial design was performed and striking factors were screened. In the second step, selected factors were investigated by RSM using central composite rotatable design (CCRD) in order to maximize the extraction efficiency of persipeptides.

Experimentals

HPLC grade acetonitrile was purchased from Merck (Darmstadt, Germany). All other organic solvent used for LLE of persipeptides, including *n*-butanol (*n*-BuOH), 1-propanol, 2-propanol, cyclohexane, dichloromethane, methanol, and chloroform were extra-pure grade and obtained from Merck (Darmstadt, Germany). HPLC grade water was produced by Barnstead/Thermolyne, USA (Model: d8992-33 Nanopure infinity).

Strain and culture conditions

The commonly used ISP2 medium (consisted of (g L⁻¹): glucose (4); yeast extract (4); and malt (10), pH 7.2) was used as growth and maintenance (supplemented with 2 g L⁻¹) and seeding media. Persipeptides were produced by the inoculation of spore suspension (1 mL of 1 × 10⁷ CFU mL⁻¹) of *S. zagrosensis* UTMC 1154 in 100-mL Erlenmeyer flasks containing 9 mL of ISP2 liquid medium, followed by 36 h of shaking (220 rpm) at 28 °C to develop seeding culture. This pre-culture was used for the subsequent inoculation of various fermentation media (50 mL) in 250-mL Erlenmeyer flasks with inoculant size of 10 % (5 mL). The inoculated production media were incubated at 28 °C on shaker incubator with 220 rpm for seven days.³ In order to examine persipeptides production, seven different media, named as candidate media (CM) 1-6 were investigated (Table 1). The optimization was done using the most productive medium.

Experimental designs and statistical analyses

In the previously reported method, the effect of critical parameters, including pH of the fermentation broth, extraction temperature, percentage of organic solvent, stirring rate, and extraction time on extraction process has not been determined.³ Therefore, an experimental design using half fraction of factorial design was employed to screen significant variables with the minimum required number of experiments. After the determination of variables with significant effect on extraction process, a three factors CCRD was employed to determine optimal conditions for critical factors. Design-Expert Version® 7.0.0 was used to fit the quadratic response surface model to the experimental information as well as to generate response surfaces, analysis of data, and contour plots diagrams, while keeping a variable constant in the second-order polynomial model. The statistical significance of an effect was evaluated by *p*-values <0.05.

The response was persipeptides peak area and actual values of independent variables (X_i) were coded to x_i according to Eqn. (1).

Table 1. Compositions of seven different production media used for enhancing persipeptides production.

Medium	C-source, g L ⁻¹	N-source, g L ⁻¹	Salt g L ⁻¹	pH
CM1	Starch (20)	Soybean (30)	MgSO ₄ ·7H ₂ O (1) and CaCO ₃ (10)	7.0
CM2	Acorn (20)	Yeast Extract (4)	-	7.0
CM3	Rape seed (10)	Malt (10)	-	7.0
CM4	Cotton seed (10)	Malt (10)	-	7.0
CM5	Sesame (20)	Malt (10)	-	7.0
CM6	Glycerol (15)	Soybean (10)	CaCO ₃ (1), NaCl (5), and COCl ₂ ·7H ₂ O (1)	7.0
ISP2	Glucose (4)	Yeast extract (4)	-	7.4

$$x_i = \frac{X_i - \bar{X}_i}{(X_{iHi} - X_{iLow})/2}, i = 1, 2, 3 \dots k \quad (1)$$

where,

x_i = coded value of independent variable;

$X_{iHi/Low}$ = real values of the independent variable;

\bar{X}_i = real values of the independent variable at the center point of the domain; and

x_1 (coded value of percentage of organic solvent),

x_2 (coded value of stirring rate), and

x_3 (coded value of extraction time) were given in Eqn. (2), (3) and (4).

$$x_1 = \frac{X_1 - 50}{25} \quad (2)$$

$$x_2 = \frac{X_2 - 225}{75} \quad (3)$$

$$x_3 = \frac{X_3 - 49}{29} \quad (4)$$

Response surface analysis of a five coded level CCRD for three factors, 20 runs (Table 2), was done using the generalized second-order polynomial model of Eqn. (5), and economically optimum conditions for LLE of persipeptides was determined by same equation.

$$Y = \beta_0 + \sum_{i=1}^k \beta_i X_i + \sum_{i=1}^k \beta_{ii} X_i^2 + \sum_{ij=1(i \neq j)}^k \beta_{ij} X_i X_j$$

(5)

where,

Y = the experimental response;

β_0 , β_i , β_{ii} , and β_{ij} = the constant (intercept) coefficient, the linear coefficient, the quadratic coefficient, and the coefficient of interaction effect, respectively; and

X_i and X_j = independent variables

The quality of the fitted model was evaluated through analysis of variance (ANOVA). Additionally, the statistical analysis of the result, the evaluation of model and factors involved, and the determination of the influence of individual factors and their interaction with other factors on persipeptides extraction from the fermentation culture matrix by LLE were performed by determination of the coefficients from eqn. (5).

Table 2. Experimental sheet for five coded level CCRD of significant factors selected by screening design.

Run	Factor 1 x_1 : BuOH %	Factor 2 x_2 : stirring rate	Factor 3 x_3 : stirring time
1	50	225	49
2	50	225	0.23
3	92	225	49
4	8	225	49
5	50	225	49
6	50	352	49
7	75	300	20
8	50	99	49
9	50	225	49
10	50	225	98
11	50	225	49
12	25	150	78
13	25	300	20
14	75	300	78
15	25	300	78
16	75	150	78
17	25	150	20
18	50	225	49
19	75	150	20
20	50	225	49

Sample preparation

The fermentation medium was harvested and divided for further experiments. Samples were prepared based on experimental conditions defined by experimental designs, then butanol containing fermentation broths were centrifuged at 2937 \times g for 10 min. One-hundred-fifty- μ L of each supernatants was separated and the solvent was removed using N_2 gas. The obtained precipitate was dissolved in 150 μ L acetonitrile-water (1:1 v/v) and analyzed by HPLC method.

HPLC instrument and analysis

A Cecil instrument with in-line-degasser (CE 4040) consisted of manual Rheodyne (Rohnert Park, CA, USA) injector with 20 μ L loop was employed. The sample was retained on an ACE (Aberdeen, UK) LiChrosob C18 column (250 \times 4.6 mm ID, particle size 5 μ m, ACE-121-2546) protected by Hichrom (Reading, UK) C18 column (NC100-5C18) and thermostated at 27 $^{\circ}$ C. The analytes were eluted by water (A) and acetonitrile (B) as mobile phase using a gradient elution, in which B was 50 % at start point, increased to 64 % in 5.5 min, then to 95 % within 1.5 min, followed by 5 min isocratic at 95 % (purge time), finally decreased to 50 % within 3 min and kept at this B % for as long as 10 min to equilibrate the column to prepare the system for next injection. Measurements were held at 210 nm and data was collected and processed by chromatography system manager and power stream software version 3.1, respectively. ³

Results and discussion

The core aim of current study was the enhancement of persipeptides retrieval. At the production step, the most effective medium basis for persipeptides biosynthesis was chosen amongst seven candidate media listed in Table 1. After cultivation, persipeptides were separately isolated from them using un-optimized LLE method previously provided.³ Results, in Table 3, indicate the CM1 medium as the most productive fermentation culture medium for persipeptides biosynthesis, which enhances its production by more than six times, reaching to 219.63 ± 2.48 , compared with ISP2 medium (36.31 ± 1.37). All other examined novel carbon sources; including acorn, sesame, cotton seed, and rape seed failed to increase the persipeptides production, compared with ISP2 and the production was in range of 33 to 39 μ g mL⁻¹. The second most promising medium after CM1 was CM6, which composed of glycerol and soybean as carbon and nitrogen sources, respectively. CM6 considerably enhanced persipeptides production (159.69 ± 27.36), and four times increased in their production was resulted, compared to that of ISP2 medium (36.31 ± 1.37). Therefore, CM1 medium was selected as the final production medium and used for further optimization of LLE.

In this study, the LLE followed by HPLC-UV was applied for the extraction and the quantification of persipeptides in fermentation broth samples, respectively. Effects of multiple factors, including volume ratio of extraction solvent, stirring rate, sample pH, extraction temperature and process time were investigated. Optimized conditions were obtained by

screening design, and subsequently, CCRD was applied for the evaluation of significant factors along with their interactions thereof.

Table 3. Production of persipeptides in different fermentation media tested.

Name	1 st trial	2 nd trial	3 rd trial	Average
CM1	220.36	216.86	221.66	219.63 ± 2.48
CM2	38.39	35.258	37.93	37.93 ± 1.69
CM3	33.65	33.57	33.97	33.73 ± 0.21
CM4	42.42	33.62	39.14	38.39 ± 4.45
CM5	36.84	37.14	37.31	37.10 ± 0.24
CM6	132.27	159.81	186.99	159.69 ± 27.36
ISP2	34.93	36.33	37.68	36.31 ± 1.37

Before starting optimization procedures, broad range of solvents, including ethyl acetate, 1-propanol, 2-propanol, cyclohexane, dichloromethane, methanol, *n*-BuOH, and chloroform were examined for obtaining maximum extraction (Data not shown). Among them, *n*-butanol was selected as the extracting solvent, as it has a high boiling point, which prevent solvent loss during extraction, and low melting point (less than -89 °C); is immiscible with aqueous solution and its density is lower than water; and is compatible with the RP-HPLC used in the quantification of persipeptides.

Screening design

Half fraction of factorial (resolution V) design is useful for preliminary purposes or in initial optimization steps owing to its great power in estimation of effects as well as considerable reduction in the number of experimental runs to be performed. Applying this design allows the estimation of all the main effects and two-factor interactions (2 FI) with the assumption that no three-factor or/and higher interactions occur/s. Therefore, half fraction factorial design was used for the screening step. Major factors, which are assumed to influence the LLE of persipeptides, include volume percentage of extraction solvent, stirring rate, sample pH, extraction temperature and process time. Levels of factors for the screening design were selected according to our knowledge, and are presented in Table 4. The overall design matrix, consisted of 20 runs of which four of them were center runs, was randomly performed in order to minimize unexplained variability effects in obtained responses due to systematic errors. Half-normal probability plot was used to choose significant effects, which were further analyzed by ANOVA and obtained results were evaluated to determine main effects (Table 5).

The standard effect was estimated for calculating a *t*-statistic for each effect. Normalized results of the performed experimental design were investigated at a 5 % of significance and analyzed by standardized Pareto chart (Figure 1). On this plot (Figure 1), effects that are now above the second vertical line, Bonferroni limit, and those between second and first vertical lines, *t*-value limit, are almost certainly and possibly significant parameters, respectively.

Table 4. Levels of factors for the screening design.

Independent Factors	CS	Levels and Ranges		
		-1 (L)	0 (M)	+1 (H)
Broth pH	A	7	9	11
Temperature (°C)	B	20	40	60
BuOH % (v/v)	C	50	63	75
Stirring rate (rpm)	D	100	200	300
Process time (min)	E	20	70	120

CS, L, M, and H stand for Coded Symbol, Low, Middle, and High, respectively.

The model F-value of 10.25 implies the significance of the model. There is only a 0.05 % chance that the model F-value of this large could have been occurred due to noise. The measured curvature F-value of 37.33 as the difference between the average of the center points and that of the factorial points implies that the curvature in the design space is significant, and there is a 0.01 % probability that it could occur due to noise. Therefore, there was a need for higher resolution design (RSM) to optimize the significant factors. Furthermore, the lack of fit F-value of 0.35 implies that it is not significant relative to the pure error, and there is an 89.72 % chance that it could occur due to noise, therefore, the model can fit. The model had the predicted R-square of 0.74, which is in reasonable agreement with the adjusted R-square of 0.78. Moreover, model adequate precision measuring the signal to noise ratio had the value of 10.217 being considerably greater than 4, and therefore, the model can be used to navigate the designed space.

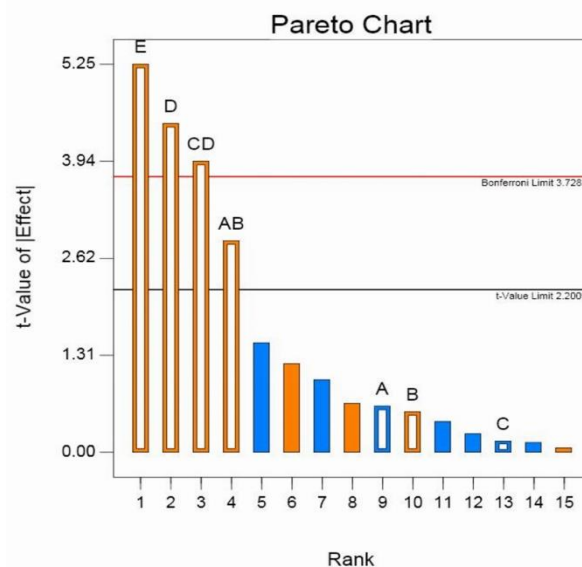


Figure 1. Pareto chart with selected main effects obtained from the half fraction of factorial design for LLE of persipeptides; A: sample pH; B: extraction temperature; C: percentage of BuOH; D: stirring rate; E: extraction time; AB and CD are 2FI between sample pH and extraction temperature, and percentage of BuOH and stirring time, respectively; 1: extraction time; 2: stirring rate; 3: 2FI between percentage of BuOH and extraction time; 4: 2FI between sample pH and extraction temperature; 5: 2FI between sample pH and extraction time; 7: 2FI between extraction temperature and stirring rate; 8: sample pH; 9: 2FI between sample pH and percentage of BuOH; 10: 2FI between sample pH and stirring rate; 11: 2FI between percentage of BuOH and extraction time; 12: 2FI between extraction temperature and percentage of BuOH; 13: 2FI between extraction temperature and extraction time; 14: extraction temperature; and 15: percentage of BuOH.

Table 5. Estimated ANOVA for half fraction of factorial design relationship between response variable (extraction yield) and independent variables (A, B, C, D, and E) in determination of significant factors to be optimized by RSM.

Source	SST	df	MS	F-Value	p-value Prob > F
Model	2438730	7	348390	10.24817	0.0005
A-pH	13219.25	1	13219.25	0.388855	0.5456
B-Temperature	10287.03	1	10287.03	0.302601	0.5933
C- BuOH %	771.4506	1	771.4506	0.022693	0.8830
D-Stirring rate	672359	1	672359	19.77798	0.0010
E-Stirring time	936685.2	1	936685.2	27.55335	0.0003
AB	278440.9	1	278440.9	8.190562	0.0155
CD	526967.1	1	526967.1	15.50116	0.0023
Curvature	1268896	1	1268896	37.32559	<0.0001
Residual	373948.7	11	33995.33		
Lack of Fit	179699.1	8	22462.39	0.34691	0.8972
Pure error	194249.6	3	64749.85		
Cor total	4081575	19			

SST, MS, and df stand for Sum of Squares, Mean Square, and Degree of Freedom, respectively.

According to Figure 1 and Table 5, duration of stirring time was the most significant factor with a negative effect on the extraction efficiency of persipeptides. The second most important negative-effect variable was the rate of stirring. Interestingly, 2 FI between percentage of BuOH and stirring rate was significant with a negative effect on the extraction process. In contrast, both pH and temperature were non-significant factors with positive and negative effect, respectively. In low temperatures, extraction is slow process with lower yield, whereas at higher temperature, solvent is more soluble in aqueous phase, and therefore its separation from aqueous solution is more complicated. Additionally, persipeptides degradation is apparent at high temperatures;³ therefore, temperature for their extraction was set at 28 °C. Moreover, the pH of the extraction process was kept the same as the pH of fermentation broth of *S. zagrosensis* (9 and 9.5).

Optimization of significant factors

In the next step, a CCRD design was applied to optimize the values of three factors (percentage of BuOH, stirring rate, and extraction time), selected from the prior screening design. The process variable of LLE of persipeptides examined using CCRD presented in Table 6. The number of experiments is determined by the expression: $(2^n + 2n + C)$, where n represents the number of factors (6) and C denoted the number of center points (3). The design of CCRD consisted of a factorial design (2^n) augmented with $(2n)$ run per axial points, which is the number of times each axial run will be performed and located at $+1.682\alpha$ and -1.682α from the center of the experiment domain to satisfy the rotatability condition of the CCRD, and central points (C). Center runs with six repetitions were employed to estimate pure error for the lack of fit test as well as provides rather uniform precision designs. This means that the error inside a sphere that has a radius equal to ± 1 level is nearly uniform. Thus, predictions in this region are equally good.

Table 6. The significant variables and the level of the central composite response design used in the optimization of the persipeptides extraction.

Factor	Level			Star points*	
	-1 (L)	0 (C)	+1 (H)	- α	+ α
x_1 : BuOH %	25	50	75	8	92
x_2 : Stirring rate	150	225	300	99	351
x_3 : Stirring time	20	49	78	0.3	98

*The value is ($\alpha = 1.682$). L, C, and H stand for Low, Central, and High, respectively

The data obtained were analyzed by ANOVA (Table 7) and then backward elimination regression, with alpha to exit equal to 0.100, was employed to improve the ANOVA results, in which the quadratic response was reduced by the elimination of x_1x_2 (2FI) and x_3^2 (Table 8).

Fitting the model

A regression evaluation (Table 8) was performed for fitting mathematical models to the experimental data aiming at an optimal area, and a quadratic model was suggested according to the results. The predicted model of the regression equation for the peak area of persipeptides was expressed as eqn. (6) in terms of coded factors.

$$Y_1 = 1604.08 - 18.95x_1 + 231.51x_2 + 267.34x_3 - 225.41x_1x_3 - 220.52x_2x_3 - 183.06x_1^2 - 138.61x_2^2 \quad (6)$$

The F-test and p -value (Table 8) were used to determine the significance of each coefficient. If the p -value becomes smaller and the absolute F-value becomes higher, the corresponding variable would be of more significant.²²

Table 7. Estimated ANOVA of relationship between response variables (extraction yield) and independent variables (x_1 , x_2 and x_3) for response surface quadratic model.

Source	SST	df	MS	F-Value	p-value Prob >F
Model	3301366	9	366818.5	3.606939	0.029
x_1	4902.709	1	4902.709	0.048209	0.8306
x_2	731993.3	1	731993.3	7.197717	<u>0.023</u>
x_3	976072.3	1	976072.3	9.597755	<u>0.0113</u>
x_1x_2	2266.328	1	2266.328	0.022285	0.8843
x_1x_3	406463.8	1	406463.8	3.996774	<u>0.0735</u>
x_2x_3	389028.2	1	389028.2	3.825328	<u>0.079</u>
x_1^2	443707	1	443707	4.362988	0.0633
x_2^2	247389.7	1	247389.7	2.432592	0.1499
x_3^2	84216.33	1	84216.33	0.828102	0.3842
Residual	1016980	10	101698		
Lack of fit	789641.9	5	157928.4	3.473428	0.099
Pure error	227337.9	5	45467.59		
Cor. total	4318346	19			

SST, MS, and df stand for Sum of Squares, Mean Square, and Degree of Freedom, respectively.

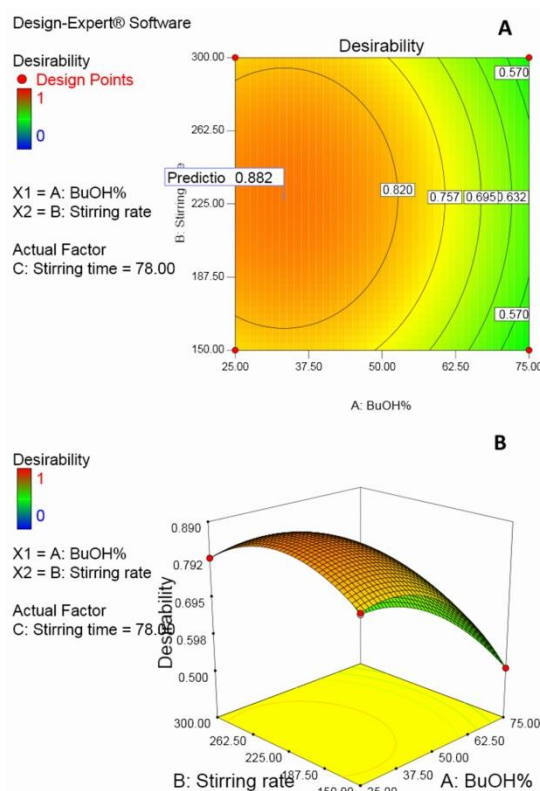
Table 8. ANOVA of relationship between response variables (extraction yield) and independent variables (x_1 , x_2 and x_3) in response surface reduced quadratic model.

Source	SST	df	MS	F-Value	p-value
Model	3214883	7	459269.1	4.994487	0.0075
x_1	4902.709	1	4902.709	0.053316	0.8213
x_2	731993.3	1	731993.3	7.960324	0.0154
x_3	976072.3	1	976072.3	10.61465	0.0069
x_1x_3	406463.8	1	406463.8	4.420237	0.0573
x_2x_3	389028.2	1	389028.2	4.230627	0.0621
x_1^2	487734.6	1	487734.6	5.304045	0.0400
x_2^2	279641.6	1	279641.6	3.041063	0.1067
Residual	1103462	12	91955.21		
Lack of fit	876124.5	7	125160.6	2.752744	0.1413
Pure error	227337.9	5	45467.59		
Cor. total	4318346	19			

It was observed that most significant variables were the linear terms of extraction time (x_3) and stirring rate (x_2).

The result suggested that the change in extraction time ($p < 0.0069$) and stirring rate ($p < 0.0154$) had considerable effects on the LLE of persipeptides. Indeed, extraction time (x_3) had a pivotal effect in LLE method and was required to be optimized in order to achieve high efficiency in extraction of the persipeptides. The procedure time was the driving force

for transportation of the persipeptides from aqueous solution to organic solvent as a result of the increase in compounds interaction with organic solvent until the extraction equilibrium has been reached. However, if the time is set erroneously high, then persipeptides will be degraded³ and in turn, the extraction efficiency will decrease. Persipeptides degradation may reach up to 21 % when fermentation broth is kept at room temperature for 24 h prior to extraction or its concentration may be decreased by up to 13 % when the broth is preserved at 4 °C in BuOH for same period of time.³ Results showed that the extraction time is in reverse relationship with the percentage of organic solvent used, justifying the existence of significant interaction between two factors, which was found in the screening design. In high percentage of organic solvent, the time of extraction could be diminished to as low as 33 min. Nevertheless, increasing the rate of stirring as high as possible (up to 300 rpm), which was the second most important factor in this process, enhanced the extraction capability. These are in accordance with other studies conducted on the effect of stirring rate, solvent amount, and hold-up on efficiency of a typical extraction process, which have reported that when stirring speed and solvent amount were increased, the efficiency increased. Additionally, it has been proposed that the efficiency of the compounds extraction increased monotonously with speeding up stirring rate.²³ Following the mathematical model fitting, multiple response method, called the desirability function (D), was employed to optimize the studied parameters.

**Figure 2.** Contour plot (A) and 3D surface graph (B) of desirability versus ratio of BuOH and stirring rate. Stirring time was 78 min, pH was 9, and temperature was 28 °C were the experiment condition.

This method was applied to meet the requirement for increasing the yield of extraction in as shortest process as possible to both decrease the expenses and prevent persipeptides degradation. The most desired value for the responses is a desirability value of one, whereas a value equal to zero represents an unacceptable value for responses.

The aim of the optimization was to improve the LLE efficiency of persipeptides. In this approach, a process with desired characteristics is obtained by combining process parameters, which has been evaluated by RSM, into a single variable for the prediction of the optimal levels of the independent variables. To achieve the highest desirability, all factors were set to within range, except the concentration of persipeptides that was set to maximum level. Figures 2A and 2B, respectively, illustrate the contour plot and 3D surface graph of desirability for LLE of persipeptides generated from 15 optimum points through numerical optimization.

Among 30 starting points, the best local maximum for LLE of persipeptides ($264 \pm 9.85 \mu\text{g mL}^{-1}$) was resulting in 34 % BuOH, 228 rpm (stirrer speed), and 78 min (stirring time) with the value of desirability of 0.88. Compared with un-optimized process (persipeptides concentration of $219.63 \pm 2.48 \mu\text{g mL}^{-1}$), the optimized conditions increased the extraction of persipeptides by 20.20 %, while decreased both time and percentage of BuOH by 67 % (162 min) and 16 %, respectively. Therefore, using optimized LLE method and suggested fermentation broth, a total of seven times increased in persipeptides production was reached. Nevertheless, from large scale prospect, the final reaction conditions *i.e.* broth pH, 9-9.5; temperature, 28 °C; stirrer speed, 228 rpm; percentage of BuOH; 34 %; and process time, 78 min have industrial compatibility.

This is because of no pre-pH adjustment requirement for LLE of persipeptides as the ambient pH of *S. zagrosensis* CM1 broth is within the mentioned range. It is worth to note that as pH increased and temperature decreased the corrosion rate of steel from different parts of extraction plants decreased, which is an astonishing feature of this optimized process. Moreover, minimum facilities and energy consumption are required for adjusting temperature at 28 °C; therefore, greatly decreases the expense of extraction. The percentage of BuOH was decreased in expense of increasing time from 33 to 78 min to minimize instrument corrosion and solvent usage and its subsequent evaporation expenses. However; despite great effort, the agitation could not be decreased and indeed increased from 150 rpm in un-optimized process to 228 rpm in further optimized method, which is inevitably still not considered as an improving step.

Conclusions

The direct impact of this optimization is on decreasing the cost of extraction as well as the time of process, whereas increasing the yield of extraction. This in turn, facilitates further clinical trial investigations, which require several of grams of purified persipeptides. This was the first attempt reported on retrieval of persipeptides from fermentation broth that has been optimized. It has been previously shown that presence of glucose plus a more slowly utilized carbon source such as malt result in production of higher secondary

metabolites, as glucose utilization results in good growth of bacteria and complex carbon source is used for antibiotic synthesis.²⁴ However, rapid catabolism of glucose has been shown to decrease the rate of antibiotic production.^{25, 26} In practice, ISP2 medium, which have been tested on the basis of this assumption failed to increase the production of persipeptides. In contrast, both CM1 and CM6 increased the production of persipeptides. These increases may be due to the fact that application of low solubility carbon sources, such as insoluble starch in CM1 and glycerol in CM6, prevents carbon catabolite regulation.²⁶ Despite the advantage of utilization of glycerol in fermentation, which contains more energy than starch and glucose on a weight-to-weight basis, it has some disadvantages, including higher oxygen requirement, increased medium viscosity, and more problematic downstream processing.²⁶ Interestingly, both CM1 and CM6, considerably enhanced persipeptides production by six and four times, respectively, compared to ISP2 medium. CM1 and CM6 contain soybean, which is a rich source of valine and phenylalanine amino acids with percentage of total weight on dry basis of 2.06 ± 0.19 and 2.16 ± 0.21 , respectively.²⁷ These amino acids are present in core structure of persipeptides with repetitions as the only utilized amino acids. CM1 contains three times more soybean than CM6, which may explain its 37 % (approximately $60 \mu\text{g L}^{-1}$) more persipeptides production, compared to CM6 by means of providing more valine and phenylalanine. It has been observed that increase in amount of CaCO_3 from 2 to 10 g L^{-1} improves the production of persipeptides (Data not shown); however, there is little knowledge on effects of various salts in biosynthesis of persipeptides. Therefore, a systematic study using a number of techniques such as labeled precursors for the study of various media components and its further optimization for exploiting the best result are required.

References

- Brown, E.D., Wright G. D., *Nature*, **2016**; 529(7586), 336.
- Mohammadipanah, F., Matasyoh, J., Hamed, J., Klenk, H. P., Laatsch, H., *Bioorg. Med. Chem.*, **2012**; 20(1), 335.
- Mohammadipanah, F., Panahi, H. K. S., Imanparast, F., Hamed, J., *Chromatographia*, **2016**, 79(19-20), 1325.
- Davidson, B. S., *Chem. Rev.*, **1993**, 93(5), 1771.
- Cody, W. L., He, J. X., Reily, M. D., Haleen, S. J., Walker, D., M., Reyner, E. L., Stewart, B. H., Doherty, A. M., *J. Med. Chem.*, **1997**, 40(14), 2228.
- Rajeswaran, W., Hocart, S. J., Murphy, W. A., Taylor, J. E., Coy, D. H., *J. Med. Chem.*, **2001**, 44(8), 1305.
- Dechantsreiter, M. A., Planker, E., Mathä, B., Lohof, E., Hölzemann, G., Jonczyk, A., Goodman, S.L., Kessler, H., *J. Med. Chem.*, **1999**, 42(16), 3033.
- Hess, S., Ovidia, O., Shalev, D., Senderovich, H., Qadri, B., Yehezkel, T., Salitra, Y., Sheynis, T., Jelinek, R., Gilon, C., Hoffman, A., *J. Med. Chem.*, **2007**, 50(24), 6201.
- Barker, P., L., Bullens, S., Bunting, S., Burdick, D., J., Chan, K., S., Deisher, T., Eigenbrot, C., Gadek T., R., Gantzios, R., *J. Med. Chem.*, **1992**, 35(11), 2040.
- Dong, M. W., *Modern HPLC for Practicing Scientists*, Wiley, Hoboken, **2006**.
- Snyder, L., R., Kirkland, J., J., Dolan, J., W., *Basic Concepts and the Control of Separation. Introduction to Modern Liquid Chromatography*, 3rd ed., Wiley, Hoboken, **2010**.

- ¹²Araujo, P. W., Brereton, R. G., *Trends Anal. Chem.*, **1996**, 15(2), 63.
- ¹³Bezerra, M. A., Santelli, R. E., Oliveira, E. P., Villar, L. S., Escalera, L. A., *Talanta*, **2008**, 76(5), 965.
- ¹⁴Ghafari, S., Aziz, H. A., Isa, M. H., Zinatizadeh, A. A., *J. Hazard. Mater.*, **2009**, 163(2), 650.
- ¹⁵Li L.Z., Zheng H., Xian M., *J. Taiwan Inst. Chem. Eng.*, **2010**, 41(3), 252.
- ¹⁶Shioya, S., Morikawa, M., Kajihara, Y., Shimizu, H., *Appl. Microbiol. Biotechnol.*, **1999**, 51 (2) 164.
- ¹⁷Zhu, Y., Chen, G., Wu, M., Miao, X., Xu, J., Wang, M., *Chin. J. Pharm.*, **2010**, 3, 014.
- ¹⁸Marques, D. A. V., Cunha, M. N. C., Araújo, J. M., Lima Filho, J. L., Converti, A., Pessoa, J. R. A., Porto, A. L., *Braz. J. Microbiol.*, **2011**, 42 (2), 658.
- ¹⁹Saval, S., Pablos, L., Sanchez, S., *Bioresour. Technol.*, **1993**, 43 (1), 19.
- ²⁰Adinarayana, K., Ellaiah, P., Srinivasulu, B., Devi, R. B., Adinarayana, G., *Process Biochem.*, **2003**, 38 (11), 1565.
- ²¹Viana Marques, D., Pessoa Júnior, A., Lima Filho, J., Converti, A., Perego, P., Porto, A., *Biotechnol. Prog.*, **2011**, 27 (1), 95.
- ²²Atkinso, A., Donev, A., *Technometrics*, **1996**, 38 (4), 333.
- ²³Abolghasemi, H., Moosavian, M., Bahmanyar, H., Maragheh, M. G., *Iran J. Chem. Eng.*, **2005**, 2 (1), 11.
- ²⁴Martín, J. F., Demain, A. L., *Microbiol. Rev.*, **1980**, 44 (2), 230.
- ²⁵Revila, G., Lopez Nieto, M. J., Luengo, J. M., Martin, J. F., *J. Antibiot.*, **1984**, 37 (7), 781.
- ²⁶Saudagar, P. S., Survase, S. A., Singhal, R. S., *Biotechnol. Adv.*, **2008**, 26 (4), 335.
- ²⁷Kovalenko, I. V., Rippke, G. R., Hurburgh, C. R., *J. Agric. Food Chem.*, **2006**, 54 (10), 3485.

Received: 21.10.2016.

Accepted: 25.11.2016,